Isotopic and Geochemical Studies of Saline-Alkaline soils, Water and Sediments of the Ganga river system: Implications to Erosion and Carbon cycle

A Thesis

submitted for the Award of Ph.D. degree of

MOHANLAL SUKHADIA UNIVERSITY

in the

Faculty of Science

by

Jayati Chatterjee

Under the supervision of

Dr. Sunil Kumar Singh

ASSOCIATE PROFESSOR

GEOSCIENCES DIVISION

PHYSICAL RESEARCH LABORATORY

AHMEDABAD – 380 009, INDIA

DEPARTMENT OF GEOLOGY
FACULTY OF SCIENCE
MOHANLAL SUKHADIA UNIVERSITY,
UDAIPUR (RAJ)

Year of submission – 2013

DECLARATION

I, **Jayati Chatterjee**, D/o Mr. Arindrajit Chatterjee, resident of UN quarter UN-14, PRL residences, Navrangpura, Ahmedabad – 380009, hereby declare that the research work incorporated in the present thesis entitled **"*Isotopic and Geochemical Studies of Saline-Alkaline soils, Water and Sediments of the Ganga river system: Implications to Erosion and Carbon cycle*"** is my own work and is original. This work (in part or in full) has not been submitted to any University for the award of a Degree or a Diploma. I have properly acknowledged the material collected from secondary sources wherever required.

I solely own the responsibility for the originality of the entire content.

Date: Jayati Chatterjee
(Author)

CERTIFICATE

I feel great pleasure in certifying that the thesis entitled “*Isotopic and Geochemical Studies of Saline-Alkaline Soils, Water and Sediments of the Ganga river system: Implications to Erosion and Carbon Cycle*” embodies a record of the results of investigations carried out by **Jayati Chatterjee** under my guidance.

She has completed the following requirements as per Ph.D. regulations of the University

(a) Course work as per the university rules

(b) Residential requirements of the university

(c) Presented her work in the departmental committee

(d) Published/accepted minimum of one research paper in a referred research journal.

I am satisfied with the analysis of data, interpretation of results and conclusions drawn.

I recommend the submission of thesis.

Date: *Name and designation of supervisor*

Sunil Kumar Singh,
Associate Professor

Countersigned by
Head of the Department

dedicated to

my parents

ACKNOWLEDGEMENTS

This thesis would not have been possible without the help of several individuals, who in one way or other contributed and extended their valuable assistance in the preparation and completion of this study.

First of all, I owe my sincere and deepest gratitude towards my thesis supervisor, Dr. Sunil K. Singh, who has supported me throughout my thesis with his patience and knowledge. His deep insight in the subject of isotope geochemistry and mass spectrometry and vast experience helped me immensely in learning the subject. It was a great experience to work with him and I consider myself fortunate to have him as my supervisor.

I take this opportunity to express my sincerest gratitude towards Prof. S. Krishnaswami for his advice and guidance. I thank Prof. M. M. Sarin, who was always supportive during my thesis work and helped me with his valuable remarks. I gratefully acknowledge Dr. Ravi Bhushan for his encouragement and support during the thesis. I am extremely thankful to Prof. J. N. Goswami, the Director, Prof. Utpal Sarkar, Dean and Prof. Anjan S. Joshipura, former Dean, Physical Research Laboratory, for providing me support and facilities for the thesis work. I thank academic committee members for timely evaluation of my research work. I would like to thank Drs. M. M. Sarin, N. M. Ashok, P. Panigrahi, R. Rangarajan, D. Angom, D. Banerjee, B. Bapat, K. P. Subramanian, V. K. Rai, K. K. Marhas, and J. S. Ray for their informative lectures during the course work.

I also like to thank all members of the Chemistry Lab for their help, support and encouragement. I specially thank Bhavsar bhai for his help during the field trips. He always gave the best suggestions throughout my thesis work. It was really nice to work with him in the lab as well as on oceanographic expeditions. I acknowledge Dr. R. Rengarajan, Dr. N. Rastogi and A. K.

Sudheer for their cooperation during my research work. I sincerely thank my labmates, Srinivas, Prashant, Vineet, Satinder, Damu, Sneha, Saweeta, Upasana, Venky, Dipjyoti, Balaji and Aslam for their help and support. I would also like to thank my ex-labmates Gyana, Rahaman, Kirpa Ram and Ashwini for their help and fruitful discussions. I duly acknowledge the help provided by Sneha, Vaishali, Trupti and Shantaben.

I am thankful to Dr. V. K. Rai and Dr. S. V. S. Murty for providing their lab facilities. Dr. Rai helped me with the measurements and shared the valuable insights in the relevance of basic operation and working of the MC–ICPMS. I am thankful to Gyana for sharing with me the basics of Inverse modeling technique. I sincerely thank Vineet, Satinder and Tapas for helping me with the computer programming.

I am grateful to all the staff-members of Library, Computer Centre, Workshop, Dispensary and Maintenance section of PRL for their assistance and cooperation.

I take an opportunity to express gratitude to all my friends at PRL. I would like to thank my batch mates of JRF07; Prashant, Srinivas, Satinder, Moumita, Tapas, Iman, Pravin, Ketan, Saxena, Ashish, Khan, and Suruchi for making my stay joyful. Much needed company of my seniors and juniors made my stay pleasant at PRL.

Finally, I would like to thank Rajdeep and in-laws, who stood by me through the good and bad times. They dealt with all of my absence from many family occasions with a smile. I acknowledge the love and care I received from Riya, Trayee and Mukti. Last but not the least; the devotion I got from my parents is something beyond acknowledgement. Without their support and sacrifice, I would not have reached this point.

ABSTRACT

This thesis deals with chemical erosion in the Ganga system and application of dissolved elemental and Sr-Nd isotope composition in apportioning the sources of dissolved ions in different reservoir and understanding the weathering processes and their controlling factors. High abundance and solubility of saline-alkaline soils in the Ganga plain makes them an important source of dissolved ions to the river waters. These soils have been chemically and isotopically characterized in the present study. Na_2CO_3, $NaHCO_3$ and Na_2SO_4 are the main components of saline-alkaline soils beside NaCl. Dissolved budget of the Ganga river system has been apportioned to various sources, e.g., silicates, carbonates, saline-alkaline soils etc, by inversion of chemical and Sr isotopic data. The results show around 40% of Na in the Ganga outflow is of saline-alkaline origin. The estimated chemical erosion rate in the Ganga plain is less than half of that in the headwaters.

The silicate chemical erosion has been apportioned in terms of litho-tectonic units e.g. Higher Himalaya, Lesser Himalaya, Deccan Basalts etc., using dissolved Sm, Nd concentration and Nd isotopic composition. Higher Himalaya seems to dominate the chemical erosion of silicates with secondary contribution from Deccan rivers. Preferential dissolution of apatite like minerals has been inferred from higher Sm/Nd in these waters and radiogenic dissolved Nd compared to its particulate counterpart in Himalayan rivers. Nd flux from the Ganga to the Bay of Bengal has been estimated to be 17000 - 34000 moles annually with ε_{Nd} -14.5±0.5. Measured dissolved Nd data from coastal region shows higher radiogenic value in the surface, which could be due to influence of the Brahmaputra. Less radiogenic deeper samples indicate towards release of Nd from the shelf sediments, which is essentially the sediment supplied by the Ganga and Brahmaputra.

Sr isotopes along with major ion chemistry have been used to delineate sources of dissolved ions in groundwater and rain water. Groundwater from Gujarat region have very high TDS with high concentration of Na. NO_3 concentration in these samples are also very high. Inversion based on chemical and Sr isotopic data shows saline-alkaline soils as an important contributor of the dissolved ions to the

groundwater. Rare precipitation of NO_3, during cyclic drying and wetting cycles, enriches that particular species in groundwater. This gives an alternate explanation of high NO_3 content in the old and deep groundwater systems, which are not susceptible to anthropogenic contamination. Groundwater from Ganga plain and Chambal basin also have moderate contribution from saline-alkaline soils. Sr isotopes have been successfully used to apportion the sources of base cations in the rain water of Ahmedabad. Good correlation between Sr and non-seasalt component of Ca and Mg validates its use as a tracer of these cations. The results indicate carbonates and basalts as important contributor of base cations to the atmosphere.

TABLE OF CONTENTS

Contents **Page**

LIST OF TABLES

LIST OF FIGURES

Chapter 1

Introduction

1.1 Introduction

The weathering and erosion in the young orogenies could be vital in influencing long time carbon cycle and climate change, and could enhance the supply of dissolved and suspended materials to the ocean. The uplift of the Himalaya since last 40 million years has changed the atmospheric circulation and climate in Asian region and has established monsoonal climate in the Indian subcontinent (Ruddiman and Prell, 1997). The rivers originating from the Himalaya contribute a major portion of global fresh water and sediment discharge to the ocean (Berner and Berner, 1996). Major ion and trace metal isotope budgets of the ocean have been influenced by the increase in the chemical weathering due to uplift of the Himalaya (Raymo and Ruddiman, 1992; Richter et al., 1992). Chemical weathering of the silicate rocks is a main sink of atmospheric CO_2 over a million year time scale, promoting several studies to estimate the contemporary silicate weathering rate and associated atmospheric CO_2 drawdown in the major Himalayan rivers (Pande et al., 1994; Krishnaswami and Singh, 1998; Singh and France-Lanord, 2002; Krishnaswami and Singh, 2005; Singh, 2007; Hren et al., 2007; Tripathy and Singh, 2010). The Ganga being one of the major rivers draining the Himalaya has been studied extensively in the headwater region (Sarin et al., 1989; Sarin et al., 1992; Palmer and Edmond, 1992; Galy and France-Lanord, 1999; Galy and France-Lanord, 2001; Bickle et al., 2003; Tipper et al., 2006; Tripathy et al., 2010). However, the plain and peninsular regions of the Ganga basin, which covers ~80% of the total drainage area, is comparatively less explored (Sarin et al., 1989; Galy and France-Lanord, 1999; Rengarajan et al., 2009; Rai et al., 2010; Lupker et al., 2012). The studies on the Ganga plain reported presence of considerable spread of saline-alkaline soils in this region (Agarwal et al., 1992; Srivastava, 2001; Pal et al., 2003), dissolution of which could contribute significantly to the river water chemistry due to their higher solubility. The impact of these saline-alkaline soils on the Ganga water chemistry is evident by increase in concentration of Na in the Ganga mainstream and few tributaries in the plain compared to the headwaters. Therefore studies dealing with rivers flowing through saline-alkaline soil regions have encountered problems in estimating silicate erosion rates (Rengarajan et al., 2009; Rai et al., 2010; Gupta et al., 2011).

Although there are a number of studies present on saline-alkaline soils, very few of them deal with their chemical characterization (Datta et al., 2002) and none of them deals with impact of these soils on the river water chemistry. Few studies (Sarin et al., 1989, Rengarajan et al., 2009, Rai et al., 2010) though highlighted their impact on water chemistry, they could not quantify its impact on river chemistry. In this study an effort has been made to chemically and isotopically characterize them and quantify the contribution of these soils to the major ion concentration and Sr isotope budget of the Ganga river system.

Silicate erosion rate in the headwaters of the Ganga has been estimated either using forward model (Krishnaswami et al., 1999; Galy and France-Lanord, 1999) or inverse model (Tripathy and Singh, 2010). In the forward model, silicate erosion has been estimated using non-chloride sodium (excess of sodium over chloride, measured in river water) as proxy of silicate weathering. The same could not be used in the Ganga plain and peninsular region as saline-alkaline soils contribute significantly to non-chloride Na to the rivers. Hence, estimates of silicate erosion rate based on non-chloride Na could be an overestimate in the Ganga plain. Gupta et al. (2010) has used K as a proxy of silicate weathering, where as Rengarajan et al., 2009 and Rai et al. (2010) have used Mg and Si respectively. But precipitation in case of Mg and participation of K and Si in biological activities make them potentially non-conservative systems in river water (Rai et al., 2010). To avoid these problems, contribution of saline-alkaline soil to the river chemistry has been estimated and further major ions in the river water have been apportioned to their various sources using inverse model in this study considering saline-alkaline soils as one of the sources in addition to silicates and carbonates (Negrel et al., 1993; Gaillardet et al., 1999; Millot, 2003; Wu et al., 2005; Moon et al., 2007; Tripathy and Singh, 2010).

Recently Lupker et al., (2012) has indicated more intense silicate weathering in the Ganga plain compared to the headwaters based on elemental composition of sediments from the plain and headwaters. It has been observed that these sediments are depleted in cations contents with respect to the headwater sediments. To calculate the weathering rate using sediment chemical composition, however, their residence time in plain over which weathering is taking place needs be considered. Information about residence times of sediment in the Ganga plain is poorly understood and is subject to large uncertainty. The Ganga-Brahmaputra delta region and the Ganga plain are made up of sediments brought by these two rivers on various time scale. These sediments have been undergoing chemical weathering since time of their deposition. It is quite possible that chemical weathering of the sediment which are being added to the rivers now were chemically weathered earlier. In such case, they will add to the sediment budget but not to the dissolved load of the river causing over estimation of weathering in the plain. This could explain the observation of higher silicate erosion rate in the plain (Lupker et al., 2012). In the present study, dissolved budget has been used to estimate the chemical erosion rate of the silicates and carbonates in the plain. Further, the contribution from saline-alkaline soils to the dissolved budgets is also being taken care. Therefore, the present study is expected to yield a more realistic estimation of chemical weathering rate in the plain.

In this context, the relation between chemical and physical weathering is not well understood. The Himalaya, where both chemical and physical weathering are important, is an excellent place to study such relations. Nd and Sr isotopes have been successfully used as a provenance tracer of physical weathering in the Himalaya as silicates from the Higher and Lesser Himalya have very distinct Nd isotopic signature. It has been observed that the Higher Himalaya (HH) controls the physical weathering and more than 65% of sediment of the Ganga is coming from the HH (Singh et al., 2008). The intensity of physical weathering depends mainly on relief and stream power. However, chemical weathering process is more complex in this respect. There are several parameters such as temperature, vegetation, amount and type of weatherable material present etc, which could control this process. Among them, the amount of fresh substrate (chemically unweathered) and surface area is a direct result of the physical weathering process. Therefore, physical weathering is also a potential controller of the chemical weathering. The Lesser Himalaya (LH) could be more conducive for chemical weathering due to higher temperature and vegetation cover. Nd isotopes can be useful to trace this process. The main advantage of using Nd isotope is that unlike Sr, very less Nd comes from the carbonates and its dissolved budget is dominated by silicate weathering. This could serve as a good proxy to locate the locus of silicate weathering in terms of lithounits. Though the mobility of Nd from rock/soils to dissolved phase is not well understood (Aubert et al., 2001; Ma et al., 2010).

Dissolved and suspended Nd in the river water world-wide was studied by Goldstein and Jacobsen as early as in 1987 and 1988, respectively (Goldstein and Jacobsen, 1987; 1988). Since then several studies (Elderfield et al., 1990; Sholkovitz et al., 1992; Allègre, 1996; Tricca et al., 1999; Ingri et al., 2000; Negrel et al., 2006) have dealt with the problem of elemental fractionation of REEs in colloidal and solution phases. Secondary mineral phases and organic matter are important in retention of the REE in the soil phase and can prevent REE from entering into dissolved phase (Aubert et al., 2001; Stille et al., 2009). The replacement of primary REE bearing minerals such as monazite, allanite, zircon and apatite by secondary LREE carrying phosphate minerals can also be importance (Stille et al., 2009). Nd is supposed to go through a congruent weathering, as both Sm and Nd belong to LREE group and behave in a similar manner (Rickli et al., 2013 and references there in). Though some isotopic difference have been observed in dissolved and suspended load in the rivers draining granite rocks (Tricca et al., 1999, Aubert et al., 2001), this has been attributed to the preferential weathering of apatite. Aubert et al., (2001) has also suggested stronger concentration of REE carrying minerals in the finest fraction (0-20 μm), based on enrichment of REEs in the same. Nesbitt and Marcovics (1997) has reported uninfluenced behavior of Sm/Nd ratio during large scale chemical weathering. Though Öhlander et al., (2000) has reported preferential release of Nd from minerals with a low Sm/Nd ratio than the bulk soil during weathering of till. Their observation has been corroborated by the study of dissolved Nd in the Kalix river, which drains the same region (Andersson et al., 2001).

Garçon et al., (2013) have studied Nd and Hf isotopic composition in bedload and suspended load in the Ganga river and its Himalayan tributaries. They have concluded that hydrodynamic sorting of minerals does not affect the Nd isotopic composition. In the present study, dissolved Nd concentration and isotopic composition has been measured in the Ganga river system from the headwaters to the outflow. This could help to identify the location of chemical weathering in the Ganga system and also to constrain the Nd flux to the Bay of Bengal from the Ganga.

Dissolved Nd isotope is widely used as water mass tracer in the oceans (Jeandel, 1995; Frank, 2002; Lacan and Jeandel, 2005) as its oceanic residence time is less than global ocean mixing time (Tachikawa, 2003). Also this isotope is used to extract paleoceanographic information from marine sediments (Piotrowski et al., 2009). A few studies in the Bay of Bengal (BoB) and in the Indian Ocean (Burton and Vance, 2000; Gourlan et al., 2010) have shown the importance of Himalayan contribution to the Nd budget of the BoB. As Nd isotopes are susceptible to exchange between water and sediments (Lacan and Jeandel, 2001), it is possible that the isotopic composition the outflow differ before and after estuary. Therefore to know the actual input from the Himalaya to BoB, samples from coastal region have also been studied for Nd isotopic composition.

Groundwater can contribute to the river water during the lean flow and the aquifers can get water from the river during monsoon depending on the water level. In arid and semi-arid regions, it is one of the most important resources of water for domestic, industrial and agricultural needs. To utilize this precious resource economically and prevent deterioration, it is necessary to understand the processes, which control its quality. Hydrological input parameters, such as precipitation, evaporation and runoff are subject to spatial and temporal variability, which in turn complicate the hydrodynamic mass balance calculation of groundwater. Geochemical and isotopic investigations are a successful alternative in determining groundwater recharge, flow paths and renewal time (Weyhenmeyer, 2002 and references there in). Local differences and short term variability do not affect the geochemical data as it integrates all water that enters the reservoir. The major ion composition of groundwater is controlled by the surface, subsurface weathering, and their residence time in the aquifer. Sr isotopes have been widely used to understand the water-rock interaction processes in the groundwater aquifers (Smalley et al., 1988; Stueber et al., 1993; Naftz et al., 1997; Katz et al., 1997; DePaolo, 2006; Hellmann et al., 2013). Groundwater also plays a significant role in the formation process of saline-alkaline soils. Therefore samples of groundwater collected during monsoon and non-monsoon were analyzed for major ions and Sr isotopic composition along with the river water samples. To better understand the nature of groundwater chemistry in the semi-arid climate where saline-alkaline soils are also present, groundwater samples from Gujarat were also analyzed.

Groundwater from some parts of the Ganga plain has been reported to have very high concentration of nitrate and fluoride (Singh et al., 2006; Sankararamakrishnan et al., 2008). Groundwater of Gujarat has very high TDS along with Na and NO_3 (Agarwal et al., 2006; present study). Nitrate contamination has been linked to agricultural activities due to nitrogenous fertilizers. Other sources of nitrate include animal waste, waste water disposal etc (Singh et al., 2006). Though a study in Hooghly district, which is agriculturally intensive, reported groundwater with nitrate content below permissible limit of WHO for drinking purposes, in spite of fairly high usage of fertilizers. Bijay-Singh et al., (1995) has indicated low fertilizer use efficiency is caused by excessive N losses via volatilization and denitrification rather leaching in developing countries of Asia. The high nitrate content in the Gujarat groundwater can not be explained by fertilizer use or waste water contamination, as these water is from a diverse region and reported to be very old (Agarwal et al., 2006). Also, groups of groundwater samples from Gambhir river basin, Rajasthan have been reported to be derived by dissolution of surface salts (Umar and Absar, 2003). Therefore, in this study an effort has been made to determine the sources contributing to dissolved budget of the groundwater using inverse model approach.

Rain waters are an important source of dissolved ions to the rivers, especially in India, where monsoonal rainfall is the main source of water to a large number of rivers. Also, rainwater chemistry has been important for its use to investigate the atmospheric conditions and the concentration of the soluble components, especially at present time when the anthropogenic activities are changing the atmospheric environment at an ever increasing pace. There have been a number of studies of the wet deposition in the Indian subcontinent to deal with the chemical components and to understand their characteristics (Saxena et al., 1996; Kulshrestha et al., 1999; Safai et al., 2004; Rastogi and Sarin, 2005; Kulshrestha et al., 2009). It has been observed that in Indian region the rainwater are mostly alkaline in nature due to abundance of primary aerosols (Ca, Mg and K) originating from the dusty soils (Kulshrestha et al., 2003; Chandra Mouli et al., 2005). Also there has been studies to detect the crustal influence on rainwater (Jain et al., 2000). It is difficult to apportion the sources of dust using the major ions only, whereas in this case Sr isotopes can be immensely helpful. In this context, the rainwater from Ahmedabad, India has been studied using Sr isotopic ratio along with other major ions to delineate the sources of base cations in terms of different lithology.

1.2 Objectives of the thesis

The major objectives of the present study is to,

a) chemically characterize saline-alkaline soils and quantification of its contribution to dissolved budget of river water in the Ganga plain.
b) estimation of silicate erosion rate and CO_2 draw down in the Ganga river system.
c) use of dissolved Nd as a provenance tracer of chemical weathering in the Ganga river system.
d) understand weathering processes of Nd in the Ganga system.
e) constrain the flux of dissolved Nd to the Bay of Bengal from the Ganga.
f) study the groundwater from the Ganga plain and Gujarat geochemically and isotopically to trace the major sources of dissolved ions.

g) delineate the sources of base cations in the rainwater from Ahmedabad, India using Sr isotope.

1.3 Structure of the thesis

This thesis is divided into seven chapters. The content of these chapters are as follows.

Chapter 1: Introduction

This chapter introduces the topics that have been addressed in this thesis. The motive of this chapter is to highlight the present level of understanding and mark the existing research gaps in the knowledge related to these topics. This chapter also provides the major objectives of this thesis.

Chapter 2: Materials and methods

This chapter provides details on the materials and various analytical methodologies used to accomplish the goals of this thesis. This chapter has been divided into two parts. The former part of the chapter details the general geology and hydrology of the sampling locations. The latter part gives a brief description of sampling river water, groundwater, rainwater and saline-alkaline soils. This part also describes various analytical methods used for their chemical and isotope analyses.

Chapter 3: Chemical and isotopic characterization of saline-alkaline soils and its impact on river water chemistry

This chapter describes the results of characterization of saline-alkaline soils chemically and using Sr isotopes. This chapter also presents major and Sr isotope data of the Ganga river system, and results of source apportionment of dissolved budget using inversion of chemical and isotopic data. Results of estimation of chemical erosion in the plain, considering the effects of saline-alkaline soils are discussed.

Chapter 4: Dissolved Nd in the Ganga river system and its flux to the Bay of Bengal

This chapter presents the results and discussions pertaining to the dissolved Nd concentration and isotopic composition in the Ganga, from headwaters to the outflow, and its major tributaries. Use of dissolved Nd as a tracer of chemical weathering in terms of different lithounits has been examined in this chapter. The effects of preferential weathering of minerals on dissolved and particulate Nd has been described. Flux of dissolved Nd from the Ganga to the Bay of Bengal has been estimated. This chapter also describes the behaviour of Nd isotope in the coastal region of Bay of Bengal.

Chapter 5: Ground water chemistry and its relation to saline-alkaline soils

This chapter details the results of chemical and Sr isotopic analyses of groundwater from the Ganga plain, Chambal basin and Gujarat. A relation between saline-alkaline soil formation process and groundwater dissolved budget has been proposed. This chapter also describes the results of source apportionment in the groundwater dissolved budget.

Chapter 6: Rain water chemistry and use of Sr as provenance tracer of base cations

This chapter provides results of chemical and Sr isotope analyses of rainwater from Ahmedabad. It describes a temporal variability in rain water major ion concentration related to precipitation amount. The use of Sr isotopes as provenance tracer of base cations in the rain water has been examined.

Chapter 7: Summary and future perspectives

This chapter summarises the major findings of this thesis and briefly outlines the future perspectives.

Chapter 2

Materials and methods

Primary objectives of this thesis, as discussed in the introduction, are to i) quantify the impact of dissolution of saline alkaline soils on geochemical budgets of the river water, ii) apportion the sources of dissolved ions of the Ganga river system to estimate the silicate erosion and CO_2 consumption rates in this basin after taking into account the contribution from saline alkaline soils, iii) study the dissolved Nd and its isotope composition in the Ganga river system and determine its flux to the Bay of Bengal, and (iv) determine the sources of solutes in rain and groundwater. Hence, a detail sampling of the Ganga river system and saline alkaline soils from its basin and rainwaters and groundwaters is a prerequisite for this purpose., A basic knowledge of the basin lithology and hydrology is necessary to address these goals. This chapter presents a brief discussion on the lithology of the sampling area, sampling locations, collection and analytical methods adopted for these studies.

2.1 Geological setting

2.1.1 The Ganga river system

The geology and hydrology of the Ganga river system is described in detail in Singh et al., 2008; Sarin et al., 1989; Dalai et al., 2002; Tripathy et al., 2010 and Rai et al., 2010. A brief description of the headwater region and the Ganga plain including the saline-alkaline soil regions is given below.

The Himalaya : The Himalayan segment of the drainage basin comprises of mainly of four lithotectonic units (Fig. 2.1), the Tethian Sedimentary Series (TSS), the Higher Himalaya (HH), The Lesser Himalaya (LH) and the Siwaliks (Singh et al, 2008).

The TSS covers Southern part of the Tibetan plateau which composed mainly of less altered lime stones, amphibole, calc-silicates with biotite, muscovite and chlorite outcrops (Galy and France-Lanord, 1999, Tripathy et al., 2010). Five major tributaries, namely Alaknanda, Ghaghra, Gandak, Kosi and Yamuna originate at this region. The HH consists of granitoid gneisses, schist, granites, metamorphosed carbonates and calc-silicates. Higher Himalayan Crystallines (HHC), which is formed of granites, gneisses and leucogranaites, are found widely in this region (Singh et al, 2008). The LH is separated from the HH by the Main Central Thrust (MCT) and composed mainly of metamorphosed Precambrian sediments, which includes greywacks, shales, slates, limestones and dolomites (Tripathy et al., 2010). The Lesser Himalayan Crystalline (LHC), which consists of granites and gneisses, separates the LH into two sedimentary sequences, the outer and inner belt (Singh et al., 2008). The southernmost part of the Himalaya, i.e. the Siwaliks composed of uplifted Mio-Pliocene sediments, eroded by the Himalayan rivers and deposited in the foreland basin (Galy and France-Lanord, 1999; Singh et al., 2008).

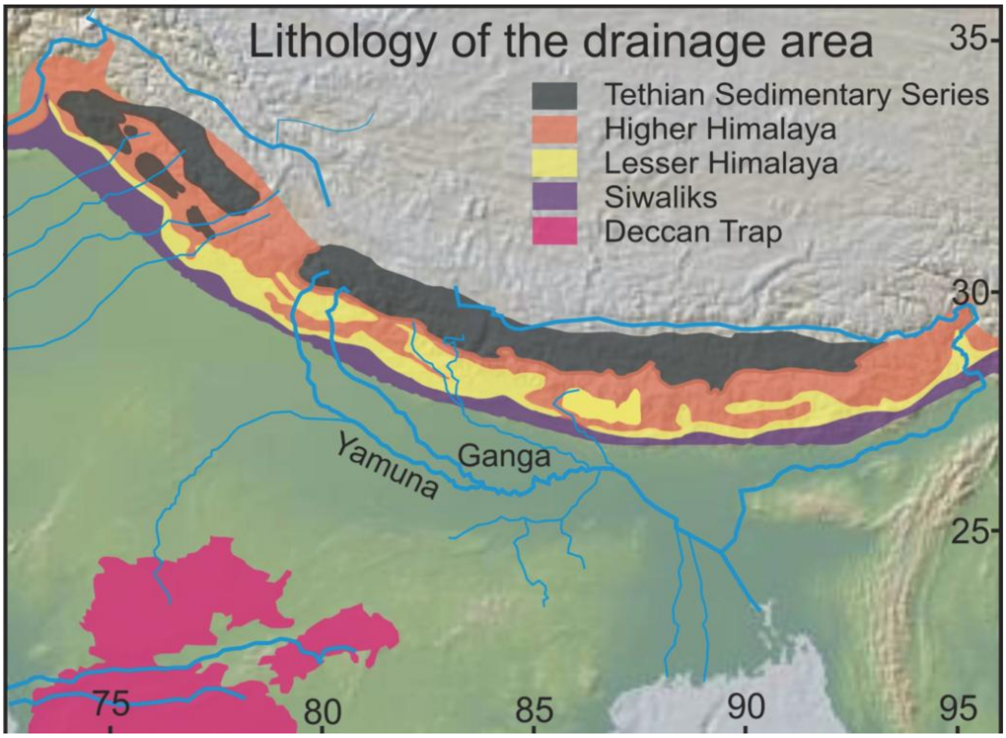

Fig. 2.1: *Major litho-tectonic units of the Himalaya and the Ganga plain.*

The Ganga plain : The Ganga plain is an accumulation of detrital material from the HH and LH. It consists of alluvial plains with beds of clay, sand and gravel (Sarin et al., 1989; Singh, 1996; Galy and France-Lanord, 2001).

Some parts of these plain are abundant with the saline and alkaline soils and irregular calcareous concretions locally known as “kankar”. The saline soils contain sodium chloride and sulphate, where as the alkaline soils mainly have sodium carbonate and bicarbonate. The kankars are mainly made of calcium carbonates, though presence of magnesium carbonate could also be found (Rengarajan et al., 2009).

The peninsular region: The Son and the Tons, tributaries of the Ganga and the Chambal, Betwa and Ken, tributaries of Yamuna flow through the peninsular India. The major lithologies present in this area are Bundelkhand crystallines, the Vindhyan sediments consisting of carbonates, shales and sandstones and Deccan Basalts.

2.1.1.1 Tributaries

The Ganga river originates at the Gangotri glacier in Kumayun Himalaya at an elevation of 7010 m (Rao, 1979) and is known as Bhagirathi there. It takes the name Ganga after the confluence of Bhagirathi and Alaknanda at Devprayag (Krishnaswami, 1999, Sarin, 1989). The drainage basin of the Ganga river system covers approximately 10^6 Km^2, which consists of the Himalaya in the North, the Ganga plain and peninsular India in the South respectively. Downstream Rajmahal at Farakka, the Ganga bifurcates into the Bhagirathi and the Padma, the later traverses through Bangladesh and joins the Brahmaputra. In the present study, Manihari, which is a place near Rajmahal, has been considered as the outflow of the Ganga river system.

The Yamuna is the most important tributary of the Ganga and it rises from the Yamunotri glacier at an elevation of 6330 m. It leaves the hill near Tajewala and joins the mainstream Ganga at Allahabad from the South. It contributes to ~60% of the average annual flow at Varanasi, and 20% of the same at the outflow (Rao, 1979). The Chambal, Betwa and Ken are its major tributaries, which join in the plain. Among them, the Chambal comprises of 139,468 km^2 in the total of 366,223 km^2 drainage area of the Yamuna. The Chambal originates from the Vindhyan range and flows majorly through the Decan Traps. It contributes to almost 40% of the average annual water flow of the Yamuna and is 25% of the same of the Ganga main stream at Varanasi. The Kali Sindh, Rewa and Khari are tributaries of the Chambal. Along the courses of the Chambal and its tributaries, significant spread of saline alkaline soils has been reported (Rengarajan et al., 2009) and observed in present study.

The Gomti is another tributary of the Ganga which has large amount of saline alkaline soil patches throughout its drainage basin, which is endoreic in nature (Rai et al., 2010). It originates at an elevation of 200m only, from the south of the foothills of the Himalaya and joins the Ganga from the north near the Ghazipur, downstream Varanasi.

The Ghaghra originates in the Nepal Himalaya near Lake Mansarovar. It has a total catchment area of 127, 953 km^2 and contributes ~25% of total annual water budget of the Ganga at Patna. The Rapti is one the major tributaries of the Ghaghra. The Gandak originates in Tibet at an elevation 7620m and joins the Ganga near Patna. It has a drainage area of 46300 km^2 and ~15% of annual water budget of the mainstream near Patna is contributed by it.

The Kosi originates in the Himalaya by confluence of Sun Kosi, Arun Kosi and Tamur Kosi. It joins the Ganga near Kursela with a drainage area of 74500 km^2. This river is known for its destructive nature caused by lateral movement. All these three tributaries (Ghaghra, Gandak and Kosi) bear a strong Himalayan signature in their water chemistry and their drainage area do not contain noticeable saline alkaline soils.

Along with bif tributaries, many smaller tributaries draining mainly the different part of the Ganga Plain has been sampled in this study. The Kramanasha originates in the Kimur range at an elevation of 350m. It has a drainage area of 11,709 km^2 and it joins the mainstream near Chaunsa. The Son rises from the Amarkantak at an elevation of 600m. It joins the mainstream upstream Patna, near Koilwar. North Koel is a tributary of the Son with a drainage area of 10360 km^2. Both of them have their drainage area in Peninsular India. Punpun is a small tributary of the Ganga with a length of only 200 km and a drainage area of 8530 km^2. It originates from the Chhota Nagpur plateau and joins the mainstream near Patna. Batane is a tributary of the Punpun. The Kiul also originates from the Chhota Nagpur plateau and has drainage area of about 16,000 km^2. Harhar is a

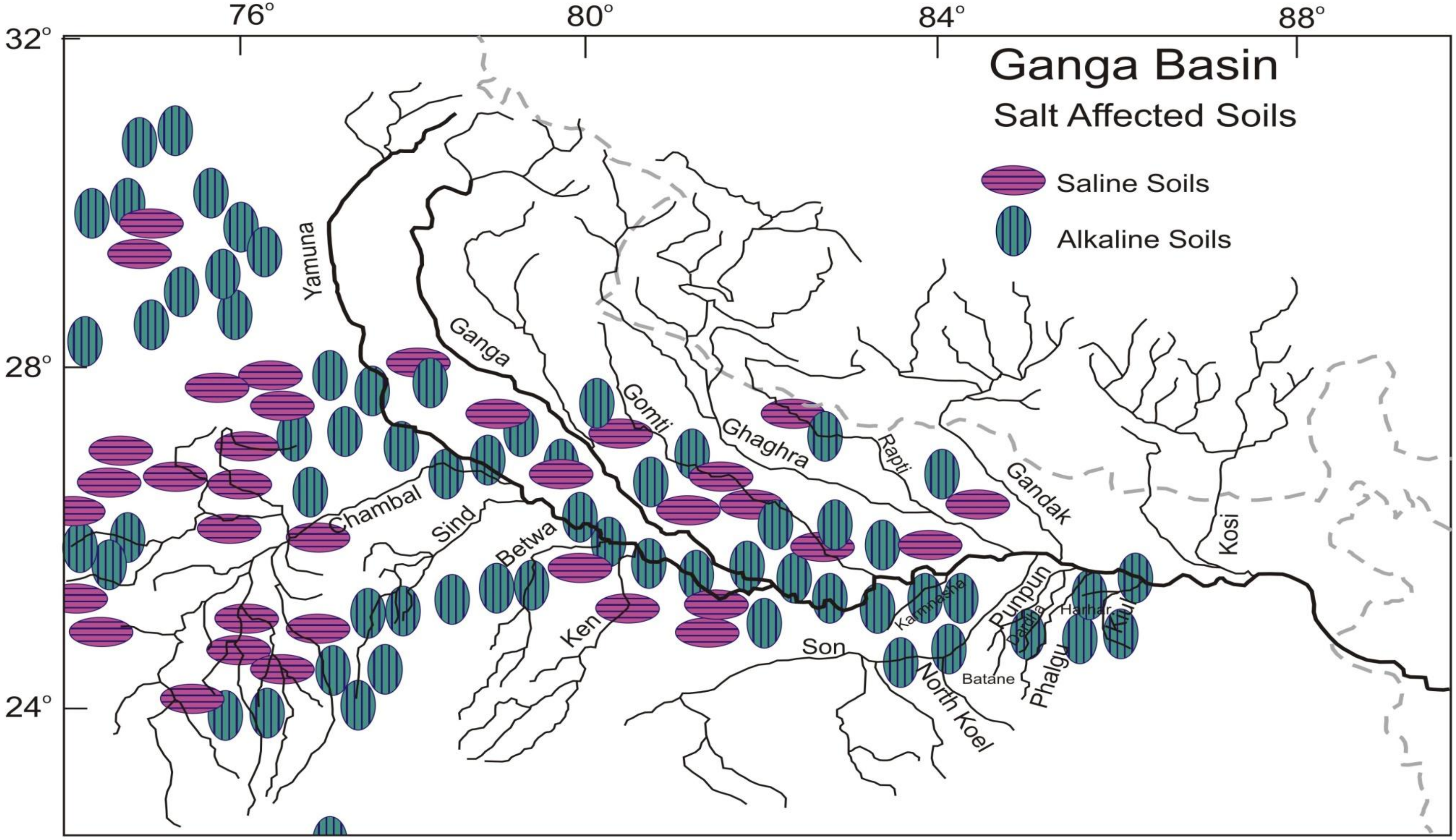

Fig. 2.2a: *Saline-alkaline soil infected regions in the Ganga plain (map redrawn from Soil regions maps by NAI and CSSSRI).*

tributary of the Kiul. The Phalgu and Dardha are two small tributaries of the Ganga. Both of them drain between the Punpun and the Kiul. All these tributaries join the mainstream from the south and are rain fed in nature. The erosion pattern of these small rivers could be interesting and would represent chemical weathering in the plain.

2.1.1.2 Saline alkaline soils in the Ganga basin

Saline-alkaline soils are mainly observed in arid and semiarid climate globally. Moreover endoreic basins with poor drainage are prone to be affected by these soils. Dissolved salts are transported to these basins or formed by weathering of minerals get concentrated due to high evaporation rate (Richards, 1954). The soluble salts accumulate in the basin in absence of adequate water to leach them out. Major exchangeable cations which are transported or weathered are Na, Ca and Mg, among them the last two tend to precipitate in concentrated soil solution in the form of $CaCO_3$ and $CaMg(CO_3)$. Therefore Na becomes the predominant cation on the soil exchanger phase. This is a main reason behind dispersion of soils, which causes low soil permeability and poor drainage (Sparks, 2003, Richards, 1995). In arid and semiarid climate, rate of evaporation can be much higher than that of humid climates. This increases the concentration of salts in soils and surface water. Further irrigation is one of the main reasons of soil salinity as the dissolved salts, supplied by the irrigation water such as canal, accumulate on the soils and make them saline/alkaline. In addition, shallow groundwater play a vital role in the formation process of saline-alkaline soils locally. The evaporation of river and flood waters, which accumulate in the micro-lows of the plains and evaporation of ground water through capillary action are responsible for the formation of saline-alkaline soils and kankars. The endoreic drainage basins are likely to accumulate river, flood and ground water, enriched in dissolved ions. These regions go through repeated cycles of wetting and drying and through these cycles the solutes from the waters precipitate during evaporation. Silica and carbonates (kankars) are prone to be deposited first; the various compounds of sodium are to be formed subsequently.

Fig. 2.2b: *Saline-alkaline soils in the Yamuna basin.*

Semi-arid climate is conducive for this formation process, and saline alkaline soils or reh, as it is called locally, are profusely present in the western part of the Ganga plain, namely the Gomti basin, the region between Yamuna and Ghaghra , in the Yamuna basin between Delhi and Allahabad, the Chambal basin (Rai et al, 2010). In the Ganga Plain, the Reh infested zone is extended from Hardoi, Shahjahanpur in the west to Sulatnpur, Pratapgarh through Lacknow, Unnao and Rae Bareli in the east (Kumar, 2005)(Fig. 2.2a). Widespread saline soils are reported in the alluvial plain covering parts of Champaran, Muzaffarpur, Darbhanga and Saharsa districts in Bihar state (Bhargava and Sharma, 1982).Typical field photograph of saline-alkaline soil is shown in Fig. 2.2b. The presence of saline-alkaline soil had been reported as early as 1871(Goldsmith and Hildyard, 1984). During that period this type of soils had been observed in Aligarh, Meerut, Kalinadi valley and also in the highly populated areas of the Ganga basin. From then onwards the extent of these soils had been increased due to excessive irrigation by canal and ground water. Srivastava et al., (1994) discussed the development of saline soils and calcretes during Holocene by dating calcretes. Pal et al., (2003) indicated the importance of micro topography in the formation process of alkaline soils. Available studies show that saline-alkaline soils in the plain contain a mineral called trona, a combination of highly dissolvable Na_2CO_3 and $NaHCO_3$ with some amount of sodium and calcium sulphate (Datta et al., 2002). These soils are likely to provide non-chloride sodium along with other ions to the river waters when leached with water.

2.1.2 Gujarat region

The groundwater samples were collected from the Ganga plain and some parts of Gujarat. The geology of the former is already discussed earlier (2.1.1). Though the state Gujarat has a wide variety strata ranging from the Archean gneiss complex to recent alluvial tracts, the groundwater samples were collected mainly from alluviam parts and Kutch region (marsh, salty waste land). Physically this state can be divided into three regions (Fig 2.3)

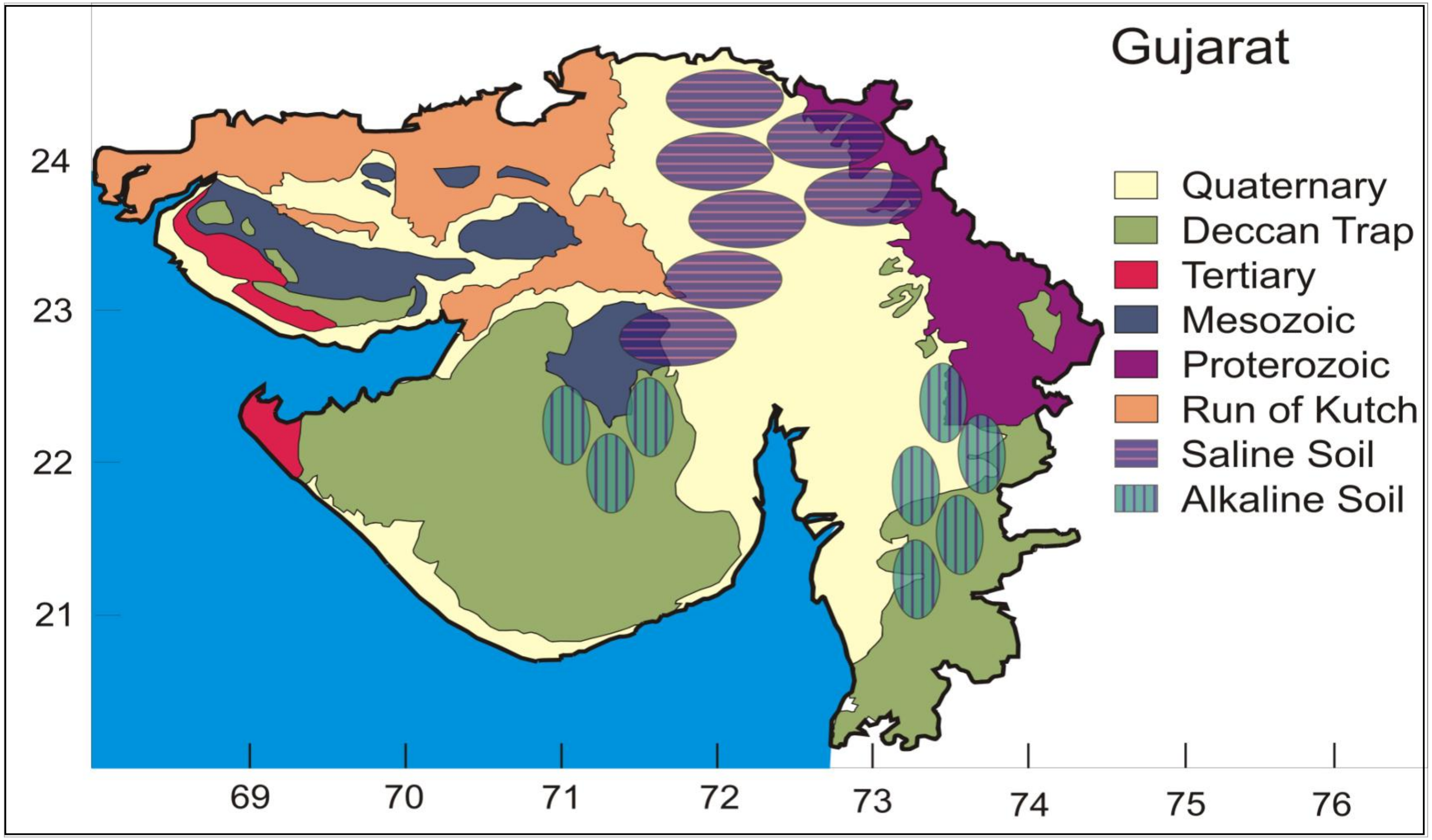

Fig 2.3: *Lithology of Gujarat with saline-alkaline soil infected regions. (based on CSSRI map)*

i) Alluvial lands stretching from Abu hills to river Daman Ganga. This alluvial plain merges into the Indian desert and the Rann of Kutch in the North and North-West.

ii) Semi arid tracts of Kutch, with a saline, sandy and barren plain originated from recession of the sea.

iii) The peninsular region in the western part of the state, i.e., Saurashtra high lands is occupied by the dark grey basalts from the Deccan traps.

Alluvium is the most recent geological formation and is ~700 m in thickness in the central part (Sukhija and Shah, 1976). Sand, silt, clay and grit are the main components of the alluvium. It was estimated that 1.2 mha of land in Gujarat and 0.7 mha in Rajasthan are affected by salts ((Bhumbla, 1978). Within alluvium, groundwater occurs in the water table conditions in the upper unconfined aquifer and under artesian pressure in lower confined aquifers. Unconfined aquifers lie within the first 50 meters and comprises of fine sand and silt. The confined aquifers extend between 50 to 150 meters, and from 300 to 700 meters. They comprise of coarse sand in the North-East and fine and medium sand in the South-West. The upper unconfined aquifers recharged by vertical infiltration followed by deep percolation. The confined aquifer seem to have its recharge area in the foot hills of the Aravalli (Agarwal et al., 2006).

Rainwater samples were collected at Ahmedabad, which is the sixth largest city in India, with a population of about 5 million. This city is located at the western part of India (23^{o}03'N, 72^{o}38'E), ~100 Km away from the coastal region of Arabian Sea. This region is dominated by aeolian sediments of quaternary age. Deccan volcanics/sediments cover a wide region in the south eastern and south western part of the site, where as Thar desert is ~500 Km away in north-west. Alluvium plain of the Ganga is present in north-east of Ahmedabad. The average annual rainfall in this region is 650-700 mm, more than 95% of which occurs within June to September, i.e. during the south-west monsoon. Rainfall in the north-western India displayed temporal variability over last 15 year. Samples for this study have been collected during the peak years of the SW monsoon, 2008, 2009 and 2011. The sampling site (23°02.18'N / 72°32.65'E) is located in a residential area with heavy traffic, though the immediate vicinity is vegetation covered.

2.2 Material

Basic objectives of this study are to characterize the chemical composition of the saline-alkaline soils present in the Ganga plain and impact of their dissolution on the dissolved chemical and isotope budget of the Ganga system and further to estimate the silicate erosion and associated CO_2 consumption in various sub-basins of the Ganga. To fulfil these objectives several samples of saline-alkaline soils present the Ganga basin and the water samples of the mainstream Ganga along with its tributaries were collected in three field campaigns, two during peak monsoon (August'08 and August'10) and another during pre-monsoon (February-March'09) in the Ganga Plain (Fig. 2.5). The details of sampling locations and data of few field based measurements are presented in Table 2.1-2.3. In addition, one water sample (GWGP-8, Table 2.2) from first order stream draining in the vicinity of saline-alkalinity soils and four surface waters (GPGW-12 to 15, Table 2.2) flowing over the saline-alkaline soil immediately after a rain event were also collected to evaluate the impact of dissolution of these soils on river chemistry.

Groundwater samples were collected from the Ganga plain and Gujarat during sampling in 2008, 2009 and 2010 (Table 2.5, Fig. 2.5). Rainwater samples were collected ~50m above the ground level using a large diameter PVC funnel manually, which was cleaned before collection. The sampler was opened after the starting of rainfall to prevent contamination from dry deposition. 10 samples were collected in 2008 from June to September, which provide information pertaining to the monthly variation in chemistry, 3 samples were collected in 2009 and 3 samples were collected in 2011.

All samples were filtered using 0.45 μm Millipore filter paper immediately after collection, and separated into two aliquots. One aliquot was kept unacidified and stored in pre-soaked (in Milli-Q water) PP bottle and the other one was acidified using concentrated HCl and stored in acid cleaned PP bottles.

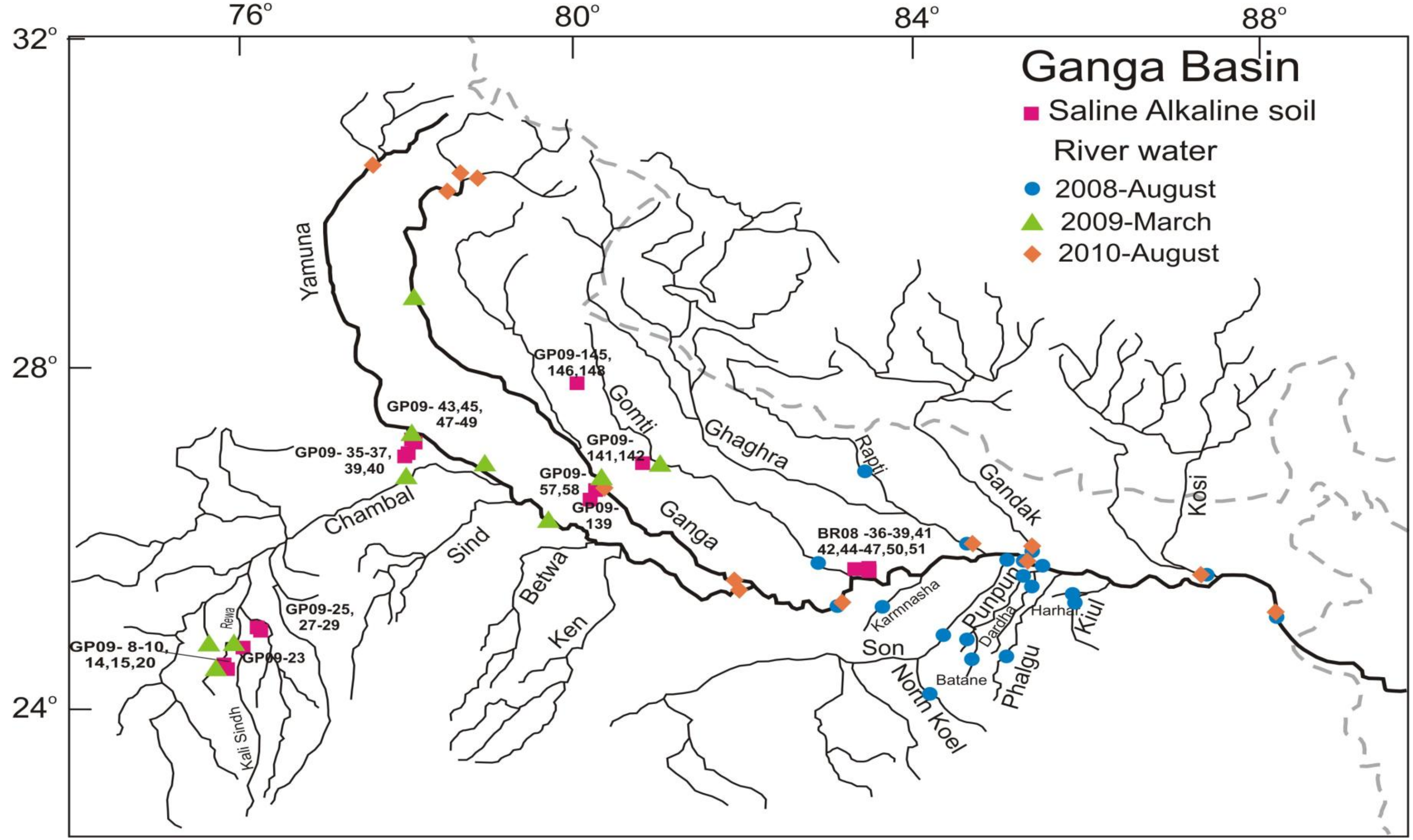

Fig. 2.4. Sampling locations in the Ganga river system.

Table 2.1: Sampling details of Saline-Alkaline Soils

Sample Code	Location	Date dd-mm-yy	Latitude N	Longitude E
BR0839	Hiranandpur	28-08-08	25°35'	83°15'
BR0842	Turna	28-08-08	25°35'	83°22'
BR0844	Turna	28-08-08	25°35'	83°22'
BR0845	Turna	28-08-08	25°35'	83°22'
BR0846	Turna	28-08-08	25°35'	83°22'
BR0847	Turna	28-08-08	25°35'	83°22'
BR0851	Turna	28-08-08	25°35'	83°21'
GP09-10	Neemthur	25-02-09	24°33'	75°49'
GP09-28	Kandauli	26-02-09	24°60'	76°16'
GP09-35	Dakhalipura	27-02-09	26°58'	77°56'
GP09-36	Dakhalipura	27-02-09	26°58'	77°56'
GP09-37	Dakhalipura	27-02-09	26°58'	77°56'
GP09-39	Birai village	27-02-09	26°59'	77°57'
GP09-40	Birai village	27-02-09	26°59'	77°57'
GP09-48	Agra, Pohia Ghat	28-02-09	27°15'	78°01'
GP09-57	Parial Town	03-02-09	26°39'	80°22'
GP09-58	Parial Town	03-02-09	26°39'	80°22'
GP09-139	Behind IIT Kanpur	03-03-09	26°31'	80°12'
GP09-141	Lucknow	04-03-09	26°54'	80°53'
GP09-142	Lucknow	04-03-09	26°54'	80°53'
GP09-145	Near Shahjahanpur	04-03-09	27°49'	80°03'
GP09-146	Near Shahjahanpur	04-03-09	27°49'	80°03'
GP09-148	Near Shahjahanpur	05-03-09	27°49'	80°03'

Table 2.2: Sampling details of streams flowing through Saline Alkaline Soil regions

Sample Code	Location	Latitude N	Longitude E	pH	Salinity	Conductivity (µS/cm)	Temp (°C)
GWGP-8	HIRANANDPUR	25°36'	83°15'	8.1	0.0	558	34.5
GWGP-12	TURNA	25°35'	83°22'	9.6	1.3	2760	33.7
GWGP-13	TURNA	25°35'	83°22'	9.4	0.4	1236	36.2
GWGP-14	TURNA	25°35'	83°22'	9.0	0.4	1170	31.7
GWGP-15	TURNA	25°35'	83°22'	9.1	0.3	1058	34.7

Table 2.3: Sampling details of the Ganga river and tributaries

Sample code	River	Place	Latitude N	Longitude E	Date dd-mm-yy	pH	Conductivity (µS/cm)	Temp. (°C)
Headwaters								
BR10-1	Yamuna	Rampur Mandi	30°27'	77°40'	18-08-10	7.7	137	22
BR10-4	Bhagirathi	Devprayag	30°09'	78°36'	19-08-10	7.2	90	18
BR10-7	Alaknanda	Devprayag	30°08'	78°37'	19-08-10	8.0	24	18
BR10-12	Ganga	Kaudiyala	30°05'	78°30'	19-08-10	8.0	106	19
Ganga Mainstream								
BR10-14	Ganga	Kanpur	26°29'	80°22'		7.4	216	29
GP09-167	Ganga	Garhmukteshwar	28°46'	78°09'	22-08-10	8.1	219	23
GP09-135	Ganga	Kanpur	26°37'	80°17'	03-03-09	8.5	461	24
BR8109	Ganga	Patna	25°37'	85°09'	17-08-08	7.5	198	30
BR8129	Ganga	Varanasi	25°19'	83°01'	21-08-08	7.6	220	29
BR8136	Ganga	Fatuha	25°33'	85°17'	22-08-08	7.6	203	30
BR08-11	Ganga	Manihari	25°20'	87°37'	25-08-08	7.5	190	31
BR10-18	Ganga	Allahabad	25°31'	81°52'	23-08-10	7.4	216	31
BR10-24	Ganga	Varanasi			24-08-10	7.6	225	29
BR10-29	Ganga	Patna	25°37'	85°11'	25-08-10	7.5	204	29
BR10-35	Ganga	Manihari	25°20'	87°37'	26-08-10	7.5	176	28
Yamuna Mainstream								
BR10-22	Yamuna	Allahabad	25°25'	81°50'	23-08-10	7.7	277	30
GP09-50	Yamuna	Pohia Ghat, Agra	27°15'	78°01'	28-02-09	8.1	1354	22
GP09-52	Yamuna	Etawah	26°45'	78°59'	28-02-09	9.0	1442	23
Himalayan Tributaries								
BR8105	Gandak	Hajipur	25°41'	85°12'	17-08-08	7.6	184	27
BR8110	Ghaghra	Revelganj	25°48'	84°38'	18-08-08	7.6	200	29
BR8121	Rapti	Gorakhpur	26°44'	83°21'	19-08-08	7.7	233	28
BR08-9	Kosi	Kursela	25°25'	87°14'	25-08-08	7.4	154	31
BR8124	Ghaghra	Dohrighat			20-08-08	7.6	200	27
BR10-26	Gandak	Sonpur (near Patna)	25°41'	85°11'	25-08-10	7.6	194	26
BR10-32	Kosi	Kursela	25°25'	87°13'	26-08-10	7.6	135	28
BR10-44	Ghaghra	Revelganj	25°47'	84°38'	27-08-10	7.4	191	29
Plain Tributaries								
BR8140	Son	Koilwar	25°34'	84°48'	23-08-08	7.4	124	32
BR08-1	Punpun	Gourichak	25°29'	85°11'	24-08-08	7.4	235	32
BR08-3	Dardha	Dhanarua	25°24'	85°10'	24-08-08	7.5	224	33
BR08-5	Harhar	Lakhisarai	25°13'	86°04'	24-08-08	7.8	180	32
BR08-7	Kiul	Lakhisarai	25°11'	86°07'	24-08-08	8.3	219	34
BR08-18	Phalgu	Gaya	24°46'	85°01'	26-08-08	8.1	242	34
BR08-20	Batane	Gheura	54°40'	84°17'	27-08-08	8.3	318	34
BR08-22	North Koel	Garikhas	24°08'	84°03'	27-08-08	8.3	294	35
BR08-24	Punpun	Aurangabad	24°50'	84°16'	27-08-08	7.6	346	31
BR08-27	Son	Dehri	24°54'	84°11'	28-08-08	7.6	175	31
BR08-34	Karmnasha	Naubatpur	25°15'	83°25'	28-08-08	7.3	161	32
BR8125	Gomti	Ghazipur	25°35'	82°60'	20-08-08	7.5	246	29
GP09-143	Gomti	Lucknow	26°54'	80°52'	04-03-09	8.1	460	24

(Continued.)

Table 2.3: Sampling details of the Ganga river and tributaries (continued)

Sample code	River	Place	Latitude N	Longitude E	Date dd-mm-yy	pH	Conductivity (μS/cm)	Temp. (°C)
Deccan rivers								
GP09-3	Rewa	Bhanpura	24°32'	75°44'	24-02-09	8.4	5570	22
GP09-21	Chambal	Gandhi Sagar Dam	24°42'	75°36'	25-02-09	8.2	348	23
GP09-24	Kali Sindh		24°55'	76°12'	26-02-09	8.0	346	27
GP09-30	Chambal	Dhaulpur	26°39'	77°54'	27-02-09	8.2	8920	22
GP09-41	Khari	Near Dhaulpur			27-02-09	8.6	913	21

Table 2.4: Sampling locations of coastal stations

Sample code	Station	Maximum depth (m)	Latitude N	Longitude E	Date dd-mm-yy	Sample depth (m)	Salinity	pH
0814-4	0814	53	20°32'	87°29'	27-11-2008	4	30.102	8.4
0814-45	0814	53	20°32'	87°29'	27-11-2008	45	32.146	8.4
0815-4	0815	40	20°59'	87°47'	27-11-2008	4	29.589	8.4
0815-30	0815	40	20°59'	87°47'	27-11-2008	30	31.051	8.4
0816-4	0816	53	20°54'	88°06'	27-11-2008	4	24.592	8.5
0816-30	0816	53	20°54'	88°06'	27-11-2008	30	31.042	8.4
0817-5	0817	79	20°50	88°30'	27-11-2008	5	30.455	8.4
0817-70	0817	79	20°50	88°30'	27-11-2008	70	33.996	8.2
0818-5	0818	71	21°00'	88°60'	27-11-2008	5	28.669	8.4
0818-60	0818	71	21°00'	88°60'	27-11-2008	60	34.029	8.2
0819-5	0819	140	20°35'	88°45'	28-11-2008	5	34.808	8.4
0819-110	0819	140	20°35'	88°45'	28-11-2008	110	31.877	8.0
0820-5	0820	114	20°35'	88°15'	28-11-2008	5	32.196	8.4
0820-110	0820	114	20°35'	88°15'	28-11-2008	110	34.779	8.0

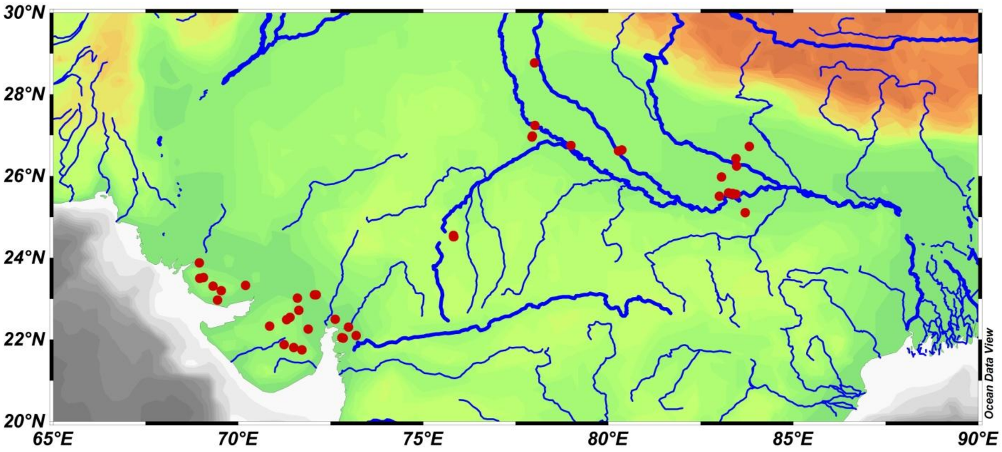

Fig 2.5: *Groundwater sampling locations.*

Table 2.5: Sampling locations and field data of groundwater

Sample Code	PLACE	Latitude N	Longitude E	Ph	Conductivity (μS/cm)	Temp (°C)	Depth (ft)
Gujarat							
GW08-1	Kundera	--	--	7.96	1761	28.5	120
GW08-2	Mamangaon	22.10	73.19	6.99	2490	30.1	280
GW08-4	Mangrun	22.04	72.84	7.34	1613	27.9	60
GW08-6	Jambusar	22.05	72.80	6.84	3790	30.9	80
GW08-7	Dilpar	22.31	72.98	7.18	991	31.1	200
GW08-8	Ishwarwada	22.50	72.62	7.44	5470	28.0	25
GW08-9	Ghatula	21.75	71.72	7.29	980	31.4	200
GW08-10	--	21.81	71.50	7.35	1348	30.3	80
GW08-11	Kherawad	21.88	71.24	7.77	365	31.6	300
GW08-12	Rajkot	22.33	70.85	6.93	1670	31.8	400
GW08-13	Sarpar	22.49	71.31	6.88	2840	30.6	300
GW08-14	Bharuka	22.55	71.40	7.67	5570	30.2	50
GW08-15	Surendranagar	22.72	71.64	6.98	2610	30.5	50
GW08-16	Olak	22.26	71.89	7.14	2810	28.6	30
GW08-17	Sakli	23.10	72.11	7.90	2220	35.4	700
Kutch							
GK08-1	Viramgam	23.10	72.06	7.60	3160	33.8	350
GK08-2	Kasiawah	23.02	71.60	6.81	8100	32.6	300
GK08-3	Buddharmoma	23.50	68.96	6.83	1563	32.8	650
GK08-4	Revapur	23.52	69.06	7.10	1691	30.8	100
GK08-27	Matanomadh	23.88	68.95	7.19	6950	33.3	--
GK08-29	Devpar	23.31	69.32	6.56	2240	29.9	--
GK08-30	Manukuwan	23.20	69.54	6.86	4270	28.3	280
GK08-33	Nana Asampiya	22.97	69.44	7.04	1807	28.9	55
GK08-35	Morgar	23.33	70.20	6.80	1723	32.1	400
GK08-36	Morgar	23.33	70.20	6.76	3360	29.5	450
Ganga Plain							
GWGP-1	Kushinagar	26.73	83.81	7.18	492	26.5	100
GWGP-2	Ghagha	26.43	83.45	7.15	657	26.4	120
GWGP-3	Mahula	26.25	83.47	7.58	148	30.9	0
GWGP-4	--	25.98	83.06	7.10	2830	27.3	140
GWGP-5	--	25.98	83.06	7.21	656	26.1	25
GWGP-6	Tisaura	25.51	83.00	7.03	828	26.9	150
GWGP-7	Pusauli	25.11	83.70	7.00	745	27.6	60
GWGP-9	Hiranandpur	25.59	83.25	7.14	788	27.5	120
GWGP-10	Hiranandpur	25.59	83.25	7.08	697	26.4	35
GWGP-11	Kusumhikala	25.56	83.45	6.91	1086	27.1	60
GWGP-16	Turna	25.58	83.36	7.3	1503	26.7	50
GWGP-17	Mahmudpur	25.56	83.36	7.11	834	27.3	30
GP09-44	Pohia Ghat, Agra	27.24	78.02	7.42	15730	25.3	--
GP09-54	Etawah	26.75	78.99	7.32	2050	27.8	--
GP09-59	Parial Town	26.64	80.37	6.97	856	26.8	--
GP09-134	Bithur, Kanpur	26.62	80.28	7.06	479	26.6	--
GP09-169	Garhmukteshwar	28.77	78.01	6.94	854	24.9	--
Chambal Basin							
GP09-4	Neemthur	24.55	75.82	8.57	877	20.3	--
GP09-12	Neemthur	24.54	75.82	7.32	5270	28.8	--
GP09-17	Bhagwanpura	24.52	75.82	7.65	18670	22.8	--
GP09-18	Usarna	24.52	75.83	8.26	8450	21.5	--
GP09-34	Dakhalipura	26.96	77.94	7.21	2050	25.7	--
GP09-38	Birai village	26.98	77.95	7.51	4610	27.1	--

For dissolved Nd measurement, river water samples were collected during monsoon sampling, (August'08) and (August'10) in the Ganga Plain and headwaters. Seawater samples from coastal region of Bay of Bengal were collected in November, 2008 at cruise SS-259. This expedition was onboard FORV Sagar Sampada of the Ministry of Earth Sciences (MoES), Govt. of India.

The details of collected samples are given in Table. 2.4. Two samples were collected from each station, one surface (4-5 m), another deep. Twelve liter Niskin bottles on 12 position CTD rosette array was used for sampling. Conductivity, temperature and depth were measure using Seabird CTD. These samples were filtered using 0.45 micron milipore cellulose filter within few hours of collection. pH of the samples was measured using a pH-meter (Radiometer, PHM 84) onboard with precision better than 0.02 unit based on repeat measurements. REE were extracted from 10-20 L samples using C-18 cartridges/ Fe precipitation onboard. One liter of filtered sample was stored in pre-cleaned (soaked in 2N HCl and cleaned with milli-Q, and filtered sample respectively) poly-propylene bottles and acidified to pH 2 using ultra-pure quartz distilled HCl.

2.3 Methodology

Some of the measurements such as temperature, pH and electrical conductivity in the water samples were measured in the field immediately after collection. Other parameters in water and soils were measured in the laboratory and a brief description of the same is given in the following section.

2.3.1. Water sample

Temperature, pH and electrical conductivity (EC): Temperature, pH and electrical conductivity (EC) were measured in all water samples using temperature, pH and EC probes (Multiline 7000) with precision ~1%. Alkalinity is measured by acid titration method with an auto titrator (Metrohm 702 SM Titrino) using dilute HCl acid in non-filtered samples with precision better than 5%.

Major ion: Major ion (Na, NH_4, K, Ca, Mg, Cl, F, NO_3, SO_4) concentrations are measured with an ion chromatograph (Dionex 500) using CS-12A, CG-12A columns for cation separation with methano sulfonic acid as eluent and AS-14, AG-14 columns for anion separation with Na_2CO_3/$NaHCO_3$ solution as eluent. The precision of these measurements are better than 5% (Rai et al., 2010)(Fig. 2.6). Dissolved Si is measured in the samples by Molybdenum blue method in a spectrophotometer (Beckman 26) using 810 nm wavelength with precision better than 10% (Rai et al., 2010).

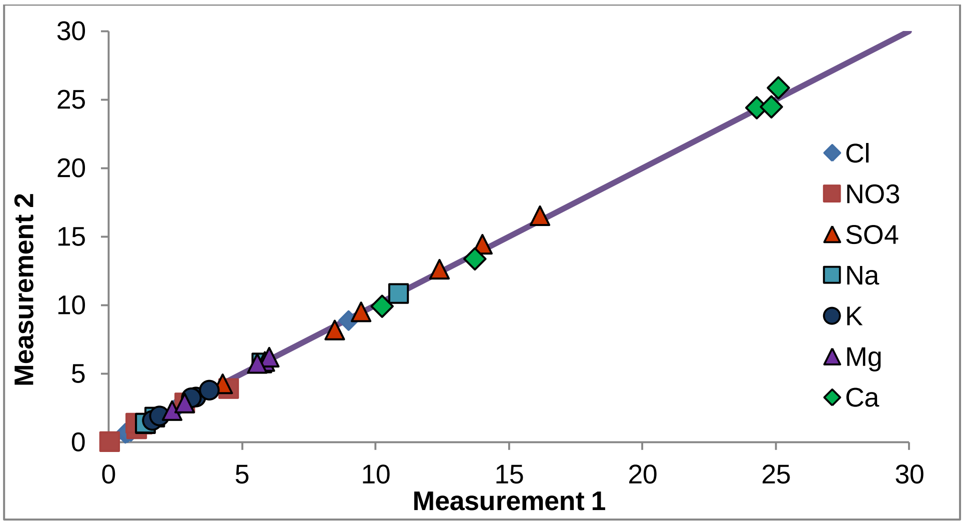

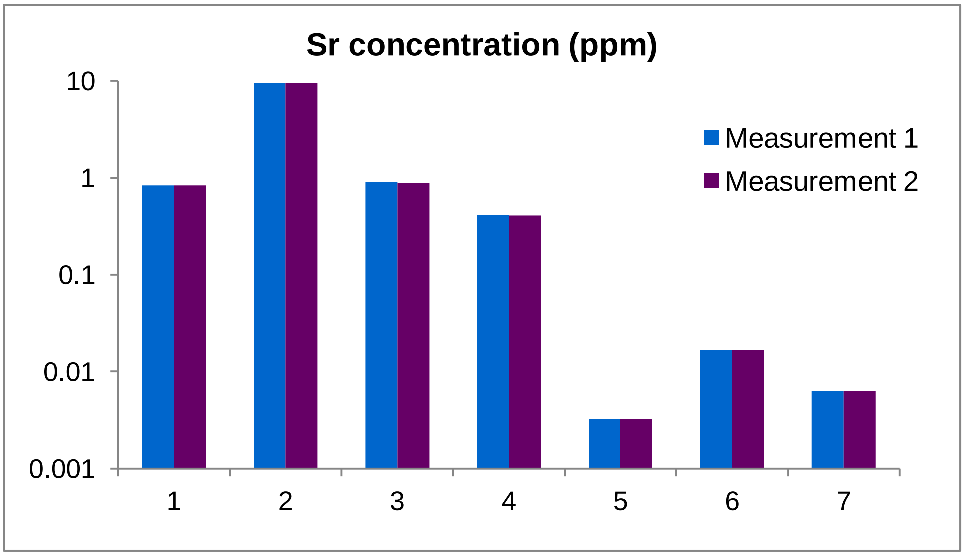

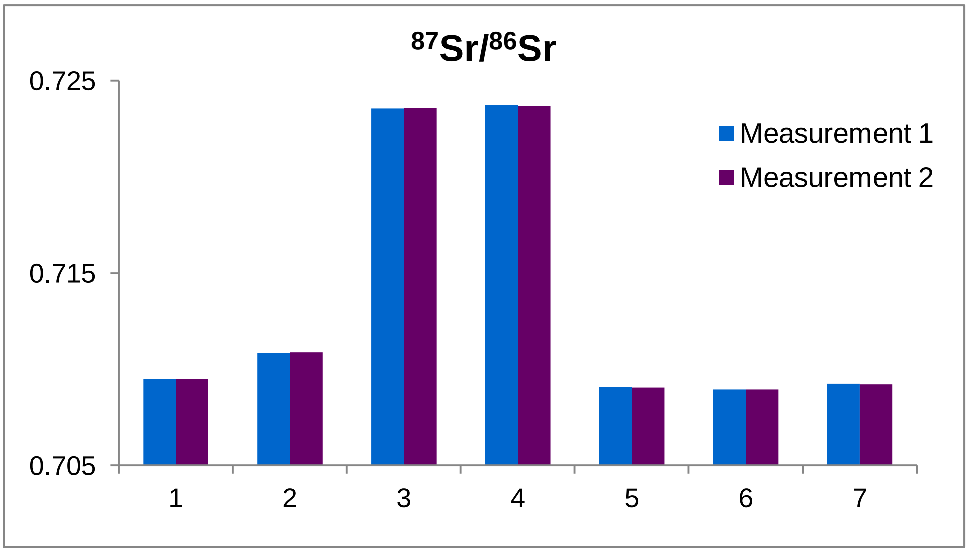

Fig. 2.6: Results of repeat measurements of major ions, Sr concentration and Sr isotopic composition.

Sr concentration and $^{87}Sr/^{86}Sr$: For Sr measurement, isotope dilution technique is used to get concentration and isotopic composition from the same aliquot. Suitable amount of filtered and acidified sample (45-50 ml for river water) is spiked using ^{84}Sr tracer and then dried in a clean laboratory. The residue is taken in 3M HNO_3 and loaded on Eichrom Sr specific resin (pre conditioned with 3M HNO_3). Pure Sr is collected after addition of milli-Q water as eluent to the column. This Sr fraction is then dried and dissolved in 2 ml HCl and loaded on degassed and oxidized Re filaments. The measurement of isotopes was carried out using a thermal ionization mass spectrometer (Isoprobe-T) in static multi collection mode. Instrumental mass fractionation was corrected using an exponential law with 0.1194 for $^{86}Sr/^{88}Sr$. The Rb contribution was corrected by the natural abundance of $^{85}Rb/^{87}Rb$, though the amount of ^{85}Rb was negligible in all samples. SRM987 standard was run with every set of samples which yielded $^{87}Sr/^{86}Sr$ ratio of 0.710217±0.000018 (1 σ, n=9). The procedural blank for Sr during river water measurement was less than 1 ng and the total Sr analyzed for the samples were always 3-4 orders of magnitude higher than the blank. In case of saline alkaline soil water extracts, milli-Q blank were around 5-6 ng, and total Sr analyzed in those samples were 2-3 orders of magnitude higher compared to the blank.

2.3.2 Dissolved Nd concentration and its isotope composition

For Nd isotope measurement, river water samples in 2008 and coastal samples (~10 ℓ of sample) is filtered and made to pH 2. This is then passed through HDEHP (REE complexant) loaded C18 cartridge, which retains all rare earth elements (REEs). The cartridge is then eluted with 50 ml 6 N HCl to collect Nd along with other REEs (Jeandel et al., 1998, Shabani et al., 1992). In river water samples from 2010, REEs were pre-concentrated by Fe co-precipitation method (Amakawa et al., 2000). The precipitated Fe is then dissolved and collected in 6N HCl. The extracted REEs from both methods were stored in acid cleaned LDPE bottles until analysis.

Nd is extracted from the pre-concentrated samples using two consecutive ion exchange chromatographies (Singh et al., 2012). The pure Nd fraction is then dried and isotopic ratio is measured in Thermal Ionisation Mass Spectrometer in static multi collector mode. Mass fractionation was corrected by normalizing ^{146}Nd/^{144}Nd ratio to 0.7219.

2.3.2.1 Sm and Nd concentration measurement

Nd concentration was determined by isotope dilution technique using Q–ICPMS using a suitable Nd tracer of known concentration (Singh et al., 2012). The concentration of Sm was determined by external calibration technique and using the total chemical extraction efficiency similar to that of Nd which was estimated based on Nd concentration determined using spike and standard calibration method.

To determine Sm and Nd concentration in water samples, precisely weighed aliquots (~500 g) of the filtered and acidified samples were spiked with known amount of ^{150}Nd tracer. After 24 hours of sample and spike equilibration, the REEs were pre-concentrated from these samples using Fe co-precipitation and purified by cation exchange separation (Tachikawa et al., 1999; Amakawa et al., 2000) on resin AG 50W–X8 (200–400 mesh). These extracts were further analyzed on Q–ICPMS for the intensities of REEs at masses 144, 146, 147, 150. Nd concentrations were calculated from the ratio of intensity at mass 150 to that at 144 after the Sm correction estimated from intensity at mass 147. Nd extraction efficiency is estimated by ratio of this true concentration as determined by isotope dilution technique to Nd concentration estimated by external calibration at mass 146. Sm concentration estimated by external calibration was corrected for this extraction efficiency. Measured blanks for Sm and Nd were less than 12 pg and 70 pg respectively.

2.3.2.2 Determination of Nd isotopic composition

Nd from the pre-concentrated REEs extracts was separated following the protocol used in our laboratory (Goswami, 2012) using column chromatography. The REE extracts were dried and dissolved in 2N HCl, which were passed through 16.5 cm long columns of AG 50W-X8 resin (200-400 mesh). The REEs were eluted using 6N HCl from the columns. This REE fraction was passed through a pre-calibrated Lanthanide specific resin column (LN-C50-B, Eichrome).

Table 2.6: Repeat measurements of Nd isotopic composition.

Sample ID	River	Place	Year	ε_{Nd}	σ_{μ}
BR8129	Ganga	Varanasi	2008	-11.5	0.2
				-11.5	0.2
BR08-11	Ganga	Manihari	2008	-13.8	0.3
				-13.8	0.2
				-14.2	0.3
				-14.2	0.4
BR10-1	Yamuna	Rampur Mandi	2010	-18.1	0.1
				-18.1	0.1

Nd isotopic composition in the river water samples from 2008, were measured in TIMS (Isoprobe-T). Towards this, the purified Nd was loaded on a triple filament (Ta-Re-Ta) assembly. Nd was loaded on one of the side filaments. The filaments were heated in vacuum before loading the Nd fraction. The analysis was done in static multi collection mode. Mass fractionation corrections were made by normalizing ^{146}Nd/^{144}Nd ratios to 0.7219. JNdi-1 standard was measured several times and gave an average value of 0.512108±0.00011 (1σ, n=14) for ^{143}Nd/^{144}Nd.

Nd isotope composition in river water samples from 2010 and coastal sea waters were measured in MC–ICPMS (Neptune) using a PFA100 nebulizer with an *APEX* introduction system as Nd^{+} in static multi-collection mode by measuring the intensities at masses 143, 144 and 146 for 40 cycles. Sm correction, if any, was done by measuring the intensity at mass 147. Amplifiers connected to Faraday cups were rotated after every 10 cycles to eliminate amplifier efficiency variations. The signal intensity of Nd at mass 144 in the samples depended on their Nd concentration, and typical values were in the range 0.2–0.6 V. Instrumental mass bias was corrected using an exponential law relative to ^{146}Nd/^{144}Nd ratio of 0.7219. JMC321 standard was run during the period of analysis. The measured average ^{143}Nd/^{144}Nd of JMC321 was 0.511029 ± 0.000012 (σ, n = 4) against the reported value of 0.511123 ± 0.000012 (Barrat and Nesbitt, 1996). The measured ^{143}Nd/^{144}Nd of JMC321 was lower compared to its reported value and hence the ^{143}Nd/^{144}Nd in samples was corrected by normalization to the reported ^{143}Nd/^{144}Nd of JMC321. The results of repeat measurements in different aliquots from the same place are given in Table 2.6.

2.3.2 Saline-Alkaline soil

Since the aim of this study is chemical characterization of the saline – alkaline soils present in Ganga basin and to determine the impact of dissolution of these soils on river water chemistry, concentration of major ions and Sr and isotope composition of Sr were measured in water leachable fraction from Saline-alkaline soils by treating them with milli-Q water. About 0.5 gm of soil with 50 ml of milli-Q water is ultra-sonicated at 60°C for 30 minutes. The solution is then centrifuged and the clear solution was collected from the top. Major ions and Sr were measured in this solution in the same way as river waters, discussed earlier.

Chapter 3

Chemical and isotopic characterization of saline - alkaline soils and its impact on river water chemistry

3.1 Introduction

The main sources of CO_2 to the atmosphere over a million year time scale are volcanic output from earth's interior (Raymo and Ruddiman, 1992) and metamorphism of carbonate rocks to silicate rocks (Berner, 2003); whereas the main sinks are chemical weathering of continental silicate rocks (Gaillardet et al., 1999), burial of organic carbon at the time of sediment deposition (France-lanord and Derry, 1997) and chemical weathering of the oceanic crust (Dessert et al., 2001). Silicate weathering is suggested to be the key factor behind the Cenozoic global cooling and hence the uplift of the Himalaya has played an important role in climate change by increasing the silicate weathering since then (Raymo and Ruddiman, 1992). The Ganga-Brahmaputra, a major river system draining the Himalaya, contributes ~3% of total dissolved material to the ocean supplied by rivers at present, higher compared to their fraction of drainage area (Sarin et al., 1989). A number of studies have been carried out in this river basin to estimate the contemporary silicate erosion and CO_2 consumption rates in this region (Rai et al., 2010 and references there in). In general, Na corrected for cyclic salts, Na* (=Na_r-Cl_r) has been used as a proxy of silicate weathering and to determine the silicate erosion rates. The mass balance equation for dissolved Na in rivers is

$Na_r = Na_a + Na_e + Na_s$ ………………………………………… (1)

where the subscripts r, a, e, s denote river, atmospheric, evaporites and silicates respectively (Krishnaswami et al., 1999). The silicate derived Na in the river basin is estimated by

$Na^* = Na_r – Cl_r$………………………………………………… (2)

where Cl_r is the chloride concentration in the river. It has been assumed in all the studies that atmospheric and evaporitic Na will be associated with equal moles of Cl, this makes Na_s=Na*.

Validity of this assumption depends on the type of evaporites present in the basin. Presence of large amount of alkaline-saline soils in the Ganga Plain challenges this assumption as these soils can supply large amount of dissolved material including Na to the river in non-chloride form. If found true, all the earlier estimates of silicate erosion rates and related CO_2 consumption in the Ganga Plain, where such soils are abundant, would be overestimate. The presence of these soils in the Ganga plain, were known since long (Sarin et al., 1989), however, their impact on the river chemistry has not been assessed yet.

Available studies show that alkaline and saline soils in the plain contain a mineral called trona (Datta et al., 2002), a combination of highly dissolvable Na_2CO_3 and $NaHCO_3$ with some amount of sodium and calcium sulphate. The dissolution of these soils can provide Na to the rivers without Cl and hence Cl correction will not be valid to estimate Na_s through Na* (eqn. 2). Therefore, it will lead to over-estimation of silicate weathering rate and associated CO_2 consumption. Their widespread presence in the plain and very high concentration of Na in the tributaries flowing exclusively through plain indicate towards their potential contribution of Na to the dissolved budget of the Ganga. In the present study, saline and alkaline soils are characterized geochemically and isotopically. Further, the role of these soils in contributing to the river geochemical and isotopic budget has been assessed using inverse model (Negrel et al., 1993; Millot et al., 2003; Tripathy and Singh, 2010). Silicate erosion rate and CO_2 consumption in different sub-basins of the Ganga river system have been re-estimated considering the contribution of saline-alkaline soils.

This study, therefore, attempts to (i) chemically and isotopically characterize the alkaline-saline soils of the Ganga plain, (ii) assess the contribution of saline-alkaline soils to the river water geochemistry as well as its significance in estimating the silicate weathering rate and hence CO_2 consumption, and (iii) compare the chemical erosion rates over the Ganga Plain and the Himalaya, and the factors influencing it.

3.2 Results and Discussion

Major ion, Sr concentration and its isotope composition in the leachable fraction of saline-alkaline soils are given in Table 3.1. The data for surface water flowing over saline-alkaline soils are in Table 3.2 whereas those of water samples of mainstream and tributaries are presented in Table 3.3.

Table 3.1: Chemical and Sr isotopic data of saline-alkaline soils

Sample code	Na µg/g	K µg/g	Mg µg/g	Ca µg/g	F µg/g	Cl µg/g	NO_3 µg/g	HCO_3 µg/g	SO_4 µg/g	SiO_2 µg/g	SAR	Sr ng/g	$^{87}Sr/^{86}Sr$
BR08-39	6131	50	40	443	25	130	93	17139	71	8442	279	1502	0.72343
BR08-42	11328	69	99	328	84	1267	149	28441	2595	7268	548	4062	0.72184
BR08-44	16842	98	97	360	104	2106	159	37873	4897	6323	788	941	0.72183
BR08-45	7281	22	52	205	54	641	394	18974	1984	2105	454	2438	0.72175
BR08-46	3905	33	13	140	7	267	559	8753	884	1418	316	935	0.72129
BR08-47	10031	31	55	245	18	819	284	26467	2571	4367	579	3857	0.72178
BR08-51	2062	83	50	691	12	91	298	7340	63	2184	76	3561	0.72118
GP09-10	2295	167	307	1470	19	451	85	9732	134	6927	54	12315	0.71320
GP09-28	3663	84	100	778	29	3691	107	11535	1203	b.d.	124	12084	0.70992
GP09-35	2770	231	201	1698	26	3162	1171	9285	4536	3695	64	9182	0.71727
GP09-36	6282	283	167	1272	27	1985	381	8957	8610	5493	166	4090	0.71664
GP09-37	13936	58	79	596	103	5207	3154	10913	12842	7525	536	2116	0.71665
GP09-39	6446	211	231	1056	47	4214	4755	3656	9300	2104	180	21896	0.71375
GP09-40	3584	142	1233	1331	14	5724	98	1329	6271	708	71	32337	0.71428
GP09-48	19957	127	439	1126	100	8514	b.d.	11892	26413	143	504	6197	0.71828
GP09-57	15449	155	87	716	4	3586	2607	6924	19774	7996	545	2129	0.72529
GP09-58	25125	98	85	751	38	4975	1537	22232	26121	10271	869	826	0.72792
GP09-139	27560	102	77	160	14	1954	62	17090	42671	5586	1790	1487	0.72017
GP09-141	31587	99	107	135	b.d.	995	1065	16768	1351	3554	2032	1719	0.72959
GP09-142	14207	90	143	712	b.d.	2094	715	17503	12457	3327	486	739	0.72924
GP09-145	14625	48	70	141	17	183	623	39258	2756	b.d.	1006	1273	0.72517
GP09-146	2688	91	148	471	38	b.d.	b.d.	10446	182	9855	108	1122	0.72448
GP09-148	3786	27	56	147	71	132	532	13884	182	1598	266	751	0.72563

b.d. - below detection limit

Table 3.2: Chemical and Sr isotopic data of streams flowing through saline-alkaline soil regions

Sample code	Na µM	K µM	Mg µM	Ca µM	F µM	Cl µM	NO_3 µM	SO_4 µM	HCO_3 µM	Si µM	TDS mg/l	Sr nM	$^{87}Sr/^{86}Sr$
GWGP-8	2838	22	1000	603	57.1	410	41.7	143	5484	134	484	2754	0.72380
GWGP-12	32297	81	43	89	156	2388	b.d.	977	26291	214	2542	893	0.72128
GWGP-13	12886	39	61	138	78	899	b.d.	545	10623	85	1041	1047	0.72128
GWGP-14	12401	36	6	19	101	697	b.d.	347	10858	125	1013	1017	0.72129
GWGP-15	11148	110	57	63	46	962	b.d.	488	9426	75	924	1211	0.72125

b.d. - below detection limit

3.2.1 Chemical Characterization of Saline-Alkaline soils

Basic objective of this study is to assess the impact of dissolution of saline-alkaline soil on the river chemistry. These soils were chemically and isotopically characterised by analysing their water leachates. The water leachates of 23 such soil samples were analyzed for their major ion (Na^+, K^+, Ca^{2+}, Mg^{2+}, Cl^-, F^-, NO_3^-, $SO_4^{2-}$and HCO_3^-) and Sr concentrations, and its isotope compositions (Table 3.1).

Na dominates the cation budget (2062 – 31587 μg/g) in these soils, which constitute up to ~3.2% of the soil in the highest case. Na constitutes up to 99% of the leachable cation fraction of these soils. Ca is the second major cation (135 – 1698 μg/g), whereas K (22 – 283 μg/g) is not significant in these samples. Mg (13 – 1233 μg/g) is less abundant compared to Ca in all samples. Bicarbonate (1329 – 39258 μg/g) is the dominant anion in most of the soils. In some samples, sulphate (63 – 42671 μg/g) concentration is also high. Chloride (91 – 8514 μg/g) and nitrate (62 – 4755 μg/g) concentrations are one to two order of magnitude lower than bicarbonate in almost all samples. Some of these soils have exceptionally high NO_3 (as high as 4755 μg/g, Table 3.1). Si concentration in these samples ranges from 143 to 10271 μg/g. There is very little difference in the major ion compositions of the saline-alkaline soils of the different sub-basins of the Ganga. However, saline-alkaline soils of the Chambal sub-basins draining the Deccan basalts have, in general, higher concentration of Sr and lower $^{87}Sr/^{86}Sr$ compared to rest of the sub-basins. Sr concentration of these soils in the Chambal basin varies from 4090 to 32337 ng/g, with marginally lower Sr isotope composition (0.70992-0.71727). The saline-alkaline soils from the sub-basins of the Ganga other than Chambal contain lower Sr content (739 – 6197 ng/g) with radiogenic $^{87}Sr/^{86}Sr$ (0.71828 - 0.72959).

In addition to water extracts of soils, four surface water samples flowing over saline-alkaline soil immediately after a rain event were analyzed for major ions, Sr and $^{87}Sr/^{86}Sr$ (Table 3.2). All these samples have very high conductivity (1058 – 2760 μS/cm) and pH (9.0 – 9.6) as shown in Table 2.2 in chapter 2. Very high concentrations of Na (11148 – 32297 μM, Table 3.2) were observed in these samples. Other cations e.g. Ca (19 – 558 μM), Mg (6 – 1992 μM), K (34 – 110 μM) are 1 to 3 orders of magnitude lower than Na. HCO_3 (9426 – 26291 μM) concentration is much higher than other anions, i.e. Cl (697 – 2388 μM), SO_4 (347 – 977 μM), F(46 – 156 μM). NO_3 (62 μM) was detected in only one sample. Sr concentration (893 – 1211 nM) and Sr isotope ratio (0.72124 – 0.72129) of these samples are quite similar to those of the soils they drain (laboratory water extracts), indicating their dissolution as important source of Sr and other ions to the water chemical budget. High concentration of Na and HCO_3 in the water flowing over saline-alkaline soils confirm their significant contribution to the dissolved load of the river water.

The saline-alkaline soils analysed in this study are classified based on total dissolved solids (TDS), Na percentage and Sodium Adsorption Ratio (SAR) determined in water leachates. SAR is defined as

$$SAR = [Na^{+}] / [Ca^{2+} + Mg^{2+}]^{1/2}$$

where brackets represent total concentration of ions in mmol/litre in the soil solution. Based on these parameters these soils can be classified in three types (Sparks, 2002).

(a) Saline soil: The soils containing more than 0.1 % of Na and SAR less than 13 has been considered as saline (Richards, 1954). A total of 18 samples have been classified in this category (Fig. 3.1). All the soils from Chambal sub-basin fall in saline soil category.

(b) Alkaline soil: the soils with high SAR and low Na fall in this category. In the present study no samples have been documented in this class.

(c) Saline-alkaline soil: Soils with high content of soluble salt as well as high SAR are characterised as saline-alkaline soils. Five samples from Ganga Plain belong to this category (Fig. 3.1).

Table 3.3: Chemical composition and Sr isotopic data of river water samples

Sample code	Na µM	K µM	Mg µM	Ca µM	F µM	Cl µM	NO_3 µM	SO_4 µM	HCO_3 µM	Si µM	TDS mg/l	Sr nM	$^{87}Sr/^{86}Sr$
Headwaters													
BR10-1	103	53	133	429	b.d.	35	40	112	1126	149	112	613	0.73484
BR10-4	61	42	101	263	b.d.	18	20	168	509	90	68	387	0.75016
BR10-7	50	54	123	356	b.d.	12	18	84	1058	95	97	392	0.73766
BR10-12	60	49	117	343	b.d.	20	16	99	1003	102	95	416	0.73871
Ganga Mainstream													
BR10-14	226	95	250	663	b.d.	75	46	129	1935	135	181	979	0.73213
GP09-167	295	67	336	634	7	61	18	120	2015	171	185	1085	0.73218
GP09-135	1056	198	777	1095	13	408	78	278	4331	156	409	2112	0.73249
BR8109	374	65	211	556	11	209	37	114	1870	134	177	1175	0.71883
BR8129	484	76	222	599	9	285	53	147	1927	136	192	1297	0.71714
BR8136	356	68	229	587	10	156	30	111	1951	131	181	1151	0.72029
BR08-11	243	75	217	585	9	105	16	119	1846	110	169	810	0.72804
BR10-18	260	101	247	657	b.d.	96	54	144	1896	139	182	1005	0.73123
BR10-24	473	96	248	626	b.d.	254	72	146	1806	147	187	1374	0.72127
BR10-29	250	84	241	606	b.d.	99	42	118	1941	126	178	1069	0.72606
BR10-35	197	84	204	597	b.d.	82	29	123	1611	131	155	885	0.73132
Yamuna Mainstream													
BR10-22	932	103	235	570	b.d.	459	95	184	1903	154	214	1781	0.71531
GP09-50	6716	413	1145	1129	30	5375	1059	672	4579	251	851	5972	0.72268
GP09-52	8024	467	1218	1537	31	6483	600	817	5865	3	998	6906	0.72211
Himalayan Tributaries													
BR8105	75	79	229	623	2	30	b.d.	174	1777	n.d.	161	833	0.73505
BR8110	139	70	272	648	6	46	b.d.	134	1990	n.d.	174	914	0.73076
BR8121	196	59	303	779	7	62	b.d.	65	2337	110	199	906	0.72881
BR08-9	180	76	157	479	10	58	3	83	1376	133	128	519	0.74774
BR8124	113	71	279	655	5	32	55	169	2034	114	186	922	0.73224
BR10-26	75	79	229	620	b.d.	28	6	159	1855	121	168	889	0.73516
BR10-32	101	68	105	471	b.d.	23	17	88	1231	124	115	494	0.74629
BR10-44	94	73	231	642	b.d.	23	20	90	1903	111	166	871	0.73118
Plain Tributaries													
BR8140	264	41	128	328	13	73.0	27	46	1070	170	103	521	0.72323
BR08-1	543	57	236	579	30	184	33	39	2100	134	188	1211	0.72161
BR08-3	654	58	252	571	28	200	37	37	2193	130	197	1260	0.72165
BR08-5	546	58	204	379	21	150	4	35	1649	138	149	902	0.72686
BR08-7	794	42	232	489	36	205	7	49	2011	111	184	885	0.73963
BR08-18	803	49	259	557	26	186	12	71	2246	395	212	836	0.73602
BR08-20	1149	42	298	769	35	215	6	51	3151	262	279	1555	0.72870
BR08-22	902	45	362	726	34	168	10	68	2887	442	262	1225	0.72995
BR08-24	999	54	387	973	29	157	51	30	3440	214	301	2118	0.71863
BR08-27	489	44	193	438	22	133	25	69	1577	267	152	724	0.72848
BR08-34	361	54	195	435	20	147	15	37	1469	108	135	837	0.71753
BR8125	801	89	313	480	16	161	25	101	2321	116	211	1220	0.72598
GP09-143	1189	99	938	979	20	133	11	112	4724	386	408	1691	0.72975
Deccan rivers													
GP09-3	682	26	288	729	5	238	8	39	2585	207	229	1811	0.71099
GP09-21	1231	95	456	696	10	785	10	262	2309	215	272	2772	0.71028
GP09-24	926	80	599	681	10	502	20	104	2949	340	285	2996	0.70997
GP09-30	2233	72	641	655	16	885	21	587	3024	75	372	4150	0.71090
GP09-41	5095	282	655	695	33	4028	162	653	3117	348	588	4519	0.72051

b.d.- below detection limit, n.d.- not determined.

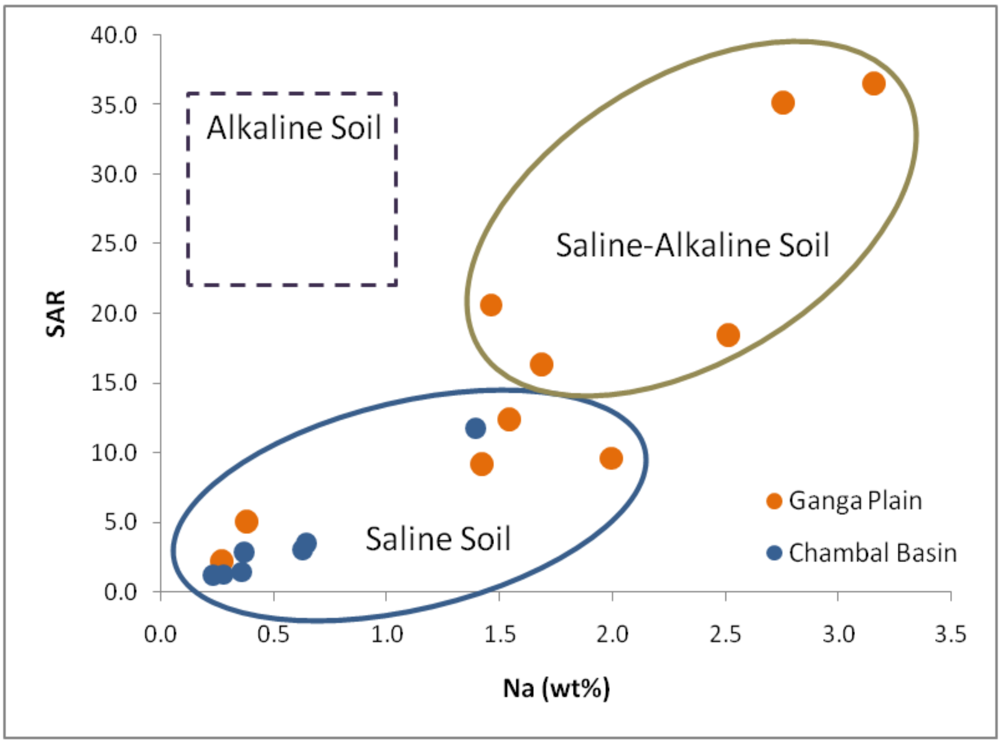

Fig. 3.1: *Classification of saline alkaline soils based on Na (wt%) and SAR. All the soils from Deccan are falling in saline soil category.*

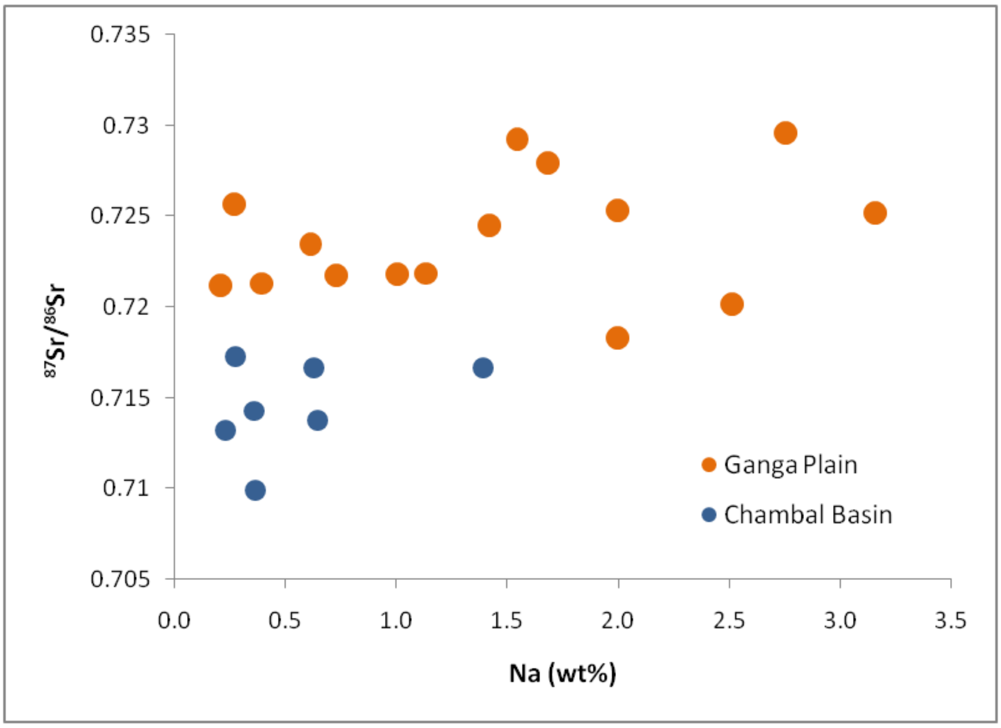

Fig. 3.2: *Sr isotopic ratio is similar for both soil types but soils from Chambal sub-basin (Deccan) have lower* $^{87}Sr/^{86}Sr$.

Sr isotopic ratio for all type of saline-alkaline soils overlaps with each other (Fig. 3.2). It is difficult to distinguish between different soil types based on their $^{87}Sr/^{86}Sr$. However, $^{87}Sr/^{86}Sr$ of soils from different sub-basin is different. $^{87}Sr/^{86}Sr$ of the Chambal sub-basin is lower compared to the other sub-basins of the Ganga. saline-alkaline soils of this basin show lower $^{87}Sr/^{86}Sr$. Na dominates the major cation budget of saline alkaline soil (Fig. 3.3). It constitutes about 90% of cation budget in majority of soil samples. HCO_3 forms the major fraction of cation budget, however, Cl and SO_4 also contribute to the anion budget of these soils. Surface water flowing through these soils mostly composed of Na and HCO_3 (Fig. 3.3).

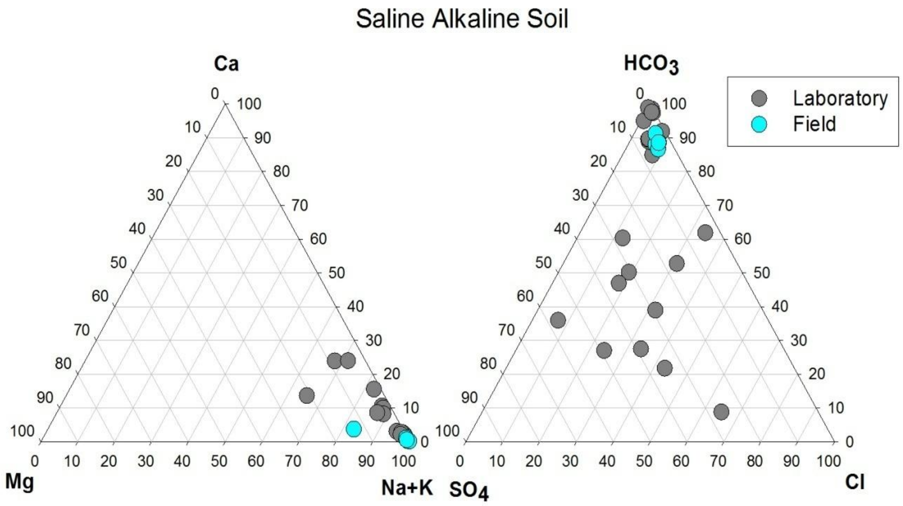

Fig. 3.3: *Ternary diagram of saline alkaline soil water extracts (Laboratory) and waters flowing through saline alkaline soil regions (Field).*

The major ion data of the water extracts of these soils display much higher concentration of Na compared to Cl in all samples except 2 (Fig. 3.4a). These results indicate presence of Na salts such as Na_2SO_4, Na_2CO_3, $NaHCO_3$, NaCl, $NaNO_3$ etc. To examine this point further, Na has been plotted with sum of all anions excluding bicarbonate (Fig. 3.4b). This plot shows excess of Na over all ions, which proves the presence of carbonate of Na minerals e.g. Na_2CO_3, $NaHCO_3$ such as trona (Datta et al., 2002) in these soils. Though bicarbonate can account for majority of Na in the soil, presence of other Na salts are required to balance entire Na in all samples (Fig. 3.4c). Fig. 3.4d shows that Na alone could balance sum of all major anions, which implies presence of NaCl, Na_2SO_4, and Na_2CO_3/$NaHCO_3$. Only one data point shows excess Na over these anions, that sample has high NO_3. Therefore, it could be inferred that $NaNO_3$ is also present in these saline-alkaline soils however it is not very common (Datta et al., 2002).

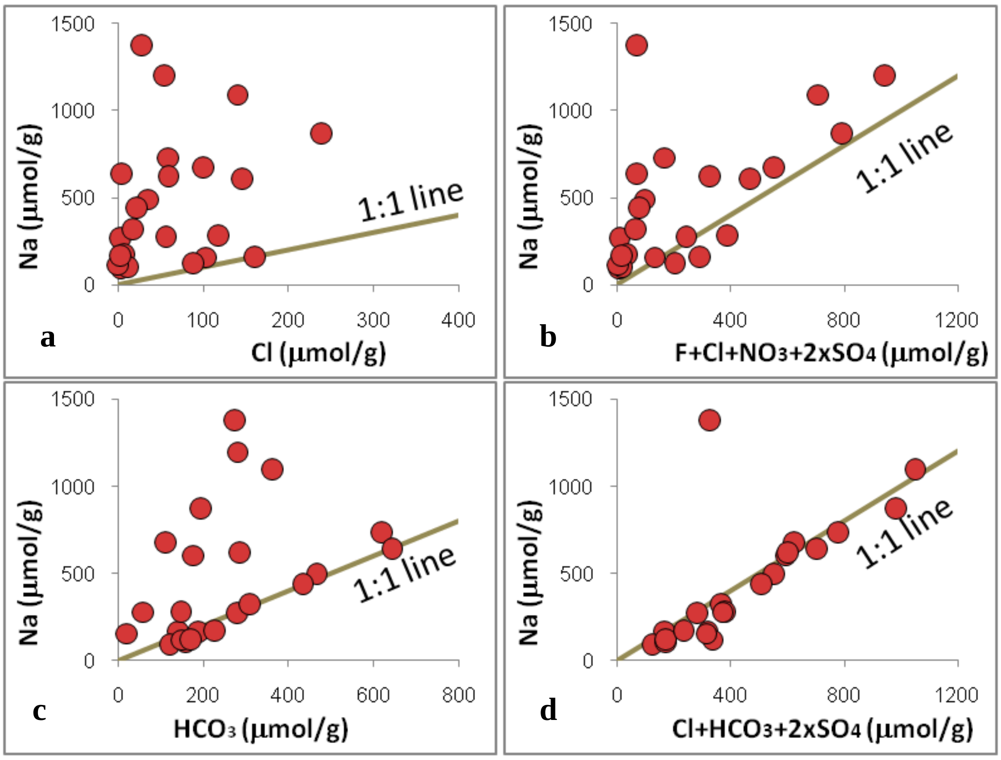

***Fig.3.4**: **a)** Higher Na concentration compared to Cl indicates presence of other soluble Na salts. **b)** Na concentration could not be balanced using all anions excluding bicarbonate. Presence of Na_2CO_3 and $NaHCO_3$ could be inferred. **c)** Excess Na over bicarbonate signifies presence of other Na salts. **d)** Chloride, bicarbonate and sulphate of sodium seem to be dominant components of the saline alkaline soils.*

It is supported by evaporite precipitation series where $NaNO_3$ precipitates at the end (Drever, 1997). Figures 3.3 and 3.4 confirm that Na_2CO_3 and $NaHCO_3$ are the major constituents of these soils with sub-ordinate contribution from NaCl and Na_2SO_4. These results indicate that dissolution of these saline-alkaline soils could significantly contribute Na to the dissolved load of river which is not associated with Cl. Therefore Cl corrected Na cannot be used as a proxy of silicate weathering in the Ganga basin as significant amount of Na to the river water could be contributed by saline-alkaline salts of carbonate compositions. Therefore any correction made to remove the impact of salt dissolution on water chemistry using Cl (Krishnaswami et al., 1999) could be an underestimate. Cl correction could not correct for Na contribution from Na_2CO_3, $NaHCO_3$ which are dominant minerals in saline–alkaline soils in the Ganga basin.

This study indicates that the saline-alkaline soils of the Ganga systems are mainly composed of $NaHCO_3$, Na_2CO_3, NaCl, Na_2SO_4 and $NaNO_3$. These minerals are highly soluble and contribute significantly to the river chemistry which will be assessed in the following section.

3.2.2 River Water Chemistry

Several studies have been carried out to study the chemistry and Sr isotope composition of river waters of the Ganga (Sarin et al., 1989; Sarin et al., 1992; Harris et al., 1998; Krishnaswami et al., 1999; Galy et al., 1999; Galy and France-Lanord, 1999; Bickle et al., 2003; Oliver et al., 2003; Quade et al., 2003; Tipper et al., 2006). In this study, river water samples have been studied for major ions and Sr concentrations and its isotopic composition (Table 3.3) with special emphasis on the contribution from saline-alkaline soils.

For this study several water samples from different locations of the Ganga mainstream, from its peninsular, Himalayan and plain tributaries were collected. These samples have been classified into following sub-sets for better understanding,

a. Headwaters: This subset includes 4 samples from Alaknada, Bhagirathi, Ganga (after confluence of those 2 rivers) collected upstream Rishikesh and Yamuna, collected at Rampur Mandi. (pH 7.2 – 8.0, conductivity 24 – 137 μS/cm)
b. Ganga mainstream: 11 samples collected from main channel of the Ganga (between Garhmukteshwar to Manihari) are included in this section.

Among them 2 were collected in non-monsoon, rest were collected during monsoon. (pH 7.4 – 8.5, conductivity 176 – 461 μS/cm)

c. Yamuna: 3 samples collected between Agra to Allahabad (1 monsoon, 2 non-monsoon) are included in this section. These have been treated separately from the Himalayan tributaries section as it receives considerable amount of water from peninsular rivers like Chambal, which flows predominantly through Deccan basalts. (pH 7.8 – 9.0, conductivity 277 – 1442 μS/cm).
d. Tributaries_Himalaya: This section includes tributaries of the Ganga which are originated in the Himalaya and joining the main channel from North, e.g. Gandak, Ghaghra, Kosi. One sample of Rapti is also added to this category. (pH 7.4 – 7.6, conductivity 135 – 233 μS/cm).
e. Tributaries_plain: This section consists of small rivers, e.g. Karmnasha, Son, Punpun, Kiul etc, which flow mainly through the Ganga plain and join main channel from the South. Samples from the Gomti are also considered in this section. The Gomti drains detritus brought from the Hiimalaya and saline-alkaline soils infected regions. This river joins the Ganga from North. It differs considerably from the Himalayan tributaries as it drains only in the Ganga plain. These tributaries will provide information of weathering processes happening in the Ganga plain. (pH 7.3– 8.3, conductivity 124 – 460 μS/cm).
f. Deccan rivers: This section includes rivers from Deccan, which directly or indirectly contribute to the Yamuna. These samples were collected during non-monsoon. (pH 8.0–8.9, conductivity 346 – 8920 μS/cm).

Major ion data along with Sr concentration and its isotope composition of these river waters are given in Table 3.3. Charge balance between measured cations and anions is within 10% in most of the river water samples, except few where it goes maximum up to 15%. The anion budget of these waters is dominated by bicarbonate in almost all samples (Fig. 3.5) expect few samples from Yamuna and Deccan rivers (Sample GP09-41, 50, 52). The cation plot shows interesting property (Fig. 3.5). The headwaters of the Ganga and the Himalayan tributaries show a Ca dominated cation budget, which gradually decreases in the Ganga mainstream downstream Rishikesh with increasing Na content.

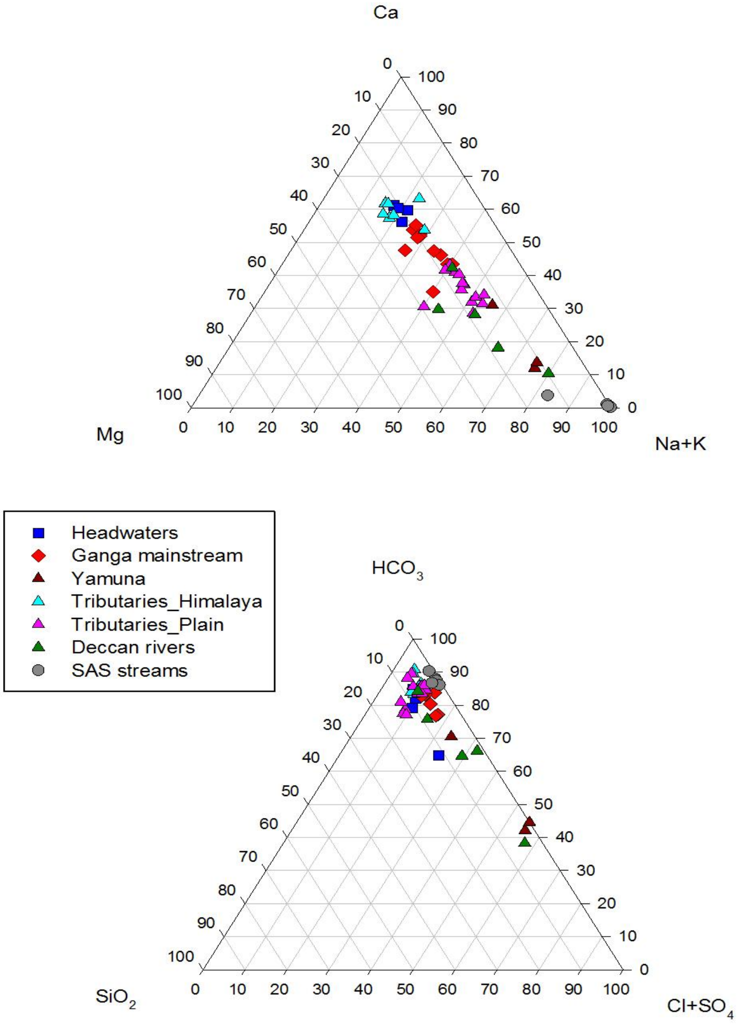

Fig. 3.5: *Cations ternary plot of river water samples shows increase in Na percentage in Ganga mainstream compared to the headwaters. Anions ternary plot mainly shows bicarbonate dominance in anion budget in almost all samples.*

Na concentration in the headwater region varies from (50-103 μM), it is almost double in the Ganga mainstream in plain (204-250 μM). Dissolved Na concentration in the tributaries from plain (264-1149 μM) is at least 3-4 times higher than that of the Himalayan tributaries (50-169 μM). The peninsular tributaries have very high Na concentration (682-5095 μM), as their drainages are infected by saline-alkaline soils. Few small stream samples, which flow through saline-alkaline soil infected region, are the rivers from plain, Deccan and Yamuna are more Na dominated. They are plotted near Na apex of the plot (Fig. 3.5). This plot (Fig. 3.5) clearly indicates the importance of saline alkaline soil contribution to cation budget of the Ganga. Ca concentration (263-779 μM) in the Himalayan tributaries is much higher than their Na content, whereas the plain and peninsular tributaries have lower Ca concentrations, (655-729μM) and (328-973μM) respectively, than their respective Na concentration. In the Ganga mainstream in plain, the Na concentration (60-1056 μM) is lower than Ca concentration (343-1095 μM) in all samples.

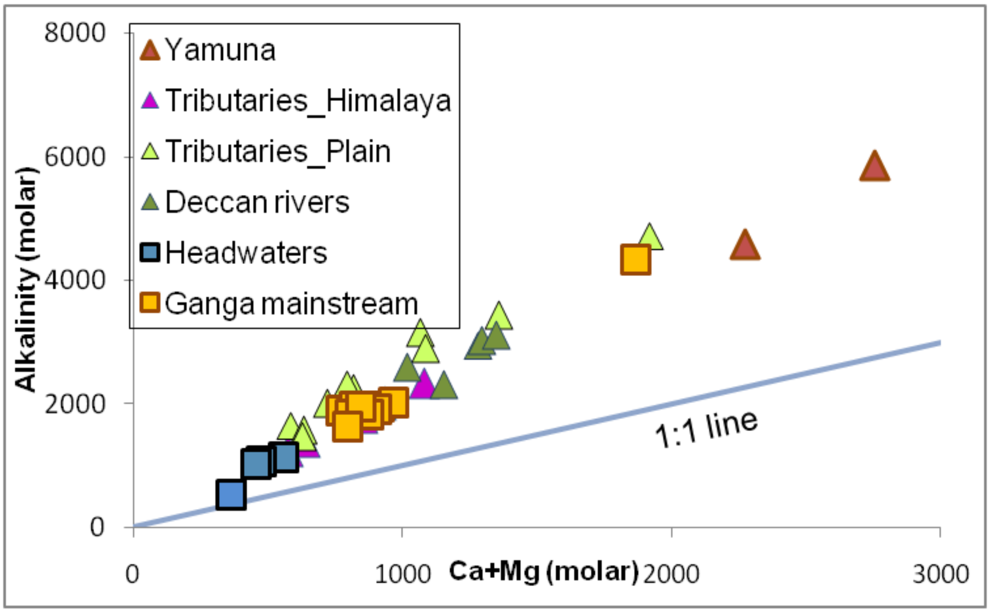

Fig. 3.6: *Higher alkalinity compared to the sum of Ca and Mg indicates towards additional sources of alkalinity in the plain.*

Alkalinity also increases in plain compared to headwaters. In the headwater region, alkalinity is almost balanced by Ca and Mg, but in plain it is higher compared to the sum of Ca and Mg (Fig. 3.6). Similar behaviour has been observed in the Ganga plain by Sarin et al., (1989). Higher alkalinity compared to their respective Ca and Mg content requires additional sources of alkalinity other than Ca, Mg carbonates. It has been already discussed in the previous section, that alkaline soils are composed of Na_2CO_3, $NaHCO_3$. Hence they can act as additional source of alkalinity to river water. SO_4 concentration does not show any increasing trend from headwaters (84-168 µM) to plain (111-147 µM). Also, Himalayan tributaries (83-169 µM) have higher SO_4 concentration compared to the tributaries from plain (30-112 µM). However, Na content in the Ganga mainstream increases progressively from headwaters to plain (Table 3.3) which has been construed as increase in intensity of silicate weathering in the plain (Lupker et al., 2012; 2013). However, Si concentration decreases in the plain compared to the headwaters.

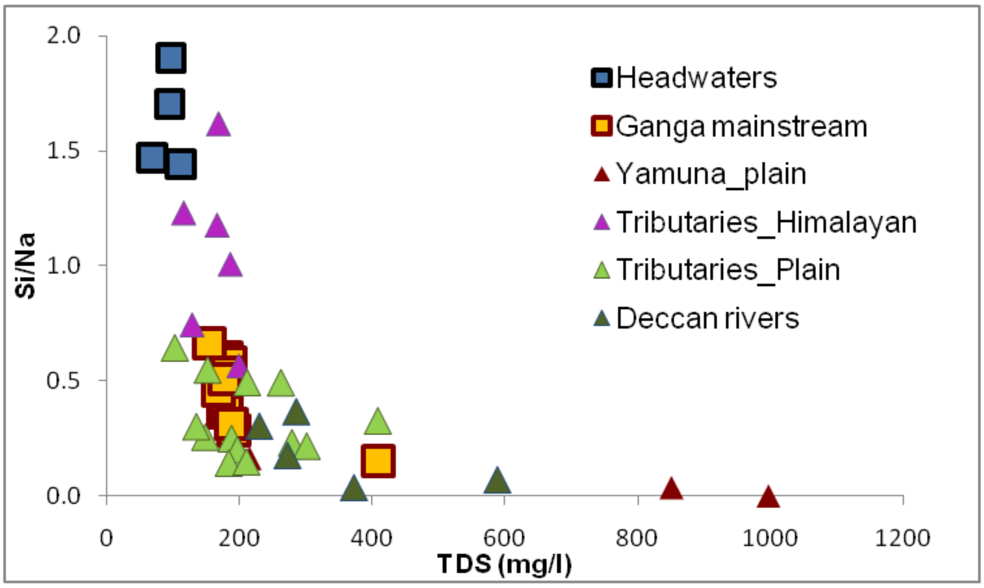

***Fig. 3.7:** Si/Na decreases with TDS due to increase in Na content from headwaters to the Ganga plain. Tributaries of the Yamuna and those of the Ganga in plain have low Si/Na indicating contribution from saline – alkaline soils.*

Si/Na decreases with increasing TDS from headwater region to the Ganga mainstream in plain (Fig. 3.7). Further, Yamuna and most of the tributaries from plain show lower value of Si/Na due to increase in Na content. If increase in the intensity of silicate weathering is the source of additional Na in river water in plain, Si/Na ratio should remain invariable. Increase in intensity of silicate weathering would increase both Si and Na keeping Si/Na ratio invariable.

Biogenic activity can remove Si from stagnant water, however during monsoon, when most of the samples are collected, biogenic activity is lower due to high river stage and turbidity (Rai et al., 2010). Therefore, additional Na specific sources other than silicate are needed in the plain. Such source could be saline-alkaline soils abundantly present in the Ganga plain.

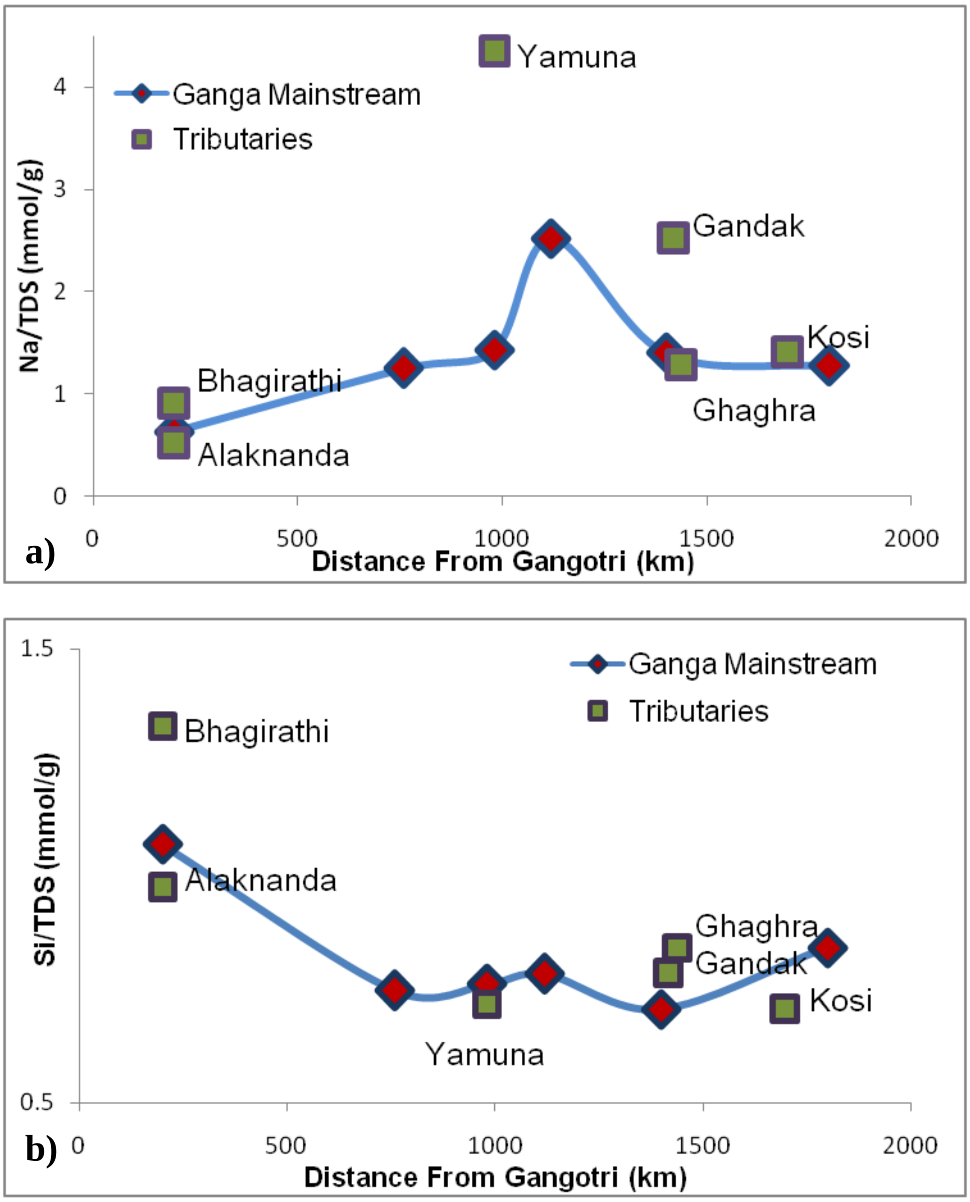

Fig. 3.8: a) *Na/TDS increases in Ganga mainstream from headwaters to the plain with highest at Varanasi indicating larger contribution from Yamuna.* ***b)*** *Si/TDS decreases in Ganga Mainstream from headwaters to the plain and increases slightly due to mixing with Himalayan tributaries.*

It is reflected in increase of Na/TDS of the Ganga in the plain with highest value at Varanasi after confluence with the Yamuna with higher Na (Fig. 3.8a), further decreasing Si/TDS in plain indicates lower silicate erosion in plain compared to headwaters. This interpretation will be examined in this study in view of presence of Na rich saline-alkaline soils in the Ganga Plain.

To assess the role of various sources on dissolved material in the Ganga and its tributaries, property plot of Ca/Na vs. Mg/Na of these waters along with possible endmembers has been used (Fig. 3.9). Most of the data of the Ganga system scatter around a linear trend defined by the mixing of carbonate and silicate endmembers (Fig. 3.9). Contribution from the Deccan Basalt seems to be minor on this plot. All the Himalayan tributaries and samples from the Ganga mainstream follow the same trend. The Yamuna and tributaries from plain and peninsular region though scatter around the silicate endmember, some of them lie below silicate endmember, requiring contribution from saline-alkaline soils. Saline-alkaline soils have different Ca/Na and Mg/Na values than silicates (Fig. 3.9).

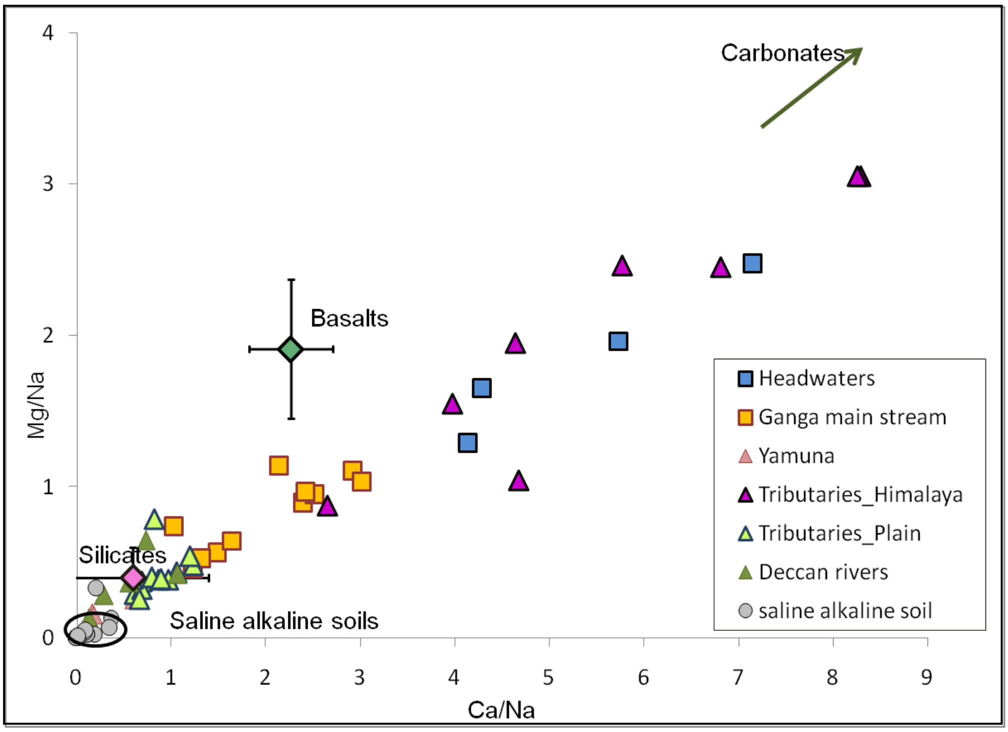

Fig. 3.9: *Major ion ratio plot does not distinguish between saline alkaline soil endmember and silicates.*

This endmember would be required to explain samples containing high Na, such as those from the Yamuna and Ganga plain.

To resolve this point further Sr isotopic composition and concentration have been used along with Na concentration (Fig. 3.10). Various endmembers, silicates, carbonates and Deccan basalts are also plotted in the same figure. From Fig. 3.10, it is clear that the Himalayan tributaries follow a mixing trend between silicates and carbonates but the plain and peninsular river cannot be explained by these two endmembers. Even mixing between silicates and basalts cannot explain all of them. Saline-alkaline soils with low Sr isotopic ratio and high Na concentration is needed as another endmember to explain them (Fig. 3.10).

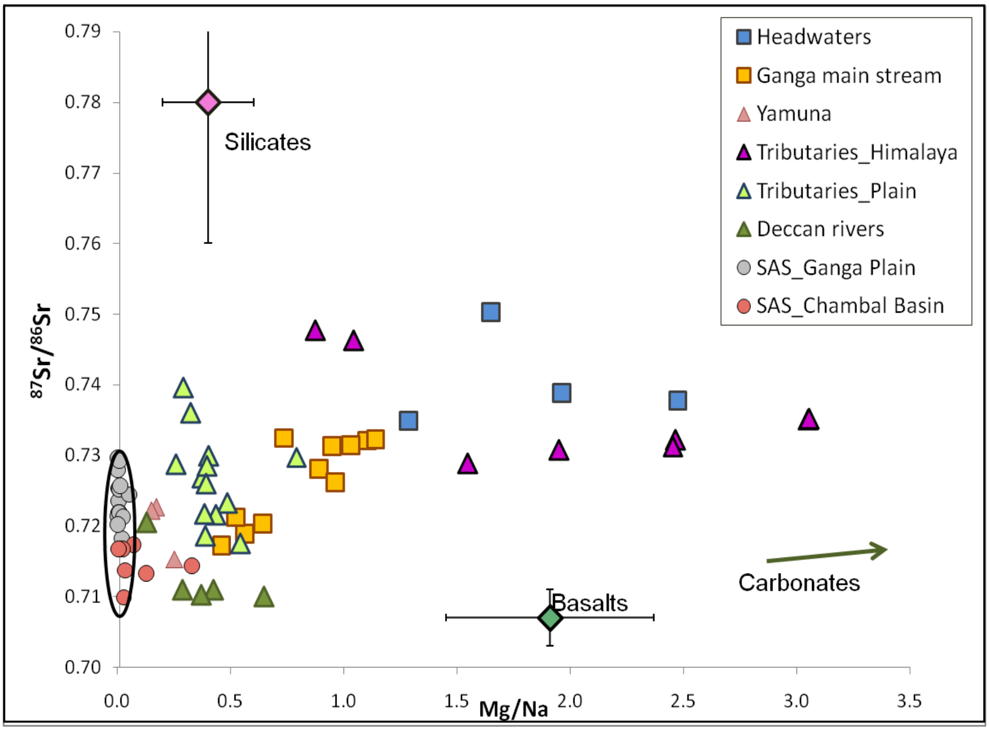

Fig. 3.10: *$^{87}Sr/^{86}Sr$ ratio plot with Sr isotopes shows the need of saline-alkaline soils as an important endmember to explain data from plain and peninsular rivers.*

It is borne out from the above discussion that in addition to Himalayan silicates, carbonates, the Deccan basalt, hotspring and rainwater sources, the Ganga system gets significant amount of dissolved material from saline-alkaline soils, rich in various Na salts other than NaCl. In such system, excess Na over Cl could not be used as a proxy to silicate weathering as has been done in many of the earlier studies (Krishnaswami et al., 1999; Galy and France-Lanord, 1999; Quade et al., 2003; Tipper et al., 2006). Mass balance calculation using forward model for the Ganga river system to apportion the sources of dissolved material in them is not possible due to multiple endmembers and absence of suitable proxy of silicate weathering. Therefore to apportion the sources of dissolved material and further to estimates the erosion rates of various sub-basins, inverse model (Negrel et al., 1993; Millot et al., 2003; Tripathy et al., 2010) has been used in this study.

3.2.3 Source apportionment of dissolved material using inverse model

It has been shown in the earlier section that water chemistry of the Ganga River system is controlled by ion contribution from rainwater and from major lithologic units of the basin such as granite/gniesses (silicates), carbonates, Deccan basalts and saline-alkaline soils. To determine the weathering rates of various lithology and associated CO_2 consumption, it is important to apportion the sources of dissolved ions in river. In this study inverse model has been used to apportion the sources of the dissolved material in the Ganga river system. The mass balance equations used for the model are given below,

□□□□= □=*1*□□□□□ ×□□□□ ……………………………….…………..(4)

87□□*86*□□ × □□□□□ = □=*1*□*87*□□*86*□□□ × □□□□□ × □□ □□ ……..………………...(5)

□=*1*□□□ □□ =*1* $\sum_{i=1}^{n} f_i\,(Na) = 1$

……………………………………………………..(6)

where X= Cl, Ca, Mg, Sr and HCO_3 and i indicates the endmember. $(X/Na)_i$ is the molar release ratio of X from i^{th} end-member. In inverse model the set of mass-balance equations are solved iteratively to get the best possible estimation of different elemental ratios of the end-members. This set of mass-balance equations correlates the observed values (observed space) with the model parameters (model space). In the model, the assumption is made that the model space should follow lognormal probability distribution and then non-linear weighted fit to the mass-balance equations, mentioned above, are performed iteratively using Quasi-Newton method (Tarantola, 2004). A set of *a-priori* values of elemental and $^{87}Sr/^{86}Sr$ ratios of various endmembers along with their uncertainties is used as input to the model. Finally, the inverse model provides the best possible estimation of the model parameters and their corresponding covariance (i.e., uncertainties). *A-priori* values used to perform the modelling of the present data set along with their references are listed in Table 3.4 and the corresponding *a-posteriori* values are listed in Table 3.5.

In this method, ratios of cations including Sr to Na in all the sources have been used as input along with an estimated fractional contribution from the sources. Rain water contribution (Galy and France-Lanord, 1999) has been subtracted from the data before inversion, considering 40% evapotranspiration in the plain and 25% of that in the headwaters. Therefore in the model, 3 sources were considered (silicate, carbonate and saline-alkaline soil) for all samples except Deccan rivers and Yamuna, in which Deccan basalt was used as fourth end member. For the Ganga headwaters, hotspring has been considered in place of saline-alkaline soil endmember as hotsprings contribute water in the Himalayan rivers.

Table 3.4: *A-priori* molar ratio of all end members

Ratio	Silicate[1]	Carbonate[2,3]	Hotsprings[4]	Deccan[5,6]	Saline Alkaline soils[7]
Cl/Na	0.0	0.0	1.2 ± 0.3	0.0	0.32 ± 0.42
Ca/Na	0.7 ± 0.3	3000 ± 2000	4.4 ± 0.8	2.3 ± 0.4	0.14 ± 0.18
Mg/Na	0.3 ± 0.2	1500 ± 1000	0.024 ± 0.012	1.9 ± 0.5	0.04 ± 0.07
Sr/Na	2.0 ± 0.8	350 ± 200	1.2 ± 0.13	3.2 ± 0.1	1.3 ± 2.2
$^{87}Sr/^{86}Sr$	0.8 ± 0.02	0.715 ± 0.02	0.77 ± 0.02	0.71 ± 0.006	0.721 ± 0.005
Alkalinity/Na	2 ± 1	8000 ± 4000	10 ± 4	2 ± 1	2.0 ± 1.3

Data source: [1]Krishnaswami et al, 1999, [2]Singh et al,1998, [3,4]Tripathy et al, 2010, [5]Das et al, 2005, [6]Rengarajan et al, 2009, [7]Present study.

Table 3.5A: *A-posteriori* results from the inverse model for the Ganga river system (3 endmembers)

Ratio	Silicates	Carbonates	Hotsprings
Headwaters			
Cl/Na	0.0	0.0	1.08 ± 0.20
Ca/Na	1.02 ± 0.37	461 ± 119	4.24 ± 0.72
Mg/Na	0.69 ± 0.27	159 ± 43	0.02 ± 0.01
Sr/Na	6.37 ± 0.67	253 ± 72	1.16 ± 0.13
^{87}Sr/^{86}Sr	0.797 ± .019	0.713 ± .020	0.770 ± .020
Alkalinity/Na	1.06 ± 0.52	1413 ± 362	7.63 ± 2.67

Ratio	Silicates	Carbonates	Saline Alkaline soils
Ganga Mainstream			
Cl/Na	0.0	0.0	0.65 ± 0.10
Ca/Na	0.49 ± 0.18	76 ± 16	0.07 ± 0.08
Mg/Na	0.61 ± 0.18	24 ± 5.9	0.03 ± 0.05
Sr/Na	0.96 ± 0.29	111 ± 23	1.39 ± .29
^{87}Sr/^{86}Sr	0.799 ± 0.020	0.715 ± 0.018	0.721 ± .005
Alkalinity/Na	2.06 ± 0.74	222 ± 47	0.95 ± 0.43
Gandak Ghaghra			
Cl/Na	0.0	0.0	0.10 ± 0.04
Ca/Na	0.62 ± 0.24	365 ± 84	1.10 ± 0.51
Mg/Na	0.62 ± 0.23	137 ± 32	0.48 ± 0.25
Sr/Na	1.41 ± 0.44	534 ± 123	0.23 ± 0.37
^{87}Sr/^{86}Sr	0.800 ± 0.020	0.717 ± 0.018	0.721 ± 0.005
Alkalinity/Na	2.71 ± 1.06	1122 ± 258	3.32 ± 1.33
Kosi			
Cl/Na	0.0	0.0	0.11 ± 0.05
Ca/Na	0.68 ± 0.29	894 ± 245	0.13 ± 0.16
Mg/Na	0.24 ± 0.16	185 ± 54	0.52 ± 0.25
Sr/Na	2.25 ± 0.89	859 ± 240	0.49 ± 0.53
^{87}Sr/^{86}Sr	0.800 ± 0.020	0.716 ± 0.019	0.721 ± 0.005
Alkalinity/Na	1.88 ± 0.94	2443 ± 668	1.80 ± 0.94
Gomti			
Cl/Na	0.0	0.0	0.18 ± 0.06
Ca/Na	0.49 ± 0.19	464 ± 171	0.09 ± 0.11
Mg/Na	0.32 ± 0.20	453 ± 159	0.02 ± 0.03
Sr/Na	1.09 ± 0.28	230 ± 122	1.39 ± 0.21
^{87}Sr/^{86}Sr	0.799 ± 0.020	0.715 ± 0.020	0.721 ± 0.005
Alkalinity/Na	1.56 ± 0.75	2269 ± 760	1.09 ± 0.57
Tributaries_Plain			
Cl/Na	0.0	0.0	0.23 ± 0.03
Ca/Na	0.48 ± 0.19	44 ± 9.6	0.04 ± 0.04
Mg/Na	0.16 ± 0.10	21 ± 4.8	0.01 ± 0.03
Sr/Na	2.78 ± 0.81	64 ± 18	0.06 ± 0.11
^{87}Sr/^{86}Sr	0.797 ± 0.020	0.710 ± 0.019	0.721 ± 0.005
Alkalinity/Na	1.32 ± 0.63	170 ± 37	0.48 ± 0.27

Table 3.5B: ***A-posteriori*** **results from the inverse model for the Ganga river system (4 endmembers)**

Ratio	Silicates	Carbonates	Saline Alkaline soils	Deccan
Ganga Mainstream_ after confuence with Yamuna				
Cl/Na	0.0	0.0	0.84 ± 0.17	0.0
Ca/Na	0.51 ± 0.21	144 ± 34	0.08 ± 0.09	2.23 ± 0.43
Mg/Na	0.19 ± 0.12	51 ± 13	0.02 ± 0.04	1.72 ± 0.41
Sr/Na	3.66 ± 0.95	146 ± 40	0.86 ± 0.65	3.23 ± 0.07
^{87}Sr/^{86}Sr	0.797 ± 0.020	0.712 ± 0.020	0.721 ± 0.005	0.710 ± 0.006
Alkalinity/Na	1.32 ± 0.64	476 ± 112	1.261 ± 0.66	1.92 ± 0.96
Yamuna monsoon				
Cl/Na	0.0	0.0	0.61 ± 0.18	0.0
Ca/Na	0.61 ± 0.26	1105 ± 490	0.08 ± 0.09	2.23 ± 0.43
Mg/Na	0.23 ± 0.15	516 ± 251	0.02 ± 0.03	1.81 ± 0.43
Sr/Na	2.00 ± 0.80	351 ± 200	1.76 ± 0.29	3.23 ± 0.07
^{87}Sr/^{86}Sr	0.800 ± 0.020	0.715 ± 0.020	0.721 ± 0.005	0.710 ± 0.006
Alkalinity/Na	1.62 ± 0.80	3573 ± 1461	0.96 ± 0.54	1.91 ± 0.95
Yamuna non-monsoon				
Cl/Na	0.0	0.0	0.89 ± 0.15	0.0
Ca/Na	0.33 ± 0.13	264 ± 126	0.04 ± 0.04	2.12 ± 0.41
Mg/Na	0.20 ± 0.13	336 ± 142	0.01 ± 0.02	1.79 ± 0.43
Sr/Na	2.90 ± 0.63	389 ± 217	0.44 ± 0.29	3.23 ± 0.07
^{87}Sr/^{86}Sr	0.799 ± 0.020	0.715 ± 0.020	0.721 ± 0.005	0.710 ± 0.006
Alkalinity/Na	1.26 ± 0.59	1577 ± 602	0.44 ± 0.24	1.76 ± 0.88
Deccan rivers non-monsoon				
Cl/Na	0.0	0.0	0.67 ± 0.09	0.0
Ca/Na	0.60 ± 0.22	243 ± 88	0.03 ± 0.04	1.65 ± 0.30
Mg/Na	0.17 ± 0.11	160 ± 68	0.02 ± 0.04	1.49 ± 0.33
Sr/Na	1.34 ± 0.45	737 ± 226	1.45 ± 0.27	3.23 ± 0.07
^{87}Sr/^{86}Sr	0.799 ± 0.020	0.714 ± 0.020	0.721 ± 0.005	0.710 ± 0.006
Alkalinity/Na	1.81 ± 0.84	1466 ± 457	0.67 ± 0.37	1.44 ± 0.71

3.2.4 Saline - Alkaline soil contribution to the dissolved ion budget

Na in the dissolved phase from saline-alkaline soil endmember varies from 27% to 70% in the Ganga mainstream in monsoon. This contribution increases in Varanasi and has the highest value (61%) and decrease gradually till Manihari (27%) (Fig. 3.11). This Na, if not apportioned properly, could be considered as silicate Na and hence would increase SER. In non-monsoon, the Ganga mainstream has 10% and 25% of Na coming from saline-alkaline soils at Garhmukteshwar and Kanpur respectively. Same behaviour is observed in the Gomti also, where Saline-alkaline Na percentage decreases from 86% in monsoon to 44% in non-monsoon. In Ghaghra and Gandak, Na contribution from saline-alkaline soil varies from 18% to 35% and 38% to 59% respectively, in monsoon.

But, as in these rivers Ca and Mg concentration is considerably higher than Na, therefore the effect of saline-alkaline soils is not very prominent in the cation budget. In the small tributaries from plain, Na from saline-alkaline soils varies from 59% to 92%, and its effect is visible in the cation budget also. Saline-alkaline soils contribute 77% of dissolved Na to the Yamuna in monsoon at Allahabad. In non-monsoon this contribution is ~95% in the Yamuna, even before mixing with its Deccan tributaries. In case of the Chambal, the saline-alkaline soil contribution of Na is ~75% in non-monsoon.

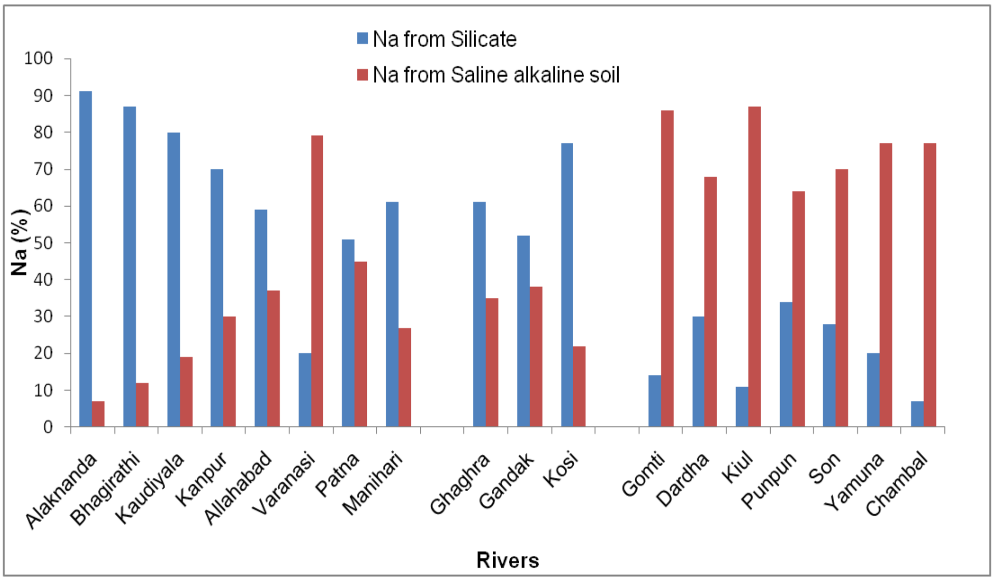

Fig. 3.11: *Na contribution from saline–alkaline soil increases in the Ganga from headwaters to the plain and also in tributaries from plain and peninsular region.*

Saline alkaline soils are not an important source of Ca and Mg to the river water. Ca and Mg from this source vary between 1-5% and 0.5-5% respectively in the Ganga mainstream in monsoon. All other rivers show similar behaviour, except Rapti, Yamuna at Etawah in non-monsoon and Kosi in monsoon, 2008, these samples show ~20% of either Ca or Mg or both from saline alkaline soils. Calcrete formation is closely related to saline alkaline soil formation. In general, calcretes are not prone to dissolution, but it seems from these data, that they can contribute along with saline alkaline soils sometimes. Bicarbonate can also be contributed by saline alkaline soils. In the Ganga mainstream and in the tributaries from plain, 2% - 18% of total alkalinity is of saline alkaline soil origin. Ghaghra and Gandak have less contribution (1% - 3%) of the same. Kosi in 2008 show a higher contribution (13%) of saline alkaline soil alkalinity than in 2010 (1%). This different behaviour of the Kosi in two different seasons has been observed in all parameters and has been attributed to flood in 2008 (discussed above). In other rivers, i.e., Gomti, Chambal and its tributaries, Yamuna, 8% - 38% of total alkalinity is of saline-alkaline soil origin.

The model results (Table 3.6A and 3.6B) show that saline-alkaline soils could contribute 4-23% of total cations to the Ganga main channel during monsoon, during non-monsoon this contribution goes up to 15±4%. From the results, it can be observed that saline-alkaline soil cation contribution in the Ganga mainstream increases suddenly at Varanasi (23±5%) after Kanpur (4±1%) and Allahabad (7±5%). This is due to contribution from the Yamuna and its tributaries from Deccan region. Extensive saline-alkaline soil patches observed in this region, are also responsible for the same. The Ganga mainstream at Patna displays varying contribution of cations from saline-alkaline soil in two monsoon seasons, 17±4% in 2008 and 6±2% in 2010. This could be due to flooding in the plain tributaries of the Ganga around Patna in 2008. The Ganga at Manihari (near Rajmahal) have 10±2% and 4±1% of saline-alkaline soil contribution in the cation budget in two different monsoon seasons, even after mixing with the other Himalayan tributaries like Gandak, Ghaghra and Kosi.

The Yamuna at Allahabad before confluence with the Ganga shows 43±11% cation contribution from saline-alkaline soils in monsoon, and up to 71±6% in non-monsoon at Etawah. In case of Gomti river, which flows through saline-alkaline soil enriched regions mainly, this contribution could be up to 46±10% in monsoon. The Gandak and Ghaghra have 2-4% of dissolved cations from saline-alkaline soils, which is clearly evident as they have lower exposure of saline-alkaline soils in their drainage basins. Kosi shows 20±6% saline-alkaline soil contribution during the flood event in 2008 and only 3±2% in another monsoon

Table 3.6A: Source apportionment of Na, Cations and Sr using 3 endmembers.

Sample	River	Place	%Na$_{\text{Sil}}$	%Na$_{\text{Carb}}$	%Na$_{\text{HS}}$	%Cation$_{\text{Sil}}$	%Cation$_{\text{Carb}}$	%Cation$_{\text{HS}}$	%Sr$_{\text{Sil}}$	%Sr$_{\text{Carb}}$	%Sr$_{\text{HS}}$
Headwaters											
BR10-7	Alaknanda	Devprayag	91 ± 3	2 ± 0.4	7 ± 3	27 ± 3	72 ± 21	3 ± 1	58 ± 22	43 ± 16	1 ± 0.3
BR10-4	Bhagirathi	Devprayag	87 ± 4	1 ± 0.2	12 ± 4	37 ± 5	46 ± 13	7 ± 2	74 ± 29	22 ± 8	2 ± 1
BR10-12	Ganga	Kaudiyala	80 ± 4	1 ± 0.3	19 ± 4	28 ± 3	66 ± 19	9 ± 2	61 ± 24	35 ± 13	3 ± 1
BR10-1	Yamuna	Rampur Mandi	73 ± 5	1 ± 0.2	26 ± 5	34 ± 5	50 ± 15	19 ± 4	72 ± 28	23 ± 9	5 ± 1
Sample	River	Place	%Na$_{\text{Sil}}$	%Na$_{\text{Carb}}$	%Na$_{\text{SAS}}$	%Cation$_{\text{Sil}}$	%Cation$_{\text{Carb}}$	%Cation$_{\text{SAS}}$	%Sr$_{\text{Sil}}$	%Sr$_{\text{Carb}}$	%Sr$_{\text{SAS}}$
Yamuna _Before mixing with Deccan tributaries											
GP09-50	Yamuna	Pohia Ghat, Agra	6 ± 7	0.04 ± 0.02	94 ± 7	12 ± 6	22 ± 9	71 ± 6	13 ± 16	16 ± 11	70 ± 16
GP09-52	Yamuna	Etawah	5 ± 7	0.04 ± 0.02	95 ± 7	11 ± 6	23 ± 9	71 ± 6	12 ± 16	17 ± 12	72 ± 16
Tributaries_Himalaya											
BR8110	Ghaghra	Revelganj	80 ± 12	2 ± 1	18 ± 12	21 ± 3	75 ± 19	4 ± 2	11 ± 4	90 ± 29	0.4 ± 0.7
BR8124	Ghaghra	Dohrighat	74 ± 15	3 ± 1	23 ± 15	15 ± 2	81 ± 20	3 ± 1	7 ± 2	94 ± 31	0.3 ± 0.6
BR10-44	Ghaghra	Revelganj	61 ± 19	4 ± 1	35 ± 19	12 ± 1	84 ± 21	4 ± 1	4 ± 2	96 ± 31	0.3 ± 0.6
BR8121	Rapti	Gorakhpur	15 ± 19	1 ± 0.3	84 ± 19	8 ± 3	66 ± 17	25 ± 6	3 ± 4	96 ± 32	3 ± 5
BR8105	Gandak	Hajipur	32 ± 26	9 ± 2	59 ± 26	9 ± 1	86 ± 22	3 ± 1	1 ± 1	99 ± 32	0.3 ± 0.5
BR10-26	Gandak	Sonpur (near Patna)	52 ± 24	9 ± 2	38 ± 24	10 ± 1	90 ± 23	2 ± 1	1 ± 1	97 ± 32	0.2 ± 0.3
BR08-9	Kosi	Kursela	23 ± 24	0.3 ± 0.1	76 ± 24	16 ± 5	64 ± 21	20 ± 6	13 ± 14	79 ± 31	9 ± 11
BR10-32	Kosi	Kursela	77 ± 24	1 ± 0.1	22 ± 24	20 ± 3	78 ± 19	3 ± 2	16 ± 8	82 ± 24	1 ± 2
Tributaries_Plain											
BR08-20	Batane	Gheura	20 ± 8	1 ± 0.3	79 ± 7	18 ± 5	42 ± 10	43 ± 4	39 ± 19	57 ± 21	4 ± 6
BR08-3	Dardha	Dhanarua	30 ± 10	2 ± 0.4	68 ± 10	25 ± 6	48 ± 11	30 ± 5	41 ± 18	54 ± 19	2 ± 4
BR08-5	Harhar	Lakhisarai	27 ± 9	1 ± 0.3	71 ± 9	25 ± 5	44 ± 11	35 ± 5	43 ± 19	52 ± 19	3 ± 4
BR08-34	Karmnasha	Naubatpur	33 ± 12	2 ± 0.6	65 ± 12	23 ± 5	55 ± 13	23 ± 4	34 ± 16	61 ± 21	2 ± 3
BR08-7	Kiul	Lakhisarai	11 ± 7	1 ± 0.3	87 ± 7	12 ± 4	42 ± 10	48 ± 4	28 ± 18	69 ± 25	5 ± 8
BR08-18	Phalgu	Gaya	6 ± 7	1 ± 0.3	92 ± 7	8 ± 4	44 ± 11	47 ± 4	16 ± 18	83 ± 30	6 ± 9
BR08-1	Punpun	Gourichak	34 ± 11	2 ± 0.5	64 ± 11	25 ± 6	53 ± 12	25 ± 4	39 ± 17	55 ± 20	2 ± 3
BR08-24	Punpun	Aurangabad	39 ± 11	2 ± 0.4	59 ± 11	28 ± 6	46 ± 11	26 ± 5	49 ± 20	49 ± 18	2 ± 3
BR8140	Son	Koilwar	28 ± 11	2 ± 0.5	70 ± 11	20 ± 5	54 ± 12	24 ± 4	33 ± 16	67 ± 24	2 ± 3
BR08-27	Son	Dehri	15 ± 9	2 ± 0.4	83 ± 8	13 ± 5	49 ± 12	37 ± 4	26 ± 17	72 ± 26	3 ± 6
BR08-22	North Koel	Garikhas	12 ± 8	2 ± 0.4	86 ± 8	11 ± 4	48 ± 11	40 ± 4	25 ± 17	74 ± 27	4 ± 7

(Continued on next page)

Table 3.6A:Source apportionment of Na, Cations and Sr using 3 endmembers* (continued).

Sample	River	Place	%Na$_{Sil}$	%Na$_{Carb}$	%Na$_{SAS}$	%Cation$_{Sil}$	%Cation$_{Carb}$	%Cation$_{SAS}$	%Sr$_{Sil}$	%Sr$_{Carb}$	%Sr$_{SAS}$
Ganga Mainstream_before mixing with Yamuna											
GP09-135	Ganga	Kanpur	59 ± 11	1 ± 0.2	40 ± 11	47 ± 7	34 ± 9	15 ± 4	27 ± 10	53 ± 17	27 ± 9
GP09-167	Ganga	Garhmukteshwar	87 ± 4	3 ± 1	10 ± 4	41 ± 5	59 ± 14	2 ± 1	19 ± 6	74 ± 22	3 ± 2
BR10-14	Ganga	Kanpur	70 ± 8	4 ± 1	25 ± 8	30 ± 3	65 ± 15	4 ± 1	12 ± 4	83 ± 24	6 ± 2
BR10-18	Ganga	Allahabad	59 ± 10	3 ± 1	37 ± 10	30 ± 4	61 ± 14	7 ± 5	12 ± 4	78 ± 23	11 ± 4
Gomti											
BR8125	Gomti	Ghazipur	14 ± 19	0.09 ± 0.03	86 ± 19	17 ± 11	40 ± 14	46 ± 10	10 ± 13	13 ± 8	75 ± 20
GP09-143	Gomti	Lucknow	56 ± 20	0.13 ± 0.04	44 ± 20	40 ± 10	44 ± 15	18 ± 8	41 ± 18	20 ± 13	42 ± 20

Table 3.6B: Source apportionment of Na, Cations and Sr using 4 endmembers*.

Sample	River	Place	%Na$_{Sil}$	%Na$_{Carb}$	%Na$_{SAS}$	%Na$_{Deccan}$	%Cat$_{Sil}$	%Cat$_{Carb}$	%Cat$_{SAS}$	%Cat$_{Deccan}$	%Sr$_{Sil}$	%Sr$_{Carb}$	%Sr$_{SAS}$	%Sr$_{Deccan}$
Yamuna														
BR10-22	Yamuna	Allahabad	20 ± 19	0.03 ± 0.02	77 ± 19	4 ± 4	24 ± 12	29 ± 14	43 ± 11	9 ± 7	20 ± 21	6 ± 4	68 ± 20	6 ± 7
Deccan Rivers														
GP09-21	Chambal	Gandhi Sagar Dam	7 ± 7	0.1 ± 0.03	75 ± 8	17 ± 6	10 ± 4	16 ± 7	40 ± 4	35 ± 8	4 ± 4	26 ± 13	47 ± 10	24 ± 8
GP09-30	Chambal	Dhaulpur	16 ± 10	0.04 ± 0.02	73 ± 9	11 ± 5	19 ± 8	10 ± 5	49 ± 6	28 ± 8	11 ± 8	15 ± 11	56 ± 12	18 ± 8
GP09-24	Kali Sindh		6 ± 6	0.2 ± 0.06	71 ± 9	23 ± 9	7 ± 3	30 ± 11	30 ± 4	38 ± 10	2 ± 2	40 ± 18	30 ± 7	21 ± 9
GP09-3	Rewa	Bhanpura	41 ± 12	0.2 ± 0.06	44 ± 10	14 ± 9	30 ± 7	27 ± 10	18 ± 4	23 ± 9	19 ± 9	45 ± 20	23 ± 7	16 ± 10
Ganga Mainstream_after mixing with Yamuna														
BR8109	Ganga	Patna	42 ± 12	1 ± 0.2	52 ± 11	5 ± 4	26 ± 5	54 ± 14	17 ± 4	7 ± 4	43 ± 16	37 ± 14	13 ± 10	4 ± 4
BR8129	Ganga	Varanasi	33 ± 13	1 ± 0.2	61 ± 12	5 ± 4	25 ± 6	45 ± 13	23 ± 5	9 ± 5	41 ± 19	33 ± 13	18 ± 14	6 ± 5
BR8136	Ganga	Fatuha	46 ± 11	1 ± 0.2	46 ± 11	7 ± 5	26 ± 5	53 ± 14	14 ± 3	9 ± 4	45 ± 16	39 ± 13	11 ± 8	6 ± 4
BR08-11	Ganga	Manihari	35 ± 13	2 ± 0.4	49 ± 11	15 ± 8	18 ± 3	58 ± 15	10 ± 2	14 ± 5	30 ± 14	54 ± 20	10 ± 8	11 ± 6
BR10-24	Ganga	Varanasi	40 ± 12	1 ± 0.2	52 ± 11	7 ± 5	28 ± 5	42 ± 12	18 ± 4	12 ± 5	45 ± 18	31 ± 12	14 ± 11	7 ± 5
BR10-29	Ganga	Patna	61 ± 10	2 ± 0.4	30 ± 9	7 ± 6	26 ± 3	63 ± 17	6 ± 2	7 ± 3	41 ± 13	48 ± 17	5 ± 4	4 ± 4
BR10-35	Ganga	Manihari	61 ± 11	2 ± 0.5	27 ± 8	9 ± 8	23 ± 3	64 ± 17	4 ± 1	7 ± 3	37 ± 11	53 ± 19	4 ± 3	5 ± 4

*The Suffixes Sil, Carb, HS, SAS and Deccan represent silicates, carbonates, hotsprings, saline alkaline soils and Deccan basalts respectively.

Samples with code GP are collected during non-monsoon.

sample. In 2008, sever small tribuatires such as the Son, Punpun, Kiul and Karmanasha and their tributaries draining mostly in plain were sampled to study the weathering in the plain. Some of them were flooded at the time of sampling. The Deccan rivers, i.e., Chambal, Rewa and Kali Sindh, were sampled during lean flow of 2009, and they have 17-38% saline-alkaline soil contribution in their major ion chemistry.

Silicate and carbonate contributions to Na and cation budgets of the Ganga system based on inverse model are given Table 3.6A and B. Based on these estimates silicate and carbonate erosion rates are estimated in the following sections.

3.2.5 Silicate and carbonate erosion rates

Silicate and carbonate erosion rates (SER and CER respectively) for the Ganga and major tributaries have been calculated after apportioning the sources of dissolved ions using the equations

$$SER = (Q/A)\times(Na_S + Ca_S + Mg_S + K + (SiO_2)_S)\ldots\ldots\ldots\ldots\ldots\ldots\ldots\ldots(7)$$

$$CER = (Q/A)\times (Na_C + Ca_C + Mg_C + (CO_3)_C)\ldots\ldots\ldots\ldots\ldots\ldots\ldots\ldots(8)$$

in units of tons/km^2/year. CO_2 consumption rate has been calculated using

$$CO_2 \text{ consumption rate} = (Q/A)\times (Na_S + K + 2\times (Ca_S + Mg_S)) \qquad \ldots\ldots\ldots.(9)$$

in units of moles/km^2/yr. In these equations Q and A represent annual water discharge and drainage area of the river respectively. The subscript S denotes contribution from silicates. Silicate fraction of SiO_2 is considered for SER estimation (eqn. 7) as some amount of silica comes from dissolution of saline - alkaline soils. This was corrected using SiO_2/Na measured in water extracts of saline-alkaline soils. Gomti (monsoon), Yamuna (monsoon) and Chambal have very low dissolved SiO_2, therefore it was assumed that all of the present SiO_2 in

Table 3.7: Silicate and carbonate erosion rates and CO_2 consumption rate of the Ganga river system.

River	Place	Date	Drainage area (10^3 Km^2)	discharge (10^9 m^3 yr^{-1})	SER (tons km^{-2} yr^{-1})	SER (mm kyr^{-1})	CER (tons km^{-2} yr^{-1})	CER (mm kyr^{-1})	CO2 consumption Rate (10^5 mol km^{-2} yr^{-1})
Headwaters									
Alaknanda	Devprayag	August 2010	11.8	14.1	12.3 ± 0.6	4.7 ± 0.2	44 ± 13	16 ± 5	2.4 ± 0.4
Bhagirathi	Devprayag	August 2010	7.8	8.3	10.9 ± 0.7	4.2 ± 0.3	19 ± 6	7 ± 2	2.4 ± 0.4
Ganga	Kaudiyala	August 2010	21.7	23.9	12.0 ± 0.7	4.6 ± 0.3	36 ± 10	13 ± 4	2.3 ± 0.4
Yamuna	Rampur Mandi	August 2010	9.6	10.8	18.2 ± 1.2	7.0 ± 0.5	36 ± 11	13 ± 4	3.8 ± 0.7
Ganga outflow									
Ganga	Manihari	August 2008	935	380	4.2 ± 0.4	2.1 ± 0.1	22 ± 6	8 ± 2	1.6 ± 0.2
Ganga	Manihari	August 2010	935	380	5.7 ± 0.4	2.2 ± 0.1	24 ± 6	9 ± 2	1.3 ± 0.2
Tributaries_Himalaya									
Yamuna	Allahabad	August 2010	366	131.7	4.5 ± 2.2	1.7 ± 0.8	17 ± 8	6 ± 3	2.0 ± 1.1
Ghaghra	Dohrighat	August 2008	128	94.4	8.5 ± 0.4	3.3 ± 0.2	55 ± 14	21 ± 5	1.5 ± 0.2
Ghaghra	Revelganj	August 2010	128	94.4	7.5 ± 0.3	2.9 ± 0.1	53 ± 14	20 ± 5	1.0 ± 0.1
Gandak	Hajipur	August 2008	46.3	52.2	11.4 ± 0.2	4.4 ± 0.1	80 ± 21	30 ± 8	1.0 ± 0.1
Gandak	Sonpur (near Patna)	August 2010	46.3	52.2	11.7 ± 0.2	4.5 ± 0.1	83 ± 22	31 ± 8	1.1 ± 0.1
Kosi	Kursela	August 2008	74.5	62	8.5 ± 0.9	3.3 ± 0.4	39 ± 13	14 ± 5	1.2 ± 0.4
Kosi	Kursela	August 2010	74.5	62	9.4 ± 0.5	3.6 ± 0.2	38 ± 10	14 ± 4	1.3 ± 0.2
Tributaries_Plain									
Gomti	Ghazipur	August 2010	30.5	7.4	2.0 ± 1.1	0.8 ± 0.4	14 ± 5	5 ± 2	0.9 ± 0.5
Karmnasha	Naubatpur	August 2008	11.7	5.8	4.3 ± 0.7	1.6 ± 0.3	23 ± 10	8 ± 2	1.3 ± 0.3
Kiul	Lakhisarai	August 2008	16.6	5.9	1.8 ± 0.6	0.7 ± 0.2	20 ± 6	7 ± 2	0.8 ± 0.3
Punpun	Gourichak	August 2008	8.5	3.6	4.7 ± 0.9	1.8 ± 0.3	26 ± 5	10 ± 2	1.8 ± 0.4
Son	Koilwar	August 2008	71.2	31.8	4.9 ± 0.4	1.9 ± 0.1	14 ± 6	5 ± 1	0.7 ± 0.2
Chambal	Dhaulpur	March 2009	23	4.8	4.2 ± 1.6	1.6 ± 0.6	7 ± 4	2 ± 1	1.9 ± 0.8

these samples are coming from saline-alkaline soils, because of their high solubility. Results of these calculations are given in Table 3.7.

SER of the Ganga at Kaudiyala (near Rishikesh) 12.0 tons/km^2/yr (Fig. 3.12) agrees well with earlier estimates e.g. 13.0 tons/km^2/yr by Tripathy et al., (2010) and 12.9 tons/km^2/yr by Krishnaswami et al., (1999). SER in the headwaters of the Ganga is higher than the global average (5.4 tons/km^2/yr). But at Manihari, SER of the Ganga has been calculated to be 4.2 and 5.7 tons/km^2/yr for 2008 and 2010 monsoons respectively, which is less than half of the earlier estimate (13.6 tons/km^2/yr by Krishnaswami et al., 1999). Erosion rates in the headwater region and plain are not same, therefore averaging of the Himalayan erosion for the whole basin would certainly give either over or under estimate of erosion rate. The SER in the Ganga plain seems to be less compared to that in the Himalaya, which explains the difference between two estimates.

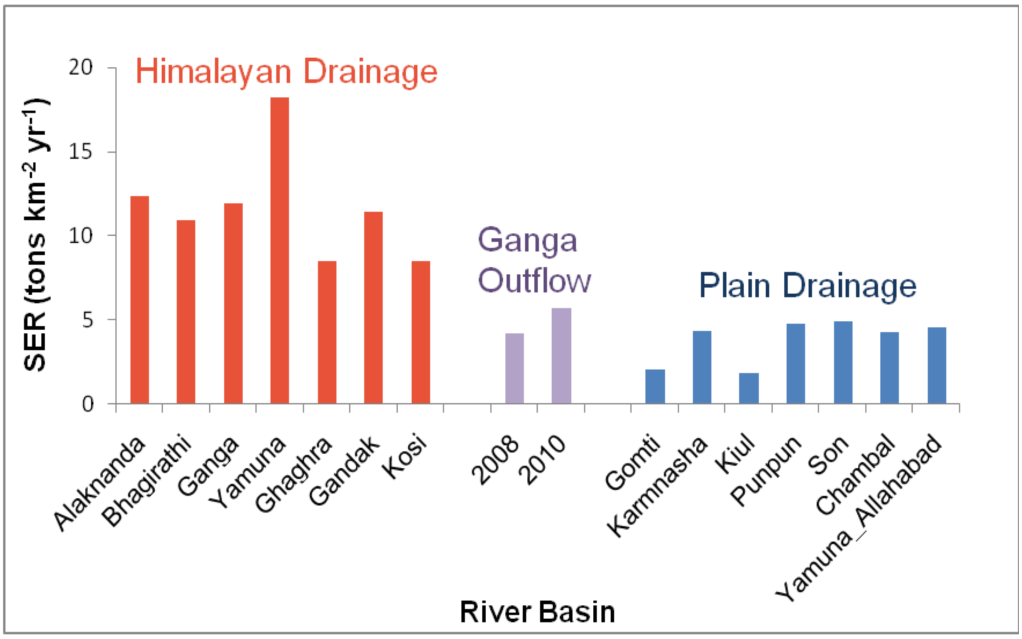

Fig. 3.12: *SER of the Ganga system in the Himalaya is higher compared to that in the Plain and peninsula*

SER of the Yamuna at Rampur Mandi, 18.2 tons/km^2/yr is considerably lower than that of the Yamuna headwaters reported by Dalai et al, 2002 (28 tons/km^2/yr) but is closer to the estimate by Tripathy et al., (2010) (13.5 tons/km^2/yr). This spatial variation in the SER of Yamuna in the headwater region has been observed earlier also (Tripathy et al., 2010). Presence of saline-alkaline soils in the lower reaches of Yamuna could give rise to over estimation in earlier estimates of SER. In the present study, the sample was collected from Rampur Mandi, and saline - alkaline soils are not very common in those area. Yamuna at Allahabad shows SER of 4.5 tons/km^2/yr which is similar to the estimation made by Rai et al., (2010), (3.9 tons/km^2/yr). This sharp decrease in SER from Himalaya to the plain, confirms the lower chemical erosion in the plain (fig. 3.12). Ghaghra and Gandak both have lower SER (for Ghaghra 8.5 and 7.5 tons/km^2/yr and for Gandak 11.4 and 11.7 tons/km^2/yr) in the plain compared to their headwaters counterpart (Tripathy et al, 2010) and the present result agrees well with Rai et al., (2010). Kosi also has lower SER (8.5 and 9.4 tons/km^2/yr respectively) in plain compared to that in the Himalaya (10.1 tons/km^2/yr) (Tripathy et al, 2010). Gomti in monsoon has a value of 2 tons/km^2/yr of SER which is lower compared toall other major tributaries and to the value reported in Rai et al., 2010 (2.6 tons/km^2/yr). The SER of the small tributaries in the plain varies between 1.8- 4.9 tons/km^2/yr, which are less than the SER of the Ganga mainstream at Manihari. Rai et al., (2010) has used chloride corrected Na as a proxy of SER in case of the Son. Their estimate (10.7 tons/km^2/yr) is double of the present estimate (4.9 tons/km^2/yr), which confirms the over-estimation by this proxy. The estimated SER of Chambal (4.2 tons/km^2/yr) is less than the value reported in Rengarajan et al., 2009 (5.7 tons/km^2/yr). They have used Si as a proxy and non-conservative behaviour of Si would only make it a lower estimate. Supply of SiO_2 from saline-alkaline soils could have resulted lower SER estimated in present study.

The above discussion shows that silicate erosion rate in the plain is less intense compared to that in the headwater region (Fig. 3.12) contrary to the study of Lupker et al., (2012) based on sediment composition of the river. The causes for difference in silicate erosion rates based on chemical composition of dissolved (this study) and particulates (Lupker et al., 2012) need to be examined. It could arise due to the large uncertainties in fluxes of water and sediments and/or contribution of paleo-weathered sediments from the plain to the rivers. In the later study difference between sediment compositions in the headwaters and plain has been used to estimate the SER. As it is difficult to determine the weathering history of the sediments in plain, the estimation of contemporary SER using dissolved components is more agreeable. Higher SER in the headwaters compared to that in the plain implies more dependence of chemical erosion on physical erosion and hence availability of freshly eroded materials compared to temperature, residence time etc.

CER of the Ganga at Kaudiyala (Rishikesh) shows a lower estimate (36±10 tons/km^2/yr) than earlier studies, e.g., 51.7 tons/km^2/yr by Krishnawami et al., (1999), 54 tons/km^2/yr by Dalai et al, (2002), but is similar to the value 45.1 tons/km^2/yr reported by Tripathy et al, 2010 based on inverse model. The reason behind this difference could be the presence of hotsprings in this region and impact on incongruent weathering, which were not accounted for in the earlier two studies. The relative amount of water coming from Bhagirathi and Alaknanda (because of dams) and calcite precipitation could also be possible causes of this difference. For the same reasons, CER of the Yamuna at Rampur Mandi (36 tons/km^2/yr) agrees well with earlier study by Tripathy et al, (2010), but is much less compared to the value (115 tons/km^2/yr) reported by Dalai et al., (2002). Yamuna at Allahabad has CER of 7 tons/km^2/yr, which is in accordance with the available study (Rai et al., 2010). Here also, the decrease in chemical weathering in the plain after the Himalaya is clearly observed. CER of Ghaghra (55 and 53 tons/km^2/yr for 2008 and 2010 respectively) shows similarity with its headwater CER (Tripathy et al., 2010). Gandak has CER of 80 and 84 tons/km^2/yr for the year 2008 and 2010 respectively, which is less than its headwaters CER (Tripathy et al., 2010). Both of these rivers have lower CER than earlier estimates in the plain (Rai et al., 2010), which could come either from difficulty in source apportionment in absence of suitable proxy or calcite precipitation. The estimated CER of the Kosi (39 and 38 tons/km^2/yr for 2008 and 2010) agrees well with the available data (Rai et al., 2010). CER of the Ganga at Manihari (22 and 24 tons/km^2/yr for 2008 and 2010 respectively) is quite lower than that of the headwaters region. All these rivers have less carbonate weathering rate in the plain compared to the headwaters except the Kosi. Lower relief and run-off in the plain along with limited supply of freshly eroded material could explain the above observation. The Kosi is different from the others in nature due to its lateral movement, which would act as a source of un-weathered material. The Gomti shows CER of 14 tons/km^2/yr which is quite lower than the earlier estimate (Rai et al., 2010). The small tributaries from plain have CER which varies from 14 to26 tons/km^2/yr. The estimated CER of the Son (14 tons/km^2/yr) is almost half of the earlier estimate (Rai et al., 2010). Possible reasons behind these differences are already discussed.

The CO_2 consumption rate (2.3±0.4 moles/km^2/yr) in Ganga headwaters is similar with earlier estimates by Tripathy et al, (2010) (2.3 moles/km^2/yr) and Dalai et al, (2002) (~2 moles/km^2/yr). The CO_2 consumption rate of the Yamuna (3.8±0.7 moles/km^2/yr) is almost double compared to the Ganga headwaters but is less than the same reported by Dalai et al., (2002). The CO_2 consumption rate calculated at Manihari (1.6 and 2.2 moles/km^2/yr) is quite less than that of headwaters and is half of the earlier estimate (Krishnaswami et al., 1999). Other tributaries also have lower CO_2 consumption rate (Ghaghra, Gandak, Kosi ~1 moles/km^2/yr) in the plain than in headwater regions (This study, Tripathy et al, 2010). The small tributaries in the plain have CO_2 consumption rate varying from 0.7 to 1.8 moles/km^2/yr which are similar to that of the mainstream. The estimated CO_2 consumption rate by silicate weathering of Gomti is 0.9 moles/km^2/yr in monsoon

The above discussion shows that weathering processes in the plain is not similar to headwater regions and hence it is not possible to average out this total drainage basin using headwater values. It is true that the Ganga has higher SER and CO_2 consumption rate in the headwater regions than most of the global rivers, but near outflow to the ocean it is not distinctly different than other global rivers. The lower erosion rate in the plain is probably due to less relief and run-off. Present study indicates towards physical erosion as the main controlling factor behind chemical erosion, and lesser importance of temperature or vegetation. This study also quantifies the contribution of saline-alkaline soils to the rivers in the Ganga plain.

3.3 Conclusion

A detailed study of the Ganga river system has been carried out with the aim of characterizing saline-alkaline soil present in the basin, determining its contribution to river chemistry and estimating the silicate and carbonate erosion rate at the outflow after accounting for the possible contribution of saline-alkaline soils. The erosion pattern in the plain was also of interest and hence, samples from a number of small tributaries have also been analyzed. An inverse model has been used to apportion the sources of dissolved ions.

The results show 4-10% cation and 27-49% of dissolved Na contribution from saline-alkaline soils at the outflow of the Ganga. This high Na contribution is particularly damaging for all forward model estimation of silicate erosion using Na as a proxy. Our results show that earlier estimates of silicate erosion rate using Na as a proxy at the outflow were considerably over-estimated.

Silicate erosion rate of the Ganga mainstream at the outflow is estimated to be 4.2 – 5.7 tons/km^2/yr, which less than half of that in the headwaters. The Hiamlayan tributaries like Ghaghra, Gandak show similar or lower silicate and carbonate erosion rate in the plain, than the headwaters. Yamuna have a high contribution from saline-alkaline soils, in monsoon as well as non-monsoon, owing to its presence in the plain and in the Deccan tributaries. The Kosi shows very different kind of erosion pattern during flood events.

60 – 92% of dissolved Na contribution in the small tributaries in plain is of saline-alkaline soil origin and silicate and carbonate erosion rates in these sub-basins are quite low compared to the Himalayan region. Though they have higher temperature, vegetation, residence time of sediments than the Himalayan rivers, physical erosion producing larger surface area and freshening of sediments is insignificant in them. The results show very low silicate cation contribution (8 – 28%) in the tributaries from plain, which indicates towards importance of physical erosion among the controlling factors of chemical erosion.

Chapter 4

Dissolved Nd in the Ganga river system and its flux to the Bay of Bengal

4.1 Introduction

As has been discussed in previous chapter, the origin and evolution of the Himalaya is an important earth surface process and has played significant role in influencing global climate and carbon and geochemical budget of the global oceans. Several studies has been carried out till date to understand geophysical and/or geochemical processes like tectonic-erosion-climate coupling (Raymo et al., 1988; Molnar and England, 1990; Raymo and Ruddiman, 1992; Sarin et al., 1992; Richter et al., 1992; France-lanord and Derry, 1997; Singh et al., 2008; Lupker et al., 2013). Major elements, Sr and Nd isotope compositions in waters and sediments of the Ganga and the Brahmaputra, an important River System of the Himalaya have been studied (Krishnaswami et al., 1999; Galy and France-Lanord, 2001; Bickle et al., 2005; Singh et al., 2006; Rai and Singh, 2007; Singh et al., 2008; Lupker et al., 2013) to understand physical and chemical erosion processes, their controlling factor and their impact on carbon, geochemical and sedimentary cycles. Sr-Nd isotope systematic of the sediments of the G-B system have been used successfully to study sediment provenance and to trace relative proportion of various litho-tectonic units, e.g., the Higher Himalaya (HH), the Lesser Himalaya (LH) etc (France-Lanord et al., 1993; Singh et al., 2008) as various litho-tectonic units of the Himalaya have very distinct Sr and Nd isotopic signatures and it has been inferred that the Higher Himalaya is the major source of sediments to these system due to higher relief and precipitation (Singh and France-Lanord, 2002; Singh et al., 2008). Sources of dissolved material to the Ganga from the different lithotectonic units of the Himalaya are still debated. It is being inferred that though physical erosion in the Himalaya is dominated by contribution from the HH, LH contributes significantly to the dissolved budget due to higher temperature, abundant vegetation and enough precipitation occurring over it. Estimates on the supply of dissolved material from some of these formations such as the Tethyan sedimentary series, Higher and Lesser Himalayan Crystallines, though, exist; they are subject to uncertainty as these estimates are based mainly on major ion and Sr isotope budget of the rivers draining through them. These chemical erosion budgets are further compounded due to the presence of carbonate in each geological unit. Isotope composition of the dissolved Nd in the Ganga river system may have the potential to track the sources of dissolved material in the basin in terms of different litho-units as they are characterised by different isotope compositions. Dissolved Nd in rivers is mostly derived from silicates with very little contribution from carbonates and hence it has the ability to track the silicate sources in the Himalaya. In view of this, a detailed study of the Nd isotope systematic in the Ganga from its headwaters to its outflow near Farakka (at Indo-Bangladesh border), is carried out as part of this thesis. It is worth mentioning here that this will be the first work on the dissolved Nd of the Himalayan rivers. This study will further provide a better understanding of Nd transport via the Ganga and its contribution to the Nd budget of the Bay of Bengal (BoB). Nd isotopic composition is used as a water mass tracer in marine environments (Frank, 2002) owing to its short residence time in the ocean. A few studies in the BoB and Indian Ocean (Burton and Vance, 2000; Gourlan et al., 2010) have brought out the importance of Himalayan contribution to the Nd budget of the BoB and inferred the variation in the Nd fluxes from the Ganga-Brahmaputra over glacial-interglacial cycles. In absence of dissolved Nd isotope composition of the G-B, earlier workers have considered its particulates' value similar to dissolved component. This study aims to provide the flux and isotope composition of dissolved Nd delivered by the Ganga river to the Bay of Bengal. In addition, Nd content and ε_{Nd} in samples collected from coastal Bay of Bengal has been analysed to assess the impact of estuarine transfer and interaction with coastal sediments (Lacan and Jeandel, 2001) as these processes lead to exchange of Nd isotope composition.

Application of dissolved Nd isotope composition in identifying the sources of chemical weathering over the Himalaya, however, would depend on how well it represents the source litho-unit. Underlying assumption in using dissolved Nd isotope composition as source indicator is its congruent weathering. It is being assumed that isotope composition of Nd is not getting fractionated while weathering. In case of particulate matter, this assumption could be valid as very small fraction of Nd of a given rocks gets chemically weathered without altering its composition in sediments, particularly in bedload. Rare Earth Elements (REEs) are hosted mostly in refractory minerals, least susceptible to weathering whereas minor component could be in minerals such as feldspar, apatite or allanite which could weather easily. Variable intensity of weathering of REE hosting minerals could lead to fractionation in Sm/Nd ratio and hence in Nd isotope composition in dissolved load with respect to its source rock. Few studies have reported such fractionation in Nd isotope composition during weathering (Öhlander et al., 2000; Viers and Wasserburg, 2004; Stille et al., 2009).In such case, it could be difficult to use Nd isotope composition of dissolved load as their source indicator. To study the impact of fractionation of Nd isotope composition during weathering in the Ganga system, Nd concentration and its isotope composition have been analysed in both particulate and dissolved phases at the same sites.

In this study, Nd isotopic composition in the dissolved phase of the Ganga river system have been analysed for two monsoon seasons to (i) assess the impact of weathering on Nd isotope composition in dissolved phase, (ii) track the sources of dissolved material based on their litho-units, i.e. the Higher and the Lesser Himalaya, (iii) provide the flux of Nd and its isotope composition to the BoB, (iv) study the behaviour of dissolved Nd in coastal BoB.

4.2 Results and Discussion

Dissolved Nd and its isotope composition in the waters of the Ganga mainstream and its tributaries were measured for two year sampling (2008 and 2010) and the results are listed in Table 4.1 and 4.2. The corresponding funnel diagram is shown in Fig. 4.1 and 4.2. Along with dissolved Nd, Table 4.1 consists of Nd isotope composition of particulate matter which were taken from Singh et al., (2008). Nd concentration in the Ganga mainstream varies from 43-541 pmol/kg. Apart from the highest value of 541 pmol/kg measured at Patna in 2008, most of them are having Nd below 100 pmol/kg. Among the Himalayan tributaries, the Kosi and the Alaknanda have highest Nd concentration, excluding Yamuna. The Gandak

Table 4.1: Dissolved Sm, Nd concentration and Nd isotopic composition in river water samples. Sediment ε_{Nd} data in last two columns are taken from Singh et al. (2008) for comparison.

Sample code	River	Place	Year	Sm (pmol/kg)	Nd (pmol/kg)	Sm/Nd	ε_{Nd}	σ_{μ}	Sediment ε_{Nd}	
									Bulk	fine (<4 μ)
Ganga Mainstream										
BR10-12	Ganga	Kaudiyala	2010	23	90	0.26	-15.8	0.1	-18.1	-17.4
BR10-14	Ganga	Kanpur	2010	18	63	0.28	-14.3	0.1	--	--
BR10-18	Ganga	Allahabad	2010	37	151	0.25	-14.0	0.2	-17.3	-15.7
BR8129	Ganga	Varanasi	2008	11	45	0.24	-11.5	0.2	-17.1	-18.8
BR10-24	Ganga	Varanasi	2010	14	52	0.26	-13.1	0.1		
BR8109	Ganga	Patna	2008	114	541	0.21	-12.0	0.2	-21.3	--
BR10-29	Ganga	Patna	2010	11	43	0.26	-13.9	0.1		
BR08-11	Ganga	Manihari	2008	19	90	0.21	-14.2	0.3	-18.1	-16.1
BR10-35	Ganga	Manihari	2010	10	44	0.23	-15.3	0.1		
Tributaries_Himalaya										
BR10-7	Alaknanda	Devprayag	2010	20	72	0.27	-16.9	0.2	-17.1	--
BR10-4	Bhagirathi	Devprayag	2010	44	165	0.27	-13.5	0.1	-19.9	--
BR10-22	Yamuna	Allahabad	2010	178	719	0.25	-12.2	0.2	-17.7	--
BR8110	Ghaghra	Revelganj	2008	19	96	0.20	-14.9	0.1	-18.2	-17.4
BR10-44	Ghaghra	Revelganj	2010	8	29	0.26	-14.7	0.1		
BR8121	Rapti	Gorakhpur	2008	n.m.	n.m.	--	-14.5	0.2	-17.0	-15.9
BR8105	Gandak	Hajipur	2008	9	41	0.22	-16.0	0.2	-18.6	--
BR10-26	Gandak	Sonpur	2010	8	40	0.21	-16.6	0.2		
BR08-9	Kosi	Kursela	2008	34	166	0.20	-14.9	0.8	-18.6	--
BR10-32	Kosi	Kursela	2010	18	74	0.24	-15.9	0.1		
Tributaries_Plain										
BR8125	Gomti	Ghazipur	2008	39	166	0.23	-14.9	0.2	-19.4	--
BR08-1	Punpun	Gourichak	2008	47	272	0.17	-16.6	0.2	--	--
BR8140	Son	Koilwar	2008	18	106	0.17	-15.2	0.3	--	--

Table 4.2: Dissolved Sm, Nd concentration and Nd isotopic composition in coastal Bay of Bengal.

Sample code	Latitude N	Longitude E	Sample depth (m)	Sm (pmol/kg)	Nd (pmol/kg)	Sm/Nd	ε_{Nd}	σ_{μ}
0814-4	20°32'	87°29'	4	29	61	0.48	-11.2	0.3
0814-45	20°32'	87°29'	45	11	49	0.23	-13.7	0.2
0815-4	20°59'	87°47'	4	14	64	0.22	-11.2	0.2
0815-30	20°59'	87°47'	30	15	71	0.21	-14.4	0.4
0816-4	20°54'	88°06'	4	14	52	0.26	-12.8	0.3
0816-30	20°54'	88°06'	30	14	54	0.26	-13.4	0.3
0817-5	20°50	88°30'	5	12	50	0.24	-12.0	0.3
0817-70	20°50	88°30'	70	16	45	0.35	-14.0	0.3
0818-5	21°00'	88°60'	5	11	47	0.24	-8.5	0.4
0818-60	21°00'	88°60'	60	8	34	0.24	-14.4	0.3
0819-5	20°35'	88°45'	5	10	49	0.21	n.m.	n.m.
0819-110	20°35'	88°45'	110	6	26	0.22	-15.3	0.4
0820-5	20°35'	88°15'	5	12	53	0.22	-14.6	0.3
0820-110	20°35'	88°15'	110	n.m.	n.m.	--	-16.0	0.5

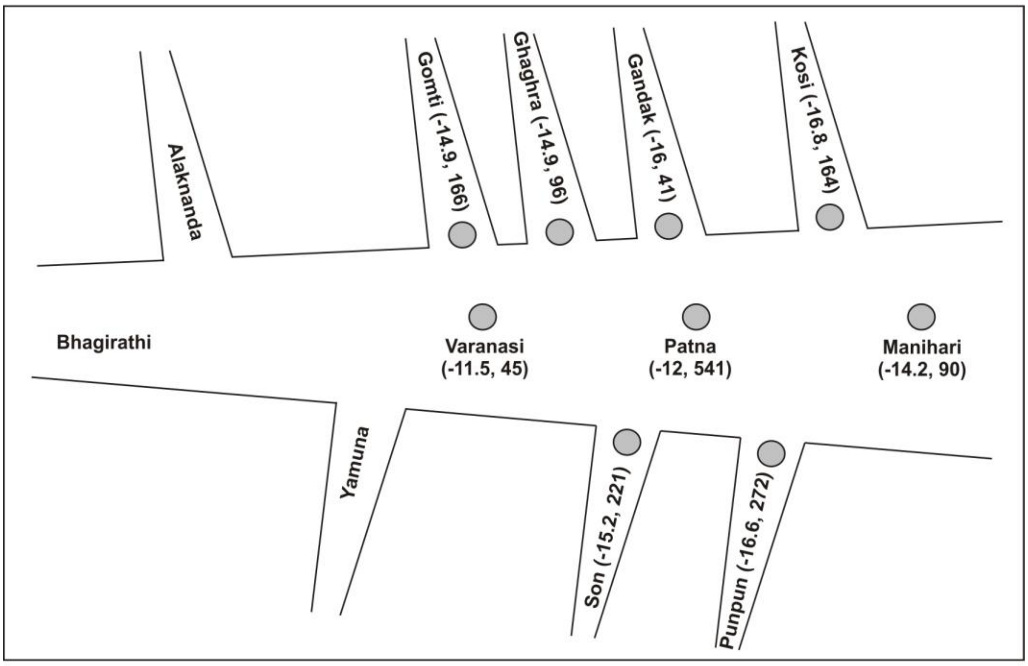

Fig. 4.1: *ε_{Nd} and Nd concentration in Ganga river system in 2008.*

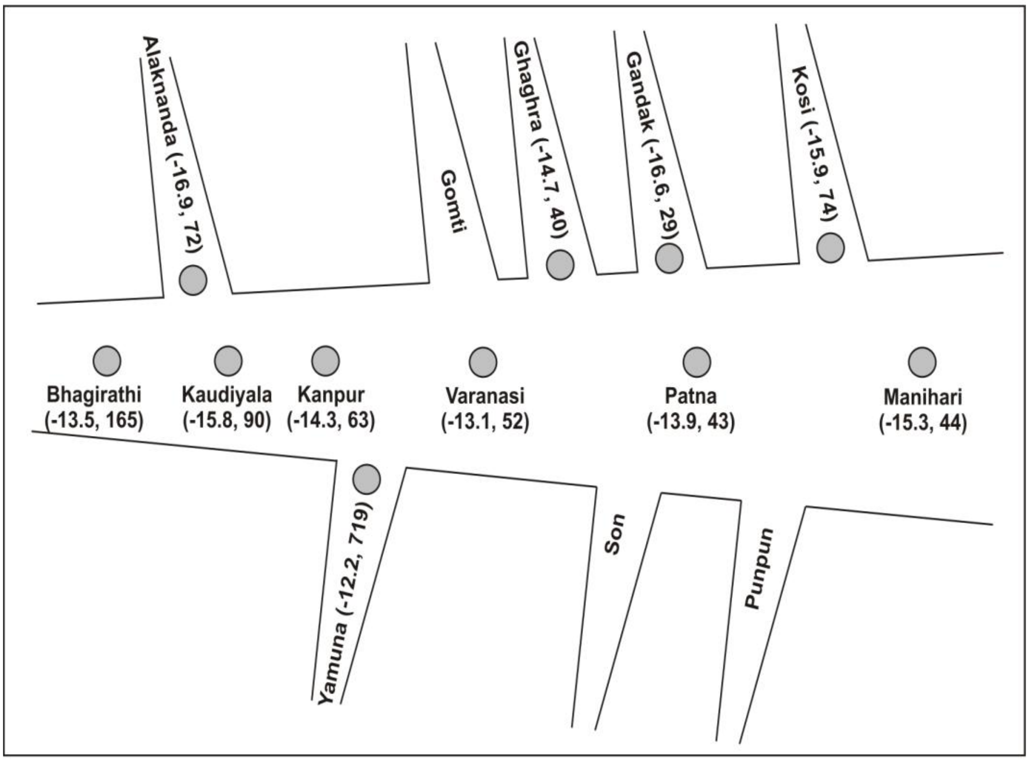

Fig. 4.2: *ε_{Nd} and Nd concentration in Ganga river system in 2010.*

shows consistent values of Nd concentration (40 pmol/kg) for both the years. Nd concentration in the Ghaghra and the Kosi display significant variability in two monsoon seasons, 29 and 74 pmol/kg (2008) and 96 and 166 pmol/kg (2010) respectively. Dissolved Nd concentration in these rivers depends on lithology they drain and the mixing proportion of various tributaries. Significant spatial variation observed in Nd concentration in these rivers could be due to its exchange with particles owing to its reactive nature or could be due to preferential leaching of Nd-rich minerals, e.g, apatite, allanite etc (Aubert, 2001; Garzanti et al., 2010; 2011). Further, it could vary with dissolved organic carbon content (Ingri et al., 2000). Small tributaries from plain (Gomti, Son, Punpun) show higher concentration of Nd compared to Himalayan tributaries. Their inputs to the Ganga during flood events could enhance the Nd concentration at Patna in 2008. The Ganga at outflow, Manihari has Nd concentration of 90 and 44 pmol/kg in 2008 and 2010 respectively. Higher Nd at outflow in 2008 could be due to higher contribution from flooded peninsular and plain rivers.

The Yamuna shows a value of 719 pmol/kg at Allahbad in 2010, which is almost one order of magnitude higher than all other tributaries, but quite in the range of the value observed in the Ganga at Patna in 2008. This exceptionally high value could be due to contribution from Deccan tributaries. The Chambal contributes almost 40% of the annual water budget of the Yamuna (Rao, 1979). It is probable that the Deccan tributaries contribute high concentration of dissolved Nd because of their basaltic lithology. Reported Average Nd concentration in the Yamuna river and its tributaries is 539 pmol/kg with a maximum of 1754 pmol/kg (Rengarajan and Sarin, 2004), which agrees well with the present data.

Dissolved Sm concentration in the Ganga mainstream range between 10 and 37 pmol/kg with one exception at Patna with 114 pmol/kg in 2008 (Table 4.1). This is the same sample having higher Nd. Sm/Nd display a range of 0.21 – 0.32 and 0.17 – 0.28 in the Ganga mainstream and its tributaries respectively. Two tributaries from plain, the Son and the Punpun has Sm/Nd ~0.17, lower compared to others rivers.

In 2008, samples were collected downstream Varanasi only. However, in 2010 samples were collected from the headwaters to the outflow. In 2010, the Ganga at Kaudiyala (near Rishikesh) shows ε_{Nd} value of -15.8 which could be explained using a mixture of the Alaknanda (-16.9) and Bhagirathi (-13.5) and represent the ε_{Nd} of the Ganga after it exits the Himalaya. By comparing the Himalayan tributaries (Ghaghra, Gandak and Kosi), it could be observed that they have nearly same ε_{Nd} value (within uncertainty) for both years. These tributaries supplying dissolved Nd with ε_{Nd} of around -16 after exiting the Himalaya to the Ganga mainstream. Samples from the small tributaries from the plain were collected in 2008 only. ε_{Nd} of the Gomti, Punpun and Son are -14.9, -16.6 and -15.2 respectively. ε_{Nd} of the Ganga is -11.5, -12.0 and -14.2 at Varanasi, Patna and Manihari respectively in 2008. But in 2010, ε_{Nd} of the Ganga at the same places are found to be less radiogenic, -13.1, -13.9 and -15.3 respectively. The radiogenic ε_{Nd} in the Ganga in 2008 compared to 2010 could be due to its higher contribution from the peninsular rivers through the Yamuna and the tributaries draining Deccan basalts. Unfortunately no data of Nd concentration or isotopic concentration of the same is available for the year 2008 due to lack of sampling. ε_{Nd} of the Yamuna is -12.2 with high concentration of Nd for 2010 sampling, which corroborates the previous explanation. ε_{Nd} in dissolved phase of the rivers draining the Deccan basalts is not available, however, sediments from Tapi river, which predominantly drains through Deccan basalts, have been reported to have radiogenic ε_{Nd} of -5.7 and -5.9 (Goswami et al., 2012). Other small west flowing rivers like Sukh, Vashishthi from the Deccan region have ε_{Nd} about -1.2 (Goswami et al., 2012). Therefore, if Chambal and other tributaries of the Yamuna draining the Deccan basalt follow the same trend in the dissolved phase, they can contribute radiogenic Nd to the Yamuna and hence to the Ganga mainstream. Moreover, the Yamuna basin was flooded during 2008 sampling, which could enhance the relative contribution of the Yamuna in the Ganga mainstream. This interpretation of higher contribution of the Yamuna to the

Ganga mainstream in 2008 compared to 2010 is also confirmed by Sr isotope composition (Fig. 4.3). $^{87}Sr/^{86}Sr$ of the Ganga mainstream downstream Varanasi is lower in 2008 compared to those in 2010 indicating enhance contribution from the Deccan region with lower $^{87}Sr/^{86}Sr$ via the Yamuna.

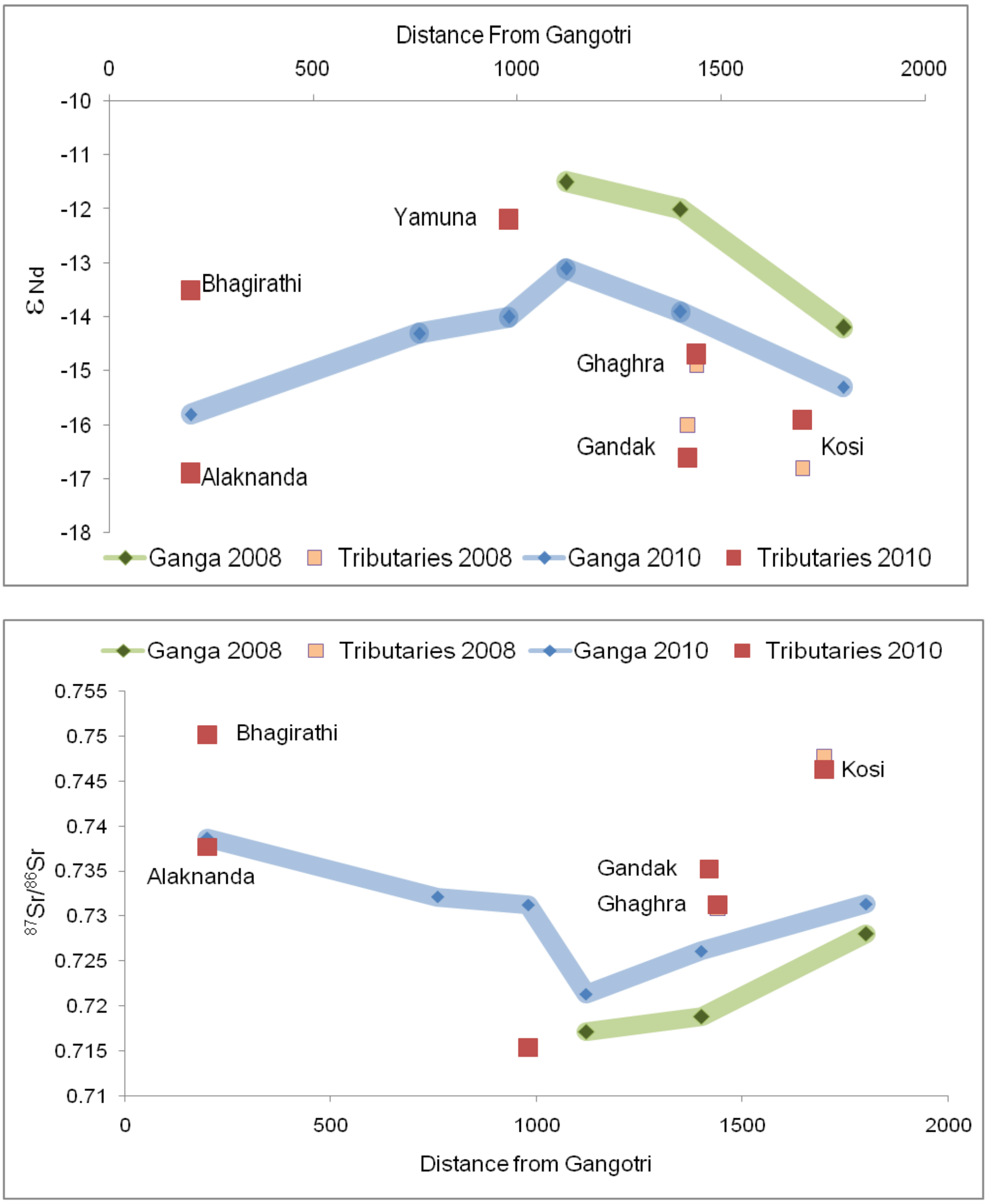

Fig. 4.3: *Variation in the Nd isotopic composition in the Ganga river system in 2008 and 2010 is probably due to higher contribution of deccan tributaries of the Yamuna in 2008. Similar variation has been observed in the Sr isotopic composition also.*

4.2.1 Sources of dissolved Nd and ε_{Nd} budget in the Ganga system

About 80% of the annual discharge of the Ganga is delivered during four monsoon months. This study has been carried out in two monsoon seasons to represent the majority of the fluxes. Most of the tributaries and the Ganga mainstream has been sampled during monsoon 2010. The Yamuna with its highest Nd content and water discharge supply much higher flux of Nd, ~9.5×10^4 moles/year compared to any other tributaries. The Kosi, Son, Ghaghra and Gandak contribute 0.46×10^4, 0.34×10^4, 0.27×10^4 and 0.20×10^4 moles Nd annually. Sum of Nd flux from all the major tributaries based on their Nd content (Table 4.1) and water discharge is ~1.1×10^5 moles/year. This estimate is much higher compared to the Nd flux of the Ganga at Manihari, ~1.7×10^4 to 3.4×10^4 moles/year. This large mismatch between the Nd flux estimated based on tributaries data and that of Ganga at Manihari is due to very high Nd flux of the Yamuna at Allahabad in 2010 (Table 4.1), reason for the same is not known at the moment. Assuming a more normal content of Nd in the Yamuna (~50 pmol/kg), the combined Nd flux of tributaries and the Ganga at the Manihari seem comparable. Such high spatial and temporal variability in Nd concentration is reported earlier in Kalix river which has been attributed to the highly particle reactive nature of Nd (Ingri et al., 2000).

In view of randomly varying Nd concentration in the river and large uncertainty in the water discharge, ε_{Nd} value of various tributaries has been used to calculate their relative contribution to the dissolve Nd budget. The Ganga gets Nd contribution mainly from the Himalaya and the peninsular basins through the rivers draining them. Himalayan contribution is derived through the Bhagirathi, Alaknanda, Ghaghra, Gandak and Kosi with ε_{Nd} of -15.7 (-15.5 in 2010), whereas the Yamuna is the main supplier from the peninsular basin with ε_{Nd} ~ -12.2. Mass balance estimate based on Nd isotope composition indicate that the Ganga receives ~64% Nd contribution from the Himalaya and ~36% from Peninsula in 2008. While in 2010, the peninsular contribution decreases merely to ~10%. ε_{Nd} of the Yamuna in 2008 has been assumed to be the same as in 2010. Though ε_{Nd}

of the Yamuna in 2008, probably, was higher than that in 2010, as suggested from the ε_{Nd} of the Ganga at Varanasi in 2008. Higher contribution of Nd from peninsular basin could be due to the huge flooding in this basin during 2008 as has been discussed earlier.

One of the objectives of this study is to determine the sources of Nd of the Ganga system in terms of the major litho-units such as the Higher Himalaya, the Lesser Himalaya and the Deccan basalt. These major lithounits are characterized by their unique ε_{Nd} making it easier to quantify their contribution. The dominance of HH in the sediment budget and physical weathering of the Ganga has already been identified by Singh et al., 2008 using Sr and Nd isotope systematic in the sediments. An effort has been made in this study to locate the silicate weathering zone using Nd isotope composition as it is derived dominantly from silicates. Impact of weathering of these major lithounits is visible in the Nd isotope composition. The Himalayan tributaries are characterized with less radiogenic Nd due its contribution from the Higher and the Lesser Himalaya. High ε_{Nd} of the Yamuna at Allahabad and that of the Ganga reflects its significant contribution from weathering of the Deccan basalt with high radiogenic Nd. The importance of Deccan tributaries in the dissolved Nd budget of the Ganga has already been discussed in the previous section. To delineate the contribution from different litho-tectonic units, ε_{Nd} has been plotted with Sm/Nd (Fig. 4.4). Though the Nd concentration in the river water is highly variable, but Sm/Nd is very well defined for these samples.

From Fig. 4.4, it could be observed that HH dominates the dissolved Nd budget in the Himalayan tributaries and in the Ganga mainstream. Deccan Basalts also contribute significantly to the dissolved Nd budget to the Yamuna and the Ganga at Varanasi after their confluence at Allahabad. Further downstream, the Ganga becomes less radiogenic under the influence of the Himalayan tributaries such as the Ghaghra, Gandak and the Kosi. The Son draining from the Archean craton could also contribute to the less radiogenic Nd of the Ganga. Mixing plot of ε_{Nd} vs Sm/Nd (Fig.4.4) indicates complete dominance to Nd budget of the Himalayan tributaries by the Higher Himalaya with very little contribution from the Lesser Himalaya. This observation is true for many of the samples from the Ganga mainstream. Deccan contribution is reflected in the Yamuna and the Ganga at Varanasi.

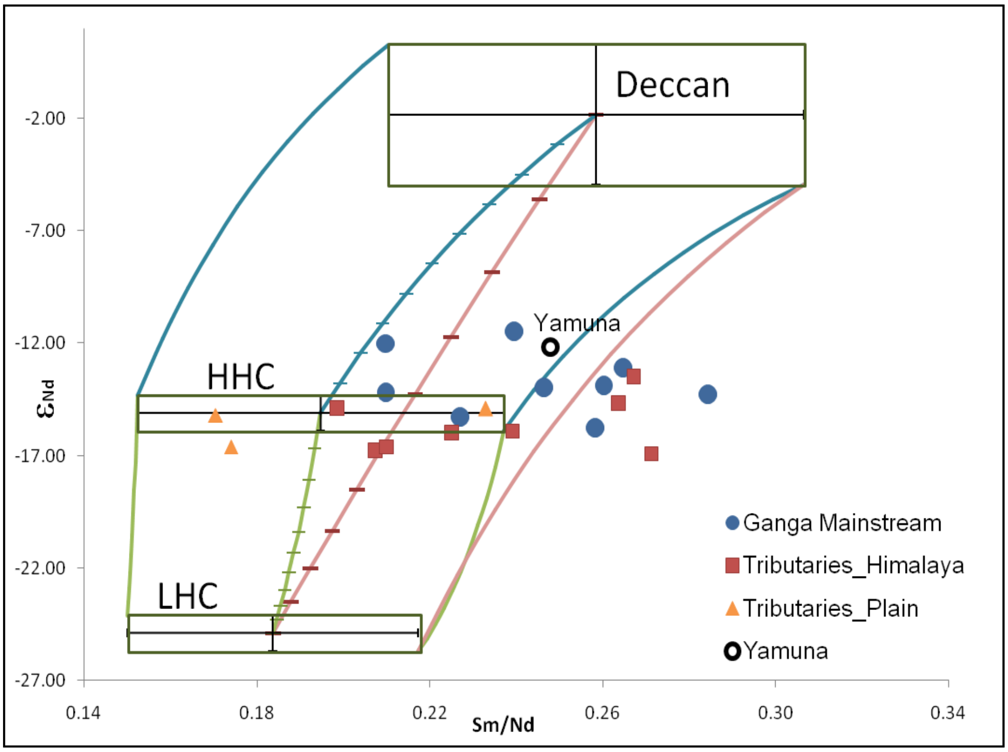

Fig. 4.4: *Dissolved Nd in the Ganga river system seems to be controlled more by Higher Himalaya compared to the Lesser Himalaya. Contribution of Deccan rivers could be observed in the Yamuna and some samples from the Ganga mainstream. Effect of preferential dissolution of apatite like minerals could be inferred from the right shift in Sm/Nd ratio.*

The observation can be interpreted in terms of supply of Nd to the Ganga due to weathering in the Higher Himalaya only with subordinate contribution from the Deccan. It is surprising to note very little or no contribution of Nd from the Lesser Himalaya indicating no silicate weathering in the Lesser Himalaya. This lithounit of the Himalaya has the higher temperature, higher vegetation cover and also higher enough precipitation. These factors are highly conducive for chemical weathering. ε_{Nd} of these rivers, however, seems to suggest that only the Higher Himalaya is getting chemically weathered. HH is responsible for entire silicate weathering, despite the fact that it supplies about 70% of sediment to the Ganga system. Though difficult, it is not impossible for HH to dominate the dissolved Nd budget of the Ganga system. Glacial erosion and its sluggish transport have left behind large amounts of fresh, finely ground rocks and soils from the HH which are getting chemical weathered in recent times (Vance et al., 2009). In addition the large area of the HH itself, it has also provided huge amount of finely sediment pulverized during last glacial period which are deposited the different part of the HH and LH (Vance et al., 2009) weathering of which could dominate the Nd budget of The Ganga.

The above proposition that the Lesser Himalaya is devoid of chemical weathering of silicates seems difficult. This could be an artefact of incongruent weathering of different minerals hosting Rare Earth Elements (REEs). It could be observed in Fig. 4.4 that Sm/Nd of many of the river waters are different compared to any of the endmembers defined in it. They lie beyond the theoretical mixing limit between HH and Deccan. They are also beyond the mixing line between LH and Deccan. All of them have high Sm/Nd ratio along with small difference in ε_{Nd}. This indicates towards the possibility of preferential dissolution of minerals having higher Sm/Nd. A mineral with higher Sm/Nd will be characterised by higher ε_{Nd}, preferential weathering of which will release higher Sm/Nd and ε_{Nd} to the water compared to source rock. It has been observed that during weathering of till in the Kalix river basin, larger part of the weathered Nd is released from minerals with a lower Sm/Nd ratio than the bulk soil (Öhlander et al., 2000). Same behavior of Sm/Nd has been observed in dissolved (including colloidal phase) Nd budget of the Kalix river (Andersson et al., 2001).

Nd is mainly enriched in the accessory minerals, such as titanite, apatite, monazite, zircon and allanite (Harlavan et al., 2009). All of them have different Sm/Nd ratios (Table. 4.3). Preferentially weathering of minerals with high Sm/Nd ratio (Table. 4.4) would increase the Sm/Nd ratio in the dissolved phase. Ayres and Harris, (1997) reported 90% of LREE in apatite and monazite of the Higher

Table 4.3: Sm, Nd concentration and Nd isotope composition of the endmembers.

Tectonic unit	Nd (ppm)	Sm (ppm)	ε_{Nd}	Sm/Nd
HHC[1]	30.3 ± 4.7	5.9 ± 0.9	-15.1 ± 0.8	0.19 ± 0.04
LH[1]	39.2 ± 4.7	7.2 ± 1	-24.9 ± 0.8	0.18 ± 0.03
Siwaliks[1]	20 ± 8.7	3.9 ± 1.6	-17.2 ± 1.2	0.20 ± 0.11
Deccan[2]	21 ± 2.9	5 ± 0.6	-2 ± 3.3	0.26 ± 0.10

(Data source: 1. Galy and France-Lanord, 2001, 2. Mahoney, 1988)

Table 4.4: Sm and Nd concentration of Nd rich minerals.

Mineral	Nd (ppm)	Sm (ppm)	Sm/Nd
Titanite	2680	655	0.24
Apatite	635	167	0.26
Monazite	94000	18000	0.19
Xenotime	2500	2587	1.03
Allanite	31000	4000	0.13

(Data source: Garzanti et al, 2010)

Himlayan Crystallines. Garzanti et al. (2010, 2011) showed that monazite, titanite, phyllosilicates, allanite and apatite are the main REE bearing minerals in suspended and bedloads of the Ganga. The Sm/Nd ratio of different minerals in bedload and suspended load of the Ganga (Table 4.4) has been reported by Garzanti et al (2010, 2011). Among these minerals, apatite has a moderately high Sm/Nd ratio (0.26). Though ε_{Nd} of these mineral phases are not known, it could be inferred that they would have higher ε_{Nd} owing to their higher Sm/Nd. They are easily weatherable. Thus, data of Fig. 4.4 indicate preferential weathering of apatite in the Ganga system which is causing higher Sm/Nd and higher ε_{Nd} of the Ganga. This is in agreement with the observations by Rengarajan and Sarin (2004) in the Yamuna river system. They reported enrichment of MREE in the dissolved phase with respect to the sediments and attributed this behaviour to the preferential dissolution of apatite. REE mobilization and fractionation due to dissolution of apatite on small scale during weathering has been reported earlier by Banfield and Eggleton (1989). Aubert et al., (2001) has shown that most of the Nd in the dissolved phase originates from apatite leaching or dissolution during granite weathering in Vosges mountain catchment.

In a laboratory dissolution experiment of granite and soil samples, Harlavan and Erel (2002) has established the weathering rates of the accessory phases as allanite>apatite>sphene. In another study of REE in the soils with varying age, Harlavan et al., (2009) has found that in early stages of weathering allanite and apatite dominate the soil labile pool of REE composition. Allanite is exhausted early with maturity of soils (2-12 kyr). In later stages of weathering (~20 kyr), dissolution of apatite alone dominates the REE concentration in the soil labile pool. Therefore in the present case, dominance of apatite weathering over other accessory minerals is not surprising.

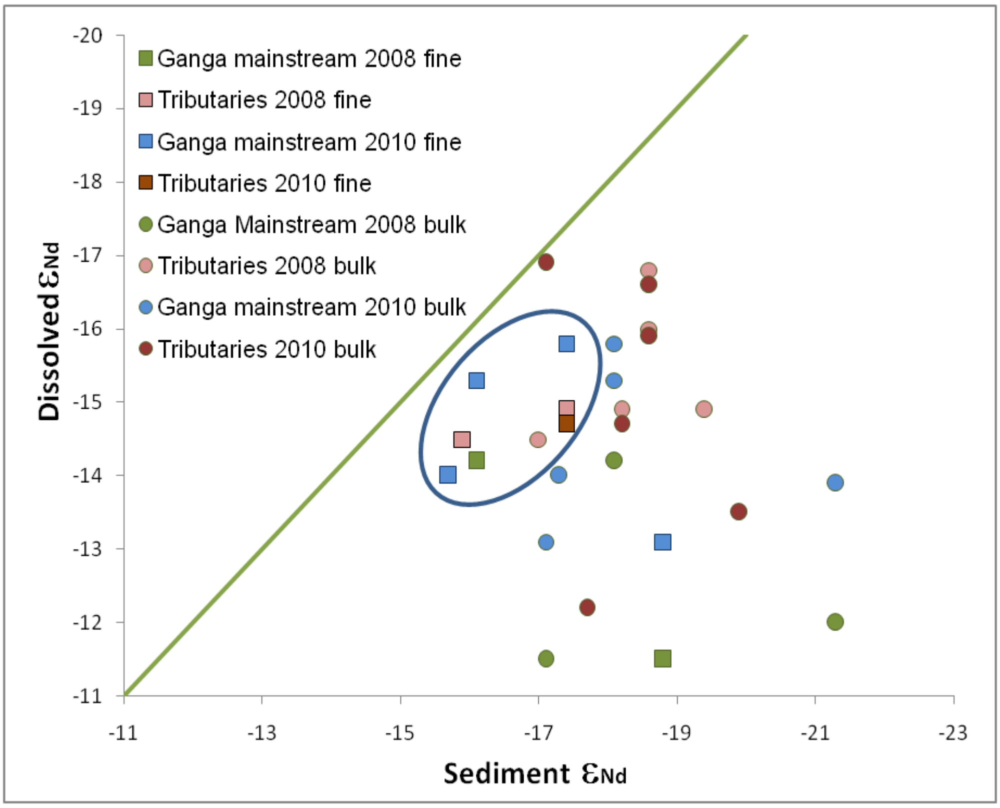

Fig. 4.5: *More radiogenic Nd in the dissolved phase compared to the sediment indicates towards preferential weathering of apatite like minerals. The same could also be obtained from different sources for sediment and dissolved budget. Finer fraction of sediment is more radiogenic than the bulk in general.*

Therefore, it could be inferred that, weathering of accessory minerals like apatite is a main factor in controlling the dissolved Nd budget in the Ganga river system. Also, chemical weathering in the Ganga river system is dominated by HH, same as physical weathering. This result also infers the importance of relief and abundance of freshly eroded material for chemical weathering over temperature and vegetation. Impact of preferential dissolution of apatite in the Ganga system is observed in a plot of ε_{Nd} of dissolved vs. particulate phases (Fig. 4.5). Data of ε_{Nd} for particulate phases are taken from Singh et al., 2008. Particulate ε_{Nd} data from the same locations have been compared with dissolved ε_{Nd}. It has been observed that dissolved phase is always more radiogenic compared to particulates at the same place (Fig.4.5). The minimum difference between sediment and dissolved phase ε_{Nd} has been observed in the sample of the Alaknanda, where both have almost same value. In all other samples dissolved ε_{Nd} is 2 to 10 e unit higher than sediment ε_{Nd}. This could be either because of different sources of dissolved and sediment budget, or due to preferential leaching of minerals with high Sm/Nd ratio (more enriched in radiogenic Nd). The first reason is linked to the relatively higher contribution of Deccan rivers to the dissolved budget. It is known that Deccan rivers contribute very little to the sediment budget in the Ganga plain (Singh et al., 2008; Lupker et al., 2012), and the deccan basalts are more radiogenic for Nd compared to the Himalayan silicates (Mahoney, 1988; Galy and France-Lanord, 2001). Therefore if the Deccan rivers contribute significantly to the dissolved budget, this kind of difference in the dissolved phase and sediments could be expected. In the absence of dissolved Nd data from rivers draining the Deccan, this point cannot be further proved. However, if ε_{Nd} of Deccan basalt (Table. 4.3) could roughly represent these rivers, this point could be logically concluded. Radiogenic Nd of sediments (Goswami et al., 2012) of the rivers flowing through Deccan region, like Tapi, supports this argument

The second reason, i.e. preferential leaching of minerals like apatite, is already discussed in the previous section. Apatite is known to be depleted in the surface and enriched in the finer fraction of sediments (Aubert et al., 2001). To examine this point further, ε_{Nd} of the finer fraction ($\leq$4 μ) from the same places (where available) has been plotted with the dissolved ε_{Nd} (Fig. 4.5). It can be observed that in majority of the samples (except 2), ε_{Nd} in the finer fraction is nearer to the dissolved ε_{Nd} than bedload. Therefore it can be concluded that, in general finer fraction is more enriched in radiogenic Nd, which indicates towards high Sm/Nd ratio in them. The possibility of adsorbed Nd in the finer fraction from the dissolved Nd also cannot be discarded (Tricca et al., 1999). As the ε_{Nd} of the finer fraction lies between the ε_{Nd} values of dissolved phase and bedload, it is possible that higher radiogenic Nd from dissolved budget gets adsorbed in the particulate phase. Considering the particle reactive nature of Nd and very high concentration of dissolved Nd in some samples, this could be another possible mechanism to explain the difference between dissolved phase, finer fraction and bedload ε_{Nd}.

4.2.2 Nd flux of the Ganga to the Bay of Bengal

Nd flux of the Ganga to the Bangladesh display large variability. In 2008, it delivered ~34000 moles Nd annually whereas only about 17000 moles/y in 2010. Based on results of two monsoon sampling, ε_{Nd} of the Ganga at the outflow, Manihari which is being supplied to the BoB is -14.5±0.5.

4.2.3 Coastal Region

It is well established that 95% of the dissolved REE budget of the rivers get removed at the estuaries (Sholkovitz, 1993; Sholkovitz and Szymczak, 2000; Jeandel et al., 2007). One of the major sources of dissolved Nd to the ocean is re-mineralization of Nd from river transported sediments (Amakawa et al., 2000; Singh et al., 2012). Therefore, to estimate Nd flux of the Ganga river system to the Bay of Bengal, samples from the coastal/shelf region (after estuary) have been analyzed for Sm, Nd concentration and Nd isotopic composition (Table 4.2).

The results show decrease in Nd concentration (Fig.4.6) from surface (average 53 pmol/kg) to deeper samples (average 47 pmol/kg), except two very shallow samples (depth 30m). This decrease could be due to biogenic activities or due to scavenging of dissolved Nd. concentration in the outflow of the Ganga is 90 pmol/kg and 44 pmol/kg in 2008 and 2010, respectively. Considering the first value, it could be interpreted as a decrease in Nd concentration in the estuary. But as discussed earlier, high Nd concentration of the Ganga is most probably due to flood events in the Yamuna and small tributaries. These samples from the coastal regions were collected during post-monsoon of the same year. At that time it is unlikely to have high Nd contribution from Deccan and peninsular rivers, which are rain fed mainly. Therefore we do not emphasize on decrease of Nd concentration between the outflow and the coastal region.

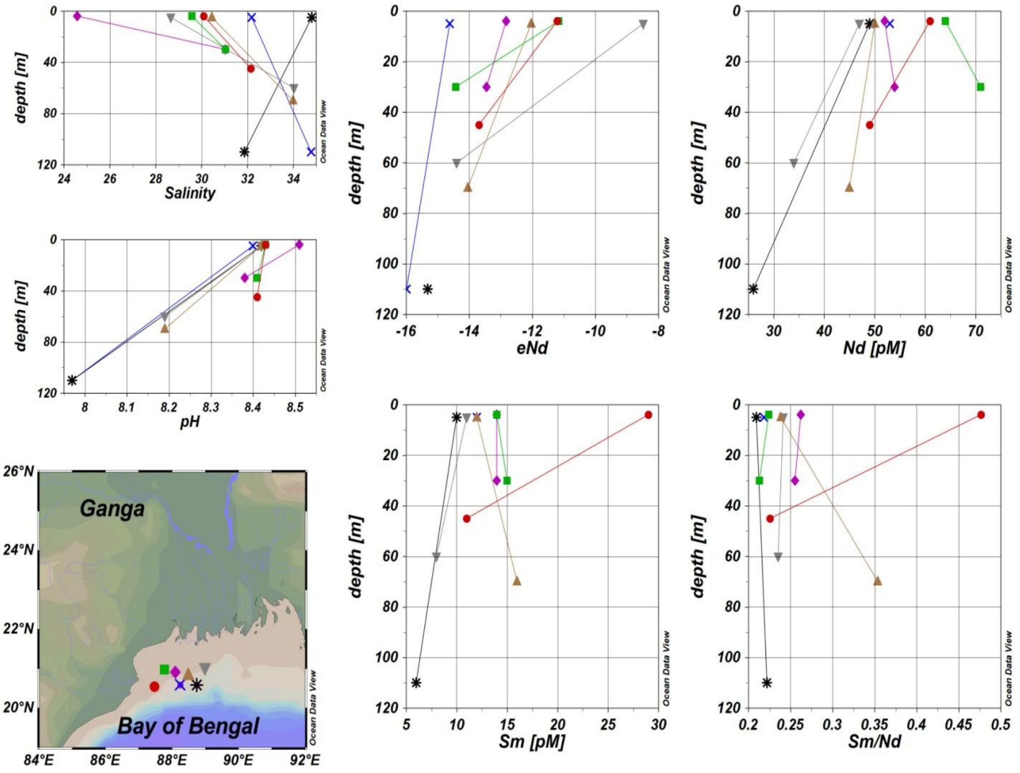

Fig. 4.6: *ε_{Nd} in the surface is more radiogenic compared to the deeper samples. Nd concentration decreases with depth for all samples except two deeper samples. Sm shows similar behaviour as Nd, except in one sample.*

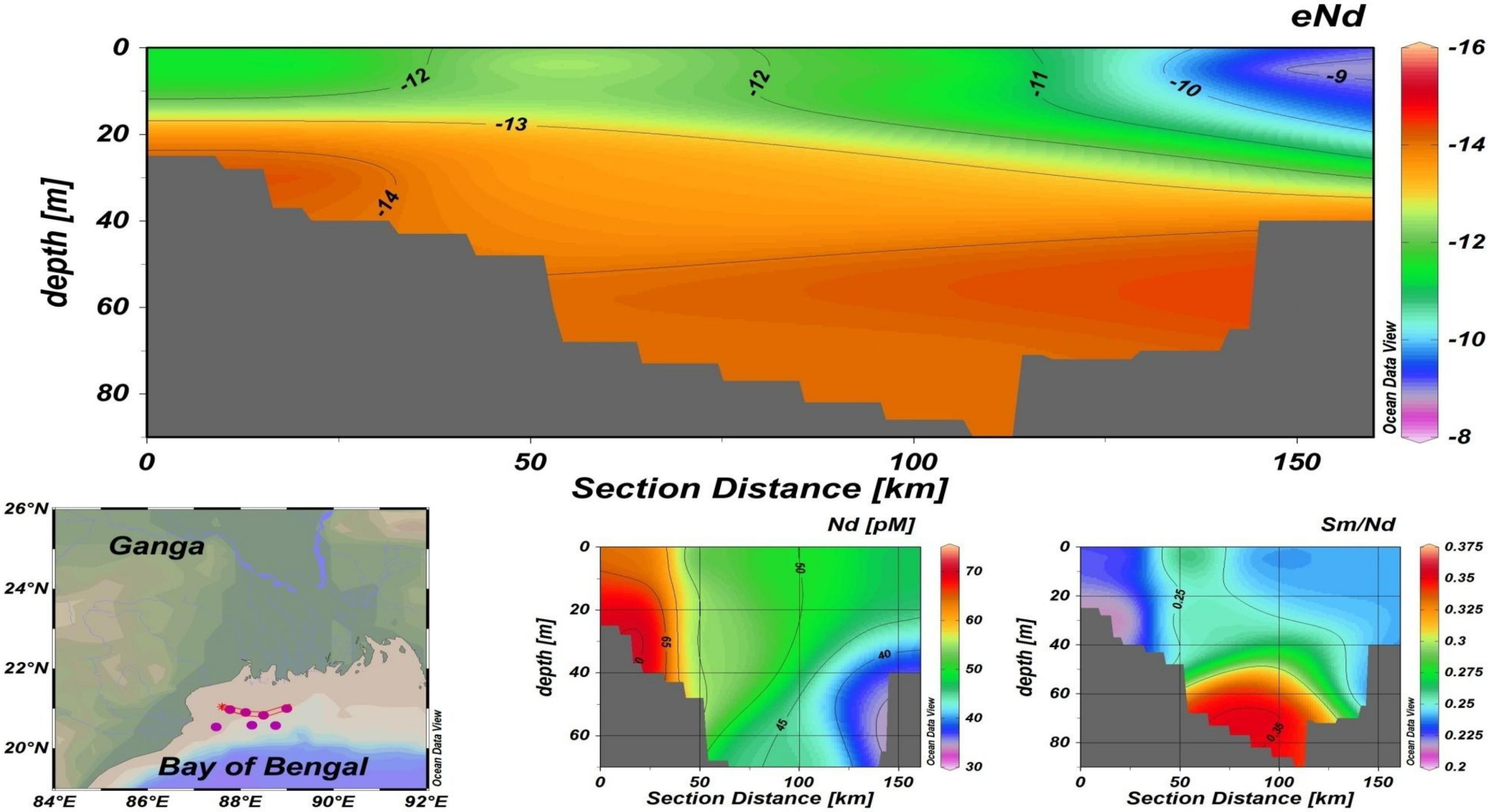

Fig. 4.7: *Profile nearer to the coast shows more radiogenic Nd at the surface compared to the Ganga outflow. The contribution of the Brahmaputra could be a possible reason.*

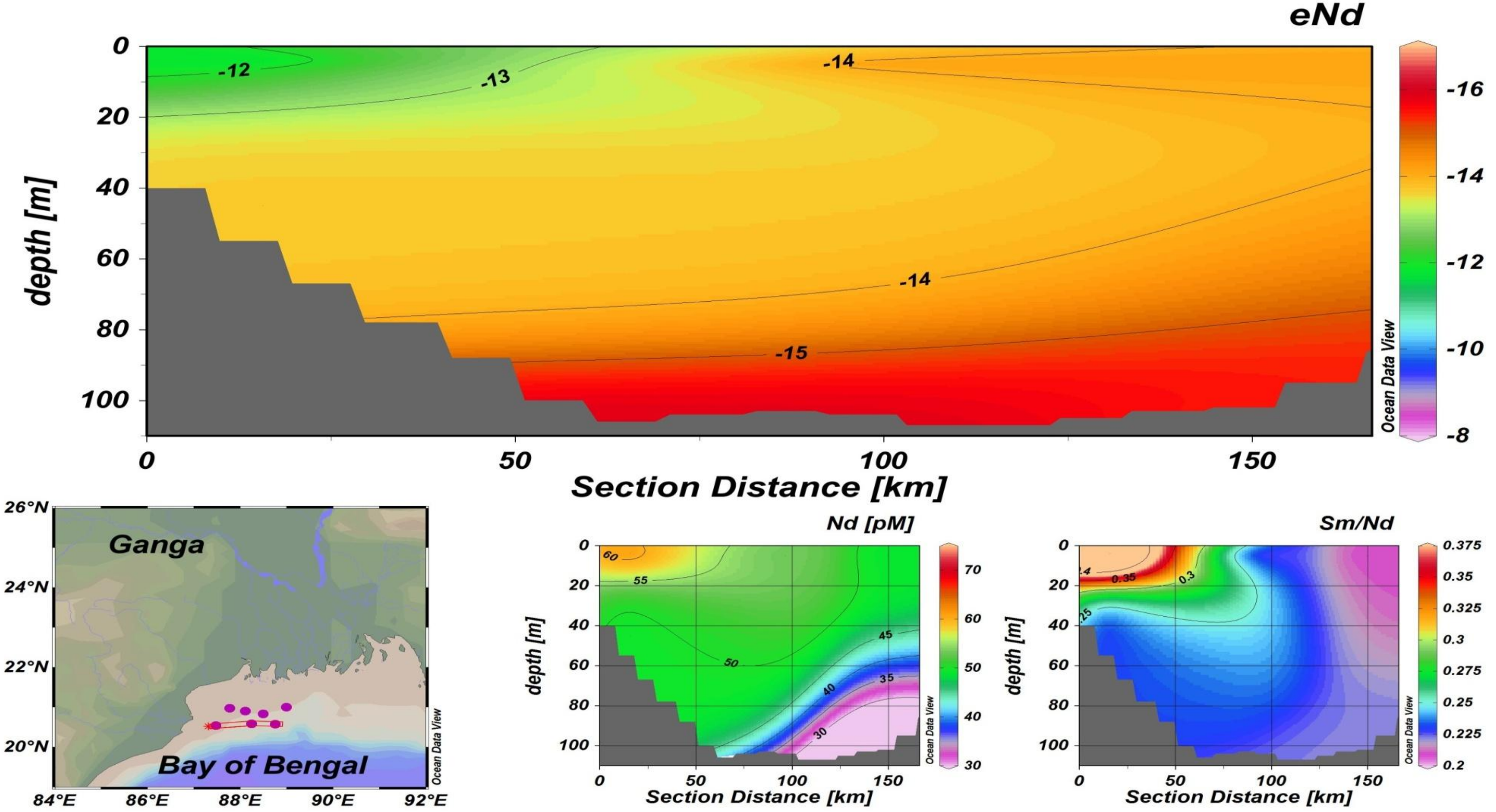

Fig. 4.8: *Desorption of less radiogenic Nd from the shelf sediments could be a reason for the less radiogenic Nd isotopic composition of the deeper samples.*

Sm concentrations in these samples also follow a similar trend. Sm/Nd in all samples is quite consistent and varies from 0.2 to 0.26, except two of them (one surface, one deep). ε_{Nd} in the surface (average -11.7) is always more radiogenic than respective deeper samples (average -14.5) (Fig. 4.6). ε_{Nd} of the surface samples is also more radiogenic (2 to 3 ε units higher) from ε_{Nd} of the Ganga outflow (-14.5±0.5). This suggests towards mixing of more radiogenic dissolved Nd from the Brahmaputra. Also, one surface sample from the north eastern part shows highly radiogenic ε_{Nd} value (-8.5) (Fig. 4.7). We can not explain this value with the present dataset, in absence of dissolved Nd data from the Brahmaputra. Only one surface sample, which shows the value -14.6 of ε_{Nd}, is the farthest one from the coast and deeper (depth 114 m) than other stations (Fig. 4.8). This is in agreement with the endmember value used for Ganga-Brahmaputra system by Singh et al., (2012).

Dissolved ε_{Nd} of the deeper samples are within the range -13.5 to -16.0. Among them, samples from shallower stations (upto 70 m) have ε_{Nd} values upto -14.4. The process of REE removal by salt-induced coagulation through colloidal phase is well established (Sholkovitz, 1992). But releasing mechanism of these elements from the sediment is not well known. One possible mechanism is leaching of river particles with seawater (Sholkovitz and Szymczak, 2000). ε_{Nd} of the Ganga bedload and finer fraction is -18.1 and -16.1 respectively at Rajmahal (Singh et al., 2008). Suspended load of the Ganga at Bangladesh have been reported to have ε_{Nd} values between -16.8 to -17.4 (Garçon et al., 2013). Though the two deeper samples (>100 m) show ε_{Nd} values in the above mentioned range (-15.3 and -16.0 respectively), the samples nearer to the coast have more radiogenic ε_{Nd}, nearer to the dissolved ε_{Nd} value of the outflow. It is possible that the dissolved Nd, which is getting removed at the estuary, is getting re-released from the shelf sediments by adsorption-desorption mechanism (Amakawa et al., 2000). This re-released Nd, which is having same ε_{Nd} value as the Ganga outflow, is acting as a source of dissolved Nd to the Bay of Bengal. The ε_{Nd} data from nearby cores (118KL, depth: 29 cm, ε_{Nd}: -14.3 by Galy et al., 2008 and V29-18, depth: 3 cm, ε_{Nd}: -15.1 by Colin et al., 1999) also supports this proposition.

4.3 Conclusions

Dissolved Nd concentration and isotopic composition has been measured in the Ganga river system. The data indicates towards more Higher Himalayan contribution in the dissolved Nd budget compared to the Lesser Himalaya. Also, the importance of Deccan tributaries in the dissolved Nd budget has been observed, though their contribution is not very consistent.

Dissolved Nd data has been compared to the bedload Nd data from literature and it has been observed that dissolved Nd is more radiogenic compared to the sediment. This difference could be due to preferential dissolution of apatite and more dissolved Nd contribution from the Deccan tributaries of the Yamuna. As these tributaries do not contribute significantly to the sediment, their higher dissolved Nd contribution could give rise to this difference. The Ganga supply around 17000 to 34000 moles Nd annually to the Bay of Bengal with ε_{Nd} -14.5±0.5.

Dissolved Nd at the coastal region of Bay of Bengal has been measured to assess the impact of its riverine supply from the Ganga. The dissolved Nd isotopic composition at the surface is 2 to 3 epsilon unit more radiogenic compared to the Ganga outflow. This indicates towards contribution of more radiogenic Nd from the Brahmaputra. Less radiogenic Nd isotopic composition has been measured in the deeper samples, indicating towards desorption of Nd from the shelf sediments of the Ganga origin.

Chapter 5

Ground water chemistry and its relation to saline - alkaline soils

5.1 Introduction

Groundwater forms the invisible and subsurface part of the hydrologic cycle. It is estimated that groundwater accounts for more than 95% of all fresh water, which is available for use, while surface water covers less than 5%. The main difference between them is that surface water is completely renewable, usually within days or weeks, while groundwater is not completely renewable, since it may take decades, centuries or even longer time to renew. The main source of the groundwater is percolation of the rainwater through porous, permeable water bearing strata, though there can be other sources, such as the water trapped in sediment at its time of deposition or magmatic water. The percolating water may have a lateral movement also, depending upon the lithology of the aquifer. Groundwater can contribute to the river water during the lean flow and the aquifers can get water from the river during monsoon depending on the water level. Groundwater also plays a significant role in the formation process of saline-alkaline soils. It is necessary to study the groundwater chemical and isotope composition to understand these processes completely.

In many cases, the water travels a large distance between its recharge and the discharge areas. Groundwater acquires dissolved component from rainwater, from the lithology through which it percolates and through which they move. The major ion composition of groundwater is controlled by the surface, subsurface weathering, and their residence time in the aquifer. Sr isotopes have been widely used to understand the water-rock interaction processes in the groundwater aquifers (Smalley et al., 1988, Stueber et al., 1993, Naftz et al., 1997, Katz et al., 1997, Depaolo, 2006), as the rocks with which groundwater interact have wide and predictable range of Sr isotopic ratio (Cartwright et al., 2007). $^{87}Sr/^{86}Sr$ ratios of the different rock type are quite different since it depends on initial $^{87}Sr/^{86}Sr$ ratio, Rb/Sr ratio and the age of the rocks (Faure, 1991). For example, old granite, gneiss has high $^{87}Sr/^{86}Sr$ compared to basalt and carbonates. Depending on the rock type the groundwater percolates or moves, it obtains $^{87}Sr/^{86}Sr$ similar to them and this ratio can be used as tracer to study what type of rocks this water has passed through. Groundwater samples from the Ganga plain and Deccan region along with that from Gujarat and Kutch region has been analyzed for chemical composition and Sr isotopic composition and Sr concentration. Their source apportionment of major ions and Sr has been done using inverse model.

5.2 Results and discussion

This study is based on the sampling in four regions having differing lithology and hence they have been divided into four groups for comparison and better understanding, e.g. a) Gujarat (includes coastal region but excludes Kutch), b) Kutch region, c) Ganga plain, d) Chambal basin. Most of the samples from Gujarat and Kutch are deep groundwater. The groundwaters of all four regions are having high total dissolved solids (TDS). TDS in groundwater of Kutch (1.03 – 4.66 g/l) and Gujarat (0.26 – 3.57 g/l) are higher compared to those from the Ganga (0.12 – 2.44 g/l) and Chambal basin (0.42 – 3.46 g/l) (Table 5.1). Na concentration in the groundwater in Gujarat varies from 1824-42709 μM. In the Kutch region the average Na concentration is higher than that in Gujarat. Ganga plain (182-19949 μM) and Chambal basin (3918-27763 μM) though contain high Na, they have lower average Na concentration compared to Gujarat and Kutch. K concentration in groundwater samples is 2-3 order of magnitude lower compared to Na concentration in all four regions. Many of the groundwater samples have higher Mg concentration compared to Ca. In Gujarat, range of dissolved Mg and Ca are measured as (212-7616 μM) and (55-4505 μM) respectively. In Kutch region, groundwater Mg and Ca varies from (376-6440 μM) and (227-6687 μM) respectively. In the Ganga plain, Mg and Ca show values between (193-5241 μM) and (344-2127 μM). Chambal basin has higher Mg concentration (192-3477 μM) compared to Ca (367-8876 μM) in majority of samples due to weathering of basalt. Cl, SO_4, HCO_3 are the major anions in these groundwaters. NO_3 concentration is also very high in some samples. Most of the samples from Ganga plain and Chambal Basin are dominated by bicarbonate in the anion budget, whereas SO_4 and Cl dominate the anion budget of samples from Gujarat and Kutch. Cl concentration in Gujarat groundwater varies from (1470-36115 μM), the same in Kutch region varies from (8175-55903 μM). In Ganga plain Cl concentration (55-8492 μM) is almost 1-2 order of magnitude less compared to

Table 5.1 Major ion and Sr concentration and Sr isotopic composition of groundwater samples.

Sample Code	Na µM	K µM	Mg µM	Ca µM	F µM	Cl µM	NO_3 µM	SO_4 µM	HCO_3 µM	Si µM	Sr nM	$^{87}Sr/^{86}Sr$	TDS mg/l
Gujarat													
GW08-1	18798	12	395	55	225	4144	355	942	13311	970	2661	0.71065	1548
GW08-2	14612	76	5294	248	b.d.	13345	1263	899	11930	1054	64105	0.70957	1872
GW08-4	9760	39	2757	921	1	9165	b.d.	454	6936	884	9535	0.70950	1146
GW08-6	21284	3234	6608	2375	14	14909	5150	4259	11692	713	121361	0.70932	2860
GW08-7	7668	48	1240	626	12	1443	439	90	9255	539	n.m.	n.m.	900
GW08-8	29737	1647	7616	5522	b.d.	36115	b.d.	4542	7954	630	69166	0.71007	3373
GW08-9	6372	5	1073	725	36	5358	155	367	3692	1090	6349	0.70951	693
GW08-10	4897	5	2135	2251	9	6308	2339	922	3824	1285	12893	0.70967	981
GW08-11	1824	3	212	434	21	1470	222	288	1419	601	1798	0.70903	262
GW08-12	2750	10	2940	4505	b.d.	7645	1789	1558	6113	869	13657	0.70862	1243
GW08-13	17468	146	2855	2813	32	18264	381	1993	3879	369	27680	0.70956	1699
GW08-14	42709	80	3980	1973	376	26565	2051	9493	6758	448	140866	0.70932	3573
GW08-15	20556	24	4279	1916	86	9335	2633	2729	15106	1055	65414	0.70894	2362
GW08-16	14970	619	2471	3303	25	17187	39	1596	6104	472	233366	0.70962	1712
GW08-17	20856	61	213	298	9	12929	b.d.	1433	3614	314	2546	0.71243	1325
Kutch													
GK08-1	23794	41	376	227	80	13685	b.d.	2439	4301	273	3813	0.71228	1558
GK08-2	51504	250	5785	6687	89	55903	433	6279	7143	313	108416	0.71084	4661
GK08-3	8317	75	1374	2150	28	9228	390	941	4446	263	26711	0.70925	1034
GK08-4	10266	240	1471	1126	27	10133	440	1251	3014	308	10655	0.70957	1026
GK08-27	38876	814	6440	6645	0	50131	b.d.	4593	4771	249	45477	0.70983	3865
GK08-29	14505	293	1560	2178	40	13113	449	1935	5926	523	33163	0.70924	1526
GK08-30	25390	230	3921	6020	9	23265	1574	4943	4809	555	31064	0.70963	2635
GK08-33	9313	72	2210	2341	24	8175	578	1847	6559	854	34948	0.70940	1292
GK08-35	9224	100	1400	2278	33	10676	439	937	4241	247	28296	0.70919	1103
GK08-36	20225	181	2726	3727	b.d.	22658	470	2049	4003	272	38242	0.70930	1969

(continued on next page)

Table 5.1: Major ion and Sr concentration and Sr isotopic composition of groundwater samples (continued).

Sample Code	Na µM	K µM	Mg µM	Ca µM	F µM	Cl µM	NO_3 µM	SO_4 µM	HCO_3 µM	Si µM	Sr nM	$^{87}Sr/^{86}Sr$	TDS mg/l
Ganga Plain													
GWGP-1	606	88	653	1571	20	221	b.d.	16.9	5188	618	2434	0.72174	440
GWGP-2	1960	115	826	1568	7	902	b.d.	181	5971	512	2493	0.72944	560
GWGP-3	182	51	193	344	14	55	b.d.	8.1	1466	43	715	0.72961	118
GWGP-4	19949	366	5241	1416	35	8492	523	1882	20606	561	10221	0.72358	2443
GWGP-5	1333	63	1743	1233	55	271	54	45	7036	459	5632	0.72416	585
GWGP-6	2220	140	2461	1161	52	456	53	199	8658	531	14254	0.71993	745
GWGP-7	3464	32	916	1356	21	561	153	161	7203	462	6302	0.71460	655
GWGP-9	4666	63	1203	989	21	141	b.d.	39.7	8908	464	5543	0.72594	744
GWGP-10	2318	68	1240	1353	25	376	76	127	7164	456	4704	0.72373	620
GWGP-11	4393	42	1725	2127	18	2684	369	543	8081	495	n.m.	n.m.	907
GWGP-16	12453	34	1992	558	114	1361	62	578	15006	365	10583	0.72161	1393
GWGP-17	3354	79	1784	1287	31	450	347	200	8338	493	7107	0.72236	754
GP09-44	1660	35	1990	1201	b.d.	3784	970	880	4462	514	15941	0.71686	701
GP09-54	15282	93	1138	634	32	7164	133	2886	7083	455	10301	0.71498	1393
GP09-59	3175	120	1309	509	14	982	116	547	5788	585	5489	0.72390	594
GP09-134	767	110	674	1074	10	253	161	226	4199	332	2647	0.72934	387
GP09-169	2101	149	1567	1392	32	1649	210	350	5296	495	3689	0.72693	590
Chambal Basin													
GP09-4	5225	35	2072	458	180	764	177	218	8989	1061	17715	0.71266	830
GP09-12	27763	299	3426	8876	2	38270	b.d.	5332	1443	252	27346	0.71868	3053
GP09-17	12940	74	1370	473	86	2459	446	587	14416	1425	9655	0.71055	1445
GP09-18	3918	94	192	367	42	670	51	170	4207	176	1743	0.71086	419
GP09-34	14023	189	2602	815	170	5677	166	3130	9703	334	98607	0.71333	1542
GP09-38	38677	140	3477	1071	331	9644	b.d.	13176	13453	277	47777	0.71375	3463

Gujarat and Kutch region. Chambal basin groundwater has moderately high Cl (670-9644 μM) with one exceptionally high value (38270 μM). HCO_3 dominates the anion budget in Ganga plain (1466-20606 μM) and Chambal basin (1443-14416 μM). HCO_3 concentration in Gujarat and Kutch groundwater varies from (1419-15106 μM) and (3014-7143 μM) respectively. SO_4 concentration in the Ganga plain (8-2886 μM) and Chambal basin (170-13176 μM) show a large range, almost 2-3 orders of magnitude. SO_4 concentration in Gujarat and Kutch region varies from (90-9493 μM) and (941-6279 μM) respectively. Inorganic charge balance of these samples are within 5% in most of the cases.

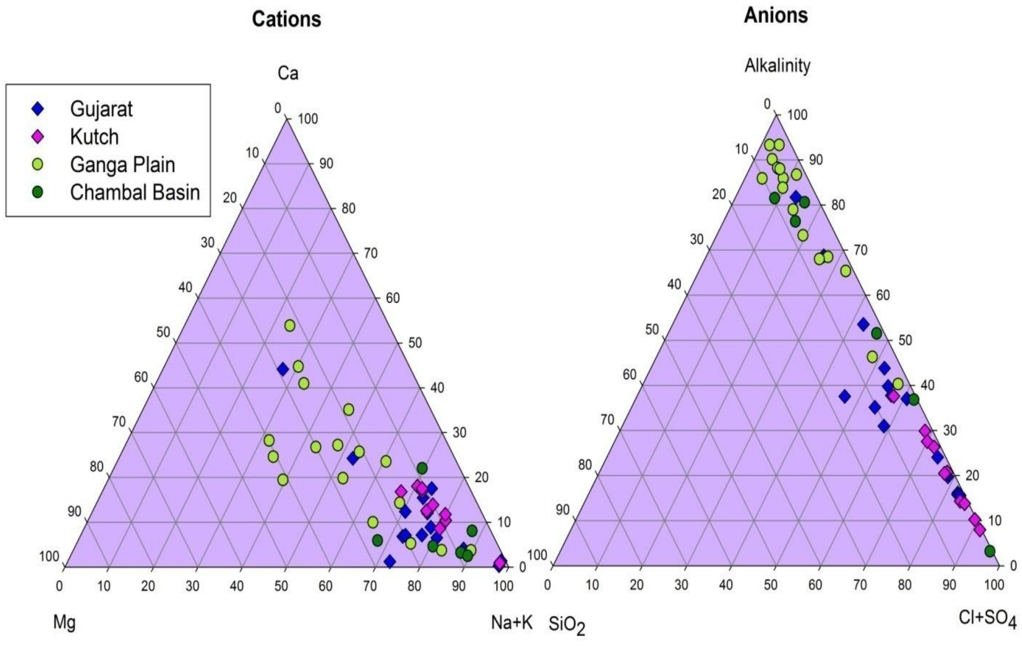

Fig. 5.1: *Cation and anion ternary diagrams of groundwater.*

The major ion concentration in the groundwater is much higher than that in river water. From the ternary diagrams (Fig. 5.1), it is clear that groundwater from Gujarat and Kutch have higher Na and K component compared to groundwater from Ganga Plain. Though the groundwater samples from Deccan have high Na and K, they are different in anion composition from Gujarat and Kutch samples. Na dominates the cation budget with a maximum of 95% contribution in TZ+ (sum of all cation charges) in few cases. Dominance of Na in cation budget is clear from the TZ+ vs. Na (Fig. 5.2a). Cl dominates the anion budget in most of the samples from Gujarat and Kutch with maximum of 69% and 78% of TZ- (sum of all anion charges) respectively. However, samples from the Ganga plain and Chambal basin need other anions to balance the TZ- (Fig. 5.2b). The Ganga plain groundwater has maximum 35% Cl contribution in the anion budget. Whereas, most of the samples in the Chambal basin have less than 26% of Cl in the anion budget with one exceptionally high value.

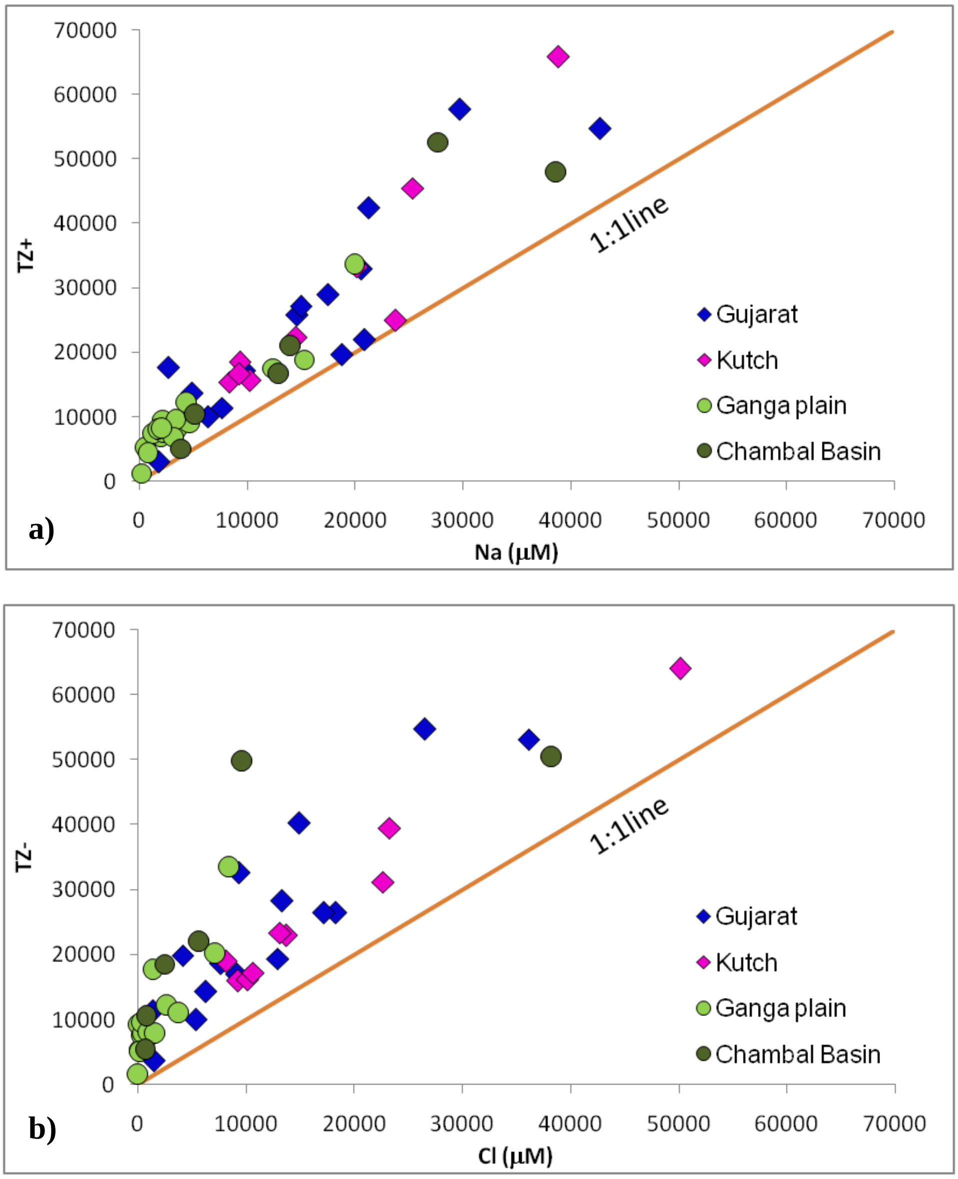

***Fig 5.2: a)**. Na is the dominating cation in groundwaters. **b)** Cl dominates the anion budget in groundwater.*

The chemical compositions of the groundwater are delineated using some major ion plots. Cl vs. Na shows excessive Na over Cl in most of the samples, though few of them have slightly higher Cl concentration compared to Na (Fig. 5.3a). The excess Cl can come from dissolution of bischofite ($MgCl_2.6H_20$), carnallite ($MgCl_2.KCl.6H_2O$) or sylvite (KCl). It has been observed that most of the groundwater samples have higher Mg concentration than Ca, which is probably due to calcite precipitation or due to interaction with Mg rich minerals of basalts, as mentioned above.

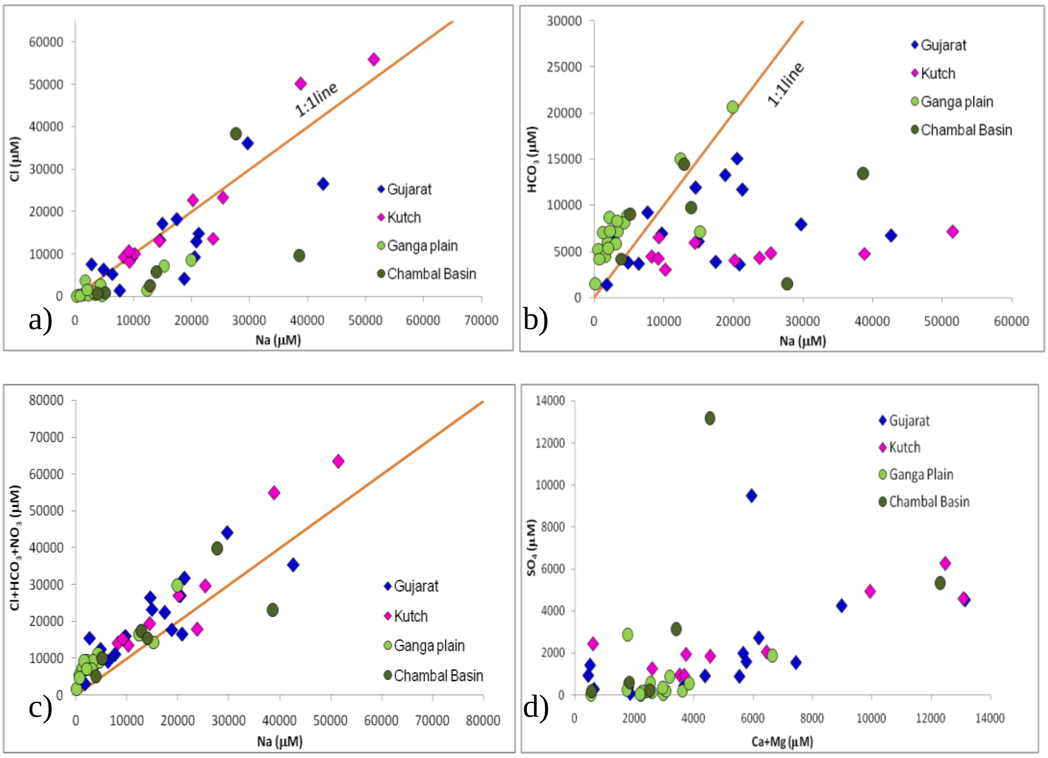

Fig. 5.3: *a) Excess Na over Cl has been observed in samples from Ganga plain and Chambal basin. b) Most of the samples from Ganga plain have higher Bicarbonate content than Na, samples from Gujarat and Kutch show just opposite behaviour. c) Na alone could balance most of the anions in groundwater. d) Good correlation between Ca, Mg with sulphate indicates towards their same source.*

Samples from the Ganga plain and Chambal basin has marginally higher HCO_3 than Na, whereas Gujarat and Kutch samples have more Na compared to HCO_3 (Fig. 5.3b). Though Ca and Mg show good correlation with SO_4, but they do not follow 1:1 line, indicating towards other sources of these ions than Gypsum. Some of the groundwater samples have very high NO_3 concentration. Sum of Cl, HCO_3 and NO_3 is almost balanced by Na (Fig. 3c), which indicates towards their common source. As has been discussed in the saline-alkaline formation process (Chapter 3), halite (NaCl), trona (Na_2CO_3) and thermonatrite (Na_2CO_3, $NaHCO_3$, $2H_2O$) are the most abundant minerals among saline-alkaline soils (Dutta et al., 2002). These salts could provide Na in association with HCO_3 and Cl. All groundwater from the Kutch and majority of Gujarat groundwaters fall on 1:1 line in Na vs Cl plot indicating their contribution from NaCl whereas those from the Ganga plain and Chambal deviates from this lines and require HCO_3 to balance the same. This observation indicates the dominance of NaCl in Kutch and Gujarat soils and Na_2CO_3 and Na_2HCO_3 in the Ganga and Chambal soils.

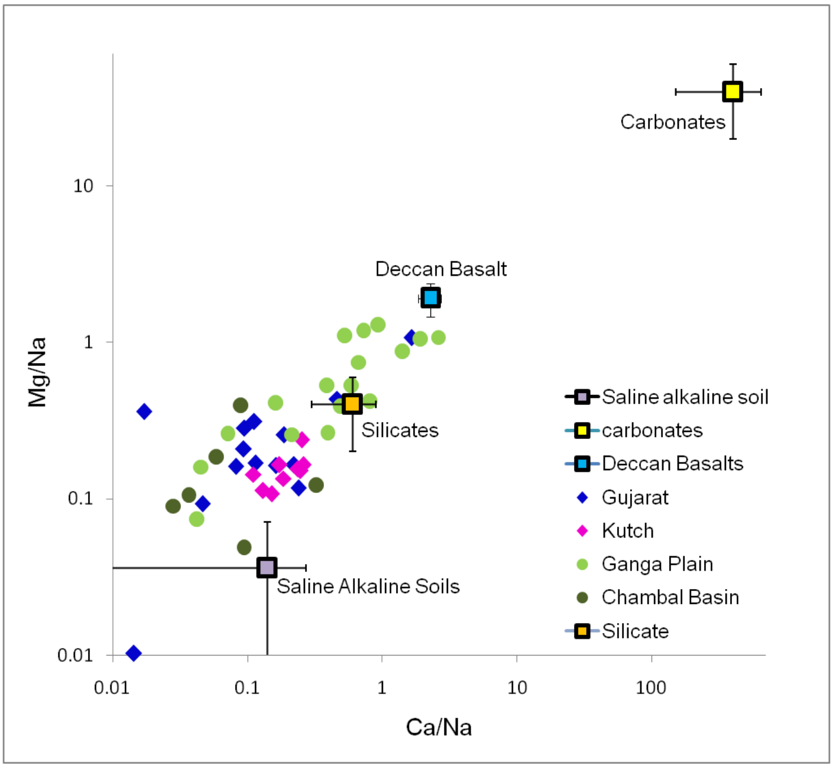

Fig. 5.4: *Major ion ratio plot shows saline-alkaline soils as an endmember for groundwater dissolved ions.*

All groundwaters contain large amount of dissolved Sr. It ranges 0.7 – 15.9 µM in the Ganga plain, 1.7 – 98.6 µM in the Chambal basin, 1.8-233.4 µM in Gujarat and 3.8 – 108.4 µM in Kutch. Similar to river water, $^{87}Sr/^{85}Sr$ in the groundwater in the Ganga plain is radiogenic (0.71498 – 0.72961). In Chambal basin it ranges

Table 5.2A: A posteriori results from the inverse model for groundwater (3 endmembers).

Ratio	Silicates	Carbonates	Saline Alkaline soils
Ganga Plain_monsoon			
Cl/Na	0.0 ± 0.0	0.0 ± 0.0	0.13 ± 0.02
Ca/Na	0.21 ± 0.09	33 ± 7	0.01 ± 0.01
Mg/Na	1.02 ± 0.21	17 ± 4	0.06 ± 0.04
Sr/Na	6.56 ± 1.13	55 ± 13	0.08 ± 0.12
$^{87}Sr/^{86}Sr$	0.792 ± 0.019	0.710 ± 0.019	0.721 ± 0.005
Alkalinity/Na	2.34 ± 0.63	132 ± 28	0.708 ± 0.166
Ganga Plain_non-monsoon			
Cl/Na	0.0 ± 0.0	0.0 ± 0.0	0.54 ± 0.05
Ca/Na	0.45 ± 0.17	114 ± 33	0.01 ± 0.02
Mg/Na	0.43 ± 0.26	195 ± 55	0.01 ± 0.02
Sr/Na	17.5 ± 5.4	277 ± 123	0.19 ± 0.27
$^{87}Sr/^{86}Sr$	0.796 ± 0.20	0.713 ± 0.020	0.721 ± 0.005
Alkalinity/Na	1.16 ± 0.55	522 ± 150	0.44 ± 0.15

Table 5.2B: A posteriori results from the inverse model for groundwater (4 endmembers).

Ratio	Silicates	Carbonates	Saline Alkaline soils	Deccan
Gujarat				
Cl/Na	0.0 ± 0.0	0.0 ± 0.0	0.77 ± 0.03	0.0 ± 0.0
Ca/Na	0.13 ± 0.05	34 ± 9	0.002 ± 0.003	0.86 ± 0.15
Mg/Na	0.16 ± 0.08	25 ± 7	0.004 ± 0.007	1.6 ± 0.3
Sr/Na	23.5 ± 3.3	68 ± 28	0.01 ± 0.02	3.2 ± 0.1
$^{87}Sr/^{86}Sr$	0.770 ± 0.019	0.710 ± 0.020	0.721 ± 0.005	0.709 ± 0.006
Alkalinity/Na	0.55 ± 0.19	64 ± 17	0.22 ± 0.06	0.96 ± 0.44
Kutch				
Cl/Na	0.0 ± 0.0	0.0 ± 0.0	1.18 ± 0.06	0.0 ± 0.0
Ca/Na	0.20 ± 0.08	34 ± 13	0.006 ± 0.007	1.4 ± 0.2
Mg/Na	0.12 ± 0.07	27 ± 11	0.004 ± 0.008	1.18 ± 0.25
Sr/Na	0.81 ± 0.31	732 ± 181	0.02 ± 0.03	3.2 ± 0.1
$^{87}Sr/^{86}Sr$	0.797 ± 0.020	0.711 ± 0.018	0.721 ± 0.005	0.710 ± 0.005
Alkalinity/Na	0.52 ± 0.24	95 ± 28	0.10 ± 0.05	0.63 ± 0.30
Chambal Basin				
Cl/Na	0.0 ± 0.0	0.0 ± 0.0	0.26 ± 0.03	0.0 ± 0.0
Ca/Na	0.12 ± 0.04	43 ± 21	0.01 ± 0.01	2.3 ± 0.4
Mg/Na	0.21 ± 0.08	119 ± 41	0.005 ± 0.009	1.5 ± 0.3
Sr/Na	10.4 ± 1.7	154 ± 85	0.05 ± 0.08	3.23 ± 0.07
$^{87}Sr/^{86}Sr$	0.787 ± 0.020	0.713 ± 0.020	0.721 ± 0.005	0.710 ± 0.006
Alkalinity/Na	0.55 ± 0.26	934 ± 296	0.11 ± 0.06	0.67 ± 0.32

Table 5.3A: Source apportionment of Na, Cations and Sr using 3 end members*.

Sample	Place	%Na$_{Sil}$	%Na$_{Carb}$	%Na$_{SAS}$	%Cation$_{Sil}$	%Cation$_{Carb}$	%Cation$_{SAS}$	%Sr$_{Sil}$	%Sr$_{Carb}$	%Sr$_{SAS}$
Ganga Plain_monsoon										
GWGP-1	Kushinagar	6 ± 8	7 ± 2	88 ± 8	5 ± 2	71 ± 16	19 ± 2	9 ± 13	89 ± 29	2 ± 3
GWGP-2	Ghagha	2 ± 3	2 ± 1	96 ± 3	5 ± 2	45 ± 10	45 ± 2	12 ± 15	86 ± 28	6 ± 9
GWGP-3	Mahula	16 ± 9	6 ± 1	77 ± 9	14 ± 3	71 ± 16	18 ± 2	23 ± 13	75 ± 24	1 ± 2
GWGP-4		4 ± 2	0.3 ± 0.1	96 ± 2	8 ± 2	12 ± 4	76 ± 3	51 ± 27	33 ± 14	15 ± 23
GWGP-5		40 ± 8	3 ± 1	57 ± 8	29 ± 5	47 ± 11	18 ± 3	61 ± 16	38 ± 13	1 ± 2
GWGP-6	Tisaura	85 ± 15	1.3 ± 0.4	14 ± 15	72 ± 11	26 ± 7	5 ± 6	86 ± 21	11 ± 4	0 ± 0
GWGP-7	Pusauli	17 ± 4	1.0 ± 0.3	82 ± 4	23 ± 4	31 ± 8	53 ± 3	61 ± 18	30 ± 11	4 ± 6
GWGP-8	Hiranandpur	7 ± 3	0.8 ± 0.2	92 ± 3	11 ± 3	25 ± 6	63 ± 3	49 ± 19	44 ± 16	8 ± 12
GWGP-9	Hiranandpur	12 ± 3	0.7 ± 0.2	88 ± 3	18 ± 3	23 ± 6	63 ± 3	64 ± 20	31 ± 12	6 ± 9
GWGP-10	Hiranandpur	15 ± 4	1.7 ± 0.4	83 ± 4	17 ± 3	42 ± 10	41 ± 2	49 ± 16	47 ± 16	3 ± 5
GWGP-16	Turna	9 ± 3	0.2 ± 0.1	90 ± 3	18 ± 4	9 ± 3	80 ± 4	73 ± 23	13 ± 6	9 ± 13
Ganga Plain_non-monsoon										
GP09-44	Pohia Ghat, Agra	46 ±15	0.5 ± 0.1	53 ± 15	30 ± 8	50 ± 15	18 ± 5	83 ± 37	14 ± 7	1 ± 1
GP09-54	Etawah	2 ± 2	0.04 ± 0.02	98 ± 2	4 ± 2	12 ± 4	90 ± 3	53 ± 42	18 ± 11	27 ± 39
GP09-59	Parial Town	6 ± 2	0.2 ± 0.1	94 ± 2	9 ± 2	36 ± 11	60 ± 2	60 ± 30	30 ± 16	10 ± 14
GP09-169	Garhmukteshwar	2 ± 3	0.4 ± 0.1	97 ± 3	5 ± 1	54 ± 16	40 ± 2	24 ± 30	67 ± 35	10 ± 15

* Suffixes Sil, Carb and SAS represent silicates, carbonates and saline alkaline soils respectively.

Table 5.3B: Source apportionment of Na, Cations and Sr using 4 end members*.

Sample	Place	%Na$_{Sil}$	%Na$_{Carb}$	%Na$_{SAS}$	%Na$_{Deccan}$	%Cat$_{Sil}$	%Cat$_{Carb}$	%Cat$_{SAS}$	%Cat$_{Deccan}$	%Sr$_{Sil}$	%Sr$_{Carb}$	%Sr$_{SAS}$	%Sr$_{Deccan}$
Gujarat													
GW08-1	Kundera	0.4 ± 0.1	0.02 ± 0.02	98 ± 1	1 ± 1	0.6 ± 0.1	1 ± 1	97 ± 1	3 ± 1	71 ± 22	9 ± 9	7 ± 11	18 ± 14
GW08-2	Mamangaon	18 ± 3	0.07 ± 0.06	78 ± 3	2 ± 2	17 ± 2	3 ± 2	58 ± 2	6 ± 3	95 ± 19	1 ± 1	0.2 ± 0.3	2 ± 2
GW08-4	Mangrun	2 ± 1	0.24 ± 0.15	89 ± 4	9 ± 4	2.4 ± 0.5	11 ± 5	65 ± 3	22 ± 7	54 ± 16	17 ± 13	1 ± 2	29 ± 15
GW08-6	Jambusar	22 ± 3	0.24 ± 0.16	68 ± 5	9 ± 5	28 ± 2	9 ± 5	44 ± 3	20 ± 7	90 ± 18	3 ± 2	0.1 ± 0.2	5 ± 3
GW08-8	Ishwarwada	8 ± 1	0.28 ± 0.16	82 ± 4	10 ± 5	10 ± 1	11 ± 5	55 ± 3	23 ± 7	76 ± 16	8 ± 6	0.4 ± 0.6	14 ± 7
GW08-9	Ghatula	2 ± 1	0.26 ± 0.15	90 ± 4	7 ± 4	3 ± 1	12 ± 5	71 ± 3	19 ± 7	59 ± 16	18 ± 13	1 ± 2	23 ± 13
GW08-10	--	7 ± 2	0.97 ± 0.33	81 ± 6	11 ± 6	5 ± 1	31 ± 9	43 ± 3	21 ± 7	60 ± 16	25 ± 13	0.3 ± 0.5	14 ± 8
GW08-11	Kherawad	2 ± 1	0.40 ± 0.19	92 ± 3	5 ± 4	2 ± 1	18 ± 7	69 ± 3	13 ± 6	55 ± 17	28 ± 18	1 ± 2	17 ± 12
GW08-12	Rajkot	9 ± 5	3.9 ± 1.0	79 ± 8	8 ± 8	3 ± 1	62 ± 16	21 ± 2	7 ± 4	41 ± 22	53 ± 26	0.2 ± 0.3	5 ± 5
GW08-13	Sarpar	5 ± 1	0.23 ± 0.14	87 ± 4	8 ± 4	5 ± 1	10 ± 5	66 ± 3	20 ± 6	73 ± 16	10 ± 7	0.5 ± 0.9	15 ± 8
GW08-14	Bharuka	13 ± 2	0.10 ± 0.08	83 ± 3	4 ± 2	15 ± 2	5 ± 2	73 ± 3	12 ± 5	93 ± 19	2 ± 2	0.3 ± 0.4	4 ± 2
GW08-15	Surendranagar	12 ± 2	0.21 ± 0.14	79 ± 4	9 ± 4	12 ± 2	9 ± 5	61 ± 3	24 ± 7	86 ± 18	4 ± 4	0.2 ± 0.4	9 ± 4
GW08-16	Olak	63 ± 9	0.27 ± 0.17	33 ± 9	4 ± 4	60 ± 8	11 ± 5	23 ± 6	9 ± 5	95 ± 19	1 ± 1	0.0 ± 0.0	1 ± 1
GW08-17	Sakli	0.3 ± 0.1	0.04 ± 0.03	98 ± 1	1 ± 1	0.6 ± 0.1	2 ± 1	97 ± 1	3 ± 2	52 ± 24	22 ± 20	8 ± 13	28 ± 21
Kutch													
GK08-1	Viramgam	8 ± 4	0.01 ± 0.01	91 ± 1	1 ± 1	10 ± 4	0.5 ± 0.3	90 ± 4	3 ± 1	41 ± 27	41 ± 32	12 ± 18	16 ± 15
GK08-2	Kasiawah	10 ± 7	0.2 ± 0.1	84 ± 6	5 ± 3	11 ± 6	12 ± 4	68 ± 5	14 ± 5	4 ± 3	84 ± 30	1 ± 1	8 ± 4
GK08-3	Buddharmoma	13 ± 8	0.4 ± 0.1	79 ± 7	8 ± 4	13 ± 6	17 ± 5	56 ± 5	19 ± 6	3 ± 2	88 ± 32	1 ± 1	8 ± 4
GK08-4	Revapur	15 ± 8	0.10 ± 0.03	79 ± 7	6 ± 3	17 ± 7	5 ± 2	18 ± 6	18 ± 5	12 ± 8	69 ± 27	2 ± 2	19 ± 9
GK08-27	Matanomadh	8 ± 6	0.1 ± 0.1	83 ± 6	9 ± 3	9 ± 5	5 ± 2	62 ± 4	24 ± 5	6 ± 5	69 ± 26	1 ± 2	25 ± 9
GK08-29	Devpar	19 ± 8	0.3 ± 0.1	76 ± 8	5 ± 3	21 ± 7	13 ± 4	60 ± 6	13 ± 5	7 ± 4	85 ± 31	1 ± 1	7 ± 4
GK08-30	Manukuwan	15 ± 8	0.10 ± 0.03	74 ± 7	11 ± 4	15 ± 6	5 ± 2	54 ± 5	28 ± 6	10 ± 6	62 ± 24	1 ± 2	29 ± 10
GK08-33	Nana Asampiya	20 ± 9	0.4 ± 0.1	71 ± 8	9 ± 5	18 ± 6	19 ± 6	48 ± 5	21 ± 7	4 ± 3	88 ± 31	0.4 ± 0.6	7 ± 4
GK08-35	Morgar	12 ± 8	0.4 ± 0.1	81 ± 7	7 ± 4	12 ± 6	16 ± 5	58 ± 5	18 ± 6	3 ± 2	88 ± 32	1 ± 1	7 ± 4
GK08-36	Morgar	11 ± 7	0.2 ± 0.1	81 ± 7	7 ± 3	12 ± 6	10 ± 3	62 ± 5	20 ± 6	5 ± 4	81 ± 29	1 ± 1	13 ± 6
Chambal Basin													
GP09-4	Neemthur	29 ± 5	0.18 ± 0.06	69 ± 5	1 ± 2	27 ± 4	19 ± 7	47 ± 4	4 ± 3	89 ± 21	8 ± 5	1 ± 2	1 ± 2
GP09-12	Neemthur	6 ± 1	0.01 ± 0.01	86 ± 2	8 ± 2	6 ± 1	1 ± 1	60 ± 2	27 ± 5	65 ± 19	1 ± 1	4 ± 7	26 ± 8
GP09-17	Bhagwanpura	5 ± 1	0.09 ± 0.03	94 ± 2	1 ± 1	6 ± 1	13 ± 5	83 ± 2	3 ± 2	71 ± 22	19 ± 12	6 ± 10	3 ± 4
GP09-18	Usarna	3 ± 1	0.06 ± 0.03	96 ± 1	1 ± 1	5 ± 1	9 ± 4	84 ± 2	6 ± 3	59 ± 25	23 ± 15	11 ± 17	10 ± 10
GP09-34	Dakhalipura	64 ± 11	0.05 ± 0.03	35 ± 11	1 ± 1	69 ± 10	7 ± 3	28 ± 8	2 ± 2	94 ± 22	1 ± 1	0.3 ± 0.4	0.3 ± 0.5
GP09-38	Birai village	10 ± 2	0.04 ± 0.02	89 ± 2	1 ± 1	13 ± 2	6 ± 2	80 ± 2	3 ± 2	87 ± 22	5 ± 3	4 ± 6	2 ± 2

* The Suffixes Sil, Carb, SAS and Deccan represent silicates, carbonates, saline alkaline soils and deccan basalts respectively.

from 0.71055 – 0.71868. Sr isotope composition is less radiogenic in Gujarat (0.70863 – 0.71243) and Kutch (0.70919 – 0.71228) groundwaters.

Major ion, Sr content and $^{87}Sr/^{86}Sr$ of the groundwaters analysed in this study indicate their significant contribution from saline-alkaline soils present in the respective basins in addition to silicates and carbonates. Major ion ratio plot of Mg/Na vs. Ca/Na (Fig. 5.4) shows that some samples from Ganga plain lie in the mixing zone between silicates and carbonates and/or Deccan basalts. Most of groundwaters from all four regions have lower Ca/Na and Mg/Na than silicates and plot between silicates and saline-alkaline soil endmembers. This could be explained as either due to Ca, Mg precipitation or due to addition of Na or both. Very high Na content of these groundwaters does indicate its addition from saline-alkaline soils and hence many of them result from mixing between silicates and saline-alkaline soils.

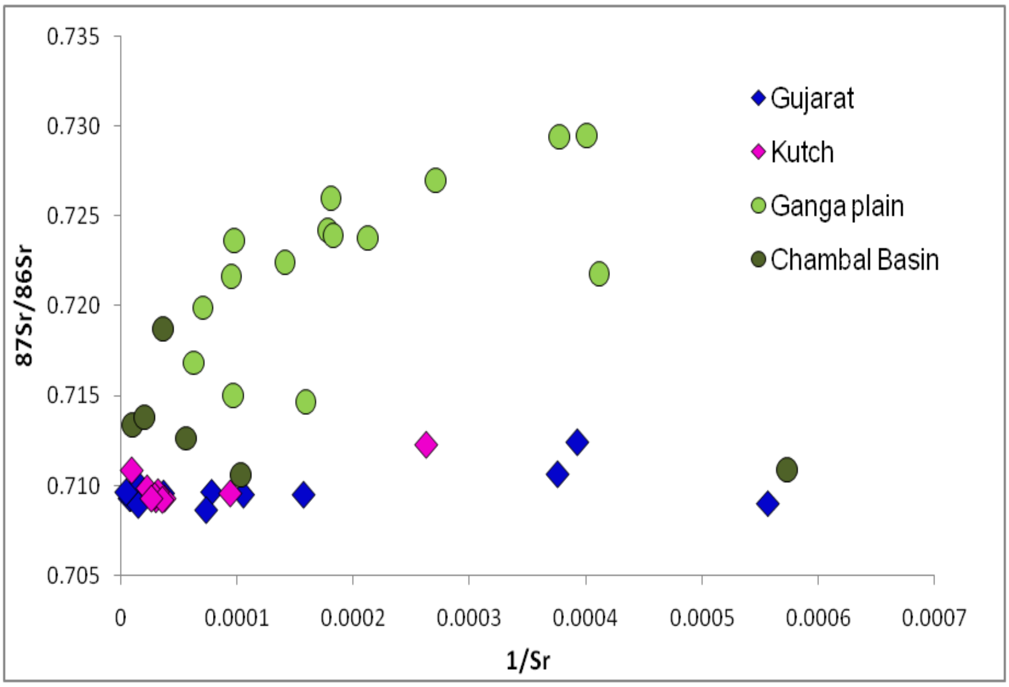

***Fig. 5.5:** Sr isotopic ratios in groundwater from different basins are distinctively different.*

The $^{87}Sr/^{86}Sr$ vs. 1/Sr plot shows a prominent distinction between samples from Gujarat (including Kutch) and Ganga plain (Fig. 5.5). The Gujarat and Kutch samples have very consistent Sr isotopic ratio (~0.71) with varying Sr concentration. Whereas samples from the Ganga plain have comparatively low Sr concentration and higher radiogenic Sr. Chambal basin Sr isotopic data is similar to Gujarat groundwater in isotopic composition and concentration. These samples have been plotted along with the four possible endmembers, viz. silicates, carbonates, Deccan basalts and saline-alkaline soils in a $^{87}Sr/^{86}Sr$ vs. Na/Sr plot (Fig. 5.6). This plot shows that most the samples are close to saline-alkaline soils and Deccan basalt endmembers, rather than silicate or carbonates. The groundwaters from the Ganga plain is defined by the mixing of saline-alkaline soils with silicates and carbonates whereas groundwaters of the Chambal basin, Gujarat and Kutch gets contribution from saline-alkaline soils, basalts and carbonates. Quantification of the dissolved material of these groundwaters from different sources is not possible from this plot due to presence of more than two endmembers.

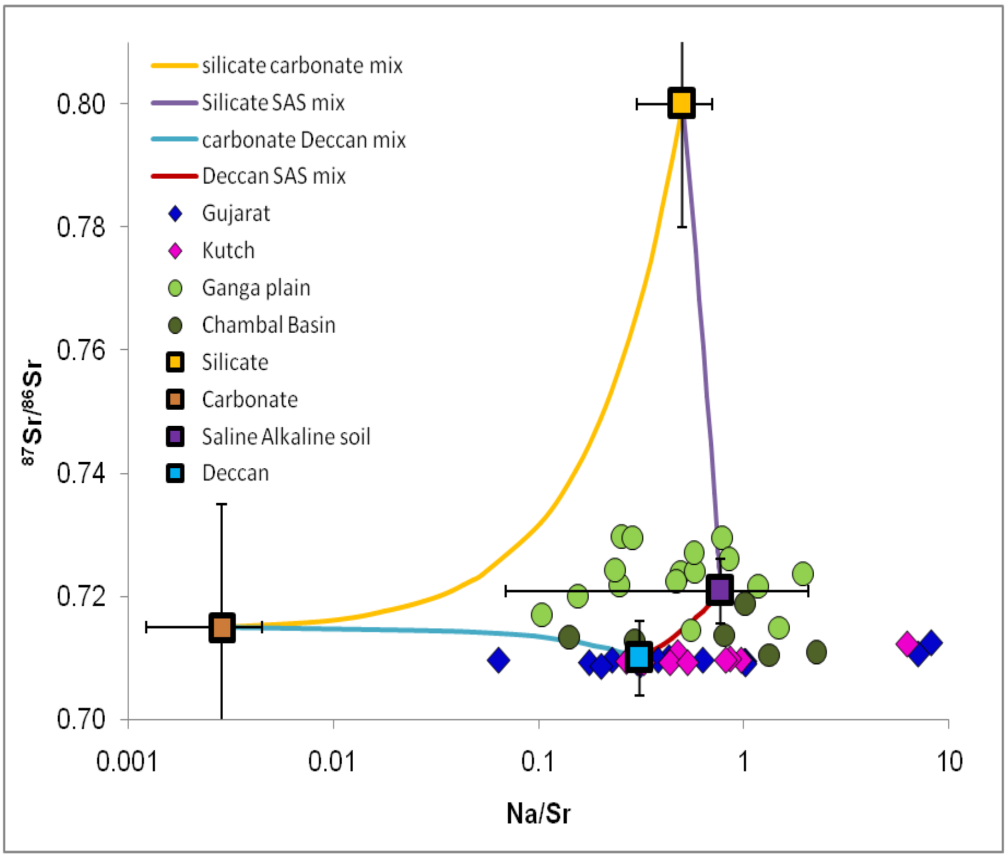

***Fig. 5.6:** Sr isotopic composition vs Na/Sr plot shows saline-alkaline soils are needed as a source endmember of groundwater dissolved ions.*

5.2.1 Source apportionment of dissolved ions using inverse model

From the above discussion, it is clear that the groundwater major ion concentration in these regions is closely related with the formation of saline-alkaline soils.

The source apportionment of dissolved material to the groundwater was done using inverse model using mass balance equations as discussed in Chapter 3.Three Sources were taken for samples from the Ganga plain, viz. silicate, carbonate and saline-alkaline soil. One additional source has been taken for Gujarat, Kutch and Chambal basin, i.e. Deccan Basalt. *A-priori* values of these four endmembers are taken similar to those given in Table 3.4. *A-posteriori* results from the model are listed in Table 5.2A and 5.2B. From table 5.2B, it could be observed that the source (endmember) chemical and isotopic composition in Gujarat and Kutch are same within uncertainty. The endmember composition of Chambal basin also follows them closely. The samples from the Ganga plain have slightly different endmember composition, also there is difference in the monsoon and non-monsoon sample endmember compositions. This could be due to difference in chemical composition of recharging rain water during monsoon vs. the riverwater during non-monsoon.

Source apportionment of Na shows saline-alkaline soils as the most important contributor of Na in majority of the samples (Table 5.3A and 5.3B). In Gujarat 33-98% of dissolved Na in the groundwater is of saline-alkaline soil origin. Whereas, in Kutch these soils contribute 79-91% of dissolved Na. Silicate contribution of Na to the groundwater of Gujarat and Kutch is less than 22% in all cases except one. Deccan basalts contribute less than 11% of Na in the groundwater of this region. In Chambal basin also, saline-alkaline soils contributes 35-96% of dissolved Na to the groundwater. Silicates and basalts contribute 3-64% and 1-8% of the same respectively in this region. In the Ganga plain, 14-96% of groundwater Na is coming from saline-alkaline soils, while, 2-85% of the same is contributed by silicates during monsoon. In non-monsoon 2-46% of dissolved Na in the groundwater is provided by silicates, whereas, 53-98% of Na is supplied by saline-alkaline soils. The cation budget in the Ganga plain has 9-71% carbonate, 5-80% saline-alkaline soils and 5-72% silicate contribution in monsoon. During non-monsoon silicates, carbonates and saline-alkaline soils supply 4-30%, 12-54% and 18-90% of cation budget respectively. Saline-alkaline soils dominate the cation budget in most of the samples from Gujarat (21-97%), Kutch (18-90%) and Chambal basin (28-84%). Carbonates contribute 1-62%, 1-19% and 1-19% of the cation budget in Gujarat, Kutch and Chambal basin respectively. Silicates provide 1-60%, 9-21% and 5-69% of cations in the groundwater in these regions. The major sources of Sr in the groundwater are carbonates and silicates with moderate supply from deccan basalts. Saline-alkaline soils contribute least Sr to the groundwater. In general residence time of the groundwater is longer than any other natural water sources. Hence, it is assumed that the groundwater gets it dissolved constituents from slow erosion of aquifer bedrocks. This study shows that presence of saline-alkaline soils in the recharge area of the groundwater can change the scenario considerably.

5.2.2 Natural sources of NO_3 to the groundwater aquifers

Groundwater samples from Gujarat and Kutch contain very high NO_3 in most of them (39-5150 μM). In general, high NO_3 concentration in groundwater has always been inferred to be derived due to anthropogenic activities. But deep groundwaters of Gujarat and Kutch, which have been reported to be very old (upto 30 ka; Agarwal et al., 2006) also contains high NO_3. These deep and old groundwater would not have acquired high NO_3 from anthropogenic activity. The sources of anthropogenic nitrate are mainly fertilizers and sewage systems. Contamination from these sources is unlikely to affect in large spatial scale like the area of present study (the state of Gujarat). Hence, it indicates towards its natural source. It is evident that Ganga plain is much more agriculturally active and densely populated than Gujarat and Kutch region. But groundwater from these regions (and from shallower depths) does not contain NO_3 concentration as high as Gujarat. Considering these points, it can be concluded that the source of the NO_3 concentration in the groundwater of Gujarat cannot be anthropogenic.

One possible mechanism for this high NO_3 concentration could be the enrichment of NO_3 in the groundwater during saline-alkaline soil formation. It is well known that cyclic wetting and drying is natural phenomenon of groundwater in the endoreic and semi-arid regions (Drever, J.I., 1997). In the dry season shallow groundwater comes up due to capillary action. This water leaches the nearby soils which increases the concentration of the dissolved ions in it. These dissolved salts precipitate when the groundwater dries in the surface. During wet season, the surface water dissolves the salts again which raise the concentration of dissolved ions. Finally, the water enriched with dissolved ions either flows through the surface to rivers or percolates to recharge the groundwater. However, NO_3 preferably remain in the dissolved phase and hence, does not precipitate along with the cations. Therefore its concentration will keep on increasing in the aquifer (due to no loss via precipitation) and its concentration will be more in relatively old groundwater. This process explains the enrichment of NO3 in groundwater in vast areas like Gujarat.

5.3 Conclusions

Salinity is one of the major contaminant of groundwater (Naftz et al., 1997). The groundwater (both deep and shallow) from Gujarat and Kutch region is almost brackish in nature. The groundwater from the Ganga plain also needs assessment due to over exploitation. In the present study groundwater samples from these two regions have been analyzed chemically and using Sr isotope systematic. The salinity of ground water could be of, a) marine origin, b) natural terrestrial origin or c) anthropogenic terrestrial origin (Weert and Gun, 2012). Seawater is not a direct source of dissolved solids in Gujarat, as rainwaters are quite dilute in TDS. The alluvial aquifers of Gujarat have their recharge area at the foothills of Aravalli (Agarwal et al., 2006), and discharge near the Kutch region. The source apportionment using inversion of chemical and Sr isotopic data shows that saline-alkaline soils are an important source of dissolved ions in the groundwater systems of the Ganga plain, the Chambal basin, Gujarat and Kutch. Presence of saline-alkaline soils in these basins confirms this conclusion. The radiocarbon dating has established the age of 2 ka near the recharge area and ~35 ka near discharge. Longer residence time along with presence of highly soluble salts could increase the dissolved component of these groundwaters. In the endoreic and semi-arid regions, cyclic wetting and drying is natural phenomenon (Drever, J.I., 1997). During wet season, the water with high concentration of soluble salts percolates to recharge the groundwater, whereas in the dry season shallow groundwater comes up due to capillary action and dissolved salts precipitate when it dries. Very low concentration of NO_3 is observed in the saline-alkaline soil water extracts. It could be suggested that NO_3 of natural origin accumulates in the groundwater as they are among the last to precipitate. Therefore the water, which percolates to the aquifer, is enriched with dissolved NO_3. The source apportionment using inversion of chemical and Sr isotopic data shows that saline-alkaline soils are an important source of dissolved ions in the groundwater systems.

Chapter 6

Rain water chemistry and use of Sr as provenance tracer of base cations

6.1 Introduction

Rain water acquires its dissolved constituents from gaseous or particulate matters present in the atmosphere. Sources of these materials could be natural or anthropogenic. Gaseous phases like SO_4 and NO_3 from anthropogenic origin dissolves in the rain water and are responsible for acid rains. Dissolvable cations such as Ca, Mg, which are of natural origin, can help to maintain the alkalinity in the rain water. They are derived from the soil dust present in the atmosphere. There have been a number of studies of the wet deposition in the Indian subcontinent to deal with the chemical components and to understand their characteristics (Saxena et al., 1996; Kulshrestha et al., 1999, 2009; Safai et al., 2004; Rastogi and Sarin, 2005). It has been observed that in Indian region the rainwater are mostly alkaline in nature due to abundance of primary aerosols (Ca, Mg and K) originating from the dusty soils (Kulshrestha et al., 2003; Chandra Mouli et al., 2005). Also there has been studies to detect the crustal influence on rainwater (Jain et al., 2000). It is important to apportion the sources of dissolved constituent present in the rainwater. Efforts has been made to determine the sources based on major ion composition of the rainwater (Safai et al., 2004; Chandra Mouli et al., 2005).It is, however, difficult to apportion the sources of dust using the major ions alone due to overlapping nature of major ion composition in various sources. Sr isotope composition of the rainwater could be useful to determine the sources of dissolved component owing to large variation in $^{87}Sr/^{86}Sr$ of the various sources contributing to the dissolved component of rainwater. Sr isotopic ratio of the rainwater has been used to delineate the sources, natural as well as anthropogenic (Dupre et al., 1994; Nakano and Tanaka, 1997; Negrel and Roy, 1998; Cheng et al., 2010). It has been used as a tracer of sources of base cations to the rainwater (Xu and Han, 2009), which are important to maintain the pH balance of the same. The Sr isotopic ratio, which has distinctively different values in various rock types, has been used extensively to track physical and chemical weathering (Gaillardet et al., 1999; Krishnaswami et al., 1999; Dessert et al., 2001; Jacobson, 2002; Singh et al., 2008, etc.). The reason behind variation in the isotopic ratio of the source rock is the difference in their Rb/Sr ratios and their age. For example carbonates having lower Rb/Sr will have lower $^{87}Sr/^{86}Sr$ compared to silicates with higher Rb/Sr. Accordingly the various lithological units in India could be differentiated, e.g., in the Himalayan Crystallines, Sr isotopic ratio varies from 0.72-0.94, in Deccan Traps .704-.716 (Das et al., 2006; Singh et al., 2008) and the Himalayan and the Vindhyan carbonates have $^{87}Sr/^{86}Sr$, ~0.71. The $^{87}Sr/^{86}Sr$ ratio in various parts of eastern Africa and middle east Asia, which could affect Ahmedabad rainwater during south-west monsoon, are also constrained, e.g. Congo craton (0.715), Ethiopian and Red sea basalts (0.704), Oman ophiolites (0.704) etc. (Sirocko, 1995). Therefore, the natural dust sources of Ca, which are same as Sr sources, could be apportioned in this region using Sr isotopes. In this context, the rainwater from Ahmedabad, India has been studied using Sr isotopic ratio along with major ions to delineate the sources of base cations in terms of different lithology. Present study reports the first data set of Sr isotopic ratio in rain water of the Indian subcontinent.

6.2 Results and Discussion

The major ion and Sr data of Ahmedabad rainwaters are given in Table 6.1. Na (3 – 66 μM), Ca (11 – 92 μM) and NH_4 (7 – 108 μM) are the major cations with relatively smaller amount of Mg (2 – 19 μM) and K (1 – 7 μM). SO_4 (7 – 60 μM), NO_3 (11 – 65 μM) and HCO_3 (2 - 101 μM) are major anions with occasionally high Cl (5 – 83 μM). All the major ion concentrations and TDS (1.7 – 17.9 mg/l) measured in the Ahmedabad rainwater during 2008, 2009 and 2011 in this study are on the lower side of the previously measured range (TDS : 1.9 – 137 mg/l) by Rastogi and Sarin, (2005) (discussed below). Sr concentration varies from 32 – 191 nM in the rainwater, whereas its isotopic ratio varies from 0.70878 - 0.71027. The statistical analysis of pH, major ions and Sr are given in Table 6.2. Average relative abundances of anions (on equivalent basis) follow the sequence SO_4^{2-}> HCO_3^->Cl^-> NO_3^- with SO_4^2- dominating the anion budget. Ca^{2+} dominates the cation budget of the rainwaters of Ahmedabad with the sequence Ca^{2+}> NH_4^+> Na^+> Mg^{2+}>K^+. SO_4 and NO_3 are the major anions which are responsible for the

Table 6.1: Major ion, Sr concentration and $^{87}Sr/^{86}Sr$ in the rain water (major ion concentrations are in μM and Sr concentration is in nM)*.

Sample	Date	Precipitation (cm)	pH	Na	K	Mg	Ca	NH_4	F	Cl	NO_3	SO_4	HCO_3	Si	Sr	$^{87}Sr/^{86}Sr$
RaW-1	30.6.08	8.20	5.16	6	4	2	12	15	b.d.	9	13	12	27	2	35	0.709359
RaW-2	01.07.08	3.60	5.22	6	4	2	11	7	b.d.	5	16	14	21	3	37	0.709080
RaW-3	02.07.08	2.17	5.46	66	3	19	92	38	b.d.	83	65	44	36	6	191	0.708974
RaW-4	28.07.08	16.26	5.31	18	1	3	13	35	b.d.	24	14	15	15	2	34	0.708975
RaW-5	29.07.08	0.37	4.81	29	7	10	70	108	1	34	33	60	b.d.	7	189	0.709893
RaW-6	02.08.08	2.62	5.40	15	2	2	13	66	b.d.	20	15	31	11	4	38	0.709890
RaW-7	12.08.08	10.54	5.31	28	2	4	19	40	b.d.	36	19	21	29	6	57	0.708991
RaW-8	26.08.08	0.54	5.39	61	2	12	68	5	1	80	12	43	101	15	171	0.709412
RaW-9	13.09.08	3.11	4.60	8	2	6	46	17	3	7	19	45	b.d.	7	112	0.709936
RaW-10	18.09.08	1.80	4.61	3	b.d.	b.d.	16	39	5	4	11	7	b.d.	7	34	0.710278
RaW-11	9.07.09	8.61	5.14	10	1	10	16	15	b.d.	11	12	15	2	3	32	0.709711
RaW-12	18.07.09	0.04	5.74	37	4	13	38	64	b.d.	44	24	50	56	8	120	0.709618
RaW-13	24.07.09	0.18	5.26	56	4	10	31	51	b.d.	67	24	41	52	4	104	0.709125
RaW-14	7.07.11	3.84	5.37	12	2	5	25	76	b.d.	9	17	28	54	n.m.	72	0.709271
RaW-15	9.07.11	4.60	5.29	23	2	5	17	39	b.d.	22	11	17	41	n.m.	48	0.708823
RaW-16	11.07.11	7.76	5.31	28	1	5	16	16	b.d.	26	8	11	36	n.m.	41	0.708789

*Precipitation data collected from Dr. R.D. Deshpande, Physical Research Laboratory, Ahmedabad.
b.d. = below detection limit
n.m. = not measured

Table 6.2: Statistical data of major ions and Sr.

Species*	Median	Mean	SD	Min	Max
pH	**5.3**	**5.2**	**0.3**	**4.6**	**5.7**
Na^+	**21**	**26**	**20**	**3**	**66**
K^+	**2**	**3**	**2**	**0**	**7**
Mg^{2+}	**5**	**7**	**5**	**0**	**19**
Ca^{2+}	**18**	**31**	**25**	**11**	**92**
NH_4^+	**38**	**39**	**28**	**5**	**108**
F^-	**1**	**1**	**2**	**0**	**5**
Cl^-	**23**	**30**	**26**	**4**	**83**
NO_3^-	**15**	**20**	**14**	**8**	**65**
SO_4^{2-}	**25**	**28**	**17**	**7**	**60**
HCO_3^-	**36**	**37**	**25**	**0**	**101**
Sr	**53**	**82**	**58**	**32**	**191**

*Major ions are in µM where as Sr is in nM.

acidic nature of the rainwater and Ca and NH_4 are major cations responsible for neutralizing these acids. Though the variation of pH (4.6 – 5.7) in these samples is not very large; all the samples have pH more than 5.0 except 3 of them. Many of these samples are having pH less than 5.6 (pH of natural rainwater in equilibrium with atmospheric CO_2) indicating that SO_4 and NO_3 are not getting neutralized by cations such as Ca, Mg and NH_4. Therefore most of the samples are in the pH range of rainwater in a clean atmosphere, where dissolution of CO_2, NO_X and SO_2 in clouds and water droplets gives the acidic pH (Xu et al., 2012), and the absence of alkaline pH could be due to absence of excess dust cations. From the major ion data, it has been observed that NH_4, Ca and Mg show very good correlation with SO_4 and NO_3 (Fig 6.1), suggesting that these cations are the main neutralizer of acids in the rain water.

6.2.1 Temporal variability in rainwater composition over Ahmedabad

The major ion data of this study has been compared with the earlier study of the same region carried out during 2000-2002 (Rastogi and Sarin, 2005, 2007). Previously measured Na (1.3 – 1030 µM), Ca (5.5 – 1057 µM), NH_4 (1.7 – 220 µM), SO_4, NO_3 and all other ions show a range much greater than this study. The major ion concentration of all the samples in this study is in the lower side of the range measured in the previous study (Rastogi and Sarin, 2007) indicating low solute rain events during 2008, 2009 and 2011.

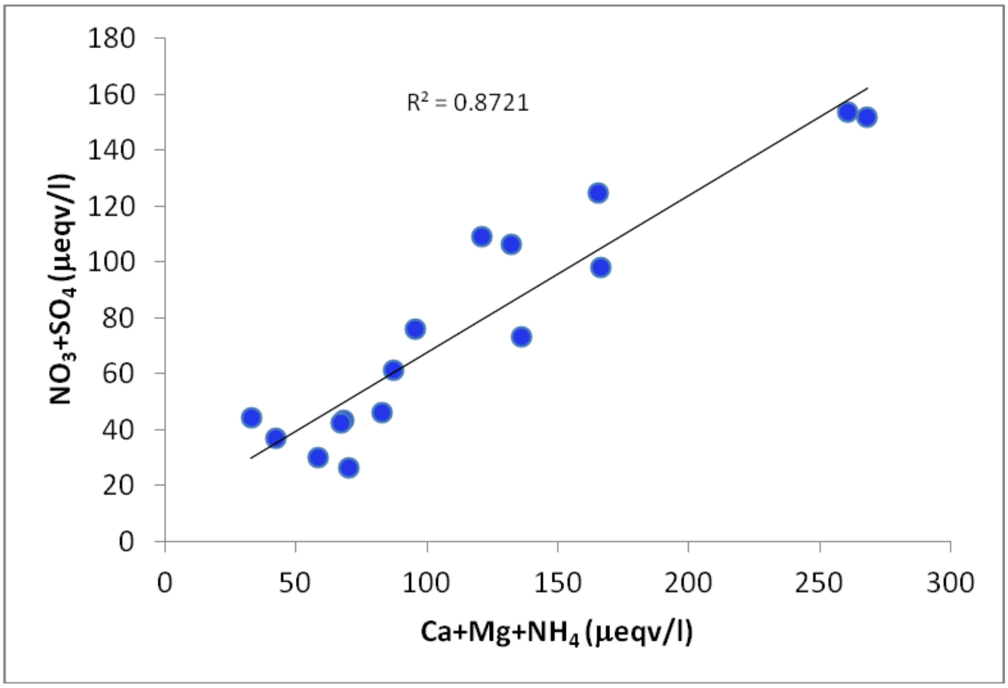

Fig. 6.1: *Good correlation between base cations and major acidic components shows that Ca, Mg and* NH_4 *act as the major acid neutralizer.*

Total dissolved solids in the rains analyzed in this study are lower compared to those measured during 2000-2002 (Rastogi and Sarin, 2007). The pH values measured in this study (4.6 – 5.7, average=5.2) are also in the lower side of the previously measured range (5.2 – 8.2, average=6.7). This could be interpreted as the signature of in cloud scavenging process rather than below cloud for these samples, as all of them were collected during high precipitation. Another possible cause could be the difference between rainfall patterns during the rainwater collection time periods. Precipitation data for North Western India from 1995 to 2010 shows that 2000-2002 were comparatively drier period compared to 2008-2010 (Fig 6.2). Comparatively less rainfall during 2000-2002 could provide more dust to the atmosphere and hence more solutes in the rainwater. This observation is corroborated by higher TDS and pH in the samples collected during 2000-2002 compared to those during 2008-2011.

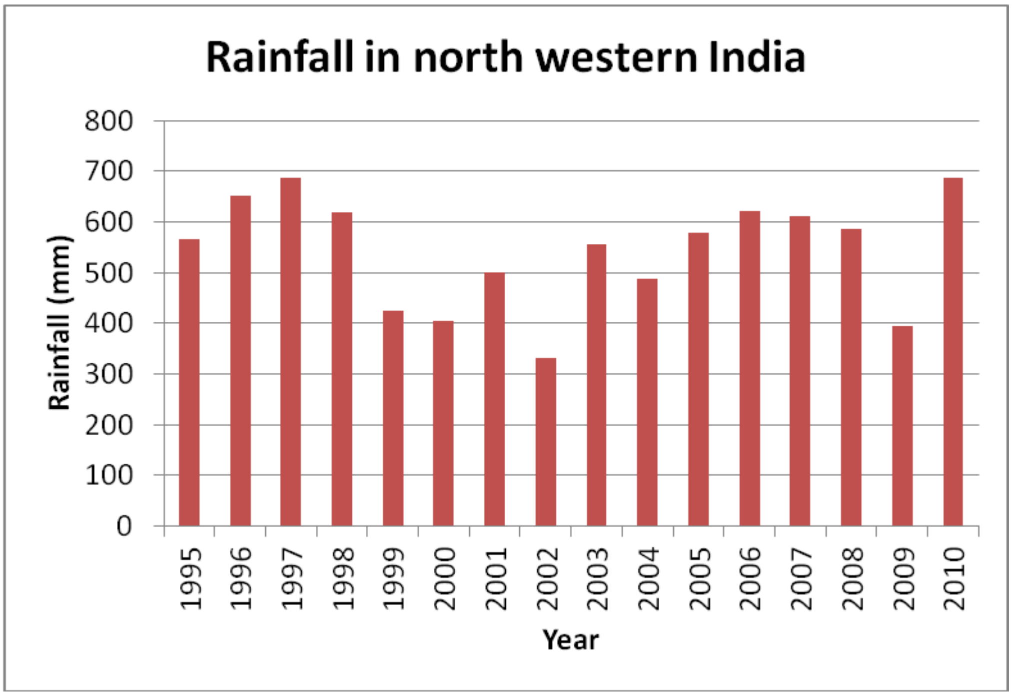

Fig. 6.2:*Temporal variation in average annual rainfall during 1995 – 2010 in north-western India. Samples for this study was collected during higher average rainfall year of 2008-2011.*

6.2.2 Sources of major cations

In most of the samples Cl correlates very well with Na and their ratio, Na/Cl, in these samples are similar to that of the seawater (Fig. 6.3). This suggests that Na and Cl in these rainwaters are mostly derived from Seawater, with very little anthropogenic contribution in the Cl ion. Further, as the sampling location, Ahmedabad is not very far from the coastal region, it can be safely assumed that all the Na in the rain water is of oceanic origin.

Further, to apportion other cations from continental sources, the non sea salt (NSS) components of various cations and anions are estimated using the formula,

$X_{NSS} = X_{Rain} - Na_{Rain} \times (X/Na)_{Seawater}$

Table 6.3: X/Na in seawater* (molar ratio).

Cl/Na	Ca/Na	Mg/Na	SO_4/Na	HCO_3/Na	Sr/Na
1.166	0.022	0.113	0.060	0.005	0.000197

*calculated from data given for seawater composition in Drever, J.I., 1997

Where X_{NSS} is the non sea salt component of the ion X; X_{Rain} and Na_{Rain} are the measured quantity of X and Na in rainwater respectively and $(X/Na)_{Seawater}$ is the ratio of X and Na in seawater (Table 6.3).

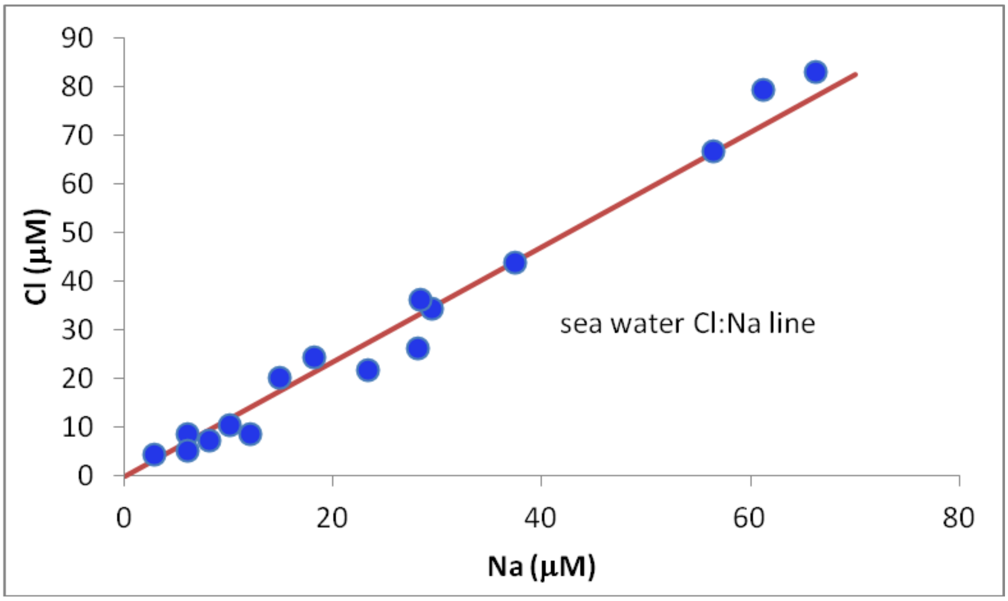

Fig. 6.3: *Chloride vs sodium ratio in Ahmedabad rainwater is almost similar to the seawater ratio indicating their contribution from seawater.*

Ca_{NSS} and Mg_{NSS} vary from 99% to 99.6% and 25% to 89% of the measured Ca and Mg respectively whereas non sea salt component of SO_4 and HCO_3 contribute 84.3% to 98.9% and 99.1% to 99.9% of their total budget respectively. Ca_{NSS}+Mg_{NSS} correlates well with HCO_{3NSS} indicating their common continental sources.

To apportion the sources of major cations of the rainwater, their Ca/Na and Mg/Na have been plotted on a mixing diagram (Fig. 6.4). The various possible endmembers contributing to the Ahmedabad rainwaters are also plotted based on their Na, Ca and Mg data. These data for the endmembers are taken from Das et al., (2005); Krishnaswami and Singh, (2005); Rengarajan et al., (2009). This mixing diagram assumes that elemental ratios of the various lithology are getting leached to rain water in same proportion as they are present in the respective lithology. The mixing diagram of Mg/Na and Ca/Na shows that the rain waters of the Ahmedabad fall on the mixing hyperbolae defined by the seawater and basalt end members and seawater and carbonate endmembers (Fig 6.4) (Krishnaswami and Singh, 2005). Fig. 6.4 indicates that carbonates and basalts, in addition to seawater, are contributing significantly to the Ca and Mg budgets of the rainwater. Other silicates do show proximity with rainwater composition, however, they do not contribute to cation budget of the rainwater (See discussion on Sr isotopes). The carbonates contributing cations to the Ahmedabad rain water could be from the Vindhyan, Aravalli, Ganga Plain, the Himalaya and/or from the African region (Negrel et al., 1993; Picouet et al., 2002). Basalts are either from the Deccan or from African region (Negrel et al., 1993; Picouet et al., 2002).

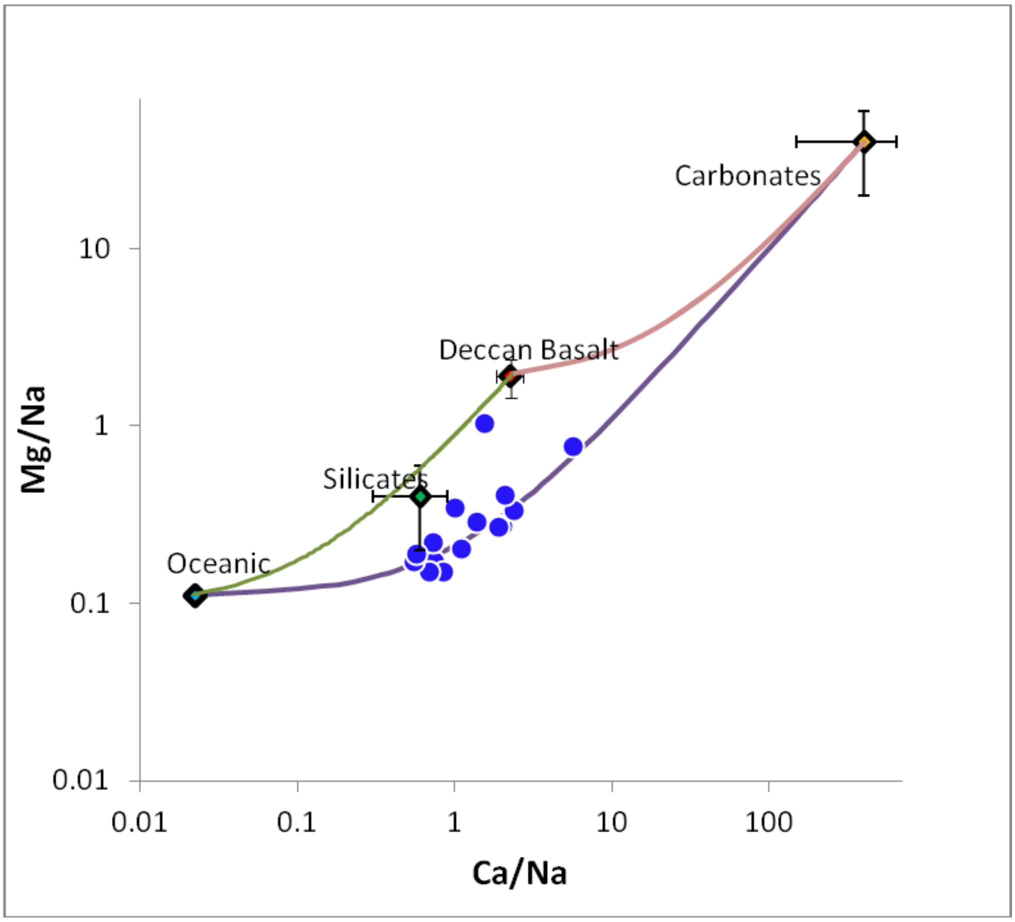

Fig. 6.4: *Ratio plot of Ca and Mg with Na shows that these ions in the rainwaters are result of mixing among three end members, oceanic, basalts and carbonates.*

6.2.3 Sr concentration and $^{87}Sr/^{86}Sr$

Sr concentration and its isotope composition in Ahmedabad rainwaters have been analyzed for the first time. Sr concentrations in these rainwaters vary by six times, from 32 to 191 nM. Its isotope composition varies from 0.70878 to 0.71027.

Sr_{NSS}varies from 87% to 98.6% with respect to measured Sr concentration in these rainwaters indicating its major contribution from continental sources. It has been observed that Sr concentration shows a very good correlation (coefficient 0.93) with the non sea salt component of Ca and Mg (Fig. 6.5), which was expected as a result of their similar source. Therefore, the use of Sr isotopes for tracking the sources of base cations is well justified.

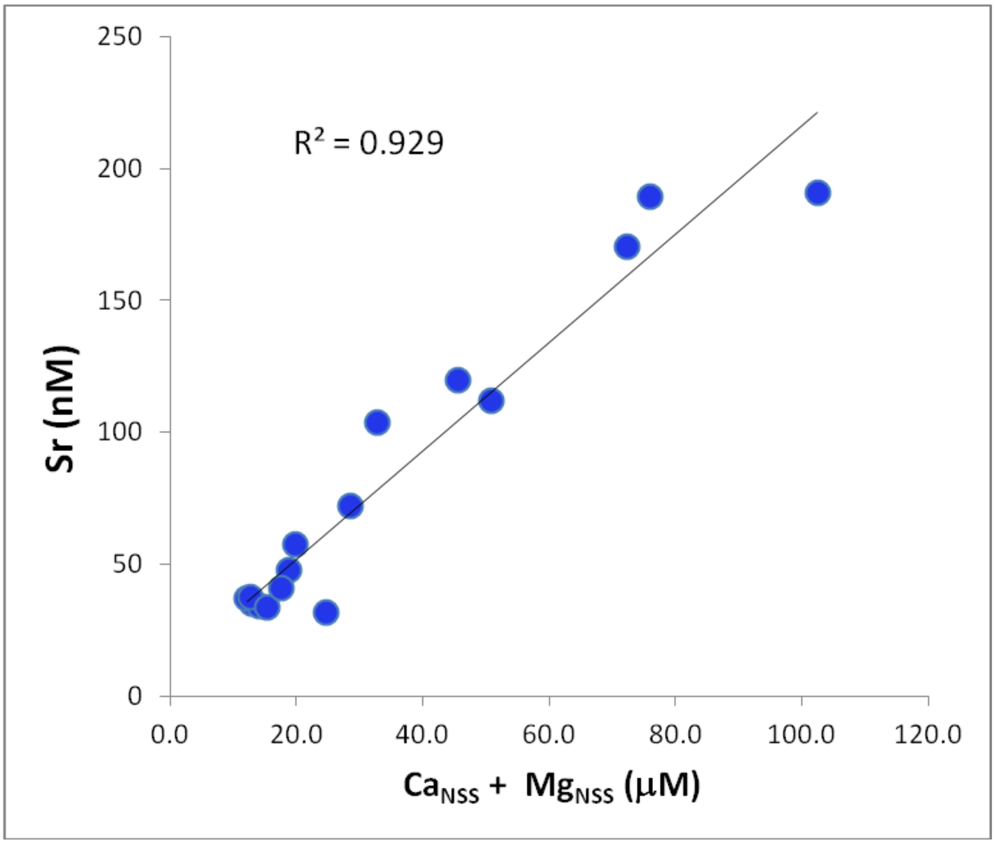

Fig. 6.5: *Good correlation between Sr and non sea salt component of the base cations indicate their similar continental sources.*

To further constrain the sources of Sr and other base cations, rainwater data has been plotted on a mixing diagram of Ca/Srvs^{87}Sr/^{86}Sr (Fig. 6.6). Along with the rainwater data, various possible endmembers are also plotted on the diagram based on their available data in the literature. One of the possible sources of these cations to the Ahmedabad rainwater is the sediments from the Thar Desert and the Ganga Plain. It has already been reported that the sediments from Thar desert and Ganga plain can be explained as mixture between Himalayan silicates and carbonates (Yadav and Rajamani, 2004; Tripathi et al., 2007). The aerosol geochemistry studied in the Thar desert region also suggests similar sources for Sr and Ca(Yadav and Rajamani, 2004). Considering this, Himalayan silicate and carbonates have been taken as endmembers in a mixing plot. It will be difficult to differentiate the Sr isotope composition of silicates and carbonates of the Aravalli and the Vindhyan from those of the Himalaya and hence silicates and carbonates endmember represent the combination of all these groups.

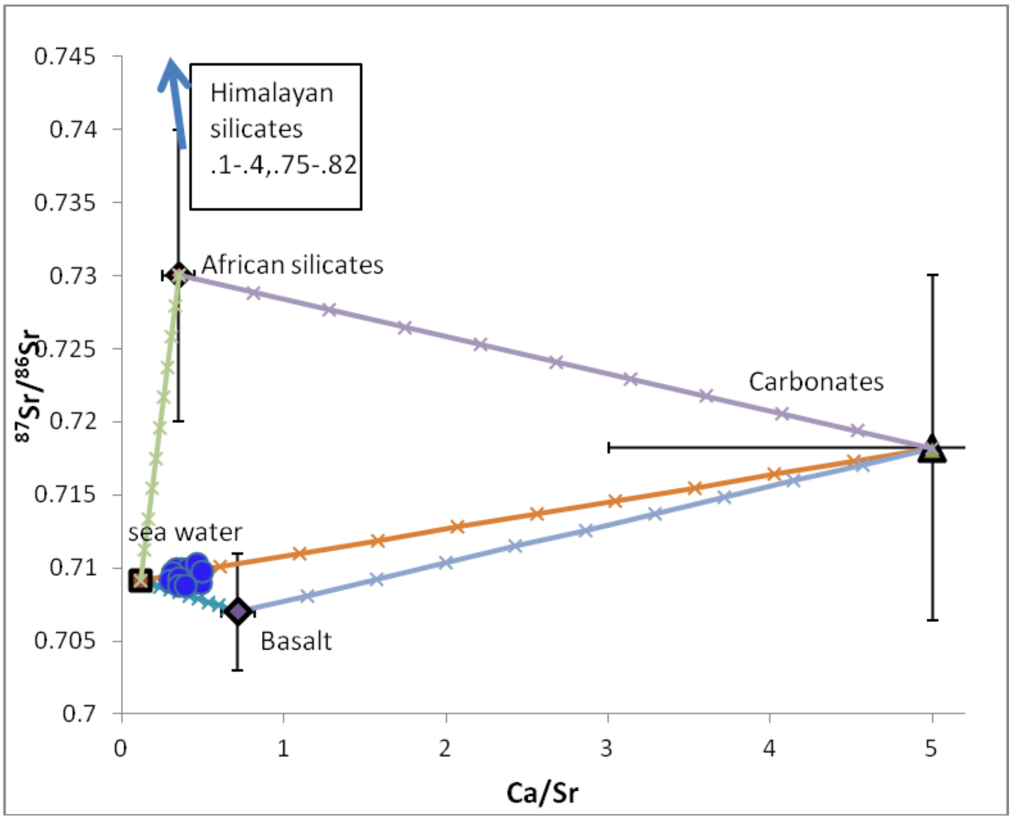

Fig.6.6: *Mixing plot between*$^{87}Sr/^{86}Sr$ *and Ca/Sr shows that Sr in rainwater of Ahmedabad is derived from carbonates, silicates and seawater. Contribution from silicates, if any, is negligible.*

The carbonates from Africa also show similar range, therefore they are not plotted separately. Silicates from the African region have similar Ca/Sr value as that of Himalaya, however they have less radiogenic Sr (Negrel et al,1993). Another lithology which could contribute dust to the rainwater of the Ahmedabad is Deccan Basalt and hence basalt has been plotted as another endmember on the mixing diagram (Fig. 6.6). This basalt endmember includes the basalts from the African region as well, as the Deccan Basalts and African Basalts are isotopically indistinguishable (Negrel et al., 1993). Due to its proximity from the sea, Ahmedabad rains could get Sr from seawater too and hence in Fig. 6.6 seawater is considered as an endmember. This figure shows that contribution from carbonates, basalts and seawater can explain the Sr budget of all the rainwater samples, as has been concluded by major ion ratio plot (Fig. 6.4). The rain water data points fall in the mixing field defined by seawater, carbonate and basalts endmembers (Fig.6.6). Therefore, the sources of Sr and Ca to the rainwater of Ahmedabad region could be specified as carbonates and basalts with small contribution from seawater. Silicates do not seem to contribute to the Sr budget of the Ahmedabad rainwaters, as that would result in more radiogenic Sr than observed. This interpretation about the sources of Sr and Ca to the Ahmedabad rainwater helps in constraining the sources better than that based on major ions only. To examine this in detail, the mixing lines have been included the percentage from each source (Fig.6.6), which shows that African silicates are less likely to contribute more than10% of the Sr isotopic budget of these rainwaters, while basalts and carbonates can explain most of the Sr budget (>50%-70%), considering the spread of these two endmembers. The rest of the Sr budget is balanced by Sr from oceanic origin.

The variation inSr isotopic ratio with time can be studied from Table 6.1. As the sea water Sr isotopic ratio is very well constrained at 0.70917±0.00001 (Nakano and Tanaka, 1997), the result indicates that the Sr is coming into the rain from sources with lower Sr isotopic signature, i.e. either Deccan Traps and/or Middle East Asia including Ethiopian basalts, whereas the higher values of Sr can come from the carbonates (Himalayan, Vindhyan or African). To have a rough idea of the wind pattern during the sampling period,7 days wind backward trajectories have been plotted with HYSPLIT model (http://www.arl.noaa.gov) (Draxler and Rolph, 2012). Four of such trajectories (two with lower Sr isotopic ratio and two with higher) are given in Figure 6.7. From Table 6.1 and Fig. 6.7 it can be seen that during July 28-29, 2008 though the collection date differs by only one day, the Sr isotopic ratio shows a large difference as the wind sources were different. In the first case (July 28, 2008) the wind has started from Arabian sea, whereas in the second case it has started from the African region, hence the higher Sr isotopic ratio is observed in the rain water collected on July 28, 2008.

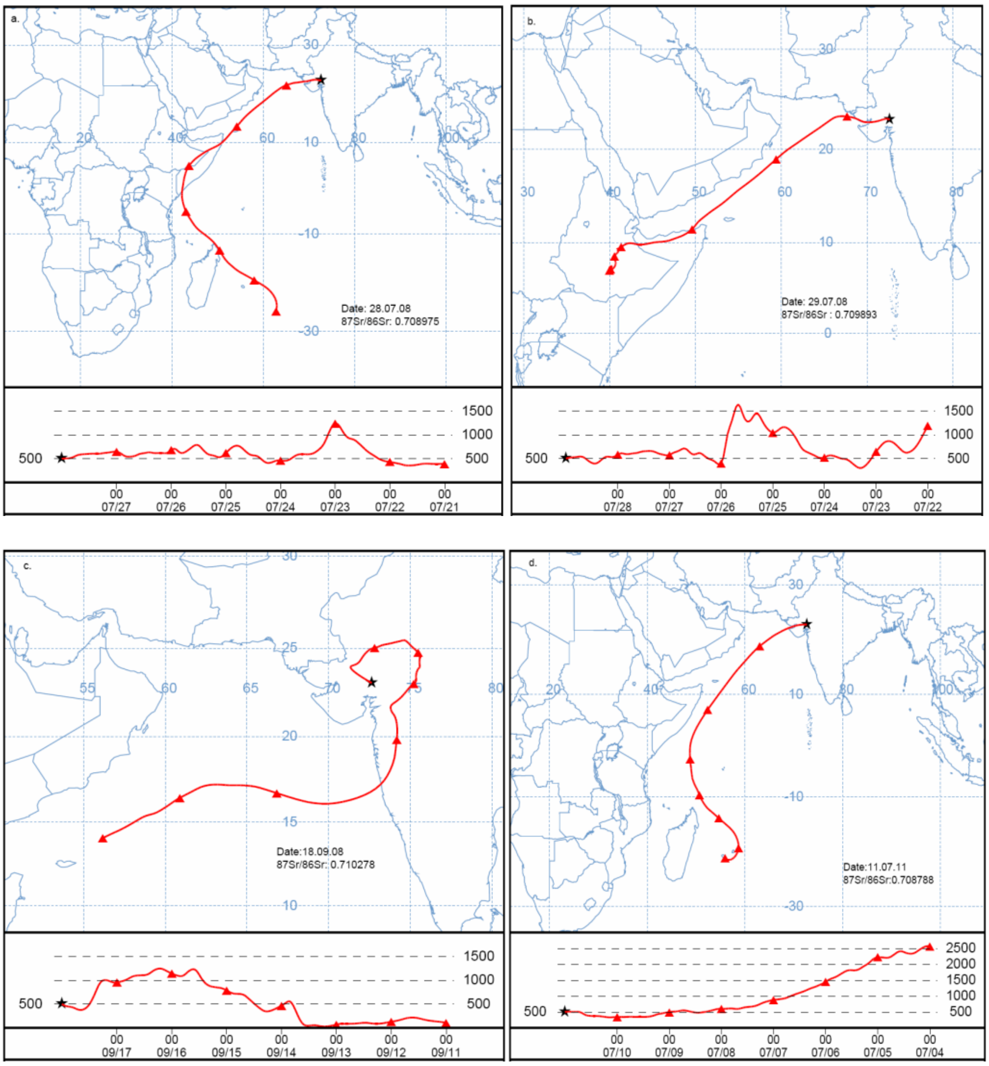

Fig.6.7: *a) 7 days wind Back trajectory starting from July 28, 2008 with Sr isotopic ratio0.708975. b) 7 days wind Back trajectory starting from July 29, 2008 with Sr isotopic ratio 0.709893. c) 7 days wind Back trajectory starting from September 18, 2008 with Sr isotopic ratio 0.710278. d) 7 days wind Back trajectory starting from July 11, 2011 with Sr isotopic ratio 0.708788.*

Similarly on September 18, 2008, when the rain water ^{87}Sr/^{86}Sr has the highest observed value (0.710278, Table 6.1), wind backward trajectory traversed a path through Aravalli and Ganga Plain region before coming to Ahmedabad (Fig.6.7c), whereas in other case (^{87}Sr/^{86}Sr, 0.708788; Fig.6.7d) it has traversed small distance inland from the Arabian Sea to Ahmedabad through the basaltic and alluvial terrains of south-west Gujarat. The above discussion shows the sensitivity of the Sr isotopic ratio in tracking the wind sources from different lithology.

6.3 Conclusions

Major ion, Sr concentrations and Sr isotope compositions were measured in the rain watersof an urban site to get an idea about the various sources of dissolved ions to rain water. The comparison of major ion data with previous studies shows the decrease in dissolved constituents in the rainwater during 2008-2011 due to higher rainfall compared to those during 2000-2002. It indicates possible influence of rain patterns (on yearly basis) over the abundance of dust in the atmosphere. The Sr concentration, which shows a very good correlation with the NSS component of Ca and Mg, has been used to delineate the dust sources to the atmosphere, assuming that they have same origin. ^{87}Sr/^{86}Sr along with major ion compositions of Ahmedabad rainwater indicate Carbonates and Basalts as important sources of dissolved base cations to the rainwater. The sources of dissolved material deduced from Sr isotopic ratio in the rainwater also agrees very well with wind back trajectory data obtained from NOAA HYSPLIT model. The present study shows the Deccan trap as a major source of Sr during the south-west monsoon. Occasional contribution from other major lithology such as Congo cratons and alluvial from the Ganga Plain have also been observed during this study. It can be concluded that Sr isotopes can be used quite satisfactorily as a provenance tracer of aerosols by measuring that in rain water.

Chapter 7

Summary and Future Perspectives

The major objectives of this thesis were to study the chemical erosion processes in the Ganga system with emphasis on the plain weathering and to quantify the relative importance of different sources of dissolved ions in river water, ground water and rain water. The Ganga plain is made of sediments having silicates and carbonates brought from the Himalaya with appreciable presence of saline-alkaline soils. Therefore, to study the chemical erosion in plain, characterization of these soils was necessary as they could be a major source of dissolved material to the river. It also helped in identifying an endmember, which was necessary to explain the major ion and Sr isotope composition of the Ganga river system. In this context, a study of the provenance of chemical weathering process of silicates in terms of litho-tectonic units in the Himalaya was also aimed. Nd isotopes in the dissolved phase were used for this purpose, for the first time in the Himalaya, its dissolved budget is controlled by silicate weathering. Further, the flux of dissolved Nd alongwith its isotope composition from the Ganga to the Bay of Bengal was to be constrained in this study. Along with this, apportionment of sources of dissolved ions in the groundwater was intended to define a relation between saline-alkaline soils and groundwater. It would also give information about long term erosion processes. The natural sources of dissolved ions in rain waters were characterised using their major ions and Sr isotopic composition. The aim was to delineate the sources of base cations to the rain water. A consorted effort has been made to achieve these goals. The major outcomes are listed below.

7.1 Characterization of saline-alkaline soils and their imapct on river geochemistry

Saline-alkaline soils are widely present in the Ganga plain. Due to their very high solubility, they can contribute large amount of dissolved ions to the rivers. Therefore, a detailed study of the Ganga river system has been carried out to characterizethe saline-alkaline soils present in the basin geochemically and isotopically. Its contribution to river chemistry has been determined. The silicate and carbonate erosion rate at the outflow have been estimated excluding the possible contribution of saline-alkaline soils. To study the erosion pattern in plain, samples from a number of small tributaries have also been analyzed. Use of forward model was not possible due to various sources of dissolved ions. Therefore, an inverse model approach has been employed to apportion the sources of dissolved budget.

The results show that saline-alkaline soils contribute 40% of total dissolved Na and 8% of the cation budget at the outflow of the Ganga. This high Na contribution is particularly damaging for all forward model estimation of silicate erosion using Na as a proxy. Our results show that chloride corrected Na cannot be used as proxy of silicate weathering in the Ganga plain as a significant amount of non-chloride Na are contributed from the saline-alkaline soils. Present estimation of silicate weathering rate of the Ganga at the outflow is 5.5-5.7 tons/km^2/yr, which is in the range of global mean. Earlier estimates of silicate erosion rate using Na as a proxy at the outflow were considerably over-estimated. The present study indicates towards lower intensity of chemical weathering in the plain compared to headwaters of the Ganga.

Other Hiamlayan tributaries like Ghaghra, Gandak also show similar or lower silicate and carbonate erosion rate in the plain, than the headwaters. Yamuna have a high contribution from saline-alkaline soils, in monsoon as well as non-monsoon, owing to its presence in the plain and contribution from the Deccan tributaries.

Small tributaries originated in the plain and peninsular regions are ideal to study the chemical erosion in the plain, as they don’t have Himalayan contribution. The results show that 60 – 92% of dissolved Na contribution in the small tributaries in plain is of saline-alkaline soil origin. The silicate and carbonate erosion rates in these sub-basins are quite low compared to the Himalayan region. Though they have higher temperature, vegetation, residence time of sediments than the Himalayan rivers, physical erosion producing larger surface area and freshening of sediments is insignificant in them. The results show very low silicate cation contribution (8 – 28%) in the tributaries from plain, which indicates towards importance of physical erosion among the controlling factors of chemical erosion.

7.2 Dissolved Nd in the Ganga river system and its flux to the Bay of Bengal

Different litho-tectonic units of the Himalaya have distinct Sr and Nd isotopic signature. Sediment Sr and Nd isotopic composition has been used to delineate the sources of physical weathering of silicates. In case of silicate chemical weathering, Sr isotopes cannot be used as it comes from carbonates also. Nd isotopes can be useful for this purpose as dissolved Nd in the river is mainly from silicates. To examine the possibility of using Nd to trace silicate chemical erosion, dissolved Nd concentration and isotopic composition has been measured in the Ganga river system. The data indicates towards more Higher Himalayan contribution in the dissolved Nd budget compared to the Lesser Himalaya. Also, the importance of Deccan tributaries in the dissolved Nd budget has been observed, though their contribution indicate significant temporal variability.

Higher ε_{Nd} in dissolved phase compared to their respective particulates and higher dissolved Sm/Nd compared to known endmembers indicate fractionation of ε_{Nd} during weathering. Possibility of preferential dissolution of minerals with different Sm/Nd ratio has also been examined. For this purpose, dissolved Nd data has been compared to the bedload Nd data from literature. The comparison shows that dissolved Nd is more radiogenic compares to the sediment. This difference could be due to preferential dissolution of apatite and more dissolved Nd contribution from the Deccan tributaries of the Yamuna. As these tributaries do not contribute significantly to the sediment, their higher dissolved Nd contribution could give rise to this difference. Nd flux of the Ganga to the Bay of Bengal has been estimated to be around 17000 to 34000 moles of Nd annually with ε_{Nd} value -14.5±0.5.

Dissolved Nd at the coastal region of Bay of Bengal has been measured to assess the impact of its riverine supply from the Ganga and to account for estuarine processes like removal or addition of REEs. The dissolved Nd isotopic composition at the surface is 2 to 3 epsilon unit more radiogenic compared to the Ganga outflow. Possible reason could be contribution of more radiogenic Nd from the Brahmaputra other than estuarine processes. Less radiogenic Nd isotopic composition has been measured in the deeper samples, indicating towards desorption of Nd from the shelf sediments of the Ganga origin. Dissolved Nd concentration in the Ganga outflow and coastal region are in the same range, though the it was marginally lower in deeper samples than surface samples.

7.3 Ground water chemistry and its relation to Saline - Alkaline Soils

Groundwater contributes to the river water during the lean flow and the aquifers are recharged during monsoon from the rivers depending on the water level. Groundwater is also an important factor in the formation process of saline-alkaline soils. On the other hand, salinity is one of the major contaminant of groundwater. It is necessary to study the groundwater chemical composition to understand these processes completely. The groundwater (both deep and shallow) from Gujarat and Kutch region are almost brackish in nature. The groundwater from the Ganga plain also needs assessment due to over exploitation. In the present study groundwater samples from these two regions have been analyzed chemically and using Sr isotope systematic. Sr isotopes can help to identify the sources of dissolved solutes to the groundwater, as Sr isotopic composition is distinctly different in different sources.

The results show very high TDS and particularly high concentration of Na in groundwater samples from Gujarat and Kutch. Seawater is not a source of dissolved constituents in groundwater of Gujarat, as has been observed from the Sr isotopic composition. The alluvial aquifers of Gujarat have their recharge area at the foothills of Aravalli (Agarwal et al., 2006), and discharge near the Kutch region. The radiocarbon dating has established the age of 2 ka near the recharge area and ~35 ka near discharge. Anthropogenic activity cannot explain presence of high NO_3 concentration in this kind of old groundwater. Therefore, we propose the natural phenomena of cyclic wetting and drying in the endoreic and semi-arid regions to be responsible for this high TDS and NO_3 in the groundwater. During wet season, the water with high concentration of soluble salts percolates to recharge the groundwater, whereas in the dry season shallow groundwater comes up due to capillary action and dissolved salts precipitate when it dries. Salinization occurs because Ca and to some extent Mg, precipitates early and they form calcretes or *Kankars,* which are not easy to dissolve. It has been observed in the saline-alkaline soil water extracts, that NO_3 concentration is very low in them. It is suggested that NO_3 of natural origin accumulates in the groundwater as they are among the last to precipitate. Therefore the water, which percolates to the aquifer, is enriched with dissolved NO_3. This study proposes an alternative explanation of high TDS in groundwater, completely unrelated to anthropogenic activities.

7.4 Rain water chemistry and use of Sr as provenance tracer of base cations

Rain water is one of the main sources of water to the rivers and groundwater recharge. Rain water acquires its dissolved constituents from gaseous or particulate matters present in the atmosphere. Major ion, Sr concentrations and Sr isotope compositions were measured in the rain waters of Ahmedabad to get an idea about the various sources of dissolved ions to rain water. The comparison of major ion data of present study with earlier studies shows the decrease in dissolved constituents in the rainwater during 2008-2011 due to higher rainfall compared to those during 2000-2002. It indicates towards possible influence of rain patterns (on yearly basis) over the abundance of dust in the atmosphere. The Sr concentration shows a very good correlation with the NSS component of Ca and Mg. therefore, it has been used to delineate the dust sources to the atmosphere, assuming that they have same origin. $^{87}Sr/^{86}Sr$ along with major ion compositions of Ahmedabad rainwater indicate Carbonates and Basalts as important sources of dissolved base cations to the rainwater. The measured data has been compared with wind back trajectory data obtained from NOAA HYSPLIT model. The results from that are in good agreement with sources of dissolved material deduced from Sr isotopic ratio in the rainwater. The present study shows the Deccan trap as a major source of Sr during the south-west monsoon. Occasional contribution from other major lithology such as Congo cratons and alluvial from the Ganga Plain have also been observed during this study. Sr isotopes in rain water haveretained their source signature and can be used quite satisfactorily as a provenance tracer of aerosols.

7.5 Future Perspectives

Research carried out as a part of this thesis has addressed issues pertaining to chemical weathering in the Ganga plain and sources of dissolved materials in river water, groundwater and rain water. There are, however, some areas related to this research which need further work. These have been listed below:

a) Chemical weathering in the Ganga plain have been studied using the dissolved composition in this study. Studies based on chemical composition of sediment indicates a much higher rate of chemical weathering in the plain compared to those based on water chemistry. This could be due to supply of paleo-weathered sediments from the plain tributaries. Sediments present in the plain could have suffered intense weathering in past causing stripping off their Na and other major ions. Such sediments could add to its contemporary budget but not to the dissolved budget. However, the time scale for such processes is not known. To understand the chemical weathering in the plain completely, a thorough study of the sediments and suspended loads from rivers draining the plain is necessary.

b) In the same context, the formation process of saline-alkaline soils could be related to the weathering of sediments. It is also related closely to the groundwater salinity. Therefore, a study on the formation process of saline-alkaline soils and its temporal scale could be helpful to understand the erosion processes in the plain better.

c) Dissolved Nd isotopes in the Ganga river system has been measured in the present study. But it is not possible to identify the processes like preferential weathering or size sorting, which control the behaviour of Nd, in such large spatial scale. To understand REEs and ε_{Nd} fractionation processes during weathering, it is important to study REEs and ε_{Nd} in dissolved, particulate, soils and minerals in small catchment in the Himalaya of known lithology and mineralogy.

d) Sr isotope has been used successfully to trace the sources of dissolved ions of the rainwater in the present study. It would be interesting to know the spatial variability of this isotope in rainwater. Also, a combined study on aerosols and rain water Sr isotopic composition, can lead towards the temporal scale of interaction between them.

References

Agarwal A. K., Rizvi M. H., Singh I. B. and Chandra S. (1992) Carbonate Deposits in Ganga Plain. In *Gangetic Plain: Terra Incognita* (ed. I. B. Singh). Lucknow University. pp. 35–43.

Agarwal M., Gupta S., Deshpande R. and Yadava M. (2006) Helium, radon and radiocarbon studies on a regional aquifer system of the North Gujarat–Cambay region, India. *Chem. Geol.* **228**, 209–232.

Allègre C. (1996) Sr_Nd_Pb isotope systematics in Amazon and Congo River systems: constraints about erosion processes. *Chem. Geol.* **131**, 93–112.

Amakawa H., Alibo D. S. and Nozaki Y. (2000) Nd isotopic composition and REE pattern in the surface waters of the eastern Indian Ocean and its adjacent seas. *Geochim. Cosmochim. Acta* **64**, 1715–1727.

Andersson P. S., Dahlqvist R., Ingri J. and Gustafsson Ö. (2001) The isotopic composition of Nd in a boreal river: a reflection of selective weathering and colloidal transport. *Geochim. Cosmochim. Acta* **65**, 521–527.

Aubert D., Stille P. and Probst A. (2001) REE fractionation during granite weathering and removal by waters and suspended loads: Sr and Nd isotopic evidence. *Geochim. Cosmochim. Acta* **65**, 387–406.

Ayres M. and Harris N. (1997) REE fractionation and Nd-isotope disequilibrium during crustal anatexis: constraints from Himalayan leucogranites. *Chem. Geol.* **139**, 249–269.

Banfield J. F. and Eggleton R. A. (1989) Apatite replacement and Rare Earth mobilization, fractionation, and fixation during weathering. *Clays Clay Miner.* **37**, 113–127.

Barrat J. A. and Nesbitt R. W. (1996) Geochemistry of the Tertiary volcanism of Northern Ireland. *Chem. Geol.* **129**, 15–38.

Berner R. A. (2003) fuels and atmospheric composition. *Nature* **426**, 323–326.

Bhargava G. P. and Sharma R. C. (1982) Saline Soils of the Indo-Gangetic Alluvial Plain (North Bihar): Their Characteristics and Genesis. *J. Indian Soc. Soil Sci.* **30**, 334–341.

Bhumbla D. R. (1978) Salinity and alkalinity problems of arid regions of India. *Proc. Indian Natl. Sci. Acad.* **44,** Part B, 331–343.

Bickle M. J., Bunbury J., Chapman H. J., Harris N. B. ., Fairchild I. J. and Ahmad T. (2003) Fluxes of Sr into the headwaters of the Ganges. *Geochim. Cosmochim. Acta* **67**, 2567–2584.

Bickle M. J., Chapman H. J., Bunbury J., Harris N. B. W., Fairchild I. J., Ahmad T. and Pomiès C. (2005) Relative contributions of silicate and carbonate rocks to riverine Sr fluxes in the headwaters of the Ganges. *Geochim. Cosmochim. Acta* **69**, 2221–2240.

Bijay-Singh, Yadvinder-Singh and Sekhon G. S. (1995) Fertilizer N use efficiency and and nitrate pollution of groundwater in developing countries. *J. Contamitant Hydrol.* **20**, 167–184.

Burton K. W. and Vance D. (2000) Glacial–interglacial variations in the neodymium isotope composition of seawater in the Bay of Bengal recorded by planktonic foraminifera. *Earth Planet. Sci. Lett.* **176**, 425–441.

Chandra Mouli P., Venkata Mohan S. and Reddy S. J. (2005) Rainwater chemistry at a regional representative urban site: influence of terrestrial sources on ionic composition. *Atmos. Environ.* **39**, 999–1008.

Cheng M.-C., You C.-F., Lin F.-J., Chung C.-H. and Huang K.-F. (2010) Seasonal variation in long-range transported dust to a subtropical islet offshore northern Taiwan: Chemical composition and Sr isotopic evidence in rainwater. *Atmos. Environ.* **44**, 3386–3393.

Colin C., Turpin L., Bertaux J., Desprairies a. and Kissel C. (1999) Erosional history of the Himalayan and Burman ranges during the last two glacial–interglacial cycles. *Earth Planet. Sci. Lett.* **171**, 647–660.

Dalai T. K., Krishnaswami S. and Sarin M. M. (2002) Major ion chemistry in the headwaters of the Yamuna river system: Chemical weathering, its temperature dependence and CO2 consumption in the Himalaya. *Geochim. Cosmochim. Acta* **66**, 3397–3416.

Das A., Krishnaswami S. and Kumar A. (2006) Sr and 87 Sr/ 86 Sr in rivers draining the Deccan Traps (India): Implications to weathering, Sr fluxes, and the marine 87 Sr/ 86 Sr record around K/T. *Geochemistry Geophys. Geosystems* **7**.

Das A., Krishnaswami S., Sarin M. M. and Pande K. (2005) Chemical weathering in the Krishna Basin and Western Ghats of the Deccan Traps, India: Rates of basalt weathering and their controls. *Geochim. Cosmochim. Acta* **69**, 2067–2084.

Datta S., Thibault Y., Fyfe W. S., Powell M. A., Hart B. R., Martin R. R. and Tripathy S. (2002) Occurrence of trona in alkaline soils of the Indo-Gangetic Plains of Uttar Pradesh(U.P.), India. *Episodes* **25**, 236–239.

DePaolo D. J. (2006) Isotopic effects in fracture-dominated reactive fluid–rock systems. *Geochim. Cosmochim. Acta* **70**, 1077–1096.

Dessert C., Dupré B., François L. M., Schott J., Gaillardet J., Chakrapani G. and Bajpai S. (2001) Erosion of Deccan Traps determined by river geochemistry: impact on the global climate and the 87Sr/86Sr ratio of seawater. *Earth Planet. Sci. Lett.* **188**, 459–474.

Draxler R. R. and Rolph G. D. (2012) HYSPLIT (HYbrid Single-Particle Lagrangian Integrated Trajectory) Model access via NOAA ARL READY Website .

Drever J. I. (1997) *The Geochemistry of Natural Waters : Surface and Groundwater Environments*. Third., Prentice hall.

Drever, J.I. (1997) *Geochemistry of natural waters: surface and groundwater environments*. 3 rd., Prentice hall, New Jersey.

Dupre B., Négrel P., Seimbille F. and Allegre C. J. (1994) 87Sr/86Sr ratio variation during a rain event. *Atmos. Environ.* **28**, 617–620.

Elderfield H., Upstill-Goddard R. and Sholkovitz E. R. (1990) The rare earth elements in rivers, estuaries, and coastal seas and their significance to the composition of ocean waters. *Geochim. Cosmochim. Acta* **54**, 971–991.

France-lanord C. and Derry L. A. (1997) letters to nature Organic carbon burial forcing of the carbon cycle from Himalayan erosion. *Nature* **390**, 65–67.

France-Lanord C., Derry L. and Michard A. (1993) Evolution of the Himalaya since Miocene time: isotopic and sedimentological evidence from the Bengal Fan. *Geol. Soc. London, Spec. Publ.* **74**, 603–621.

Frank M. (2002) Radiogenic isotopes: Tracers of past ocean circulation and erosional input. *Rev. Geophys.* **40**.

Gaillardet J., Dupré B. and Allègre C. J. (1999) Geochemistry of large river suspended sediments: silicate weathering or recycling tracer? *Geochim. Cosmochim. Acta* **63**, 4037–4051.

Gaillardet J., Dupre B., Louvat P. and Allegre C. J. (1999) Global silicate weathering and CO2 consumption rates deduced from the chemistry of large rivers. *Chem. Geol.* **159**, 3–30.

Galy A. and France-Lanord C. (2001) Higher erosion rates in the Himalaya: Geochemical constraints on riverine fluxes. *Geology* **29**, 23.

Galy A. and France-Lanord C. (1999) Weathering processes in the Ganges–Brahmaputra basin and the riverine alkalinity budget. *Chem. Geol.* **159**, 31–60.

Galy A., France-Lanord C. and Derry L. A. (1999) The strontium isotopic budget of Himalayan rivers in Nepal and Bangladesh. *Geochim. Cosmochim. Acta* **63**, 1905–1925.

Galy V., François L., France-Lanord C., Faure P., Kudrass H., Palhol F. and Singh S. K. (2008) C4 plants decline in the Himalayan basin since the Last Glacial Maximum. *Quat. Sci. Rev.* **27**, 1396–1409.

Garçon M., Chauvel C., France-Lanord C., Huyghe P. and Lavé J. (2013) Continental sedimentary processes decouple Nd and Hf isotopes. *Geochim. Cosmochim. Acta* **121**, 177–195.

Garzanti E., Andó S., France-Lanord C., Censi P., Vignola P., Galy V. and Lupker M. (2011) Mineralogical and chemical variability of fluvial sediments 2. Suspended-load silt (Ganga–Brahmaputra, Bangladesh). *Earth Planet. Sci. Lett.* **302**, 107–120.

Garzanti E., Andò S., France-Lanord C., Vezzoli G., Censi P., Galy V. and Najman Y. (2010) Mineralogical and chemical variability of fluvial sediments1. Bedload sand (Ganga–Brahmaputra, Bangladesh). *Earth Planet. Sci. Lett.* **299**, 368–381.

Goldsmith E. and Hildyard N. (1984) Salting the earth : the problem of salinisation. In *The Social and Environmental Effects of Large Dams: Volume 1*

Goldstein S. J. and Jacobsen S. B. (1988) Nd and Sr isotopic systematics of river water suspended material: implications for crustal evolution. *Earth Planet. Sci. Lett.* **87**, 249–265.

Goldstein S. J. and Jacobsen S. B. (1987) The Nd and Sr isotopic systematics of river-water dissolved material: Implications for the sources of Nd and Sr in seawater. *Chem. Geol. Isot. Geosci. Sect.* **66**, 245–272.

Goswami V. (2012) Spatial and temporal variations of Os , Nd , Sr isotopes and redox sensitive elements in waters and sediments of the Arabian Sea and their implications. Thesis, Mohanlal Sukhadia University, Udaipur.

Goswami V., Singh S. K., Bhushan R. and Rai V. K. (2012) Temporal variations in 87 Sr/ 86 Sr and eNd in sediments of the southeastern Arabian Sea: Impact of monsoon and surface water circulation. *Geochemistry Geophys. Geosystems* **13**.

Gourlan A. T., Meynadier L., Allègre C. J., Tapponnier P., Birck J.-L. and Joron J.-L. (2010) Northern Hemisphere climate control of the Bengali rivers discharge during the past 4 Ma. *Quat. Sci. Rev.* **29**, 2484–2498.

Gupta H., Chakrapani G. J., Selvaraj K. and Kao S.-J. (2011) The fluvial geochemistry, contributions of silicate, carbonate and saline–alkaline components to chemical weathering flux and controlling parameters: Narmada River (Deccan Traps), India. *Geochim. Cosmochim. Acta* **75**, 800–824.

Harlavan Y. and Erel Y. (2002) The release of Pb and REE from granitoids by the dissolution of accessory phases. *Geochim. Cosmochim. Acta* **66**, 837–848.

Harlavan Y., Erel Y. and Blum J. D. (2009) The coupled release of REE and Pb to the soil labile pool with time by weathering of accessory phases, Wind River Mountains, WY. *Geochim. Cosmochim. Acta* **73**, 320–336.

Harris N., Bickle M., Chapman H., Fairchild I. and Bunbury J. (1998) The significance of Himalayan rivers for silicate weathering rates: evidence from the Bhote Kosi tributary. *Chem. Geol.* **144**, 205–220.

Hellmann R., Pitsch H., Négrel P., Millot R., Petelet-Giraud E., Malcuit E. and Brenot A. (2013) Impact of Rock Weathering on the Chemical Composition of Groundwater Determined by Inverse Modeling in Large Sedimentary Basins. *Procedia Earth Planet. Sci.* **7**, 615–619.

Hren M., Chamberlain C., Hilley G., Blisniuk P. and Bookhagen B. (2007) Major ion chemistry of the Yarlung Tsangpo–Brahmaputra river: Chemical weathering, erosion, and CO2 consumption in the southern Tibetan plateau and eastern syntaxis of the Himalaya. *Geochim. Cosmochim. Acta* **71**, 2907–2935.

Ingri J., Widerlund A., Land M., Gustafsson Ö., Andersson P. and Öhlander B. (2000) Temporal variations in the fractionation of the rare earth elements in a boreal river; the role of colloidal particles. *Chem. Geol.* **166**, 23–45.

Jacobson A. D., Blum J. D. and Walter L. M. (2002) Reconciling the elemental and Sr isotope composition of Himalayan weathering fluxes: insights from the carbonate geochemistry of stream waters. *Geochim. Cosmochim. Acta* **66**, 3417–3429.

Jain M., Kulshrestha U. ., Sarkar a. . and Parashar D. . (2000) Influence of crustal aerosols on wet deposition at urban and rural sites in India. *Atmos. Environ.* **34**, 5129–5137.

Jeandel C. (1995) Exchange of neodymium and its isotopes between seawater and small and large particles in the Sargasso Sea. *Geochim. Cosmochim. Acta* **59**, 535–547.

Jeandel C., Arsouze T., Lacan F., Techine P. and Dutay J. (2007) Isotopic Nd compositions and concentrations of the lithogenic inputs into the ocean: A compilation, with an emphasis on the margins. *Chem. Geol.* **239**, 156–164.

Katz B. G., Coplen T. B., Bullen T. D. and Davis J. H. (1997) Use of Chemical and Isotopic Tracers to Characterize the Interactions Between Ground Water and Surface Water in Mantled Karst. *Ground Water* **35**, 1014–1028.

Krishnaswami S. and Singh S. K. (2005) Chemical weathering in the river basins of the Himalaya , India. *Curr. Sci.* **89**, 841–849.

Krishnaswami S. and Singh S. K. (1998) Silicate and carbonate weathering in the drainage basins of the Ganga-Ghaghara-Indus head waters: Contributions to major ion and Sr isotope geochemistry. *Proc. Indian Acad. Sci.* **107**, 283–291.

Krishnaswami S., Singh S. K. and Dalai T. K. (1999) Silicate weathering in the Himalaya : Role in contributing to major ions and radiogenic Sr to the Bay of Bengal. In *Ocean Science, Trends and Future Directions* (ed. B. L. . Somayajulu). Indian National Science Academy. pp. 23–51.

Kulshrestha U. C., Jain M., Mandal T. K., Gupta P. K., Sarkar A. K. and Parashar D. C. (1999) Measurements of acid rain over Indian Ocean and surface measurements of atmospheric aerosols at New Delhi during INDOEX pre-campaigns. *Curr. Sci.* **76**, 968–973.

Kulshrestha U. C., Kulshrestha M. J., Sekar R., Sastry G. S. R. and Vairamani M. (2003) Chemical characteristics of rainwater at an urban site of south-central India. *Atmos. Environ.* **37**, 3019–3026.

Kulshrestha U. C., Reddy L. A. K., Satyanarayana J. and Kulshrestha M. J. (2009) Real-time wet scavenging of major chemical constituents of aerosols and role of rain intensity in Indian region. *Atmos. Environ.* **43**, 5123–5127.

Kumar G. (2005) *Geology of Uttar Pradesh and Uttaranchal*. First., Geological Society of India, Bangalore.

Lacan F. and Jeandel C. (2005) Acquisition of the neodymium isotopic composition of the North Atlantic Deep Water. *Geochemistry Geophys. Geosystems* **6**.

Lacan F. and Jeandel C. (2001) Tracing Papua New Guinea imprint on the central Equatorial Pacific Ocean using neodymium isotopic compositions and Rare Earth Element patterns. *Earth Planet. Sci. Lett.* **186**, 497–512.

Lupker M., France-Lanord C., Galy V., Lavé J., Gaillardet J., Gajurel A. P., Guilmette C., Rahman M., Singh S. K. and Sinha R. (2012) Predominant floodplain over mountain weathering of Himalayan sediments (Ganga basin). *Geochim. Cosmochim. Acta* **84**, 410–432.

Lupker M., France-Lanord C., Galy V., Lavé J. and Kudrass H. (2013) Increasing chemical weathering in the Himalayan system since the Last Glacial Maximum. *Earth Planet. Sci. Lett.* **365**, 243–252.

Ma J., Wei G., Xu Y. and Long W. (2010) Variations of Sr–Nd–Hf isotopic systematics in basalt during intensive weathering. *Chem. Geol.* **269**, 376–385.

Mahoney J. J. (1988) Deccan Traps. In *Continental Flood Basalts* (ed. J. D. Macdougall). Kluwer Academic Publishers. pp. 151–193.

Millot R., Gaillardet J., Dupré B. and Allegre C. J. (2003) Northern latitude chemical weathering rates: clues from the Mackenzie River Basin, Canada. *Geochim. Cosmochim. Acta* **67**, 1305–1329.

Molnar P. and England P. (1990) Late Cenozoic uplift of mountain ranges and climate change: chicken or egg? *Nature* **346**, 29–34.

Moon S., Huh Y., Qin J. and Vanpho N. (2007) Chemical weathering in the Hong (Red) River basin: Rates of silicate weathering and their controlling factors. *Geochim. Cosmochim. Acta* **71**, 1411–1430.

Naftz D. L., Peterman Z. E. and Spangler L. E. (1997) Using d87Sr values to identify sources of salinity to a freshwater aquifer , Greater Aneth Oil Field , Utah , USA. *Chem. Geol.* **84**, 195–209.

Nakano T. and Tanaka T. (1997) Variation of the Provenance of Base Cations in Rain Water at Kawakami, Central Japan. *Atmos. Environ.* **3**, 4237–4245.

Negrel P., Allegre C. J., Dupre B. and Lewin E. (1993) Erosion sources determined by inversion of major and trace element ratios and strontium isotopic ratios in river water: The Congo Basin case. *Earth Planet. Sci. Lett.* **120**, 59–76.

Negrel P., Casanova J. and Brulhet J. (2006) REE and Nd Isotope Stratigraphy of a Late Jurassic Carbonate Platform, Eastern Paris Basin, France. *J. Sediment. Res.* **76**, 605–617.

Negrel P. and Roy S. (1998) Chemistry of rainwater in the Massif Central (France): a strontium isotope and major element study. *Appl. Geochemistry* **13**, 941–952.

Öhlander B., Ingri J., Land M. and Schöberg H. (2000) Change of Sm-Nd isotope composition during weathering of till. *Geochim. Cosmochim. Acta* **64**, 813–820.

Oliver L., Harris N., Bickle M., Chapman H., Dise N. and Horstwood M. (2003) Silicate weathering rates decoupled from the 87Sr/86Sr ratio of the dissolved load during Himalayan erosion. *Chem. Geol.* **201**, 119–139.

Pal D. K., Srivastava P., Durge S. L. and Bhattacharyya T. (2003) Role of microtopography in the formation of sodic soils in the semi-arid part of the Indo-Gangetic Plains, India. *Catena* **51**, 3–31.

Pal D., Srivastava P., Durge S. L. and Bhattacharyya T. (2003) Role of microtopography in the formation of sodic soils in the semi-arid part of the Indo-Gangetic Plains, India. *Catena* **51**, 3–31.

Palmer M. and Edmond J. (1992) Controls over the strontium isotope composition of river water. *Geochim. Cosmochim. Acta* **56**, 2099–2111.

Pande K., Sarin M. M., Trivedi J. R., Krishnaswami S. and Sharma K. K. (1994) The Indus river system (India-Pakistan): Major-ion chemistry, uranium and strontium isotopes. *Chem. Geol.* **116**, 245–259.

Picouet C., Dupre B., Orange D. and Valladon M. (2002) Major and trace element geochemistry in the upper Niger river (Mali): physical and chemical weathering rates and CO 2 consumption. *Chem. Geol.* **185**, 93 – 124.

Piotrowski A. M., Banakar V. K., Scrivner A. E., Elderfield H., Galy A. and Dennis A. (2009) Indian Ocean circulation and productivity during the last glacial cycle. *Earth Planet. Sci. Lett.* **285**, 179–189.

Quade J., English N. and DeCelles P. G. (2003) Silicate versus carbonate weathering in the Himalaya: a comparison of the Arun and Seti River watersheds. *Chem. Geol.* **202**, 275–296.

Rai S. K. and Singh S. K. (2007) Temporal variation in Sr and 87 Sr/ 86 Sr of the Brahmaputra: Implications for annual fluxes and tracking flash floods through chemical and isotope composition. *Geochemistry Geophys. Geosystems* **8**, 1–14.

Rai S. K, Singh S. K. and Krishnaswami S. (2010) Chemical weathering in the plain and peninsular sub-basins of the Ganga : Impact on major ion chemistry and elemental fluxes. *Geochim. Cosmochim. Acta* **74**, 2340–2355.

Rao K. L. (1979) *India's Water Wealth.*, Orient Blackswan.

Rastogi N. and Sarin M. (2005) Chemical characteristics of individual rain events from a semi-arid region in India: Three-year study. *Atmos. Environ.* **39**, 3313–3323.

Rastogi N. and Sarin M. M. (2007) Chemistry of Precipitation Events and Inter-Relationship with Ambient Aerosols over a Semi-Arid Region in Western India. *J. Atmos. Chem.* **56**, 149–163.

Raymo M. E. and Ruddiman W. F. (1992) Tectonic forcing of late Cenozoic climate. *Nature* **359**, 117–122.

Raymo M. E., Ruddiman W. F. and Froelich P. N. (1988) Influence of late Cenozoic mountain building on ocean geochemical cycles. *Geology* **16**, 649–653.

Rengarajan R. and Sarin M. M. (2004) Distribution of rare earth elements in the Yamuna and the Chambal rivers , India. *Geochem. J.* **38**, 551–569.

Rengarajan R., Singh S. K., Sarin M. M. and Krishnaswami S. (2009) Strontium isotopes and major ion chemistry in the Chambal River system, India: Implications to silicate erosion rates of the Ganga. *Chem. Geol.* **260**, 87–101.

Richards L. A. (1954) *Diagnosis and improvement of saline and alkali soils.*, U.S.G.P.O.

Richter F. M., Rowley D. B. and DePaolo D. J. (1992) Sr isotope evolution of seawater: the role of tectonics. *Earth Planet. Sci. Lett.* **109**, 11–23.

Rickli J., Frank M., Stichel T., Georg R. B., Vance D. and Halliday A. N. (2013) Controls on the incongruent release of hafnium during weathering of metamorphic and sedimentary catchments. *Geochim. Cosmochim. Acta* **101**, 263–284.

Ruddiman W. F. and Prell W. L. (1997) Introduction to the Uplift-Climate Connection. In *Tectonic Uplift and Climate Change* (ed. W. F. Ruddiman). Plenum Press, New York. pp. 3–15.

Safai P. D., Rao P. S. P., Momin G. A., Ali K., Chate D. M. and Praveen P. S. (2004) Chemical composition of precipitation during 1984–2002 at Pune, India. *Atmos. Environ.* **38**, 1705–1714.

Sankararamakrishnan N., Sharma A. K. and Iyengar L. (2008) Contamination of nitrate and fluoride in ground water along the Ganges Alluvial Plain of Kanpur district, Uttar Pradesh, India. *Environ. Monit. Assess.* **146**, 375–82.

Sarin M. M., Krishnaswami S., Dilli K., Somayajulu B. L. K. and Moore W. S. (1989) Major ion chemistry of the Ganga-Brahmaputra river system: Weathering processes and fluxes to the Bay of Bengal. *Geochim. Cosmochim. Acta* **53**, 997–1009.

Sarin M. M., Krishnaswami S., Trivedi J. R. and Sharma K. K. (1992) Major ion chemistry of the Ganga source waters: Weathering in the high altitude Himalaya. *Proc. Indian Acad. Sci.* **101**, 89–98.

Saxena a., Kulshrestha U. C., Kumar N., Kumari K. M. and Srivastava S. S. (1996) Characterization of precipitation at Agra. *Atmos. Environ.* **30**, 3405–3412.

Sholkovitz E. ., Shaw T. . and Schneider D. . (1992) The geochemistry of rare earth elements in the seasonally anoxic water column and porewaters of Chesapeake Bay. *Geochim. Cosmochim. Acta* **56**, 3389–3402.

Sholkovitz E. R. (1992) Chemical evolution of rare earth elements: fractionation between colloidal and solution phases of filtered river water. *Earth Planet. Sci. Lett.* **114**, 77–84.

Sholkovitz E. R. (1993) The geochemistry of rare earth elements in the Amazon River estuary. *Geochim. Cosmochim. Acta* **57**, 2181–2190.

Sholkovitz E. and Szymczak R. (2000) The estuarine chemistry of rare earth elements: comparison of the Amazon, Fly, Sepik and the Gulf of Papua systems. *Earth Planet. Sci. Lett.* **179**, 299–309.

Singh I. B. (1996) Geological evolution of Ganga plain- an overview. *J. Paleontol. Soc. India* **41**, 99–137.

Singh K. P., Singh V. K., Malik A. and Basant N. (2006) Distribution of nitrogen species in groundwater aquifers of an industrial area in alluvial Indo-Gangetic Plains--a case study. *Environ. Geochem. Health* **28**, 473–85.

Singh S. K. (2007) Erosion and Weathering in the Brahmaputra River System. In *Large Rivers: Geomorphology and Management* (ed. A. Gupta). Wiley & Sons, Ltd. pp. 373–393.

Singh S. K. and France-Lanord C. (2002) Tracing the distribution of erosion in the Brahmaputra watershed from isotopic compositions of stream sediments. *Earth Planet. Sci. Lett.* **202**, 645–662.

Singh S. K., Kumar A. and France-Lanord C. (2006) Sr and 87Sr/86Sr in waters and sediments of the Brahmaputra river system: Silicate weathering, CO2 consumption and Sr flux. *Chem. Geol.* **234**, 308–320.

Singh S. K., Rai S. K. and Krishnaswami S. (2008) Sr and Nd isotopes in river sediments from the Ganga Basin: Sediment provenance and spatial variability in physical erosion. *J. Geophys. Res.* **113**, 1–18.

Singh S. P., Singh S. K., Goswami V., Bhushan R. and Rai V. K. (2012) Spatial distribution of dissolved neodymium and εNd in the Bay of Bengal: Role of particulate matter and mixing of water masses. *Geochim. Cosmochim. Acta* **94**, 38–56.

Sirocko F. (1995) Abrupt change in monsoonal climate: Evidence from the geochemical composition of Arabian sea sediments, Habilitation thesis, University of Kiel. Thesis, University of Kiel.

Smalley P. C., Blomqvist R. and Raheim A. (1988) Sr isotopic evidence for discrete saline components in stratified ground waters from crystalline bedrock , Outokumpu , Finland. *Geology* **16**, 354–357.

Sparks D. L. (2002) *Environmental Soil Chemistry, Second Edition.*, Academic Press.

Srivastava P. (2001) Paleoclimatic implications of pedogenic carbonates in Holocene soils of the Gangetic Plains, India. *Palaeogeogr. Palaeoclimatol. Palaeoecol.* **172**, 207–222.

Srivastava P., Prakash B., Sehgal J. L. and Kumar S. (1994) Role of neotectonics and climate in development of the Holocene geomorphology and soils of the Gangetic Plsins between the Ramganga and Rapti rivers. *Sediment. Geol.*, 129–151.

Stille P., Pierret M.-C., Steinmann M., Chabaux F., Boutin R., Aubert D., Pourcelot L. and Morvan G. (2009) Impact of atmospheric deposition, biogeochemical cycling and water–mineral interaction on REE fractionation in acidic surface soils and soil water (the Strengbach case). *Chem. Geol.* **264**, 173–186.

Stueber A. M., Walter L. M., Huston T. J. and Pushkar P. (1993) Formation waters from Mississippian-Pennsylvanian reservoirs, Illinois basin, USA: Chemical and isotopic constraints on evolution and migration. *Geochim. Cosmochim. Acta* **57**, 763–784.

Sukhija B. S. and Shah C. R. (1976) Conformity of groundwater recharge rate by tritium method and mathematical modelling. *J. Hydrol.* **30**, 167–178.

Tachikawa K. (2003) Neodymium budget in the modern ocean and paleo-oceanographic implications. *J. Geophys. Res.* **108**, 1–13.

Tachikawa K., Jeandel C. and Roy-Barman M. (1999) A new approach to the Nd residence time in the ocean: the role of atmospheric inputs. *Earth Planet. Sci. Lett.* **170**, 433–446.

Tarantola A. (2004) *Inverse Problem Theory and Methods for Model Parameter Estimation.*, SIAM: Society for Industrial and Applied Mathematics.

Tipper E., Bickle M., Galy a, West a, Pomies C. and Chapman H. (2006) The short term climatic sensitivity of carbonate and silicate weathering fluxes: Insight from seasonal variations in river chemistry. *Geochim. Cosmochim. Acta* **70**, 2737–2754.

Tipper E., Galy a and Bickle M. (2006) Riverine evidence for a fractionated reservoir of Ca and Mg on the continents: Implications for the oceanic Ca cycle. *Earth Planet. Sci. Lett.* **247**, 267–279.

Tricca A., Stille P., Steinmann M., Kiefel B. and Samuel J. (1999) Rare earth elements and Sr and Nd isotopic compositions of dissolved and suspended loads from small river systems in the Vosges mountains ž France / , the river Rhine and groundwater. *Chem. Geol.*

Tripathi J., Ghazanfari P., Rajamani V. and Tandon S. (2007) Geochemistry of sediments of the Ganges alluvial plains: Evidence of large-scale sediment recycling. *Quat. Int.* **159**, 119–130.

Tripathy G. R., Goswami V., Singh S. K. and Chakrapani G. J. (2010) Temporal variations in Sr and 87 Sr / 86 Sr of the Ganga headwaters : estimates of dissolved Sr flux to the mainstream. *Hydrol. Process.*

Tripathy G. R. and Singh S. K. (2010) Chemical erosion rates of river basins of the Ganga system in the Himalaya: Reanalysis based on inversion of dissolved major ions, Sr, and 87 Sr/ 86 Sr. *Geochemistry Geophys. Geosystems* **11**, 1–20.

Umar R. and Absar A. (2003) Chemical characteristics of groundwater in parts of the Gambhir River basin, Bharatpur District, Rajasthan, India. *Environ. Geol.* **44**, 535–544.

Vance D., Teagle D. a H. and Foster G. L. (2009) Variable Quaternary chemical weathering fluxes and imbalances in marine geochemical budgets. *Nature* **458**, 493–6.

Viers J. and Wasserburg G. J. (2004) Behavior of Sm and Nd in a lateritic soil profile1. *Geochim. Cosmochim. Acta* **68**, 2043–2054.

Wayne Nesbitt H. and Markovics G. (1997) Weathering of granodioritic crust, long-term storage of elements in weathering profiles, and petrogenesis of siliciclastic sediments. *Geochim. Cosmochim. Acta* **61**, 1653–1670.

Weyhenmeyer C. E. (2002) Groundwater Evolution in an Arid Coastal Region of the Sultanate of Oman based on Geochemical and Isotopic Tracers. In *Water-Rock Interaction* (eds. I. Stober and K. Bucher). Springer Netherlands, Dordrecht. pp. 1–38.

Wu L., Huh Y., Qin J., Du G. and Vanderlee S. (2005) Chemical weathering in the Upper Huang He (Yellow River) draining the eastern Qinghai-Tibet Plateau. *Geochim. Cosmochim. Acta* **69**, 5279–5294.

Xu Z. and Han G. (2009) Chemical and strontium isotope characterization of rainwater in Beijing, China. *Atmos. Environ.* **43**, 1954–1961.

Xu Z., Tang Y. and Ji J. (2012) Chemical and strontium isotope characterization of rainwater in Beijing during the 2008 Olympic year. *Atmos. Res.* **107**, 115–125.

Yadav S. and Rajamani V. (2004) Geochemistry of aerosols of northwestern part of India adjoining the Thar desert1. *Geochim. Cosmochim. Acta* **68**, 1975–1988.

Agarwal A. K., Rizvi M. H., Singh I. B. and Chandra S. (1992) Carbonate Deposits in Ganga Plain. In *Gangetic Plain: Terra Incognita* (ed. I. B. Singh). Lucknow University. pp. 35–43.

Agarwal M., Gupta S., Deshpande R. and Yadava M. (2006) Helium, radon and radiocarbon studies on a regional aquifer system of the North Gujarat–Cambay region, India. *Chem. Geol.* **228**, 209–232.

Allègre C. (1996) Sr_Nd_Pb isotope systematics in Amazon and Congo River systems: constraints about erosion processes. *Chem. Geol.* **131**, 93–112.

Amakawa H., Alibo D. S. and Nozaki Y. (2000) Nd isotopic composition and REE pattern in the surface waters of the eastern Indian Ocean and its adjacent seas. *Geochim. Cosmochim. Acta* **64**, 1715–1727.

Andersson P. S., Dahlqvist R., Ingri J. and Gustafsson Ö. (2001) The isotopic composition of Nd in a boreal river: a reflection of selective weathering and colloidal transport. *Geochim. Cosmochim. Acta* **65**, 521–527.

Aubert D., Stille P. and Probst A. (2001) REE fractionation during granite weathering and removal by waters and suspended loads: Sr and Nd isotopic evidence. *Geochim. Cosmochim. Acta* **65**, 387–406.

Ayres M. and Harris N. (1997) REE fractionation and Nd-isotope disequilibrium during crustal anatexis: constraints from Himalayan leucogranites. *Chem. Geol.* **139**, 249–269.

Banfield J. F. and Eggleton R. A. (1989) Apatite replacement and Rare Earth mobilization, fractionation, and fixation during weathering. *Clays Clay Miner.* **37**, 113–127.

Barrat J. A. and Nesbitt R. W. (1996) Geochemistry of the Tertiary volcanism of Northern Ireland. *Chem. Geol.* **129**, 15–38.

Berner R. A. (2003) fuels and atmospheric composition. *Nature* **426**, 323–326.

Bhargava G. P. and Sharma R. C. (1982) Saline Soils of the Indo-Gangetic Alluvial Plain (North Bihar): Their Characteristics and Genesis. *J. Indian Soc. Soil Sci.* **30**, 334–341.

Bhumbla D. R. (1978) Salinity and alkalinity problems of arid regions of India. *Proc. Indian Natl. Sci. Acad.* **44, Part B**, 331–343.

Bickle M. J., Bunbury J., Chapman H. J., Harris N. B. ., Fairchild I. J. and Ahmad T. (2003) Fluxes of Sr into the headwaters of the Ganges. *Geochim. Cosmochim. Acta* **67**, 2567–2584.

Bickle M. J., Chapman H. J., Bunbury J., Harris N. B. W., Fairchild I. J., Ahmad T. and Pomiès C. (2005) Relative contributions of silicate and carbonate rocks to riverine Sr fluxes in the headwaters of the Ganges. *Geochim. Cosmochim. Acta* **69**, 2221–2240.

Bijay-Singh, Yadvinder-Singh and Sekhon G. S. (1995) Fertilizer N use efficiency and and nitrate pollution of groundwater in developing countries. *J. Contamitant Hydrol.* **20**, 167–184.

Burton K. W. and Vance D. (2000) Glacial–interglacial variations in the neodymium isotope composition of seawater in the Bay of Bengal recorded by planktonic foraminifera. *Earth Planet. Sci. Lett.* **176**, 425–441.

Chandra Mouli P., Venkata Mohan S. and Reddy S. J. (2005) Rainwater chemistry at a regional representative urban site: influence of terrestrial sources on ionic composition. *Atmos. Environ.* **39**, 999–1008.

Cheng M.-C., You C.-F., Lin F.-J., Chung C.-H. and Huang K.-F. (2010) Seasonal variation in long-range transported dust to a subtropical islet offshore northern Taiwan: Chemical composition and Sr isotopic evidence in rainwater. *Atmos. Environ.* **44**, 3386–3393.

Colin C., Turpin L., Bertaux J., Desprairies a. and Kissel C. (1999) Erosional history of the Himalayan and Burman ranges during the last two glacial–interglacial cycles. *Earth Planet. Sci. Lett.* **171**, 647–660.

Dalai T. K., Krishnaswami S. and Sarin M. M. (2002) Major ion chemistry in the headwaters of the Yamuna river system: Chemical weathering, its temperature dependence and CO2 consumption in the Himalaya. *Geochim. Cosmochim. Acta* **66**, 3397–3416.

Das A., Krishnaswami S. and Kumar A. (2006) Sr and 87 Sr/ 86 Sr in rivers draining the Deccan Traps (India): Implications to weathering, Sr fluxes, and the marine 87 Sr/ 86 Sr record around K/T. *Geochemistry Geophys. Geosystems* **7**.

Das A., Krishnaswami S., Sarin M. M. and Pande K. (2005) Chemical weathering in the Krishna Basin and Western Ghats of the Deccan Traps, India: Rates of basalt weathering and their controls. *Geochim. Cosmochim. Acta* **69**, 2067–2084.

Datta S., Thibault Y., Fyfe W. S., Powell M. A., Hart B. R., Martin R. R. and Tripathy S. (2002) Occurrence of trona in alkaline soils of the Indo-Gangetic Plains of Uttar Pradesh(U.P.), India. *Episodes* **25**, 236–239.

DePaolo D. J. (2006) Isotopic effects in fracture-dominated reactive fluid–rock systems. *Geochim. Cosmochim. Acta* **70**, 1077–1096.

Dessert C., Dupré B., François L. M., Schott J., Gaillardet J., Chakrapani G. and Bajpai S. (2001) Erosion of Deccan Traps determined by river geochemistry: impact on the global climate and the 87Sr/86Sr ratio of seawater. *Earth Planet. Sci. Lett.* **188**, 459–474.

Draxler R. R. and Rolph G. D. (2012) HYSPLIT (HYbrid Single-Particle Lagrangian Integrated Trajectory) Model access via NOAA ARL READY Website .

Drever J. I. (1997) *The Geochemistry of Natural Waters : Surface and Groundwater Environments*. Third., Prentice hall.

Drever, J.I. (1997) *Geochemistry of natural waters: surface and groundwater environments*. 3 rd., Prentice hall, New Jersey.

Dupre B., Négrel P., Seimbille F. and Allegre C. J. (1994) 87Sr/86Sr ratio variation during a rain event. *Atmos. Environ.* **28**, 617–620.

Elderfield H., Upstill-Goddard R. and Sholkovitz E. R. (1990) The rare earth elements in rivers, estuaries, and coastal seas and their significance to the composition of ocean waters. *Geochim. Cosmochim. Acta* **54**, 971–991.

France-lanord C. and Derry L. A. (1997) letters to nature Organic carbon burial forcing of the carbon cycle from Himalayan erosion. *Nature* **390**, 65–67.

France-Lanord C., Derry L. and Michard A. (1993) Evolution of the Himalaya since Miocene time: isotopic and sedimentological evidence from the Bengal Fan. *Geol. Soc. London, Spec. Publ.* **74**, 603–621.

Frank M. (2002) Radiogenic isotopes: Tracers of past ocean circulation and erosional input. *Rev. Geophys.* **40**.

Gaillardet J., Dupré B. and Allègre C. J. (1999) Geochemistry of large river suspended sediments: silicate weathering or recycling tracer? *Geochim. Cosmochim. Acta* **63**, 4037–4051.

Gaillardet J., Dupre B., Louvat P. and Allegre C. J. (1999) Global silicate weathering and CO2 consumption rates deduced from the chemistry of large rivers. *Chem. Geol.* **159**, 3–30.

Galy A. and France-Lanord C. (2001) Higher erosion rates in the Himalaya: Geochemical constraints on riverine fluxes. *Geology* **29**, 23.

Galy A. and France-Lanord C. (1999) Weathering processes in the Ganges–Brahmaputra basin and the riverine alkalinity budget. *Chem. Geol.* **159**, 31–60.

Galy A., France-Lanord C. and Derry L. A. (1999) The strontium isotopic budget of Himalayan rivers in Nepal and Bangladesh. *Geochim. Cosmochim. Acta* **63**, 1905–1925.

Galy V., François L., France-Lanord C., Faure P., Kudrass H., Palhol F. and Singh S. K. (2008) C4 plants decline in the Himalayan basin since the Last Glacial Maximum. *Quat. Sci. Rev.* **27**, 1396–1409.

Garçon M., Chauvel C., France-Lanord C., Huyghe P. and Lavé J. (2013) Continental sedimentary processes decouple Nd and Hf isotopes. *Geochim. Cosmochim. Acta* **121**, 177–195.

Garzanti E., Andó S., France-Lanord C., Censi P., Vignola P., Galy V. and Lupker M. (2011) Mineralogical and chemical variability of fluvial sediments 2. Suspended-load silt (Ganga–Brahmaputra, Bangladesh). *Earth Planet. Sci. Lett.* **302**, 107–120.

Garzanti E., Andò S., France-Lanord C., Vezzoli G., Censi P., Galy V. and Najman Y. (2010) Mineralogical and chemical variability of fluvial sediments1. Bedload sand (Ganga–Brahmaputra, Bangladesh). *Earth Planet. Sci. Lett.* **299**, 368–381.

Goldsmith E. and Hildyard N. (1984) Salting the earth : the problem of salinisation. In *The Social and Environmental Effects of Large Dams: Volume 1*

Goldstein S. J. and Jacobsen S. B. (1988) Nd and Sr isotopic systematics of river water suspended material: implications for crustal evolution. *Earth Planet. Sci. Lett.* **87**, 249–265.

Goldstein S. J. and Jacobsen S. B. (1987) The Nd and Sr isotopic systematics of river-water dissolved material: Implications for the sources of Nd and Sr in seawater. *Chem. Geol. Isot. Geosci. Sect.* **66**, 245–272.

Goswami V. (2012) Spatial and temporal variations of Os , Nd , Sr isotopes and redox sensitive elements in waters and sediments of the Arabian Sea and their implications. Thesis, Mohanlal Sukhadia University, Udaipur.

Goswami V., Singh S. K., Bhushan R. and Rai V. K. (2012) Temporal variations in 87 Sr/ 86 Sr and eNd in sediments of the southeastern Arabian Sea: Impact of monsoon and surface water circulation. *Geochemistry Geophys. Geosystems* **13**.

Gourlan A. T., Meynadier L., Allègre C. J., Tapponnier P., Birck J.-L. and Joron J.-L. (2010) Northern Hemisphere climate control of the Bengali rivers discharge during the past 4 Ma. *Quat. Sci. Rev.* **29**, 2484–2498.

Gupta H., Chakrapani G. J., Selvaraj K. and Kao S.-J. (2011) The fluvial geochemistry, contributions of silicate, carbonate and saline–alkaline components to chemical weathering flux and controlling parameters: Narmada River (Deccan Traps), India. *Geochim. Cosmochim. Acta* **75**, 800–824.

Harlavan Y. and Erel Y. (2002) The release of Pb and REE from granitoids by the dissolution of accessory phases. *Geochim. Cosmochim. Acta* **66**, 837–848.

Harlavan Y., Erel Y. and Blum J. D. (2009) The coupled release of REE and Pb to the soil labile pool with time by weathering of accessory phases, Wind River Mountains, WY. *Geochim. Cosmochim. Acta* **73**, 320–336.

Harris N., Bickle M., Chapman H., Fairchild I. and Bunbury J. (1998) The significance of Himalayan rivers for silicate weathering rates: evidence from the Bhote Kosi tributary. *Chem. Geol.* **144**, 205–220.

Hellmann R., Pitsch H., Négrel P., Millot R., Petelet-Giraud E., Malcuit E. and Brenot A. (2013) Impact of Rock Weathering on the Chemical Composition of Groundwater Determined by Inverse Modeling in Large Sedimentary Basins. *Procedia Earth Planet. Sci.* **7**, 615–619.

Hren M., Chamberlain C., Hilley G., Blisniuk P. and Bookhagen B. (2007) Major ion chemistry of the Yarlung Tsangpo–Brahmaputra river: Chemical weathering, erosion, and CO2 consumption in the southern Tibetan plateau and eastern syntaxis of the Himalaya. *Geochim. Cosmochim. Acta* **71**, 2907–2935.

Ingri J., Widerlund A., Land M., Gustafsson Ö., Andersson P. and Öhlander B. (2000) Temporal variations in the fractionation of the rare earth elements in a boreal river; the role of colloidal particles. *Chem. Geol.* **166**, 23–45.

Jacobson A. D., Blum J. D. and Walter L. M. (2002) Reconciling the elemental and Sr isotope composition of Himalayan weathering fluxes: insights from the carbonate geochemistry of stream waters. *Geochim. Cosmochim. Acta* **66**, 3417–3429.

Jain M., Kulshrestha U. ., Sarkar a. . and Parashar D. . (2000) Influence of crustal aerosols on wet deposition at urban and rural sites in India. *Atmos. Environ.* **34**, 5129–5137.

Jeandel C. (1995) Exchange of neodymium and its isotopes between seawater and small and large particles in the Sargasso Sea. *Geochim. Cosmochim. Acta* **59**, 535–547.

Jeandel C., Arsouze T., Lacan F., Techine P. and Dutay J. (2007) Isotopic Nd compositions and concentrations of the lithogenic inputs into the ocean: A compilation, with an emphasis on the margins. *Chem. Geol.* **239**, 156–164.

Katz B. G., Coplen T. B., Bullen T. D. and Davis J. H. (1997) Use of Chemical and Isotopic Tracers to Characterize the Interactions Between Ground Water and Surface Water in Mantled Karst. *Ground Water* **35**, 1014–1028.

Krishnaswami S. and Singh S. K. (2005) Chemical weathering in the river basins of the Himalaya , India. *Curr. Sci.* **89**, 841–849.

Krishnaswami S. and Singh S. K. (1998) Silicate and carbonate weathering in the drainage basins of the Ganga-Ghaghara-Indus head waters: Contributions to major ion and Sr isotope geochemistry. *Proc. Indian Acad. Sci.* **107**, 283–291.

Krishnaswami S., Singh S. K. and Dalai T. K. (1999) Silicate weathering in the Himalaya : Role in contributing to major ions and radiogenic Sr to the Bay of Bengal. In *Ocean Science, Trends and Future Directions* (ed. B. L. . Somayajulu). Indian National Science Academy. pp. 23–51.

Kulshrestha U. C., Jain M., Mandal T. K., Gupta P. K., Sarkar A. K. and Parashar D. C. (1999) Measurements of acid rain over Indian Ocean and surface measurements of atmospheric aerosols at New Delhi during INDOEX pre-campaigns. *Curr. Sci.* **76**, 968–973.

Kulshrestha U. C., Kulshrestha M. J., Sekar R., Sastry G. S. R. and Vairamani M. (2003) Chemical characteristics of rainwater at an urban site of south-central India. *Atmos. Environ.* **37**, 3019–3026.

Kulshrestha U. C., Reddy L. A. K., Satyanarayana J. and Kulshrestha M. J. (2009) Real-time wet scavenging of major chemical constituents of aerosols and role of rain intensity in Indian region. *Atmos. Environ.* **43**, 5123–5127.

Kumar G. (2005) *Geology of Uttar Pradesh and Uttaranchal*. First., Geological Society of India, Bangalore.

Lacan F. and Jeandel C. (2005) Acquisition of the neodymium isotopic composition of the North Atlantic Deep Water. *Geochemistry Geophys. Geosystems* **6**.

Lacan F. and Jeandel C. (2001) Tracing Papua New Guinea imprint on the central Equatorial Pacific Ocean using neodymium isotopic compositions and Rare Earth Element patterns. *Earth Planet. Sci. Lett.* **186**, 497–512.

Lupker M., France-Lanord C., Galy V., Lavé J., Gaillardet J., Gajurel A. P., Guilmette C., Rahman M., Singh S. K. and Sinha R. (2012) Predominant floodplain over mountain weathering of Himalayan sediments (Ganga basin). *Geochim. Cosmochim. Acta* **84**, 410–432.

Lupker M., France-Lanord C., Galy V., Lavé J. and Kudrass H. (2013) Increasing chemical weathering in the Himalayan system since the Last Glacial Maximum. *Earth Planet. Sci. Lett.* **365**, 243–252.

Ma J., Wei G., Xu Y. and Long W. (2010) Variations of Sr–Nd–Hf isotopic systematics in basalt during intensive weathering. *Chem. Geol.* **269**, 376–385.

Mahoney J. J. (1988) Deccan Traps. In *Continental Flood Basalts* (ed. J. D. Macdougall). Kluwer Academic Publishers. pp. 151–193.

Millot R., Gaillardet J., Dupré B. and Allegre C. J. (2003) Northern latitude chemical weathering rates: clues from the Mackenzie River Basin, Canada. *Geochim. Cosmochim. Acta* **67**, 1305–1329.

Molnar P. and England P. (1990) Late Cenozoic uplift of mountain ranges and climate change: chicken or egg? *Nature* **346**, 29–34.

Moon S., Huh Y., Qin J. and Vanpho N. (2007) Chemical weathering in the Hong (Red) River basin: Rates of silicate weathering and their controlling factors. *Geochim. Cosmochim. Acta* **71**, 1411–1430.

Naftz D. L., Peterman Z. E. and Spangler L. E. (1997) Using d87Sr values to identify sources of salinity to a freshwater aquifer , Greater Aneth Oil Field , Utah , USA. *Chem. Geol.* **84**, 195–209.

Nakano T. and Tanaka T. (1997) Variation of the Provenance of Base Cations in Rain Water at Kawakami, Central Japan. *Atmos. Environ.* **3**, 4237–4245.

Negrel P., Allegre C. J., Dupre B. and Lewin E. (1993) Erosion sources determined by inversion of major and trace element ratios and strontium isotopic ratios in river water: The Congo Basin case. *Earth Planet. Sci. Lett.* **120**, 59–76.

Negrel P., Casanova J. and Brulhet J. (2006) REE and Nd Isotope Stratigraphy of a Late Jurassic Carbonate Platform, Eastern Paris Basin, France. *J. Sediment. Res.* **76**, 605–617.

Negrel P. and Roy S. (1998) Chemistry of rainwater in the Massif Central (France): a strontium isotope and major element study. *Appl. Geochemistry* **13**, 941–952.

Öhlander B., Ingri J., Land M. and Schöberg H. (2000) Change of Sm-Nd isotope composition during weathering of till. *Geochim. Cosmochim. Acta* **64**, 813–820.

Oliver L., Harris N., Bickle M., Chapman H., Dise N. and Horstwood M. (2003) Silicate weathering rates decoupled from the 87Sr/86Sr ratio of the dissolved load during Himalayan erosion. *Chem. Geol.* **201**, 119–139.

Pal D. K., Srivastava P., Durge S. L. and Bhattacharyya T. (2003) Role of microtopography in the formation of sodic soils in the semi-arid part of the Indo-Gangetic Plains, India. *Catena* **51**, 3–31.

Pal D., Srivastava P., Durge S. L. and Bhattacharyya T. (2003) Role of microtopography in the formation of sodic soils in the semi-arid part of the Indo-Gangetic Plains, India. *Catena* **51**, 3–31.

Palmer M. and Edmond J. (1992) Controls over the strontium isotope composition of river water. *Geochim. Cosmochim. Acta* **56**, 2099–2111.

Pande K., Sarin M. M., Trivedi J. R., Krishnaswami S. and Sharma K. K. (1994) The Indus river system (India-Pakistan): Major-ion chemistry, uranium and strontium isotopes. *Chem. Geol.* **116**, 245–259.

Picouet C., Dupre B., Orange D. and Valladon M. (2002) Major and trace element geochemistry in the upper Niger river (Mali): physical and chemical weathering rates and CO 2 consumption. *Chem. Geol.* **185**, 93 – 124.

Piotrowski A. M., Banakar V. K., Scrivner A. E., Elderfield H., Galy A. and Dennis A. (2009) Indian Ocean circulation and productivity during the last glacial cycle. *Earth Planet. Sci. Lett.* **285**, 179–189.

Quade J., English N. and DeCelles P. G. (2003) Silicate versus carbonate weathering in the Himalaya: a comparison of the Arun and Seti River watersheds. *Chem. Geol.* **202**, 275–296.

Rai S. K. and Singh S. K. (2007) Temporal variation in Sr and 87 Sr/ 86 Sr of the Brahmaputra: Implications for annual fluxes and tracking flash floods through chemical and isotope composition. *Geochemistry Geophys. Geosystems* **8**, 1–14.

Rai Santosh K, Singh S. K. and Krishnaswami S. (2010) Chemical weathering in the plain and peninsular sub-basins of the Ganga : Impact on major ion chemistry and elemental fluxes. *Geochim. Cosmochim. Acta* **74**, 2340–2355.

Rai Santosh K., Singh S. K. and Krishnaswami S. (2010) Chemical weathering in the plain and peninsular sub-basins of the Ganga: Impact on major ion chemistry and elemental fluxes. *Geochim. Cosmochim. Acta* **74**, 2340–2355.

Rao K. L. (1979) *India's Water Wealth.*, Orient Blackswan.

Rastogi N. and Sarin M. (2005) Chemical characteristics of individual rain events from a semi-arid region in India: Three-year study. *Atmos. Environ.* **39**, 3313–3323.

Rastogi N. and Sarin M. M. (2007) Chemistry of Precipitation Events and Inter-Relationship with Ambient Aerosols over a Semi-Arid Region in Western India. *J. Atmos. Chem.* **56**, 149–163.

Raymo M. E. and Ruddiman W. F. (1992) Tectonic forcing of late Cenozoic climate. *Nature* **359**, 117–122.

Raymo M. E., Ruddiman W. F. and Froelich P. N. (1988) Influence of late Cenozoic mountain building on ocean geochemical cycles. *Geology* **16**, 649–653.

Rengarajan R. and Sarin M. M. (2004) Distribution of rare earth elements in the Yamuna and the Chambal rivers , India. *Geochem. J.* **38**, 551–569.

Rengarajan R., Singh S. K., Sarin M. M. and Krishnaswami S. (2009) Strontium isotopes and major ion chemistry in the Chambal River system, India: Implications to silicate erosion rates of the Ganga. *Chem. Geol.* **260**, 87–101.

Richards L. A. (1954) *Diagnosis and improvement of saline and alkali soils*., U.S.G.P.O.

Richter F. M., Rowley D. B. and DePaolo D. J. (1992) Sr isotope evolution of seawater: the role of tectonics. *Earth Planet. Sci. Lett.* **109**, 11–23.

Rickli J., Frank M., Stichel T., Georg R. B., Vance D. and Halliday A. N. (2013) Controls on the incongruent release of hafnium during weathering of metamorphic and sedimentary catchments. *Geochim. Cosmochim. Acta* **101**, 263–284.

Ruddiman W. F. and Prell W. L. (1997) Introduction to the Uplift-Climate Connection. In *Tectonic Uplift and Climate Change* (ed. W. F. Ruddiman). Plenum Press, New York. pp. 3–15.

Safai P. D., Rao P. S. P., Momin G. A., Ali K., Chate D. M. and Praveen P. S. (2004) Chemical composition of precipitation during 1984–2002 at Pune, India. *Atmos. Environ.* **38**, 1705–1714.

Sankararamakrishnan N., Sharma A. K. and Iyengar L. (2008) Contamination of nitrate and fluoride in ground water along the Ganges Alluvial Plain of Kanpur district, Uttar Pradesh, India. *Environ. Monit. Assess.* **146**, 375–82.

Sarin M. M., Krishnaswami S., Dilli K., Somayajulu B. L. K. and Moore W. S. (1989) Major ion chemistry of the Ganga-Brahmaputra river system: Weathering processes and fluxes to the Bay of Bengal. *Geochim. Cosmochim. Acta* **53**, 997–1009.

Sarin M. M., Krishnaswami S., Trivedi J. R. and Sharma K. K. (1992) Major ion chemistry of the Ganga source waters: Weathering in the high altitude Himalaya. *Proc. Indian Acad. Sci.* **101**, 89–98.

Saxena a., Kulshrestha U. C., Kumar N., Kumari K. M. and Srivastava S. S. (1996) Characterization of precipitation at Agra. *Atmos. Environ.* **30**, 3405–3412.

Sholkovitz E. ., Shaw T. . and Schneider D. . (1992) The geochemistry of rare earth elements in the seasonally anoxic water column and porewaters of Chesapeake Bay. *Geochim. Cosmochim. Acta* **56**, 3389–3402.

Sholkovitz E. R. (1992) Chemical evolution of rare earth elements: fractionation between colloidal and solution phases of filtered river water. *Earth Planet. Sci. Lett.* **114**, 77–84.

Sholkovitz E. R. (1993) The geochemistry of rare earth elements in the Amazon River estuary. *Geochim. Cosmochim. Acta* **57**, 2181–2190.

Sholkovitz E. and Szymczak R. (2000) The estuarine chemistry of rare earth elements: comparison of the Amazon, Fly, Sepik and the Gulf of Papua systems. *Earth Planet. Sci. Lett.* **179**, 299–309.

Singh I. B. (1996) Geological evolution of Ganga plain- an overview. *J. Paleontol. Soc. India* **41**, 99–137.

Singh K. P., Singh V. K., Malik A. and Basant N. (2006) Distribution of nitrogen species in groundwater aquifers of an industrial area in alluvial Indo-Gangetic Plains--a case study. *Environ. Geochem. Health* **28**, 473–85.

Singh S. K. (2007) Erosion and Weathering in the Brahmaputra River System. In *Large Rivers: Geomorphology and Management* (ed. A. Gupta). Wiley & Sons, Ltd. pp. 373–393.

Singh S. K. and France-Lanord C. (2002) Tracing the distribution of erosion in the Brahmaputra watershed from isotopic compositions of stream sediments. *Earth Planet. Sci. Lett.* **202**, 645–662.

Singh S. K., Kumar A. and France-Lanord C. (2006) Sr and 87Sr/86Sr in waters and sediments of the Brahmaputra river system: Silicate weathering, CO2 consumption and Sr flux. *Chem. Geol.* **234**, 308–320.

Singh S. K., Rai S. K. and Krishnaswami S. (2008) Sr and Nd isotopes in river sediments from the Ganga Basin: Sediment provenance and spatial variability in physical erosion. *J. Geophys. Res.* **113**, 1–18.

Singh S. P., Singh S. K., Goswami V., Bhushan R. and Rai V. K. (2012) Spatial distribution of dissolved neodymium and εNd in the Bay of Bengal: Role of particulate matter and mixing of water masses. *Geochim. Cosmochim. Acta* **94**, 38–56.

Sirocko F. (1995) Abrupt change in monsoonal climate: Evidence from the geochemical composition of Arabian sea sediments, Habilitation thesis, University of Kiel. Thesis, University of Kiel.

Smalley P. C., Blomqvist R. and Raheim A. (1988) Sr isotopic evidence for discrete saline components in stratified ground waters from crystalline bedrock , Outokumpu , Finland. *Geology* **16**, 354–357.

Sparks D. L. (2002) *Environmental Soil Chemistry, Second Edition*., Academic Press.

Srivastava P. (2001) Paleoclimatic implications of pedogenic carbonates in Holocene soils of the Gangetic Plains, India. *Palaeogeogr. Palaeoclimatol. Palaeoecol.* **172**, 207–222.

Srivastava P., Prakash B., Sehgal J. L. and Kumar S. (1994) Role of neotectonics and climate in development of the Holocene geomorphology and soils of the Gangetic Plsins between the Ramganga and Rapti rivers. *Sediment. Geol.*, 129–151.

Stille P., Pierret M.-C., Steinmann M., Chabaux F., Boutin R., Aubert D., Pourcelot L. and Morvan G. (2009) Impact of atmospheric deposition, biogeochemical cycling and water–mineral interaction on REE fractionation in acidic surface soils and soil water (the Strengbach case). *Chem. Geol.* **264**, 173–186.

Stueber A. M., Walter L. M., Huston T. J. and Pushkar P. (1993) Formation waters from Mississippian-Pennsylvanian reservoirs, Illinois basin, USA: Chemical and isotopic constraints on evolution and migration. *Geochim. Cosmochim. Acta* **57**, 763–784.

Sukhija B. S. and Shah C. R. (1976) Conformity of groundwater recharge rate by tritium method and mathematical modelling. *J. Hydrol.* **30**, 167–178.

Tachikawa K. (2003) Neodymium budget in the modern ocean and paleo-oceanographic implications. *J. Geophys. Res.* **108**, 1–13.

Tachikawa K., Jeandel C. and Roy-Barman M. (1999) A new approach to the Nd residence time in the ocean: the role of atmospheric inputs. *Earth Planet. Sci. Lett.* **170**, 433–446.

Tarantola A. (2004) *Inverse Problem Theory and Methods for Model Parameter Estimation*., SIAM: Society for Industrial and Applied Mathematics.

Tipper E., Bickle M., Galy a, West a, Pomies C. and Chapman H. (2006) The short term climatic sensitivity of carbonate and silicate weathering fluxes: Insight from seasonal variations in river chemistry. *Geochim. Cosmochim. Acta* **70**, 2737–2754.

Tipper E., Galy a and Bickle M. (2006) Riverine evidence for a fractionated reservoir of Ca and Mg on the continents: Implications for the oceanic Ca cycle. *Earth Planet. Sci. Lett.* **247**, 267–279.

Tricca A., Stille P., Steinmann M., Kiefel B. and Samuel J. (1999) Rare earth elements and Sr and Nd isotopic compositions of dissolved and suspended loads from small river systems in the Vosges mountains ž France / , the river Rhine and groundwater. *Chem. Geol.*

Tripathi J., Ghazanfari P., Rajamani V. and Tandon S. (2007) Geochemistry of sediments of the Ganges alluvial plains: Evidence of large-scale sediment recycling. *Quat. Int.* **159**, 119–130.

Tripathy G. R., Goswami V., Singh S. K. and Chakrapani G. J. (2010) Temporal variations in Sr and 87 Sr / 86 Sr of the Ganga headwaters : estimates of dissolved Sr flux to the mainstream. *Hydrol. Process.*

Tripathy G. R. and Singh S. K. (2010) Chemical erosion rates of river basins of the Ganga system in the Himalaya: Reanalysis based on inversion of dissolved major ions, Sr, and 87 Sr/ 86 Sr. *Geochemistry Geophys. Geosystems* **11**, 1–20.

Umar R. and Absar A. (2003) Chemical characteristics of groundwater in parts of the Gambhir River basin, Bharatpur District, Rajasthan, India. *Environ. Geol.* **44**, 535–544.

Vance D., Teagle D. a H. and Foster G. L. (2009) Variable Quaternary chemical weathering fluxes and imbalances in marine geochemical budgets. *Nature* **458**, 493–6.

Viers J. and Wasserburg G. J. (2004) Behavior of Sm and Nd in a lateritic soil profile1. *Geochim. Cosmochim. Acta* **68**, 2043–2054.

Wayne Nesbitt H. and Markovics G. (1997) Weathering of granodioritic crust, long-term storage of elements in weathering profiles, and petrogenesis of siliciclastic sediments. *Geochim. Cosmochim. Acta* **61**, 1653–1670.

Weyhenmeyer C. E. (2002) Groundwater Evolution in an Arid Coastal Region of the Sultanate of Oman based on Geochemical and Isotopic Tracers. In *Water-Rock Interaction* (eds. I. Stober and K. Bucher). Springer Netherlands, Dordrecht. pp. 1–38.

Wu L., Huh Y., Qin J., Du G. and Vanderlee S. (2005) Chemical weathering in the Upper Huang He (Yellow River) draining the eastern Qinghai-Tibet Plateau. *Geochim. Cosmochim. Acta* **69**, 5279–5294.

Xu Z. and Han G. (2009) Chemical and strontium isotope characterization of rainwater in Beijing, China. *Atmos. Environ.* **43**, 1954–1961.

Xu Z., Tang Y. and Ji J. (2012) Chemical and strontium isotope characterization of rainwater in Beijing during the 2008 Olympic year. *Atmos. Res.* **107**, 115–125.

Yadav S. and Rajamani V. (2004) Geochemistry of aerosols of northwestern part of India adjoining the Thar desert1. *Geochim. Cosmochim. Acta* **68**, 1975–1988.

List of Publications

1. Chatterjee J., Singh S.K., ^{87}Sr/^{86}Sr and major ion composition of rainwater of Ahmedabad, India: Sources of base cations, (2012) Atmospheric Environment, 63, doi:10.1016/j.atmosenv.2012.08.060

2. Chatterjee J., Singh S. K., Sr Isotope Ratio in the Rainwater from, Ahmedabad, an Urban site in India, (2011) Proceedings of Fourteenth ISMAS Symposium cum Workshop on Mass Spectrometry, ISBN: 978-81-904442-4-8.

Atmospheric Environment 63 (2012) 60–67

Contents lists available at SciVerse ScienceDirect

Atmospheric Environment

journal homepage: www.elsevier.com/locate/atmosenv

$^{87}Sr/^{86}Sr$ and major ion composition of rainwater of Ahmedabad, India: Sources of base cations

Jayati Chatterjee*, Sunil Kumar Singh

Geosciences Division, Physical Research Laboratory, Navrangpura, Ahmedabad 380009, India

HIGHLIGHTS

- ► Chemical composition and Sr isotopic ratio are measured in rainwater samples.
- ► Chemical composition of rainwater display decadal variation.
- ► Sr isotopic ratio has been used to trace the sources of base cations for the first time in the Indian subcontinent.
- ► Base cations in the rainwaters of the Ahmedabad are derived from carbonates and basalts in addition to seawater.

ARTICLE INFO

Article history:
Received 15 March 2012
Received in revised form
5 August 2012
Accepted 28 August 2012

Keywords:
Rainwater
Chemical composition
Sr isotopic composition
Base cations
Provenance tracer
Ahmedabad, India

ABSTRACT

Rainwater samples from Ahmedabad, an urban site in India are analysed for their chemical composition and Sr isotopic ratio. Dominance of Ca in the cation budget indicates its importance in the acid neutralization whereas SO_4 and NO_3 dominate the anion budget. The major ion concentrations measured in this study are on the lower side of the range reported in the previous study (Rastogi and Sarin, 2007) from the same site. Na and Cl show very good correlation with ratio similar to the seawater ratio, implying their marine origin. Na concentration in these samples has been used as a proxy to calculate the non sea salt fraction of other major ions. Non sea salt Ca and Mg vary from 99.0% to 99.6% and 24.6% to 89.1% of the measured Ca and Mg respectively whereas non sea salt component of SO_4 and HCO_3 contribute 84.3% to 98.9% and 99.1% to 99.9% respectively. Sr concentrations in these rainwaters vary from 32 to 191 nM and $^{87}Sr/^{86}Sr$ ranges from 0.70878 to 0.71027. Sr concentration shows a very good correlation (coefficient 0.93) with the non-sea salt component of Ca and Mg indicating their continental sources and having similar provenances. Carbonates and basalts seem to contribute significantly to dissolved base cations of the rainwaters. The basalts from Deccan region, which is isotopically indistinguishable from the African basalts and the silicate and carbonates from African region along with the sediments from the Ganga plain (which is originated from the Himalayan lithologies) could be potential dust sources for this particular site. The sources of dissolved base cations deduced from Sr isotope composition of the rainwaters are consistent with wind back trajectory data obtained from NOAA HYSPLIT model.

1. Introduction

The rainwater chemistry has been important for its use to investigate the atmospheric conditions and the concentration of the soluble components, especially at present time when the anthropogenic activities are changing the atmospheric environment at an ever-increasing pace. Rainwater acquires dissolved cations and anions from the dissolution of gaseous and particulate material present in the atmosphere which could be of natural or anthropogenic origin. Cations such as Ca, Mg and anions such as HCO_3 are derived from the soil dust present in the atmosphere whereas SO_4 and NO_3 could come from anthropogenic sources in addition to natural precursors. There have been a number of studies of the wet deposition in the Indian subcontinent to deal with the chemical components and to understand their characteristics (Saxena et al., 1996; Kulshrestha et al., 1999, 2009; Safai et al., 2004; Rastogi and Sarin, 2005). It has been observed that in Indian region the rainwater are mostly alkaline in nature due to abundance of primary aerosols (Ca, Mg and K) originating from the dusty soils (Kulshrestha et al., 2003; Chandra Mouli et al., 2005). Also there have been studies to detect the crustal influence on rainwater (Jain

---

* Corresponding author. Tel.: +91 79 2631 4316; fax: +91 79 2631 4900.
E-mail addresses: jayati27@gmail.com, jayatic@prl.res.in (J. Chatterjee), sunil@prl.res.in (S.K. Singh).

1352-2310/$ – see front matter © 2012 Elsevier Ltd. All rights reserved.
http://dx.doi.org/10.1016/j.atmosenv.2012.08.060

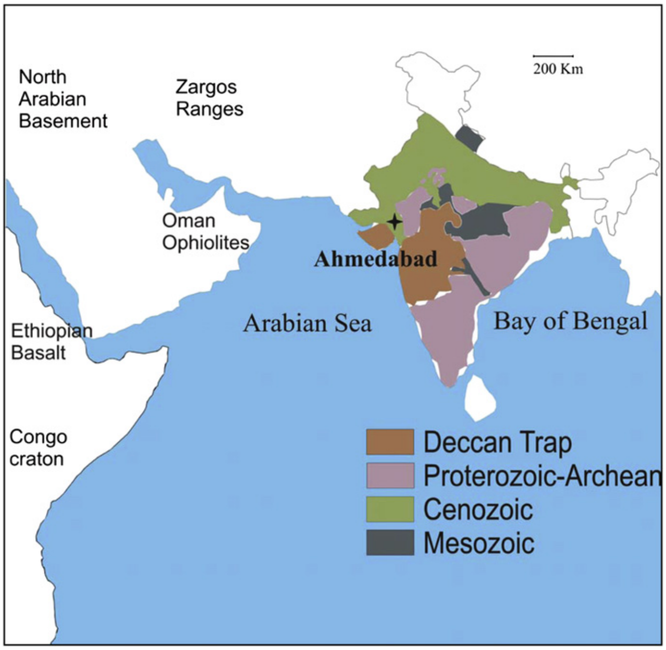

Fig. 1. Sampling location and various lithological units which could contribute base cations to the rainwater at sampling site.

et al., 2000). It is important to apportion the sources of dissolved constituent present in the rainwater. Efforts have been made to determine the sources, based on major ion composition of the rainwater in the Indian region (Safai et al., 2004; Chandra Mouli et al., 2005). It is, however, difficult to apportion the sources of dust using the major ions alone due to overlapping nature of major element composition in various sources. Sr isotope composition of the rainwater could be of immense help to determine the sources of dissolved component owing to large variation in $^{87}Sr/^{86}Sr$ of the various sources contributing to the dissolved component of rainwater. Sr isotopic ratio of the rainwater has been used to delineate the sources, natural as well as anthropogenic (Dupre et al., 1994; Nakano and Tanaka, 1997; Negrel and Roy, 1998; Chabaux et al., 2005; Cheng et al., 2010). It has been used as a tracer of sources of base cations to the rainwater (Xu and Han, 2009), which are important to maintain the pH balance of the same. The Sr isotopic ratio, which has distinctively different values in various rock types, has been used extensively to track physical and chemical weathering (Negrel et al., 1993; Negrel and Deschamps, 1996; Gaillardet et al., 1999; Krishnaswami et al., 1999; Dessert et al., 2001; Jacobson et al., 2002; Singh et al., 2008). The reason behind variation in the isotopic ratio of the source rock is the difference in their Rb/Sr ratios and their age. For example carbonates having lower Rb/Sr will have lower $^{87}Sr/^{86}Sr$ compared to silicates with higher Rb/Sr. Accordingly the various lithological units in India could be differentiated (Table 3), e.g. in the Himalayan Crystallines, Sr isotopic ratio varies from 0.72 to 0.94, in Deccan Traps 0.704–0.716 (Das et al., 2006; Singh et al., 2008) and the Himalayan and the Vindhyan carbonates have $^{87}Sr/^{86}Sr$, ~0.71, which is similar to the African carbonates from the Congo basin (0.7088) (Negrel et al., 1993). The $^{87}Sr/^{86}Sr$ ratio in various parts of eastern Africa and middle east Asia, which could affect Ahmedabad rainwater during south-west monsoon, are also constrained (Fig. 1), e.g. Congo craton (0.715), Ethiopian and Red sea basalts (0.704), Oman ophiolites (0.704) etc. (Sirocko, 1995). The silicates from the African region is considered to have Sr isotopic value of 0.73 ± 0.01 (Negrel et al., 1993). Therefore, the natural dust sources of Ca, which are same as Sr sources, could be apportioned in this region using Sr isotopes.

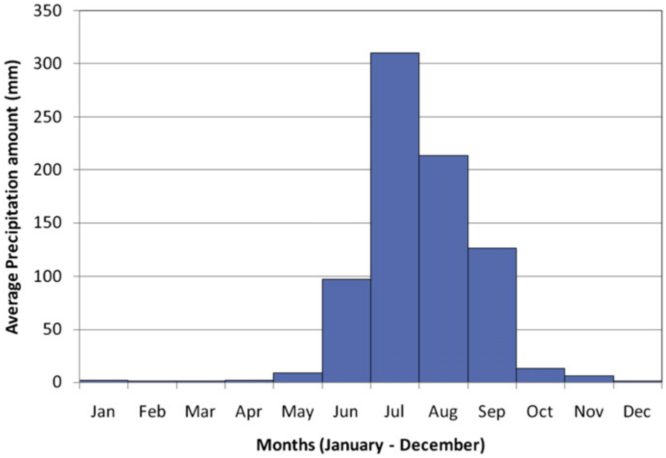

Fig. 2. Average rainfall data (1901–2000) over Ahmedabad from January to December.

In this context, the rainwater from Ahmedabad, India has been studied using Sr isotopic ratio along with major ions to delineate the sources of base cations in terms of different lithologies. This paper reports the first data set of Sr isotopic ratio in rainwater of the Indian subcontinent.

2. Sampling and experimental method

Rainwater samples were collected at Ahmedabad, which is the sixth largest city in India, with a population of about 5 million. This city is located at the western part of India (23°03′N, 72°38′E), ~100 km away from the coastal region of Arabian Sea (Fig. 1). This region is dominated by aeolian sediments of quaternary age. Deccan volcanics/sediments cover a wide region in the south eastern and south western part of the site, whereas Thar desert is ~500 km away in north-west. Alluvium plain of the Ganga is present in north-east of Ahmedabad. The average annual rainfall in this region is 650–700 mm, more than 95% of which occurs within June–September, i.e. during the south-west monsoon (Fig. 2). Rainfall in the north-western India displayed temporal variability over last 15 year (Fig. 3). Samples for this study have been collected during the peak years of the SW monsoon, 2008, 2009 and 2011 (Fig. 3).

The sampling site (23°02.18′N/72°32.65′E) is located in a residential area with heavy traffic, though the immediate vicinity is vegetation covered. Samples were collected ~35 m above the

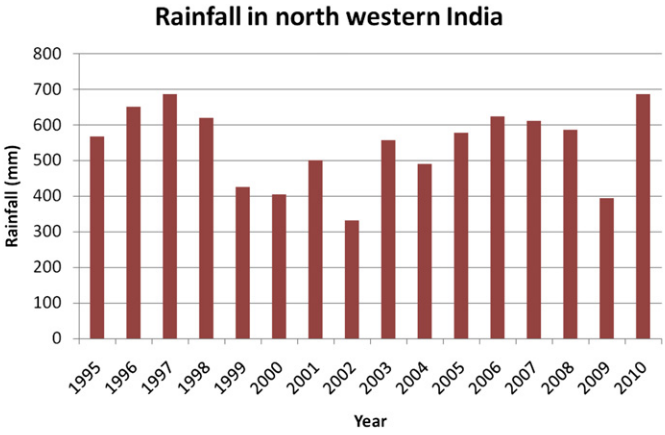

Fig. 3. Temporal variation in average annual rainfall during 1995–2010 in north-western India. Samples for this study was collected during higher average rainfall year of 2008–2011.

Table 1

Major ion, Sr concentration and $^{87}Sr/^{86}Sr$ in the rainwater (major ion concentrations are in μM and Sr concentration is in nM).[a]

Sample	Date	Precipitation (cm)	pH	Na	K	Mg	Ca	NH_4	F	Cl	NO_3	SO_4	HCO_3	Si	Sr	$^{87}Sr/^{86}Sr$
RaW-1	30.6.08	8.20	5.16	6	4	2	12	15	b.d.	9	13	12	27	2	35	0.709359
RaW-2	01.07.08	3.60	5.22	6	4	2	11	7	b.d.	5	16	14	21	3	37	0.709080
RaW-3	02.07.08	2.17	5.46	66	3	19	92	38	b.d.	83	65	44	36	6	191	0.708974
RaW-4	28.07.08	16.26	5.31	18	1	3	13	35	b.d.	24	14	15	15	2	34	0.708975
RaW-5	29.07.08	0.37	4.81	29	7	10	70	108	1	34	33	60	b.d.	7	189	0.709893
RaW-6	02.08.08	2.62	5.40	15	2	2	13	66	b.d.	20	15	31	11	4	38	0.709890
RaW-7	12.08.08	10.54	5.31	28	2	4	19	40	b.d.	36	19	21	29	6	57	0.708991
RaW-8	26.08.08	0.54	5.39	61	2	12	68	5	1	80	12	43	101	15	171	0.709412
RaW-9	13.09.08	3.11	4.60	8	2	6	46	17	3	7	19	45	b.d.	7	112	0.709936
RaW-10	18.09.08	1.80	4.61	3	b.d.	b.d.	16	39	5	4	11	7	b.d.	7	34	0.710278
RaW-11	9.07.09	8.61	5.14	10	1	10	16	15	b.d.	11	12	15	2	3	32	0.709711
RaW-12	18.07.09	0.04	5.74	37	4	13	38	64	b.d.	44	24	50	56	8	120	0.709618
RaW-13	24.07.09	0.18	5.26	56	4	10	31	51	b.d.	67	24	41	52	4	104	0.709125
RaW-14	7.07.11	3.84	5.37	12	2	5	25	76	b.d.	9	17	28	54	n.m.	72	0.709271
RaW-15	9.07.11	4.60	5.29	23	2	5	17	39	b.d.	22	11	17	41	n.m.	48	0.708823
RaW-16	11.07.11	7.76	5.31	28	1	5	16	16	b.d.	26	8	11	36	n.m.	41	0.708789

b.d. = below detection limit.
n.m. = not measured.
[a] Precipitation data collected from Dr. R.D. Deshpande, Physical Research Laboratory, Ahmedabad.

ground level on the roof of a 8 storey building using a large diameter PVC funnel, which was cleaned before collection. The sampler was opened after the starting of rainfall to prevent contamination from dry deposition. 10 samples were collected in 2008 from June to September, which provide information pertaining to the monthly variation in chemistry, 3 samples were collected in 2009 and 3 samples were collected in 2011.

All samples were filtered using 0.45 μm Millipore filter paper immediately after collection, and separated into two aliquots. One aliquot was kept unacidified and stored in pre-soaked (in Milli-Q water) polypropylene bottle and the other one was acidified using quartz distilled concentrated HCl and stored in acid cleaned polypropelene bottles. Major ion (Na, NH_4, K, Ca, Mg, Cl, F, NO_3, SO_4) concentrations were measured with an ion chromatograph (Dionex 500) using CS-12A,CG-12A columns for cation separation with methane sulfonic acid as eluent and AS-14,AG-14 columns for anion separation with Na_2CO_3/$NaHCO_3$ solution as eluent. The precision of these measurements is better than 5%. pH and alkalinity were measured in unfiltered samples using an auto-titrator (Metrohm) with an attached glass electrode, the precision of this measurement was better than 10%. Dissolved Si was measured in the samples by Molybdenum blue method in a spectrophotometer (Beckman 26) using 810 nm wavelength with precision better than 5%.

For Sr measurement, isotope dilution technique was used to get concentration and isotopic composition from the same aliquot. 80–100 ml filtered and acidified sample was spiked using ^{84}Sr tracer and then dried in a clean laboratory. The residue was taken in 3 M HNO_3 and loaded on Eichrom Sr specific resin (pre conditioned with 3 M HNO_3). Pure Sr was eluted from the resin using Milli-Q water as eluent. This Sr fraction was then dried and dissolved in 2 μl HCl and loaded on degassed and oxidized Re filaments. The measurement of Sr isotope composition was carried out using a thermal ionization mass spectrometer (Isoprobe-T) in static multi collection mode. Instrumental mass fractionation was corrected using an exponential law with 0.1194 for $^{86}Sr/^{88}Sr$. The Rb contribution, if any, was corrected by measuring ^{85}Rb and using the natural abundance of $^{85}Rb/^{87}Rb$, though the signal of ^{85}Rb was negligible. SRM987 standard was run with every set of samples which yielded $^{87}Sr/^{86}Sr$ ratio of 0.710217 ± 0.000018 (σ, $n = 9$). The procedural blank for Sr during rainwater measurement was less than 1 ng and the total Sr analysed for the samples were ~0.4 μg, which were 2–3 orders of magnitude higher than the blank.

3. Results and discussion

The major ion and Sr data of Ahmedabad rainwaters are given in Table 1. Na (3–66 μM), Ca (11–92 μM) and NH_4 (7–108 μM) are the major cations with relatively smaller amount of Mg (2–19 μM) and K (1–7 μM). SO_4 (7–60 μM), NO_3 (11–65 μM) and HCO_3 (2–101 μM) are major anions with occasionally high Cl (5–83 μM). All the major ion concentrations and TDS (1.7–17.9 mg l^{-1}) measured in the Ahmedabad rainwater during 2008, 2009 and 2011 in this study are on the lower side of the previously measured range (TDS: 1.9–137 mg l^{-1}) by Rastogi and Sarin (2005) (discussed below). Sr concentration varies from 32 to 191 nM in the rainwater, whereas its isotopic ratio varies from 0.70878 to 0.71027.

Average relative abundances of anions (on equivalent basis) follow the sequence $SO_4 > HCO_3 > Cl > NO_3$ with SO_4 dominating the anion budget. Ca dominates the cation budget of the rainwaters of Ahmedabad with the sequence $Ca > NH_4 > Na > Mg > K$. SO_4 and NO_3 are the major anions which are responsible for the acidic nature of the rainwater and Ca and NH_4 are major cations responsible for neutralizing these acids. Though the variation of pH (4.6–5.7) in these samples is not very large, all the samples have pH more than 5.0 except 3 of them. Many of these samples are having pH less than 5.6 (pH of natural rainwater in equilibrium with atmospheric CO_2) indicating that SO_4 and NO_3 are not getting neutralized by

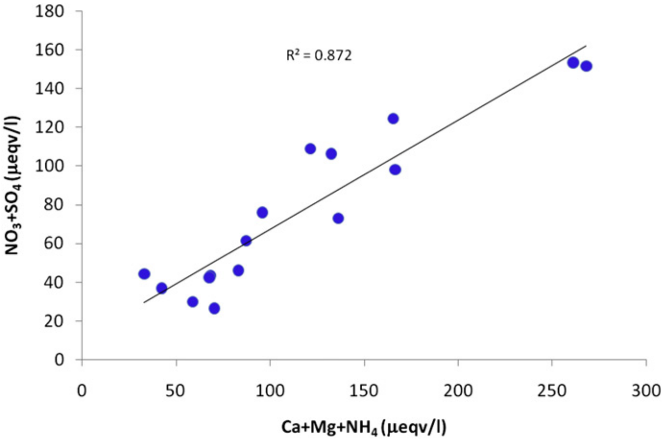

Fig. 4. Good correlation between base cations and major acidic components shows that Ca, Mg and NH_4 act as the major acid neutralizer.

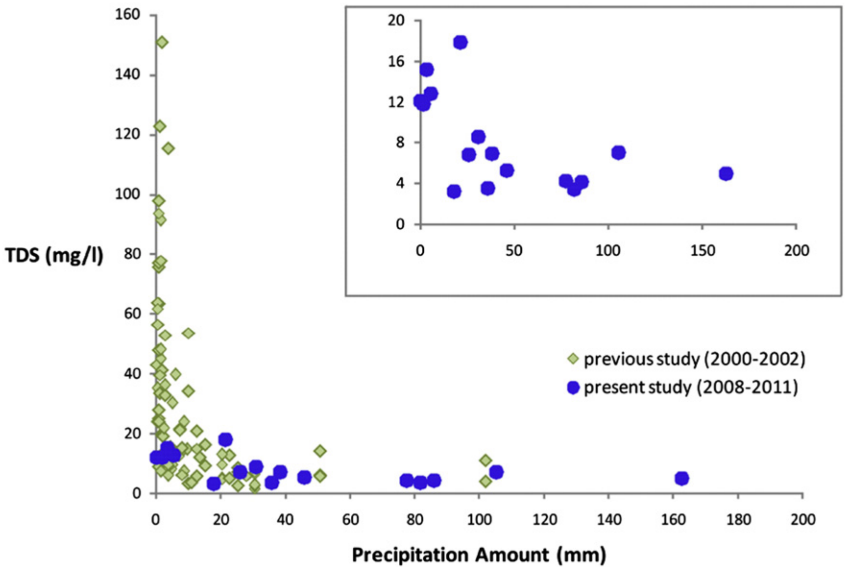

Fig. 5. Comparison of total dissolved solids between previous study (Rastogi and Sarin, 2007) and present one. This figure (inset) also shows the inverse relation between total dissolved solids and precipitation amount (mm).

cations such as Ca, Mg and NH_4. Therefore most of the samples are in the pH range of rainwater in a clean atmosphere, where dissolution of CO_2, NO_x and SO_2 in clouds and water droplets gives the acidic pH (Xu et al., 2012), and the absence of alkaline pH could be due to absence of excess dust cations. From the major ion data, it has been observed that NH_4, Ca and Mg show very good correlation with SO_4 and NO_3 (Fig. 4), suggesting that these cations are the main neutralizer of acids in the rainwater.

3.1. *Temporal variability in rainwater composition over Ahmedabad*

The major ion data of this study has been compared with the earlier study of the same region carried out during 2000–2002 (Rastogi and Sarin, 2005, 2007). Previously measured Na (1.3–1030 µM), Ca (11–2114 µM), NH_4 (1.7–220 µM), SO_4 (9.6–862 µM), NO_3 (1.3–115 µM) and all other ions in 91 samples show a range much greater than this study. The pH values measured in this study (4.6–5.7, average = 5.2) are in the lower side of the previously measured range (5.2–8.2, average = 6.7). The major ion concentration of all the samples in this study is in the lower side of the range measured in the previous study by Rastogi and Sarin (2007) indicating low solute rain events for this set of samples. The comparison of total dissolved solids (TDS) with precipitation amount from both the studies confirms this (Fig. 5). This could be interpreted as the signature of in cloud scavenging process rather than below cloud for these samples, as majority of them were collected during high precipitation (Table 1). The low pH of these samples can be explained as either less availability of dust cations during high precipitation events or increase in NO_x and SO_4 in the ambient air and hence precipitation or both. The first reason i.e. less availability of dust can possibly be related to the difference between rainfall patterns during the rainwater collection time periods. Precipitation data for North Western India from 1995 to 2010 shows that 2000–2002 were comparatively drier period compared to 2008–2010 (Fig. 3). Comparatively less rainfall during 2000–2002 could provide more dust to the atmosphere and hence more solutes in the rainwater. The second reason also cannot be ignored as during the time gap between both the studies the car/vehicular traffic in Ahmedabad has increased considerably. The comparison of the NO_3 and SO_4

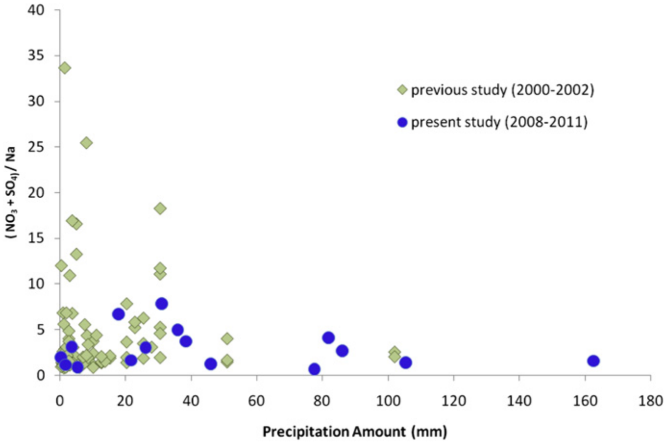

Fig. 6. Comparison between relative enrichment of $(NO_3 + SO_4)$/Na of the present study with that of the previous study (Rastogi and Sarin, 2007) does not show much difference.

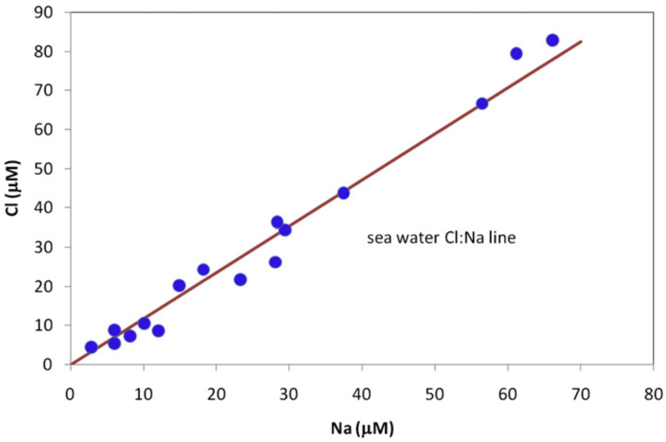

Fig. 7. Chloride vs sodium ratio in Ahmedabad rainwater is almost similar to the seawater ratio indicating their contribution from seawater.

Table 2
X/Na in seawater[a] (molar ratio).

Cl/Na	Ca/Na	Mg/Na	SO_4/Na	HCO_3/Na	Sr/Na
1.166	0.022	0.113	0.060	0.005	0.000197

[a] Calculated from data given for seawater composition in Drever (1997).

data of the present study with those of the previous one does not show much difference. To examine this point closely, a relative enrichment of ($NO_3 + SO_4$) to Na (molar ratios) has been considered and compared with the precipitation amount (Fig. 6). Though most samples from the present study are plotted towards the higher range of the previous study, but there is no drastic increase in the relative enrichment of anthropogenic inputs with time. Here it has to be remembered that no discrimination has been done between high and low solute events. These samples roughly show an inverse trend between solute concentration and precipitation amount (Fig. 5) as had been observed in the previous study (Rastogi and Sarin, 2007).

3.2. Sources of major cations

In most of the samples, Cl correlates very well with Na and their ratio, Na/Cl, in these samples are similar to that of the seawater (Fig. 7). The slope of the Na vs Cl trend is 1.26, which is not very different from the seawater ratio (1.17). Moreover, there is no relationship between Cl/Na ratio and ($NO_3 + SO_4$)/Na ratio. Therefore, anthropogenic Cl contribution is unlikely in these samples, which implies that Na and Cl in these rainwaters are mostly derived from Seawater. Further, as the sampling location, Ahmedabad is not very far from the coastal region (Fig. 1), it can be safely assumed that all the Na and Cl in the rainwater are of oceanic origin.

To apportion other cations from continental sources, the non-sea salt (NSS) components of various cations and anions are estimated using the formula,

$$X_{NSS} = X_{Rain} - Na_{Rain} \times (X/Na)_{Seawater}$$

Where X_{NSS} is the non sea salt component of the ion X; X_{Rain} and Na_{Rain} are the measured quantity of X and Na in rainwater respectively and $(X/Na)_{Seawater}$ is the ratio of X and Na in seawater (Table 2). Ca_{NSS} and Mg_{NSS} vary from 99.0% to 99.6% and 24.6%–89.1% of the measured Ca and Mg respectively whereas non-sea salt component of SO_4 and HCO_3 contribute 84.3%–98.9% and 99.1%–99.9% of their total budget respectively.

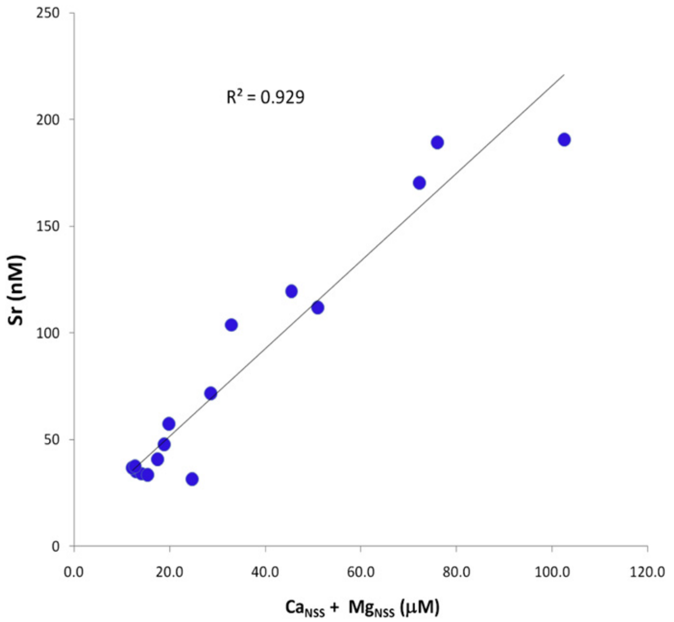

Fig. 9. Good correlation between Sr and non sea salt component of the base cations indicate their similar continental sources.

To apportion the sources of major cations of the rainwater, their Ca/Na and Mg/Na have been plotted on a mixing diagram (Fig. 8). The various possible endmembers contributing to the Ahmedabad rainwaters are also plotted based on their Na, Ca and Mg data. These data for the endmembers are taken from Das et al. (2005), Krishnaswami and Singh (2005), Rengarajan et al. (2009), Negrel et al. (1993). This mixing diagram assumes that elemental ratios of the various lithologies are getting leached to rainwater in same

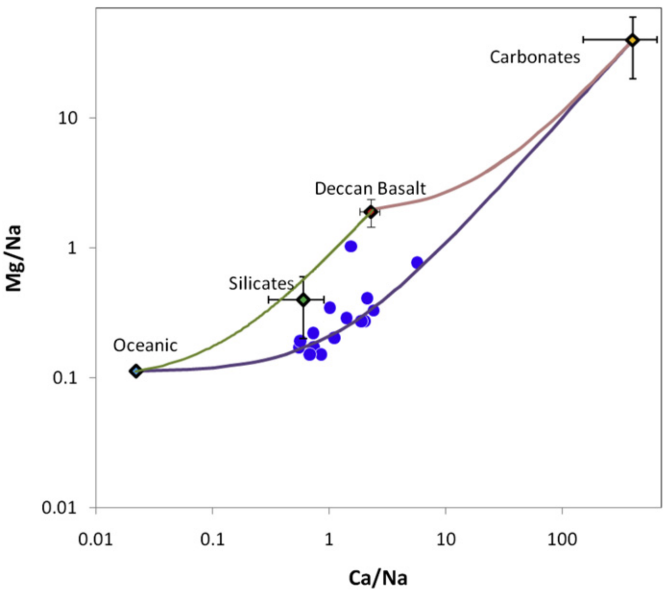

Fig. 8. Ratio plot of Ca and Mg with Na shows that these ions in the rainwaters are result of mixing among three endmembers, oceanic, basalts and carbonates.

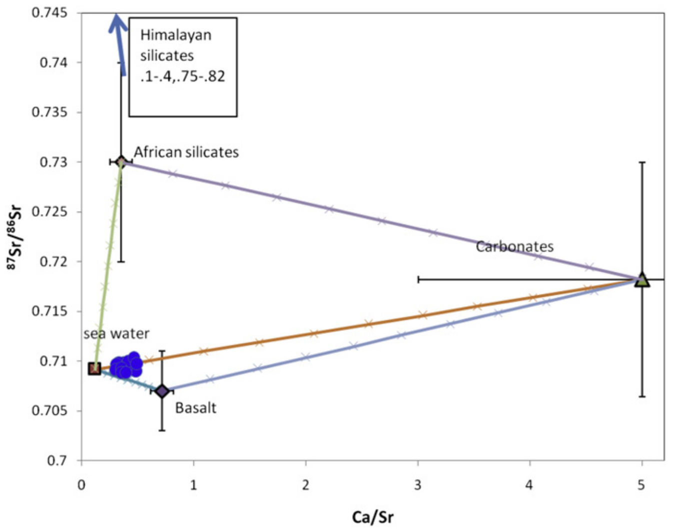

Fig. 10. Mixing plot between $^{87}Sr/^{86}Sr$ and Ca/Sr shows that Sr in rainwater of Ahmedabad is derived from carbonates, basalts and seawater. Contribution from silicates, if any, is negligible. Data source: Silicates, Carbonates from Himalaya: Krishnaswami et al. (1999); Basalts: Das et al. (2006); Silicates and carbonates from Africa: Negrel et al. (1993).

Table 3
Major ion and Sr isotopic ratios of various related endmembers.

Endmembers	Ca/Na	Mg/Na	Ca/Sr (mM/nM)	^{87}Sr/^{86}Sr
Seawater	0.022	0.113	0.1157	0.70917
Himalayan silicates	0.6 ± 0.3	0.4 ± 0.2	0.1–0.4	0.75–0.82
African silicates	0.35 ± 0.25	0.25 ± 0.15	0.35 ± 0.1	0.73 ± 0.01
Deccan basalts	2.27 ± 0.44	1.91 ± 0.46	0.71 ± 0.01	0.707 ± 0.004
Carbonates	400 ± 300	40 ± 20	5 ± 2	0.718 ± 0.01

Data compiled from Negrel et al. (1993), Krishnaswami et al. (1999), Krishnaswami and Singh (2005), Rengarajan et al. (2009).

proportion as they are present in the respective lithology. The mixing diagram of Mg/Na and Ca/Na shows that the rainwaters of the Ahmedabad fall on the mixing hyperbolae defined by the seawater and carbonate endmembers with subordinate contribution from basalt (Fig. 8, Krishnaswami and Singh, 2005). The endmember values of silicates and carbonates from Africa are not plotted separately, as they have similar values to their counter parts from Indian region, and are indistinguishable within their spreads. Fig. 8 indicates that carbonates could contribute to the Ca and Mg

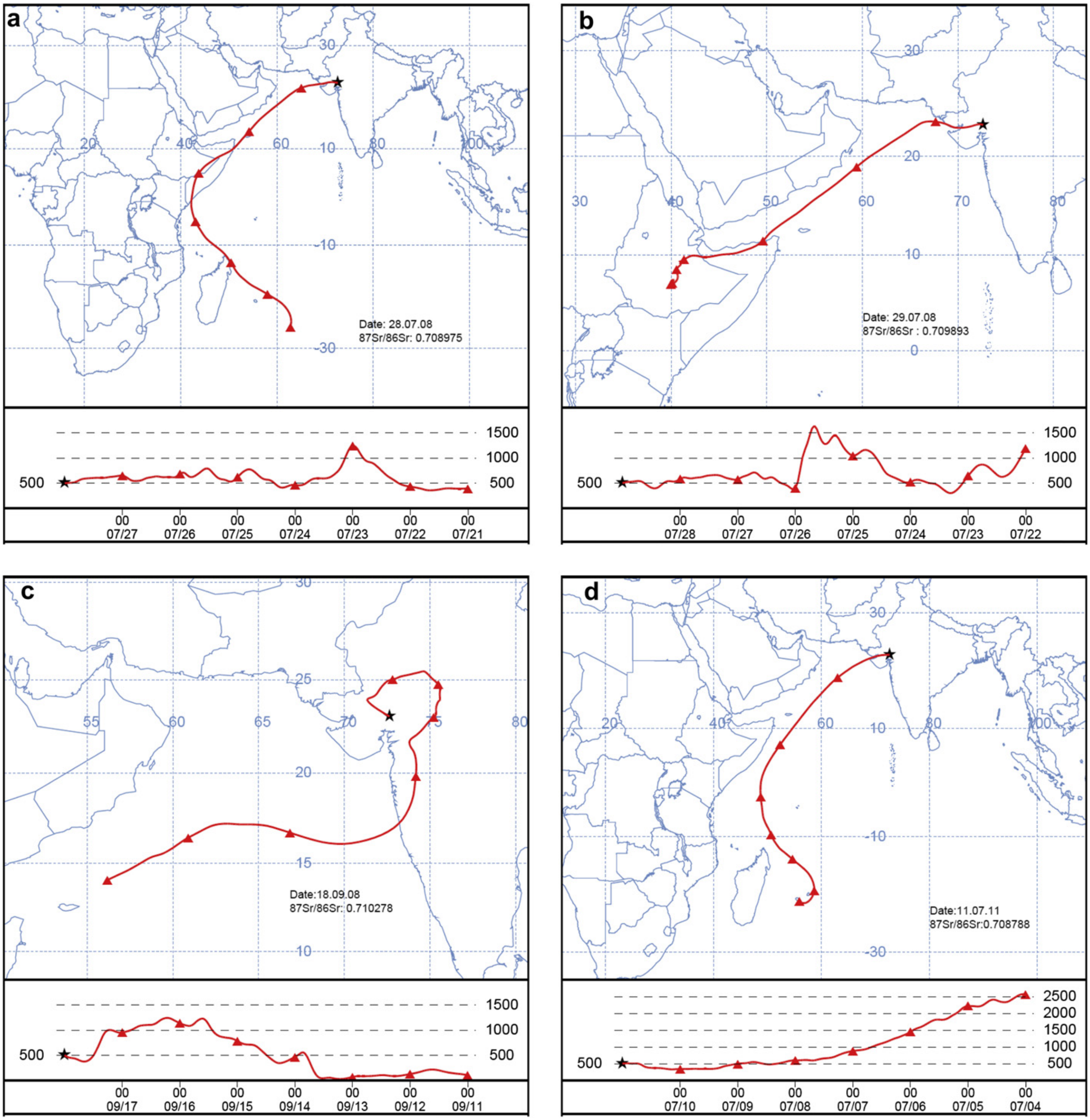

Fig. 11. a: 7 Days wind back trajectory starting from July 28, 2008 with Sr isotopic ratio 0.708975. b: 7 days wind back trajectory starting from July 29, 2008 with Sr isotopic ratio 0.709893. c: 7 days wind back trajectory starting from September 18, 2008 with Sr isotopic ratio 0.710278. d: 7 days wind back trajectory starting from July 11, 2011 with Sr isotopic ratio 0.708788.

budgets of the rainwater, basalts playing the secondary role. The carbonates contributing cations to the Ahmedabad rainwater could be from the Vindhyan, Aravalli, Ganga Plain, the Himalaya and/or from the African region (Negrel et al., 1993; Picouet et al., 2002). Basalts are either from the Deccan or from African region (Negrel et al., 1993; Picouet et al., 2002). The silicates do show close proximity to the data points, even if the mixing between slilicates, seawater and basalt cannot encompass the entire sample space, but their contribution is needed to be studied more closely. Towards this, the Sr concentration and isotopic ratio would be helpful.

3.3. *Sr concentration and $^{87}Sr/^{86}Sr$*

Sr concentration and its isotope composition in Ahmedabad rainwaters have been analysed for the first time. Sr concentrations in these rainwaters vary by six times, from 32 to 191 nM. Its isotope composition varies from 0.70878 to 0.71027. Sr_{NSS} varies from 86.5% to 98.6% with respect to measured Sr concentration in these rainwaters indicating a major contribution of continental sources. It has been observed that Sr concentration shows a very good correlation ($r^2 = 0.93$) with the non-sea salt component of Ca and Mg (Fig. 9), which was expected as a result of their similar continental source. Therefore, the use of Sr isotopes for tracking the sources of base cations is well justified.

To further constrain the sources of Sr and other base cations, rainwater data has been plotted on a mixing diagram of Ca/Sr vs $^{87}Sr/^{86}Sr$ (Fig. 10). Along with the rainwater data, various possible endmembers are also plotted on the diagram based on their available data in the literature (Table 3). One of the possible sources of these cations to the Ahmedabad rainwater is the sediments from the Thar Desert and the Ganga Plain. It has already been reported that the sediments from Thar desert and Ganga plain can be explained as mixture between Himalayan silicates and carbonates (Yadav and Rajamani, 2004; Tripathi et al., 2007). The aerosol geochemistry studied in the Thar desert region also suggests similar sources for Sr and Ca (Yadav and Rajamani, 2004). Considering this, Himalayan silicate and carbonates have been taken as endmembers in a mixing plot. It will be difficult to differentiate the Sr isotope composition of silicates and carbonates of the Aravalli and the Vindhyan from those of the Himalaya and hence silicates and carbonates endmember represent the combination of all these groups. The carbonates from Africa also show similar range, therefore they are not plotted separately. Silicates from the African region have similar Ca/Sr value as that of Himalaya, however they have less radiogenic Sr (Negrel et al., 1993). Another lithology which could contribute dust to the rainwater of the Ahmedabad is Deccan Basalt and hence basalt has been plotted as another endmember on the mixing diagram (Fig. 10). This basalt endmember includes the basalts from the African region as well, as the Deccan Basalts and African Basalts are isotopically indistinguishable (Negrel et al., 1993). Due to its proximity from the sea, Ahmedabad rains could get Sr from seawater too and hence in Fig. 10 seawater is considered as an endmember. This figure shows that contribution from carbonates, basalts and seawater can explain the Sr budget of all the rainwater samples, as has been concluded by major ion ratio plot (Fig. 8). The rainwater data points fall in the mixing field defined by seawater, carbonate and basalts endmembers (Fig. 10). Therefore, the sources of Sr and Ca to the rainwater of Ahmedabad region could be specified as carbonates and basalts with small contribution from seawater. Silicates do not seem to contribute to the Sr budget of the Ahmedabad rainwaters, as that would result in more radiogenic Sr than observed. This interpretation about the sources of Sr and Ca to the Ahmedabad rainwater helps in constraining the sources better than that based on major ions only. To examine this in detail, the mixing lines have been included the percentage from each source (Fig. 10), which shows that African silicates are less likely to contribute more than 10% of the Sr isotopic budget of these rainwaters, while basalts and carbonates can explain most of the Sr budget (>50%–70%), considering the spread of these two endmembers. The rest of the Sr budget is balanced by Sr from oceanic origin.

The variation in Sr isotopic ratio with time can be studied from Table 1. As the seawater Sr isotopic ratio is very well constrained at 0.70917 ± 0.00001 (Nakano and Tanaka, 1997), the result indicates that the Sr is coming into the rain from sources with lower Sr isotopic signature, i.e. either Deccan Traps and/or Middle East Asia including Ethiopian basalts. Whereas the higher values of Sr can come from the carbonates (Himalayan, Vindhyan or African). To have a rough idea of the wind pattern during the sampling period, 7 days wind backward trajectories have been plotted with HYSPLIT model (http://www.arl.noaa.gov) (Draxler and Rolph, 2012). Four of such trajectories (two with lower Sr isotopic ratio and two with higher) are given in Fig. 11. From Table 1 and Fig. 11 it can be seen that during July 28–29, 2008 though the collection date differs by only one day, the Sr isotopic ratio shows a large difference as the wind sources were different. In the first case (July 28, 2008) the wind has started from Arabian Sea, whereas in the second case it has started from the African region, hence the higher Sr isotopic ratio is observed in the rainwater collected on July 28 2008. Similarly on September 18, 2008, when the rainwater $^{87}Sr/^{86}Sr$ has the highest observed value (0.710278, Table 1), wind backward trajectory traversed a path through Aravalli and Ganga Plain region before coming to Ahmedabad (Fig. 11c), whereas in other case ($^{87}Sr/^{86}Sr$, 0.708788; Fig. 11d) it has traversed small distance inland from the Arabian Sea to Ahmedabad through the basaltic and alluvial terrains of south-west Gujarat. The above discussion shows the sensitivity of the Sr isotopic ratio in tracking the wind sources from different lithologies.

4. Conclusions

Major ion, Sr concentrations and Sr isotope compositions were measured in the rainwaters of an urban site to get an idea about the various sources of dissolved ions to rainwater. The comparison of major ion data with previous studies shows the decrease in dissolved constituents in the rainwater during 2008–2011 due to higher rainfall compared to those during 2000–2002. It indicates possible influence of rain patterns (on yearly basis) over the abundance of dust in the atmosphere. The Sr concentration, which shows a very good correlation with the NSS component of Ca and Mg, has been used to delineate the dust sources to the atmosphere, assuming that they have same origin. $^{87}Sr/^{86}Sr$ along with major ion compositions of Ahmedabad rainwater indicate carbonate and basalts as important sources of dissolved base cations to the rainwater. The sources of dissolved material deduced from Sr isotopic ratio in the rainwater also agrees very well with wind back trajectory data obtained from NOAA HYSPLIT model. The present study shows the carbonates and basalts are major sources of Sr during the south-west monsoon. Occasional contribution from other major lithologies such as African carbonates/basalts and alluvial from the Ganga Plain have also been observed during this study. It can be concluded that Sr isotopes can be used quite satisfactorily as a provenance tracer of aerosols by measuring that in rainwater.

Acknowledgements

We thank Dr. R.D. Deshpande for kindly providing rainfall data. The comments of the two reviewers have helped immensely to improve the manuscript.

References

Chabaux, F., Riotte, J., Schmitt, A.-D., Carignan, J., Herckes, P., Pierret, M.-C., Wortham, H., 2005. Variations of U and Sr isotope ratios in Alsace and Luxembourg rain waters: origin and hydrogeochemical implications. Comptes Rendus Geoscience 337, 1447–1456.

Chandra Mouli, P., Venkata Mohan, S., Reddy, S.J., 2005. Rainwater chemistry at a regional representative urban site: influence of terrestrial sources on ionic composition. Atmospheric Environment 39, 999–1008.

Cheng, M.-C., You, C.-F., Lin, F.-J., Chung, C.-H., Huang, K.-F., 2010. Seasonal variation in long-range transported dust to a subtropical islet offshore northern Taiwan: chemical composition and Sr isotopic evidence in rainwater. Atmospheric Environment 44, 3386–3393.

Das, A., Krishnaswami, S., Kumar, A., 2006. Sr and $^{87}Sr/^{86}Sr$ in rivers draining the Deccan Traps (India): implications to weathering, Sr fluxes, and the marine $^{87}Sr/^{86}Sr$ record around K/T. Geochemistry Geophysics Geosystems 7.

Das, A., Krishnaswami, S., Sarin, M., Pande, K., 2005. Chemical weathering in the Krishna Basin and Western Ghats of the Deccan Traps, India: rates of basalt weathering and their controls. Geochimica et Cosmochimica Acta 69, 2067–2084.

Dessert, C., Dupré, B., François, L.M., Schott, J., Gaillardet, J., Chakrapani, G., Bajpai, S., 2001. Erosion of Deccan Traps determined by river geochemistry: impact on the global climate and the $^{87}Sr/^{86}Sr$ ratio of seawater. Earth and Planetary Science Letters 188, 459–474.

Draxler, R.R., Rolph, G.D., 2012. HYSPLIT (HYbrid Single-Particle Lagrangian Integrated Trajectory) Model Access Via NOAA ARL READY Website.

Drever, J.I., 1997. Geochemistry of Natural Waters: Surface and Groundwater Environments, third ed. Prentice hall, New Jersey.

Dupre, B., Négrel, P., Seimbille, F., Allegre, C.J., 1994. $^{87}Sr/^{86}Sr$ ratio variation during a rain event. Atmospheric Environment 28, 617–620.

Gaillardet, J., Dupré, B., Allègre, C.J., 1999. Geochemistry of large river suspended sediments: silicate weathering or recycling tracer? Geochimica et Cosmochimica Acta 63, 4037–4051.

Jacobson, A.D., Blum, J.D., Walter, L.M., 2002. Reconciling the elemental and Sr isotope composition of Himalayan weathering fluxes: insights from the carbonate geochemistry of stream waters. Geochimica et Cosmochimica Acta 66, 3417–3429.

Jain, M., Kulshrestha, U.C., Sarkar, A.K., Parashar, D.C., 2000. Influence of crustal aerosols on wet deposition at urban and rural sites in India. Atmospheric Environment 34, 5129–5137.

Krishnaswami, S., Singh, S.K., 2005. Chemical weathering in the river basins of the Himalaya, India. Current Science 89, 841–849.

Krishnaswami, S., Singh, S.K., Dalai, T.K., 1999. Silicate weathering in the Himalaya: role in contributing to major ions and radiogenic Sr to the Bay of Bengal. In: Somayajulu, B.L. (Ed.), Ocean Science, Trends and Future Directions. Indian National Science Academy, pp. 23–51.

Kulshrestha, U.C., Jain, M., Mandal, T.K., Gupta, P.K., Sarkar, A.K., Parashar, D.C., 1999. Measurements of acid rain over Indian Ocean and surface measurements of atmospheric aerosols at New Delhi during INDOEX pre-campaigns. Current Science 76, 968–973.

Kulshrestha, U.C., Kulshrestha, M.J., Sekar, R., Sastry, G.S.R., Vairamani, M., 2003. Chemical characteristics of rainwater at an urban site of south-central India. Atmospheric Environment 37, 3019–3026.

Kulshrestha, U.C., Reddy, L.A.K., Satyanarayana, J., Kulshrestha, M.J., 2009. Real-time wet scavenging of major chemical constituents of aerosols and role of rain intensity in Indian region. Atmospheric Environment 43, 5123–5127.

Nakano, T., Tanaka, T., 1997. Variation of the provenance of base cations in rain water at Kawakami, central Japan. Atmospheric Environment 3, 4237–4245.

Negrel, P., Allegre, C.J., Dupre, B., Lewin, E., 1993. Erosion sources determined by inversion of major and trace element ratios and strontium isotopic ratios in river water: the Congo Basin case. Earth and Planetary Science Letters 120, 59–76.

Negrel, P., Deschamps, P., 1996. Natural and anthropogenic budgets of a small watershed in the massif central (France): chemical and strontium isotopic characterization of water and sediments. Aquatic Geochemistry 2.

Negrel, P., Roy, S., 1998. Chemistry of rainwater in the Massif Central (France): a strontium isotope and major element study. Applied Geochemistry 13, 941–952.

Picouet, C., Dupre, B., Orange, D., Valladon, M., 2002. Major and trace element geochemistry in the upper Niger river (Mali): physical and chemical weathering rates and CO_2 consumption. Chemical Geology 185, 93–124.

Rastogi, N., Sarin, M., 2005. Chemical characteristics of individual rain events from a semi-arid region in India: three-year study. Atmospheric Environment 39, 3313–3323.

Rastogi, N., Sarin, M.M., 2007. Chemistry of precipitation events and inter-relationship with ambient aerosols over a semi-arid region in western India. Journal of Atmospheric Chemistry 56, 149–163.

Rengarajan, R., Singh, S.K., Sarin, M.M., Krishnaswami, S., 2009. Strontium isotopes and major ion chemistry in the Chambal River system, India: implications to silicate erosion rates of the Ganga. Chemical Geology 260, 87–101.

Safai, P.D., Rao, P.S.P., Momin, G.A., Ali, K., Chate, D.M., Praveen, P.S., 2004. Chemical composition of precipitation during 1984–2002 at Pune, India. Atmospheric Environment 38, 1705–1714.

Saxena, A., Kulshrestha, U.C., Kumar, N., Kumari, K.M., Srivastava, S.S., 1996. Characterization of precipitation at Agra. Atmospheric Environment 30, 3405–3412.

Singh, S.K., Rai, S.K., Krishnaswami, S., 2008. Sr and Nd isotopes in river sediments from the Ganga Basin: sediment provenance and spatial variability in physical erosion. Journal of Geophysical Research 113, 1–18.

Sirocko, F., 1995. Abrupt Change in Monsoonal Climate: Evidence From the Geochemical Composition of Arabian Sea Sediments, Habilitation thesis, University of Kiel.

Tripathi, J., Ghazanfari, P., Rajamani, V., Tandon, S., 2007. Geochemistry of sediments of the Ganges alluvial plains: evidence of large-scale sediment recycling. Quaternary International 159, 119–130.

Xu, Z., Han, G., 2009. Chemical and strontium isotope characterization of rainwater in Beijing, China. Atmospheric Environment 43, 1954–1961.

Xu, Z., Tang, Y., Ji, J., 2012. Chemical and strontium isotope characterization of rainwater in Beijing during the 2008 Olympic year. Atmospheric Research 107, 115–125.

Yadav, S., Rajamani, V., 2004. Geochemistry of aerosols of northwestern part of India adjoining the Thar desert. Geochimica et Cosmochimica Acta 68, 1975–1988.